Department of Natural Resources, Mines and Energy
Geological Survey of Queensland

The Geochemistry Tool Kit

A geochemical exploration reference for northwest Queensland

Keith Hannan[1], Richard Lilly[2] and Joseph Tang[3]
[1] GeoChem Pacific, [2] University of Adelaide,
[3] Geological Survey of Queensland

Queensland Government

The Geochemistry Tool Kit

A geochemical exploration reference for northwest Queensland

Keith Hannan[1], Richard Lilly[2] and Joseph Tang[3]
[1] GeoChem Pacific, [2] University of Adelaide, [3] Geological Survey of Queensland

Address for correspondence:

Geological Survey of Queensland
Department of Natural Resources, Mines and Energy
PO Box 15216 City East QLD 4002
Email: geological_info@dnrme.qld.gov.au

Cover photographs: Left, clumps of spinifex amongst outcrop of a siliceous member of the mid-Proterozoic Corella Formation, 56 km northwest of Cloncurry (2008, K. Hannan); right, grass-covered black soil plain on 30 metres of post-Paleozoic sedimentary cover, north of Cloncurry and 7 km southwest of Ernest Henry mine (2009, R. Lilly).

ISBN 978-1-9256-0906-6 (Hardcopy)
ISBN 978-1-9256-0907-3 (Online)
Issued: August 2018

Reference: HANNAN, K., LILLY, R. & TANG, J., 2018: *The Geochemistry Tool Kit. A geochemical exploration reference for northwest Queensland*. Geological Survey of Queensland, Department of Natural Resources, Mines and Energy, Brisbane.

Contents

Figures

Tables

Appendices

Data and internal reports (online only)

Data relating to Chapters 1–7 and pdf versions of unpublished internal reports

Preface

The Mount Isa region of Queensland is one of the world's highly endowed zinc, lead, silver, copper and gold mineral provinces, hosting numerous world class deposits. After more than 70 years of mineral exploration, and at a time of depleting production at established mines, explorers are now drilling longer holes to test deeper targets and are increasingly searching at the periphery of the Mount Isa Inlier, and beyond, where prospective Proterozoic rock units and structures are buried under sediments of the Carpentaria, Eromanga and Georgina basins. Accordingly, the challenge of replenishing the ore inventory of the region is an increasingly technological one.

Since about 1950, the Mount Isa region has been covered by more than 3500 exploration tenements, most of which were explored with geochemistry as the primary means of investigation and final assessment. This remains the situation today even though geophysical data influence the siting of many pre-discovery (reconnaissance) drill holes. Yet, during the recent 25-year period of high profile geoscience initiatives and multiple post-graduate research programs, little attention, other than company-confidential projects, has been given to the evaluation of surface geochemical exploration techniques suitable for the detection of buried and blind orebodies, or the challenge of chemical data optimisation for primary halo detection in drill hole samples.

The Geochemical Tool Kit (GTK) addresses these shortcomings by providing reviews, case studies, instruction, expert advice and learned opinion. Its primary aims are to guide and enhance geochemical exploration practice in northwest Queensland and encourage more companies to explore the 'greenfields' covered domain.

The GTK is the product of collaboration between experienced industry exploration geochemists and the Geological Survey of Queensland. Industry contributors, by way of data or internal reports, include MIM Resource Development PL (MIMRD), Minotaur Exploration Ltd, South32 Ltd and Chinova Resources PL. The project was funded by the Queensland Government's *Strategic Resources Exploration Program* to increase mining activity and expedite mineral discoveries in northwest Queensland.

Introduction

The growing global demand for metals and decreasing rates of discovery in established mineral belts underscores a trend to increasing search depths and the unavoidable challenge of exploring extensions of favourable geologic domains beneath transported cover. The Geochemistry Tool Kit (GTK) addresses the challenge for Queensland's premier mineral region, the Mount Isa Inlier, by promoting optimal geochemical exploration practice for deep targets, both in areas of exposed Proterozoic bedrock and targets beneath as much as 200 metres (m) of transported cover.

The publication is primarily concerned with the chemical detection and recognition of buried targets in surficial regolith and drill hole samples. Overviews of conventional and innovative sampling and analytical methods are provided, and the relevance of each to typical exploration settings encountered in the Mount Isa region is demonstrated. Near-surface and outcropping mineralisation is also treated, but only in the context of data coverage and optimisation. The following framework links exploration setting and chemical exploration tactics as the major themes of the GTK:

- identifying locally sourced secondary dispersions at the surface (conventional surface geochemical)
- identifying deeply sourced secondary dispersions at the surface (non-conventional surface geochemical exploration)
- identifying secondary dispersions from drill hole samples within, and at the base of, transported cover (unlithified or lithified).

The first half of the document comprises four chapters in which conventional sampling and chemical analytical methods are discussed. The subject matter includes: the quality and effectiveness of compiled surface geochemical data (DNRME, open-file), the optimisation of future surface and drill hole sample geochemical data, and the applicability of isotopic and mineral-based technologies. The second half, Chapters 5 to 8, concerns sampling and chemical analytical methods designed, or intended for, the measurement of chemically introduced secondary dispersions. Topics covered include: chemical transport mechanisms in transported cover, sample media and sampling procedures, nature of the data and the identification of anomalies.

To complement the GTK, updated thickness of cover contours and a derived geochemical exploration domain map will shortly be completed by the Geological Survey of Queensland (GSQ) to assist the planning of soil geochemical and base of cover drilling programs for the covered domain.

Underlying the instructional aspects of the GTK are specific agendas of a strategic nature for the mining industry and the Queensland government. They include:

- promotion of the prospective, covered extensions of the Mount Isa Inlier as desirable, accessible and logistically feasible exploration terrain

- encouragement of the acquisition of high quality lithogeochemical (whole rock) data, as a growing strategic resource for the modelling and recognition of distal primary dispersions (i.e., haloes)
- as above, for groundwater data, both for the modelling and recognition of distal secondary dispersions (to ore) and as a resource for long term aquifer management.

Keywords:
Geochemistry, geochemical exploration, analytical method, data analysis and interpretation, surface geochemistry, concealed ore deposits, pathfinder elements, metal migration, dispersion and anomalies, gossans, lead and stable isotopes, hydrogeochemistry, biogeochemistry, stratiform deposits, IOCG, fracture control, Mount Isa Proterozoic.

Acknowledgements

The Geochemistry Toolkit is a collaboration between the Geological Survey of Queensland, GeoChem Pacific Ltd (NZ) and the University of Adelaide. Primary authorship was undertaken by Dr. Keith Hannan (Geochem Pacific).

The following are acknowledged with gratitude for professional and expert input:

> primary reviewer Dr Neil Rutherford of Rutherford Mineral Resource Consultants PL
>
> contributing reviewers Douglas Brewster and geoscientists of the DNRME especially Dr Micaela Preda, David Purdy and Dominic Brown
>
> editorial and digital publishing staff of the DNRME including Sharon Beeston, Jonathan Garde, Paula Deacon, and Gina Nuttall.

Staff of MIM RD are thanked for generous access to in-house geochemical R&D data and reports.

Chapter 1
Surface geochemistry: Outcrop domain

Introduction

The chemical analyses and supporting information for almost a million soil, rock chip and stream sediment samples from open-file mineral exploration reports provide an essential platform for exploration activity in northwest Queensland. The data are current to September 2016 and accessible through the online services of the Queensland Department of Natural Resources, Mines and Energy. This chapter concerns the 85–90% of samples located within areas of outcropping Proterozoic rock (*i.e.*, the Mount Isa Inlier).

The geochemical data has been accumulated over 60 years, during a period of substantial change in analytical technologies and evolving field sampling practices. Consequently, the data for individual elements vary enormously in quality and sensitivity, and therefore utility. Stated explicitly, the compilation comprises 26 subgroups of physically distinct material analysed by more than 1000 laboratory routines at more than 150 laboratories. Therefore, it is not surprising that the task of re-evaluating and interpreting anything larger than prospect-scale subsets of the data is challenging and time-consuming, even for the expert.

Accordingly, the first part of this chapter informs the user of the essential strengths and weaknesses of the data for each of the three major sample types (soils, stream sediments and rock chips) and provides examples of processing and data optimisation. The second section examines how future soil, rock chip and stream sediment sampling in the outcrop domain can be aligned with drill sample geochemistry, and the challenge of detecting and recognising the distal expressions of undiscovered blind ore deposits.

Chapter 1

Overview of compiled surface geochemical data

Soil samples

The northwest Queensland compilation contains 457,904 soil sample data points, 84% of which are located within the area shown as outcropping Proterozoic rock in Figure 1.

For elements such as Cu, Pb and Zn, the coverage is comprehensive for rock units historically regarded as prospective, and it could be argued that further work is unlikely to reveal new areas of outcropping and significant base metal mineralisation. Nonetheless, very large areas of outcrop remain unsampled and present opportunities for explorers to pursue with new concepts and base metal mineralisation models. Moreover, the soils compilation is an agglomeration of widely differing sample types, sample grain sizes and analytical methods—much more so than the stream sediment and rock chip data sets. Therefore, it is possible that processing, by levelling or normalisation, could reveal distribution patterns (gradients) in individual or combined commodity metals (including Au), at scales which encompass multiple historical soil surveys.

The complexity of the data is illustrated by Table 1.1, which identifies the two main sample types as (a) sieved soil followed by a conventional laboratory digestion, and (b) the gold-focussed bulk cyanide leach or BCL type. The 360,000, or so, conventional soil samples were prepared in the field with 52 different types of sieve (mesh classes), and the 41,000 BCL samples by 17. Fortunately, the mesh classes can be consolidated into four well separated groups, ranging from very fine (-80# through -200# sieves) to coarse (4.7 to 6.7 mm sieves), which should reveal, after levelling, variation in background and anomaly amplitudes controlled by grain size variation. Those samples without a mesh class designation must be processed as a separate population (right-most column, Table 1.2); in the case the case of the BCL type, many were probably bulk-sampled in the field.

The remaining 58,100 samples consist primarily of the following sample types: lag (13,100), radiation readings (9200), magnetic separates (6,000, including a lag subgroup), auger (4000), weak/selective extraction (7500, four separate extraction types), soil by RAB drill (3100), soil by portable XRF (2600), termite mounds (2000) and heavy mineral concentrates (3000, for kimberlite indicator minerals).

The compiled soil data are comparatively free of misattributed abundance units, with notable exception of the weak/selective extraction data (recorded with a “PD” for “partial digestion” in the sample type field of the data base). In detail, the elemental data for about half of the 7500 MMI, Enzyme Leach, Regoleach etc. samples are about 3 orders of magnitude higher than the other half, indicating that they retain their lab-designated ppb units (*i.e.*, require conversion to ppm). The units of supplementary elements associated with some groups of BCL samples are also suspect (*e.g.*, high Pb, As, Bi, Ag, Mo values that require factoring by 0.001).

Table 1.1. Summary of major soil sample types and mesh classes (DNRM, 2016 release).

Sample type	Sub-total	Mesh classes	Sieved grainsize maximum (mm)					Unknown preparation (NA or UNK)
			Very fine 0.18	fine 0.2–1.2	medium 1.7–4.0	Coarse 4.7–6.7	oversize various	
Soil Conventional	359,111	52	228,757	74,386	21,491	7970	615	26,507
BCL	40,693	17	1608	0	3101	24,102	261	11,621
Other	58,100							
Total	457,904							

Table 1.2: Compiled soil data (2016)—selected element frequencies and utility scores.

Element	Number of readings	Proportion of 458,000 samples (%)	Applied detection limit for routine exploration	Effective proportion (%) for routine exploration	
				Readings	Samples
Pb	388,300	85	10 ppm	98	83
Zn	328,000	72	25 ppm	100	72
Ag	278,000	61	0.5 ppm	84	51
As	193,000	42	5 ppm	99	41
Au	184,000	40	0.05 ppm	98	39
Cu	172,000	38	25 ppm	100	38
Bi	114,000	25	1 ppm	77	19
Mo	95,500	21	2 ppm	72	15
Sb	39,300	8.5	1 ppm	81	6.9
Tl	33,800	7.4	5 ppm	78	5.8
Sn	26,600	5.8	2 ppm	97	5.6
U	22,900	5	2 ppm	79	4.0
Pt	22,800	5	0.05 ppm	78	3.9
La	16,300	3.6	10 ppm	100	3.6
Lu	3200	0.7	2 ppm	100	0.7

Significantly, most of the Cu, Pb, Zn, Ag, As and Au data were acquired with sufficiently low detection limits to reveal common rock type background distributions and anomalous populations. This is shown in Table 1.2, which identifies the proportion of assays for each element that are reported with detection limits considered to be appropriate for reconnaissance level exploration. Thus, even if data levelling is not undertaken, individual survey data is, by and large, fit for prospect-scale, and in some cases, district-scale prospectivity reassessments. That said, the coverage is clearly dominated by Pb and Zn, reflecting the priorities of explorers in the 1960s and 1970s, whereas 'effective' readings for pathfinders, such as Bi, Sb and U, are available for less than 20% of the total data set (right-most column of Table 1.2).

Recommended soil sampling procedures and essential laboratory specifications for the recognition and mapping of distal expressions of ore systems, as gradients or halos in non-commodity elements (*i.e.*, pathfinders) are identified later in the chapter on page 13.

Rock chip samples

The northwest Queensland compilation contains 108,004 rock chip sample data points, most of which are located within the area shown as outcropping Proterozoic rock in Figure 1.2. The overall pattern of coverage is like that for soil samples (Figure 1.1), favouring long established areas of perceived mineral potential but with generally more spread at the scale of individual districts and prospect clusters.

The compilation is dominated by older base metal data acquired before the routine availability of multi-element ICP technology (represented by Fe and Mn in Table 1.3). Thus, more than 75% of all samples have Cu, Pb and Zn determinations whilst 'utility' pathfinders such as Bi, Mo, Sb, and U, are present in less than 20% of cases. Metallogenically specific metals such as Sn and Pt are strongly under-represented (<2%) and there are very few rare earth element data (REE), despite the availability of La (±Ce) in most ICP routines in the last 10 years. Gold is moderately represented (45%), of which 75% are accompanied by other elemental data other than just Cu (±Ag).

The rock chip data are comparatively free of misattributed units (*c.f.*, stream sediment data) and can be used for large area evaluations of a preliminary nature without the need for time

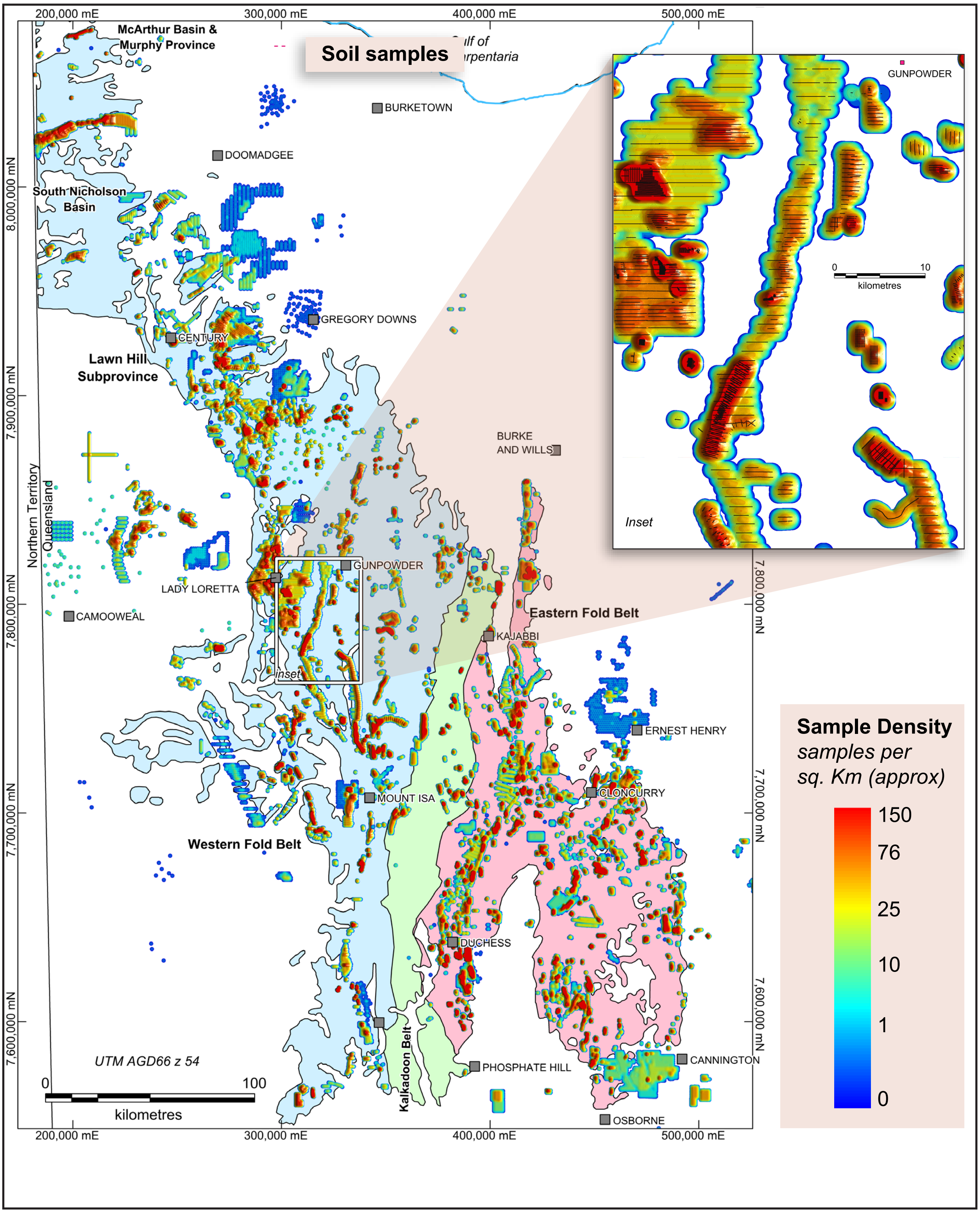

Figure 1.1. Image of gridded northwest Queensland soil sample distributions on a map of outcropping bedrock (Proterozoic, 500K scale); with inset to demonstrate relationship of colour gradients to sample line spacings and sample intervals (Gunpowder – Lady Loretta area).

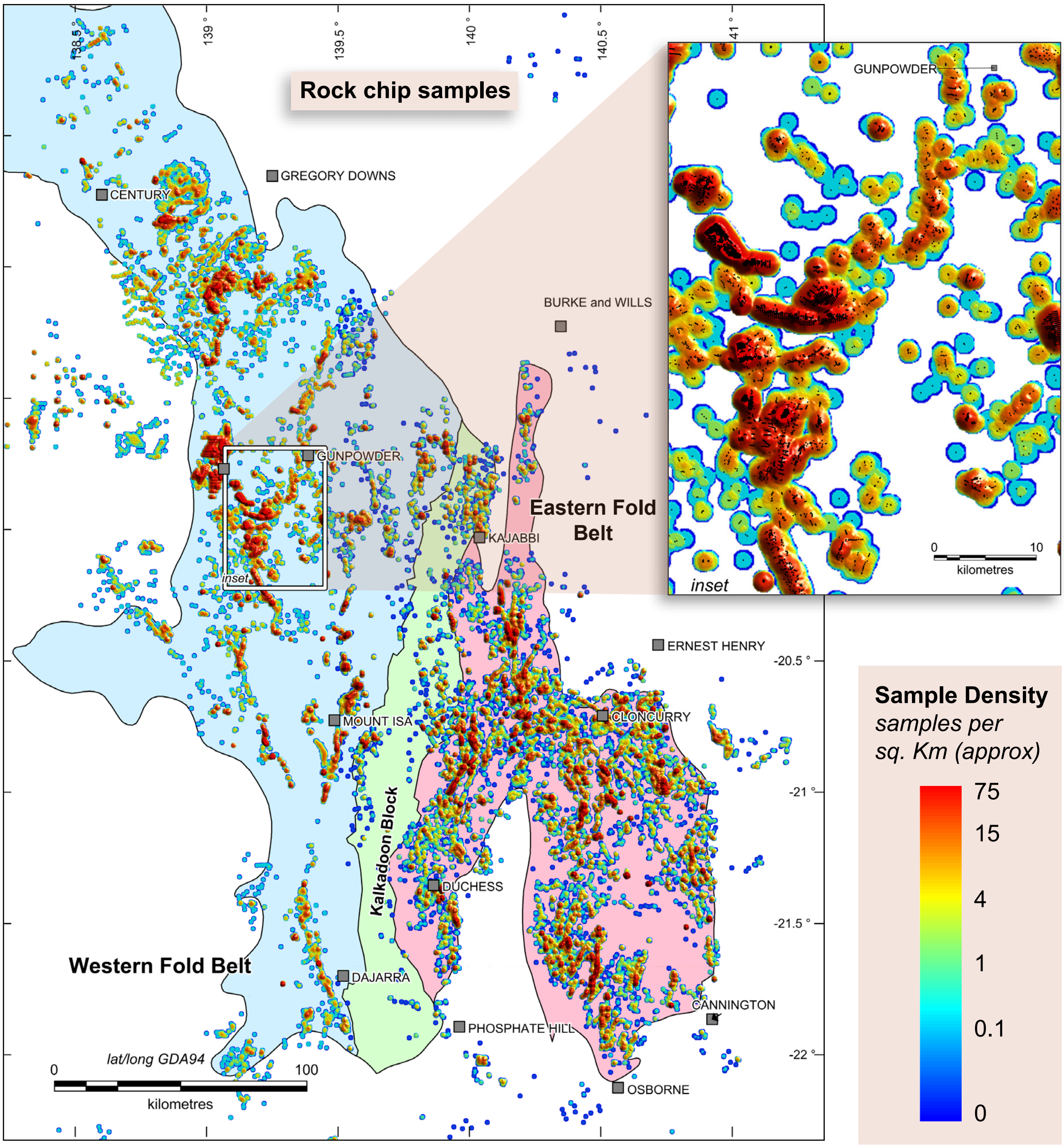

Figure 1.2. Image of gridded northwest Queensland rock chip sample distributions on a map of outcropping bedrock (Proterozoic, 500K scale); with inset to demonstrate relationship of colour gradients to sample line spacings and sample intervals (Gunpowder area).

consuming error checking or levelling. Significantly, most of the Cu, Pb, Zn, Ag, As and Au data were acquired with sufficiently low detection limits to be utilised in combinations for multi-element assessments of a reconnaissance nature. This is shown in Table 1.3, which identifies the proportion of assays for each element that are reported with detection limits considered necessary for reconnaissance level exploration (refer to 'reconnaissance' column). As an example of potential application, a simple gossan discriminant, described in Chapter 2 and referred to as the regional filter, is applied to the rock chip data to map chemically anomalous outcrop, as single channel factor, for comparison with soil Cu at district scale in Figure 1.3.

Table 1.3 also identifies the proportion of assays for each element that were analysed with detection limits more likely to permit the recognition of single metal gradients and weak or distal expressions of mineralisation at varying scales of enquiry. Importantly, only those mineralogically "tricky" elements accumulated by explorers since the earliest days of geochemical exploration are significantly affected by the tightened sensitivity band *i.e.*, Ag, Pb,

Table 1.3: Compiled rock chip (2016)—selected element frequencies and utility scores.

Element	Number of readings	Proportion (of 108,000) %	Reconnaissance		Optimised proportion	
			DL (ppm) maximum	% effective	DL (ppm) maximum	% effective
Cu	94,200	87	25	100	5	97
Zn	83,300	77	25	100	5	99
Pb	81,800	76	10	98	2	78
Ag	59,400	55	0.5	83	0.2	40
Au	48,300	45	0.05	95	0.01	91
As	34,700	37	5	93	2	79
Mn	34,300	32	50	100	-	-
Fe	25,000	23	100	100	-	-
Mo	17,200	16	2	82	0.5	67
Bi	13,500	13	1	41	0.2	40
Sb	8800	8	1	57	0.2	53
U	7400	7	2	74	0.2	73
Tl	4364	4	5	68	1	64
Sn	4200	4	2	66	0.5	65
La	3012	3	10	98	2	95
Pt	520	0.5	0.05	99	0.01	96
Lu	272	0.3	2	100	0.2	95

DL = detection limit

As and Mo. By contrast, the relatively small number of data for trace elements and ‘pathfinders’ accumulated in recent years such as Bi, Sb, U, Tl, Sn, LREE and Pt complements the exploration campaigns. However, most of these ‘pathfinders’ are refractory elements which are dependent on analytical methodology for completeness of digestion, and it is important to subset data according to analytical methods. Obviously, *areas* of coverage by modern data (which often includes refractory elements such as Y, Nb, and Zr), and the nature of the digestion used, need to be taken into account when applying the data statistically or for lithogeochemical purposes.

To conclude, portions of the rock chip data compilation will be identifiable, with care, for comparison and integration with new data, both for outcrop and drill hole samples, that are acquired with a view to the detection and recognition of distal expressions of large, buried or blind mineral systems. Specific recommendations in this regard are provided in the next section on page 15.

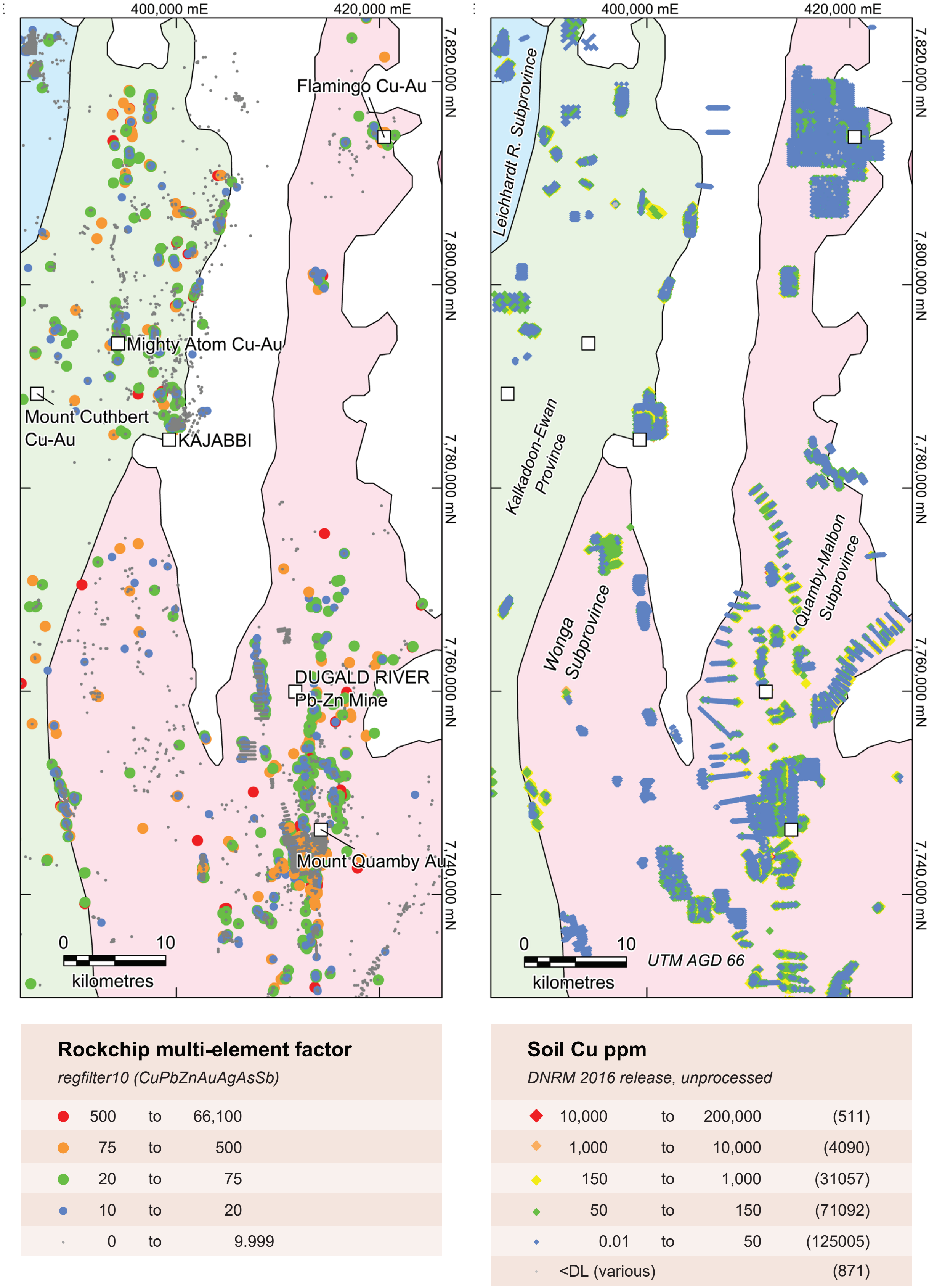

Rockchip multi-element factor

regfilter10 (CuPbZnAuAgAsSb)

●	500	to	66,100
●	75	to	500
●	20	to	75
●	10	to	20
·	0	to	9.999

Soil Cu ppm

DNRM 2016 release, unprocessed

◆	10,000	to	200,000	(511)
◆	1,000	to	10,000	(4090)
◆	150	to	1,000	(31057)
◆	50	to	150	(71092)
◆	0.01	to	50	(125005)
·	<DL (various)			(871)

Figure 1.3. Rock chip sample regfilter10 values (left frame) and soil sample Cu (right frame) for the northern part of the Eastern Fold Belt and Kalkadoon-Ewan Subprovince; labelled with selected prospects and mine sites; on background of outcropping bedrock (Proterozoic, 500K scale).

Stream sediment samples

The northwest Queensland compilation contains 207,000 stream sediment data points, of which 185,000 are located within the area shown as outcropping Proterozoic rock in Figure 1.4. As discussed for soil samples, the drainage sample data is heterogeneous, comprising varied sample sub-types (*e.g.* bulk, sieved, panned concentrates) and laboratory preparation-analytical protocols (*e.g.*, weak leach, aqua regia, BCL).

Clearly, stream sediment coverage is almost comprehensive (Figure 1.4), particularly of rock units and districts traditionally regarded as prospective. For repeatedly explored localities and districts, extreme sample densities of more than 25 per square kilometre are common (*e.g.*, inset frame, Figure 1.4). Peripheral areas that remain unsampled either lack sufficient topographic relief for the method or have onlapping Tertiary or Cambrian sedimentary cover. 'Internal' areas without recorded sampling include: northern blocks of the Haslingden Group (WFB), remnants of Tertiary cover in the Lawn Hill Province (WFB), large areas of Ewen Granite and Leichhardt Volcanics in the infrequently explored Kalkadoon Belt, and parts of the Sybella Batholith and Squirrel Hills Granite (southern WFB and EFB, respectively).

Given the relative ease of accessibility of the region, it is fair to say that the intensity of the historical stream sediment sampling was excessive and comparatively ineffective—all significant and outcropping base metal deposits were discovered by visual inspection of exposures, rock chip sampling and/or soil sampling. Indeed, in the authors' knowledge, the only discovery that can be directly attributed to the recognition of a stream sediment chemical anomaly is that of the Tick Hill gold deposit by MIM Exploration in 1990.

What, then, of the utility of the compiled data or the relevance of the method for future exploration of the region?

Copper, lead and zinc

It is evident that the data for Cu, Pb and Zn are generally adequate, in terms of analytical sensitivity, for the identification of population backgrounds and geochemical anomalies. The issue is then one of judging if the influence of local factors, such as Cu signal reduction in drainages with carbonate-bearing rock types, or the need to normalise results for size fraction or strength of chemical digestion for large area assessments, has prevented the recognition of potentially significant and exposed base metal mineralisation.

Trace metals

In the case of other pathfinder metals, like Ag, Bi, As, Mo, Sb, Cd, Tl, and U, much of the older data is the product of comparatively insensitive instrumentation and detection limits above the abundances typically encountered in alluvium (*viz*., DLs of 1–10 ppm or more, for backgrounds of less than 1 ppm). Even today, the commonly available ICP-OES routines are simply too insensitive to produce informative trace element assays for samples of alluvium. The problem is illustrated in the maps of Figure 1.5, where the abundance distributions of Ag and Bi display discontinuities corresponding to surveys with varying analytical detection limits (mostly inadequate) and, to a lesser extent, sample mesh. There are also legacy data errors related to misreported units *e.g.*, most of the Ag values more than 2 ppm and probably all the Bi data above 2 ppm require factoring by 0.001. In short, the multi-element data of the compiled stream sediment data are of little use to the explorer seeking to discriminate styles of mineralisation or even recognise dispersion patterns from point sources.

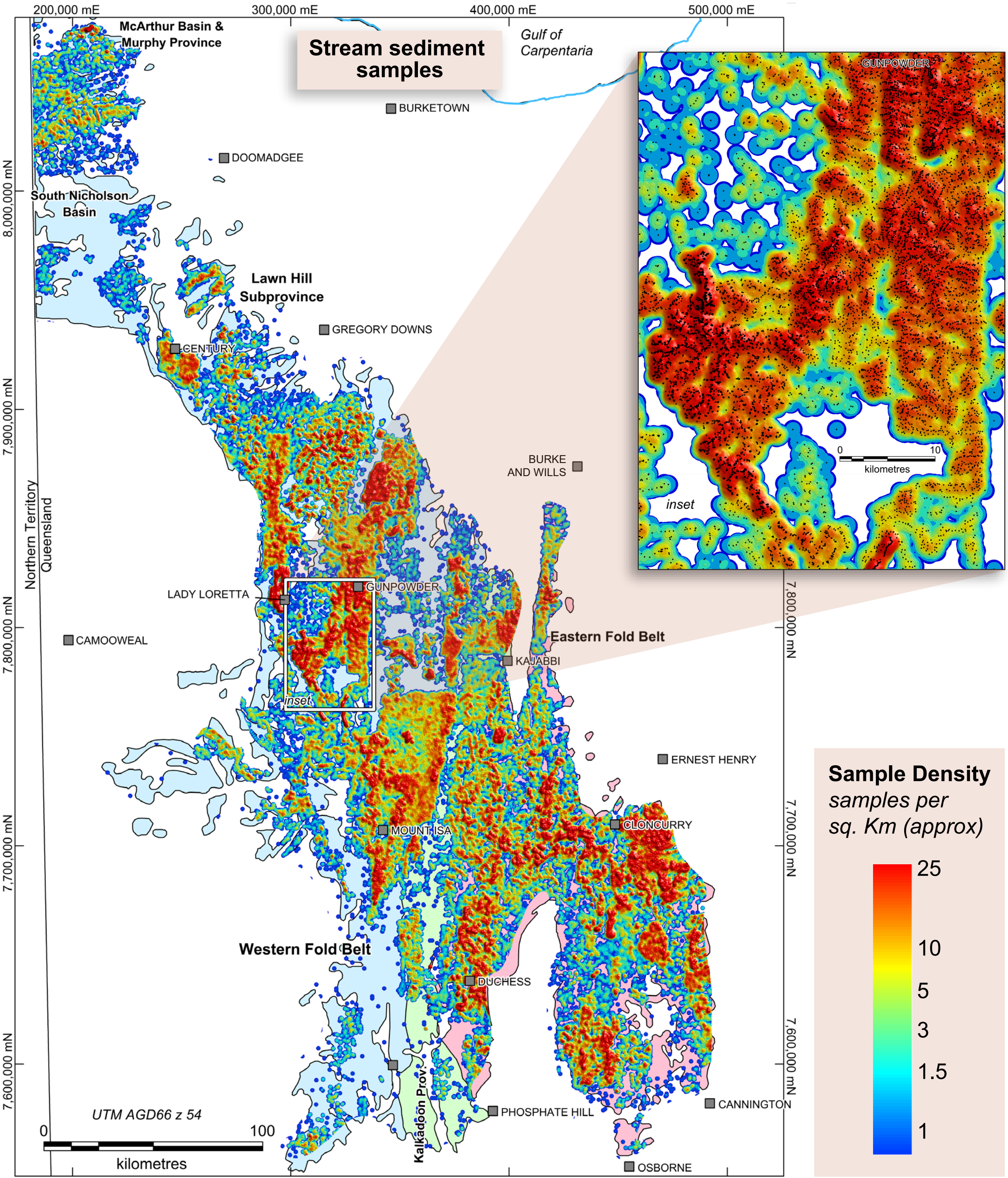

Figure 1.4. Image of gridded northwest Queensland stream sediment sample distributions clipped to areas of outcropping bedrock (Proterozoic, 500K scale); with inset to demonstrate relationship of colour gradients to sample line spacings and sample intervals (Gunpowder area).

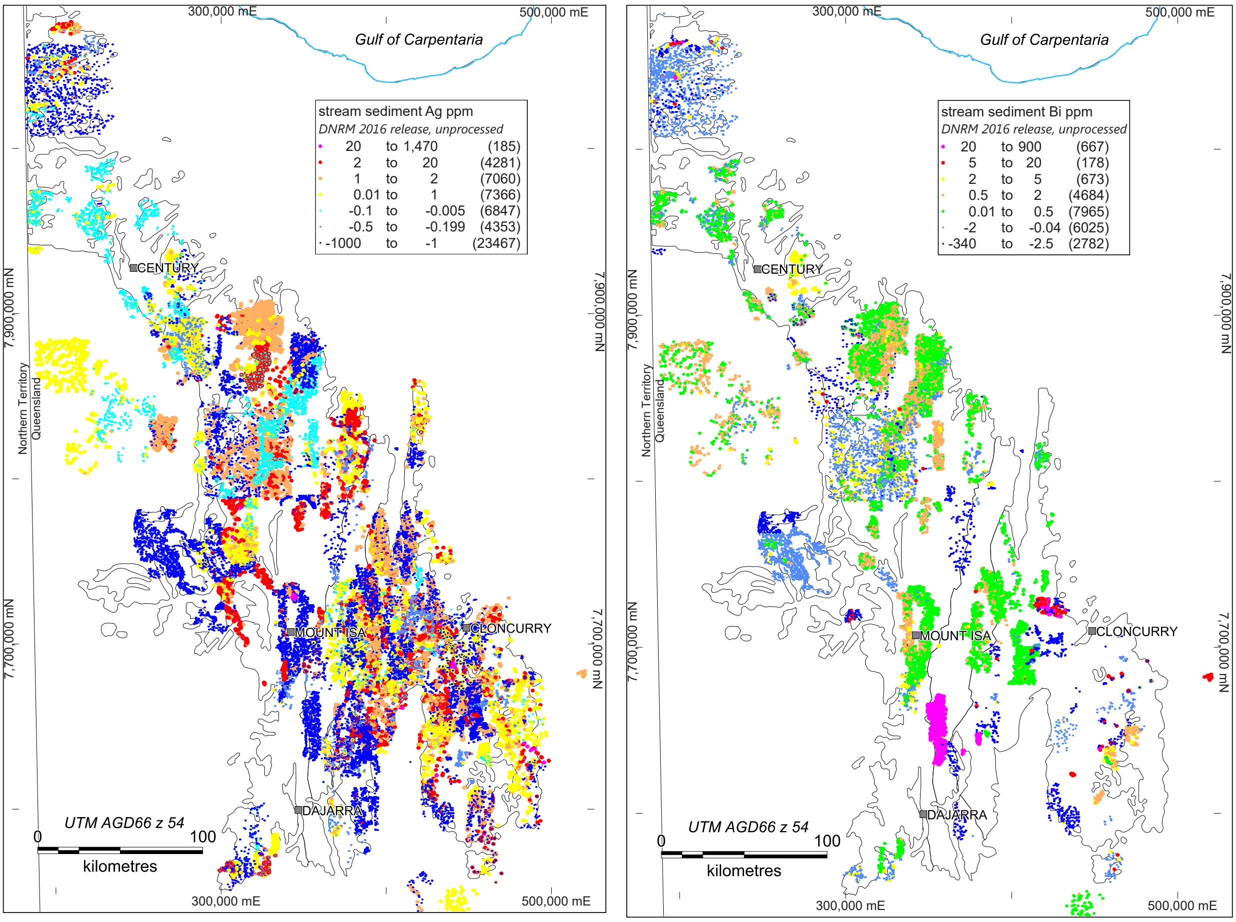

Figure 1.5. Ag and Bi abundances in stream sediment samples of the northwest Queensland compilation, coloured to show the predominance of < DL results and illustrate the very limited utility of compiled multi-element data (background map of outcropping Proterozoic, 500K scale).

Gold

The distribution of compiled stream sediment Au analyses is mapped as unprocessed point data in Figure 1.6 in relation to the grey-scale version of the cumulative sample density grid (as for Figure 1.4). It shows minimal drainage Au coverage for most of the Lawn Hill Subprovince and large areas of the central north and southern Western Fold Belt and Kalkadoon subprovinces. Some low relief and/or granitic areas of the Eastern Fold Belt also lack recorded sampling.

As discussed for pathfinder metals, much of the oldest data is compromised by historically elevated DLs. Most of the data within the <DL bin (dark blue points, Figure 1.6) are sub-5, 10, 50 and even 100 ppb results. Areas uniquely populated by such data are inadequately tested for drainage Au. Legacy data errors are also present, with most results above 25 ppb found, upon cross laboratory method details, to be mis-factored by 1000 (red and magenta points of Figure 1.6).

Nevertheless, some 45,000 of the 65,000 Au data points have Au values between 0.05 and 25 ppb and can be treated as fit-for-purpose with due care. Levelling to sample mesh and major classes of digestion (*e.g.*, BCL v aqua regia) is therefore possible and may reveal otherwise obscure trends and patterns for further investigation. An example is provided in Figure 1.7, which compares unprocessed and levelled Au stream sediment data for the northern part of the Eastern Fold Belt at the metallogenically complex intersection of the Wonga, Quamby-Malbon and Kalkadoon subprovinces (noting, with the example of the Dugald River Zn-Pb deposit, the minimal open file data for the vicinity of mine sites and long-held Mining Leases).

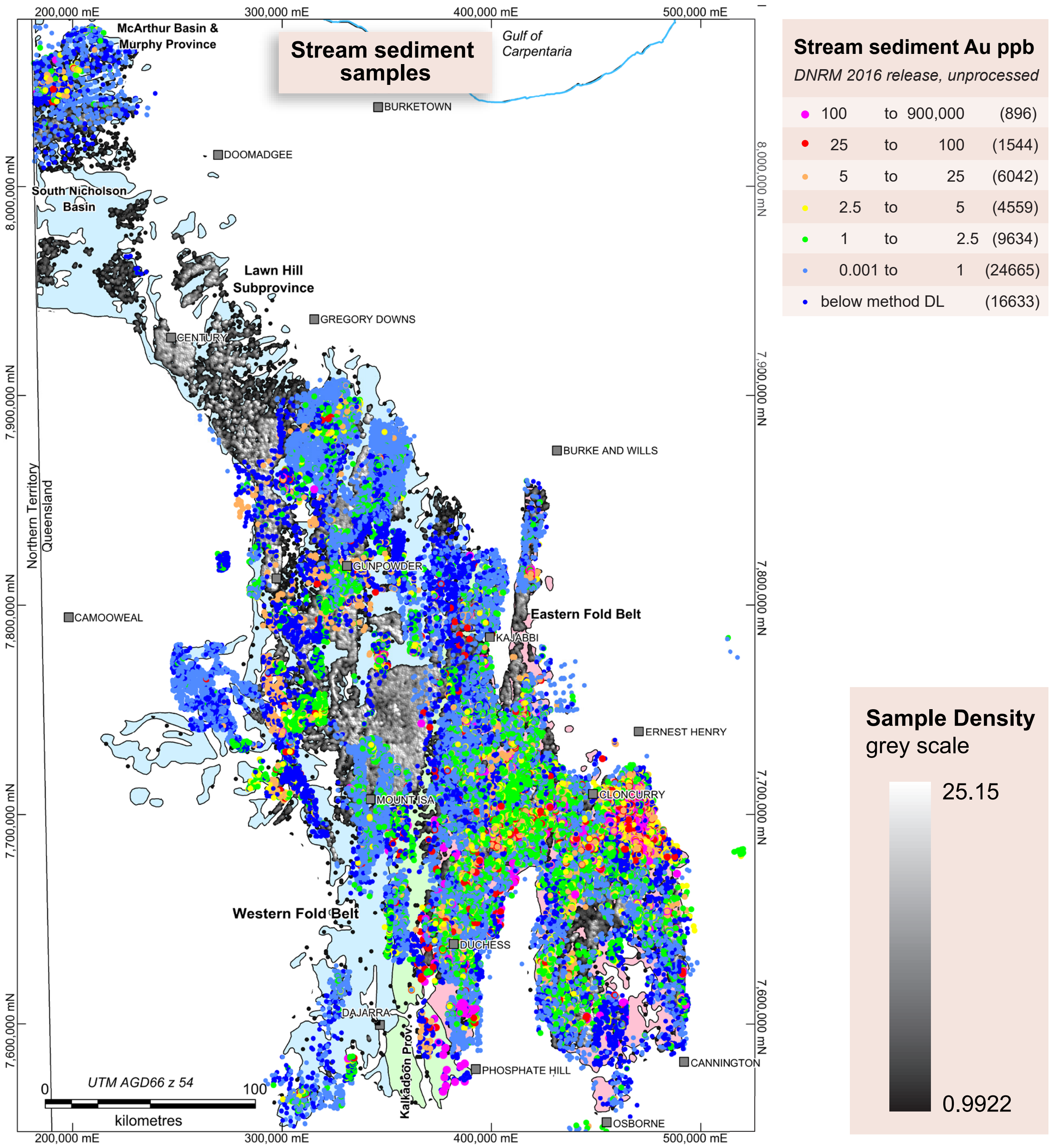

Figure 1.6. Gold abundances of northwest Queensland stream sediment samples distributions as unprocessed point data, with backdrop of gridded sample density (grey-scale equivalent of Figure 4 grid) clipped to areas of outcropping bedrock (Proterozoic, 500K scale).

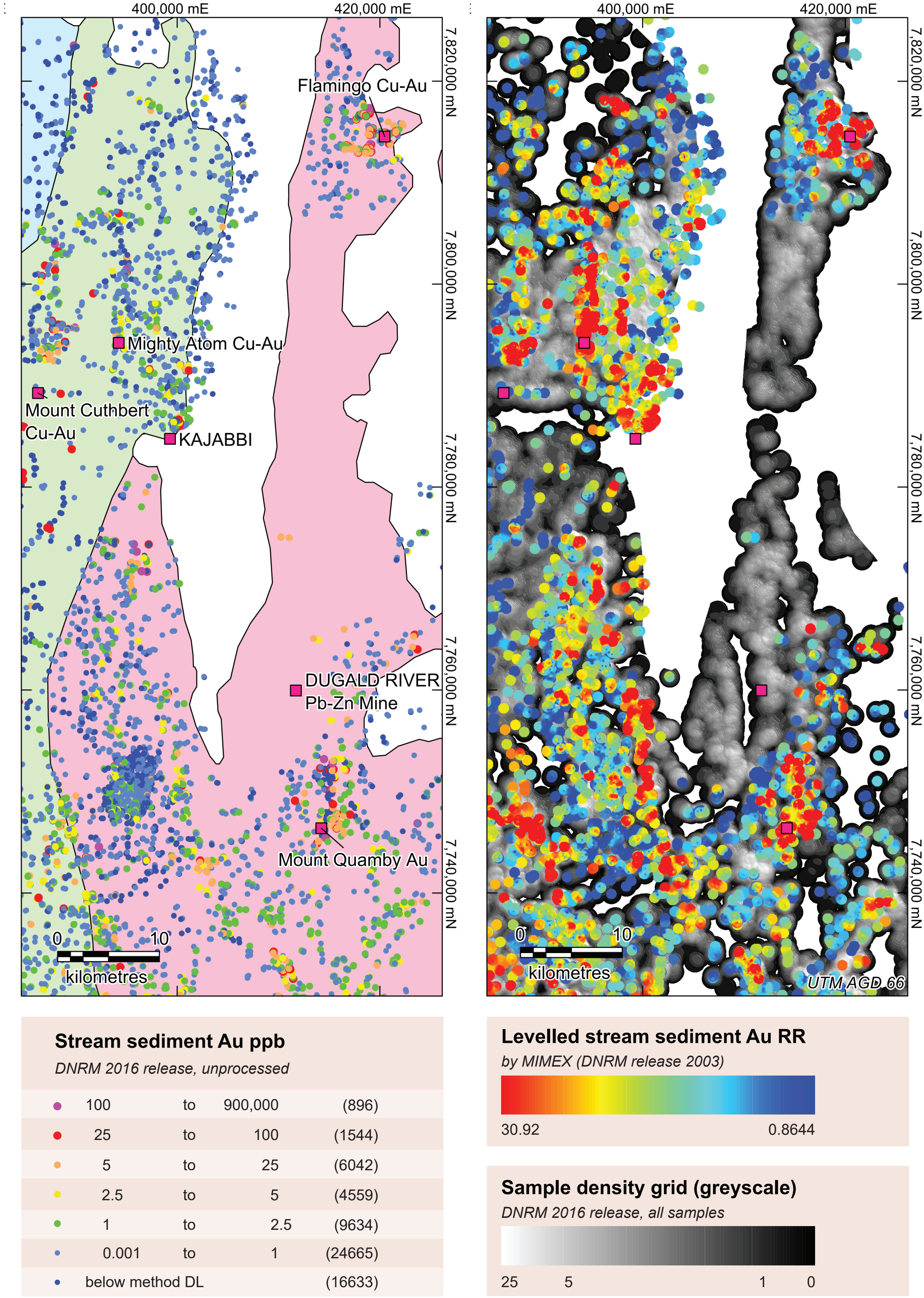

Figure 1.7. Unprocessed Au (left frame) and levelled Au (right frame) in stream sediment samples of the northern part of the Eastern Fold Belt and Kalkadoon-Ewan Subprovince; labelled with significant Au prospects and/or historical production sites.

Optimising future geochemical practice in the outcrop domain

Conventional soil geochemistry

Preamble

There is some potential for the astute explorer to leverage the existing historical compilation by either re-evaluating carefully levelled data or identifying areas of low quality coverage for locating "missed" opportunities at near surface. However, the greatest opportunity lies in the reinvestigation of entire districts for signs of buried or blind economic mineralisation through the mapping of pathfinder metal gradients and taking advantage of the cumulative advances in analytical geochemistry. The focus of this chapter is therefore on the acquisition of high quality data from low sample-density grids, for both trace-metal distribution mapping and improved alignment with rock multi-element data (gossan, rock chip and drill holes).

Recommended laboratory analytical schema

Digestion by aqua regia

Aqua regia is an effective solvent for most of the secondary minerals and organic compounds that develop in soil and regolith in response to rock weathering. Thus, the metal content of sulphates, sulphides, oxides, sesquioxides, carbonates and native metals, including gold, is almost quantitatively accessible to aqua regia (typically, a 3:1 mixture hydrochloric and nitric acid). The unavailable portion, locked within residual silicates and resistate minerals (*e.g.*, magnetite) can generally be safely disregarded, based on a wealth of comparative data showing that metal assays by aqua regia are very rarely more than 20% less than those by hydrofluoric acid-assisted digestions or X-ray fluorescence (XRF).

Though not suitable for *quantitative* lithogeochemical characterisation, the aqua regia method, with sample weights of 25–50 g, is robust and produces precise analytical data. Therefore, the partial yields of the major elements and traces such as the light rare earths (LREE) and Y, can be used to chemically map rock type and alteration assemblage distributions from spatially discrete data sets (*e.g.*, individual soil sample and RAB drill hole grids).

Four acids digestion

The four acids digest is the most cost-effective commercial method for the near-total dissolution of silicates and oxides. By using a combination of hydrochloric, nitric, hydrofluoric and perchloric acids even the most refractory minerals are at least partly dissolved; the resulting data are therefore generally adequate for lithogeochemical and petrogenetic characterisation. This digestion is required for Sn, W, Nb, Ta, Cr, Ti, Y, Hf, Re, U and rare earths, and up to 50 elements are commonly available in standardised packages.

Measurement by ICP

Elemental measurement by ICP Optical Emission Spectroscopy (ICP-OES) is sufficient for most elements, but the enhanced sensitivity and lower detections limits provided by mass spectrometry (ICP-MS) is required for metallogenically informative metals such as Ag, Bi, Cd, Mo, Sb, Tl, U, and W). Above all, ICP-MS offers the advantage of improved analytical resolution without the complication of overlapping spectra. A separate digestion for Au (and platinoids), by aqua regia or fire assay, is generally needed for the high degree of resolution required for most exploration campaigns (*i.e.*, a detection limit of less than 5 ppb). Although some laboratories offer variants of aqua regia routines to provide high resolution Au and path finder metals under one method code, care is required to ensure that major elements such as Fe, K and Mn, and abundant metals like Cu, Pb and Zn remain resolvable (*i.e.*, have stated upper DLs).

This analytical schema is identical to the minimal cost option recommended for gossans and strongly weathered rock in outcrop (this volume). The resulting data is of sufficient quality and sensitivity to be used for single element anomaly mapping and discriminants such Regfilter10 (refer to Chapter 2, *Discrimination of gossans and ironstones*).

Recommended field sampling procedures

At the intended sample site, clear an area of about 0.5 x 0.5 m of surface debris and remove the upper 10 cm of regolith. Then, loosen the regolith over an area of 0.3 x 0.3 m within the primary excavation to a depth of about 25 cm and process through a 5 mm sieve (plastic, aluminium or stainless steel). Bag 1.5–2 kg of the sieved material for laboratory preparation and analysis (pulverisation, splitting and chemical analysis, as described, above). A slightly larger area of excavation may be needed for regolith dominated by very coarse fragments or lag.

A relatively large area and consistent depth and thickness of excavation enhances sample site representability and sampling precision (repeatability). These sampling steps are also applicable to soil grids in the covered domain, where weaker chemical reagents, loosely referred to as ‘selective extraction’ or ‘selex’ methods, target material at the root zone of grasses and the interval of evaporative accumulation (Chapter 5).

A systematic approach to sample site selection, description and/or photography is also encouraged to support data interpretation. Table 1.4 lists the essential *non-geologic* parameters, and their common variants, that account for most sample site settings in areas of exposed Proterozoic bedrock in the Mount Isa region.

Table 1.4: Essential soil sample site parameters (non-geologic)

Site parameter	Options
Landscape	*general setting of sample site in the landscape* ridge or crest, upper/mid/lower slope, erosional plain, swale or valley floor
Regolith class	*nature of exposure* fresh rock/saprock/saprolite; continuous/patchy/sparse
Soil class	*nature of sampled regolith (soil), in broad terms* “black soil”, clay, loam, silt, sandy, stony; % alluvium/colluvium/lag/pisoliths
Soil colour	*common variants* red, brown, grey (pale-, mid-, or dark); secondary colour if mottled or variegated
Vegetation cover	*ground covered for 10 m radius centred on sample site; % tree canopy where present* *e.g.,* 30% bare, else spinifex, grass, scrub (for 100%); 10% tree canopy
Interference	*Human activity-related influences—comment* *e.g.*, refuse, dam over flow, road, oil spill, stock pad; distance from sample site
Soil pH	*Required for surveys using leachant or soil-gas methods*

Discussion

For the numerous samples typically associated with a soil survey, the recommended analytical procedure is comparatively expensive on a per sample basis. However, it is explicitly intended for a new generation of strategic sample grids, often over larger areas, and at greater sample and line spacings, than those typically designed for prospect-scale and post-discovery investigations.

The rationale for the sub-5mm fraction, rather than a finely sieved fraction (*e.g.*, -80#/<0.18 mm, which seems to be the industry default), is the capture of as many lithic fragments as possible. By doing so, the proportion of fines is reduced and thereby the effects of metals segregation by weathering and/or signal dilution by aeolian fine sand and silt are also reduced (relevant to southern parts of the region). More discussion and alternatives can be sought in the literature (*e.g.*, Rose *et al.*, 1979, Butt *et al.*, 2005), but the over-riding imperative is that individual explorers maintain consistent and transparently recorded sampling practices and fully utilise ICP-MS.

For Au-focussed explorers, the precision-enhancing advantage of large volume soil sampling for analysis by bulk cyanide leach (BCL) still applies, but fewer labs now offer the service due to environmental restrictions. Where available, sample size limits and cyanide disposal costs increasingly apply (*i.e.*, the day of 5 or 10 kg sample BCL soils surveys is long past). Significantly, the sampling procedure, described herein, is essentially the same as that for ‘modern’ BCL sampling (1–3 kg of regolith sieved to less than 2 or 5mm). Therefore, provided industry standard pulverisation and subsampling practices are followed, the recommended procedure replicates the large sample volume quality of the BCL methodology for Au.

Rock chip geochemistry

A consistent theme of this document is the acquisition of rock chemical data suitable for the detection and identification of subtle, weak, and by potential implication, distal expressions of blind or buried mineralisation with economic potential. Today, with the widespread availability of ICP-MS and other high resolution chemical instrumentation, the exploration industry can contribute to the growth of a strategic geochemical data resource that is fit for this challenge.

Therefore, it is recommended that explorers build into their future rock chip sampling activities a component of high resolution data acquisition for key trace elements, especially those conventionally referred to as chalcophiles or ‘pathfinders’. A list is provided in Table 1.5; it is not optimised for lithogeochemical characterisation but includes Li and Co to accommodate niche commodities relevant to the Mount Isa region, and Ba as a non-trace indicator for a wide range of mineralisation types. Modern laboratories offer competitive packages for the analysis of multiple elements at ultra-low limits of detection.

Three scenarios are envisaged where rock chip sampling can be optimised for strategic data acquisition. Each is paired with at least one of the lab schemas listed in Table 1.5 (which are also appropriate for drill hole samples):

1. Standard, or routine, reconnaissance-type sampling where the material sampled is comparatively unweathered (fresh rock or saprock) and weakly mineralised at most (*i.e.*, < 2–5%, by volume, of visible sulfide or its pseudomorphs).

   These conditions are suitable for metallogenic fingerprinting and, where needed, lithogeochemical characterisation; at key or selected sites use lab schema 1 for an acceptable degree of control of both parameters, or schema 2 for optimised fingerprinting, or schema 3 for optimal wholerock chemical and acceptable fingerprinting information (this schema includes the commonly available lithium metaborate flux/fused disc wholerock variant by which major elements are measured by ICP-MS rather than XRF).

2. Standard, or routine, reconnaissance-type sampling where the material sampled is comprehensively weathered and weakly mineralised at most (*i.e.*, < 2–5%, by volume, of former sulfide)

   Not suitable for lithogeochemistry, but O.K. for fingerprinting; at key or selected sites use lab schema 2.

3. Gossan sampling or known prospect sampling, *viz*., strongly weathered rock with evidence of moderate to strong mineralisation (*i.e.*, nominally more than 5%, by volume, of evidence of former sulfide)

   Not suitable for lithogeochemistry, but ideal for fingerprinting; at key or selected sites use lab schema 2.

Table 1.5: Recommended laboratory methods for optimised rock chip sampling

Element	Required DL	MS needed	Schema 1 HF-assisted digestion	Schema 2 Aqua Regia digestion	Schema 3 Fusion/XRF
			Comment	Comment	Comment
Ag	0.05	yes			
Au	0.005		Aqua Regia or Fire		Aqua Regia or Fire
As	1	yes			
Ba	10		semi-quantitative	non-quantitative	reported as BaO
Bi	0.1	yes			
Co	1				
La	1	yes	represents light REE	semi-quantitative	represents LREE
Li	10			semi-quantitative	
Lu	0.2	yes	represents heavy REE	semi-quantitative	represents HREE
Mo	0.2	yes		can be semi-Q	
S	1000				reported as SO_3
Sb	0.2	yes			
Sn	0.5	yes		semi-quantitative	
Tl	0.5	yes			
Pt	0.005		Aqua Regia or Fire	represents platinoids	Aqua Regia or Fire
U	0.5	yes			
W	0.5	yes		semi-quantitative	
majors	-		-	semi-quantitative	+ LOI

Stream sediment geochemistry

As discussed in the overview section, areas of exposed Proterozoic bedrock in the Mount Isa region traditionally regarded as prospective have been intensively stream sediment sampled. Despite the variability of data quality and the need for levelling to obtain coherent views of large-scale element distributions, re-sampling is unlikely to lead to the identification of previously missed exposed and significant mineralisation. Therefore, future sampling should be confined to areas without historical coverage, *unless* the search is for previously untested commodities such as Sn, the platinoids, REE, and perhaps Ni—*i.e.*, in circumstances where the inherent advantage of drainage geochemistry for broad-area reconnaissance can be exercised. Even so, well planned rock chip and soil sampling is likely to produce more definitive outcomes, at little extra cost, given the favourable accessibility of the region.

Recommended laboratory analytical schema

Digestion by aqua regia

- refer to the equivalent paragraph of the *Soil sampling geochemistry* sub-section (page 13).

Measurement

- by ICP for most metals and pathfinder elements (as per *Soil sampling geochemistry* sub-section);
- optimal detection limits are required for Au, Ag and platinoids (preferably 0.5 ppb or lower) which are easily achieved for 25 or 50 g samples by aqua regia digestion, or 1–3 kg samples by bulk cyanide leaching (BCL).

Recommended field sampling procedures

The following suggestions are based on field experience in a wide range of physiographic settings and specific familiarity with the Mount Isa region. More discussion and alternatives can be sought in the literature (*e.g.*, Rose *et al.*, 1979, Butt *et al.*, 2005, Marjoribanks, 2010).

List of essential procedures for future stream sediment sampling:

- choose sample sites in the upstream half of longitudinal mid-channel or lateral gravel bars
- remove upper cobbles (‘lag’) and excavate over an area of about 0.4 x 0.4 m
- sieve material from a depth interval of 15–30 cm
- if precious metals (Au and Pt) are not required, sieve about 0.5–1 kg of -80 mesh material and sub-sample 50 g for the lab
- if precious metals are required, then in addition to a -80 mesh sample, either:
  a) sieve about 10 kg of -5 mm material and sub-sample about 2 kg for the lab (for BCL Au ±Ag, Cu, Pt, Mo, Bi etc.); or
  b) if logistically manageable, wet sieve about 0.2–0.5 kg of -200 mesh material and sub-sample 50–100 g for the lab.

Surface geochemistry by field portable XRF (fpXRF)

During the last 10 years, the analytical sensitivity and stability of portable X-ray Fluorescence instrumentation have improved to such a degree that the handheld instruments are now in common use in several industries, including the mining and mineral exploration sectors.

The instruments are fundamentally suited to the transition metals, especially Fe and Mn and the commodity base metals Cu, Zn and Pb (in order of decreasing sensitivity). Spot readings of fine-grained and dry media, such as soil and reverse circulation (RC) drill spoil are demonstrably precise for many elements and almost quantitative for some (well calibrated instruments). For optimal results, samples should be prepared and analysed using a consistent methodology. The best results are achieved on finely sieved samples using constant instrumental settings and run-times.

Therefore, with appropriate care, *fp*XRF can be used with confidence to:

- map base metal distributions, at varied scales of investigation, with similar effect to conventional sampling and laboratory analytical practice (illustrated by Figure 1.8)
- provide real time and indicative metal abundance measures for reconnaissance campaigns (soils and rocks)
- improve the efficiency of conventional sampling programs, especially in remote regions, by real-time scout analysis of soils, rocks, and alluvium.

Under conditions stipulated in the JORC Code (2012), fpXRF data is now acceptable for the public reporting of exploration results and resource estimates for appropriate commodities.

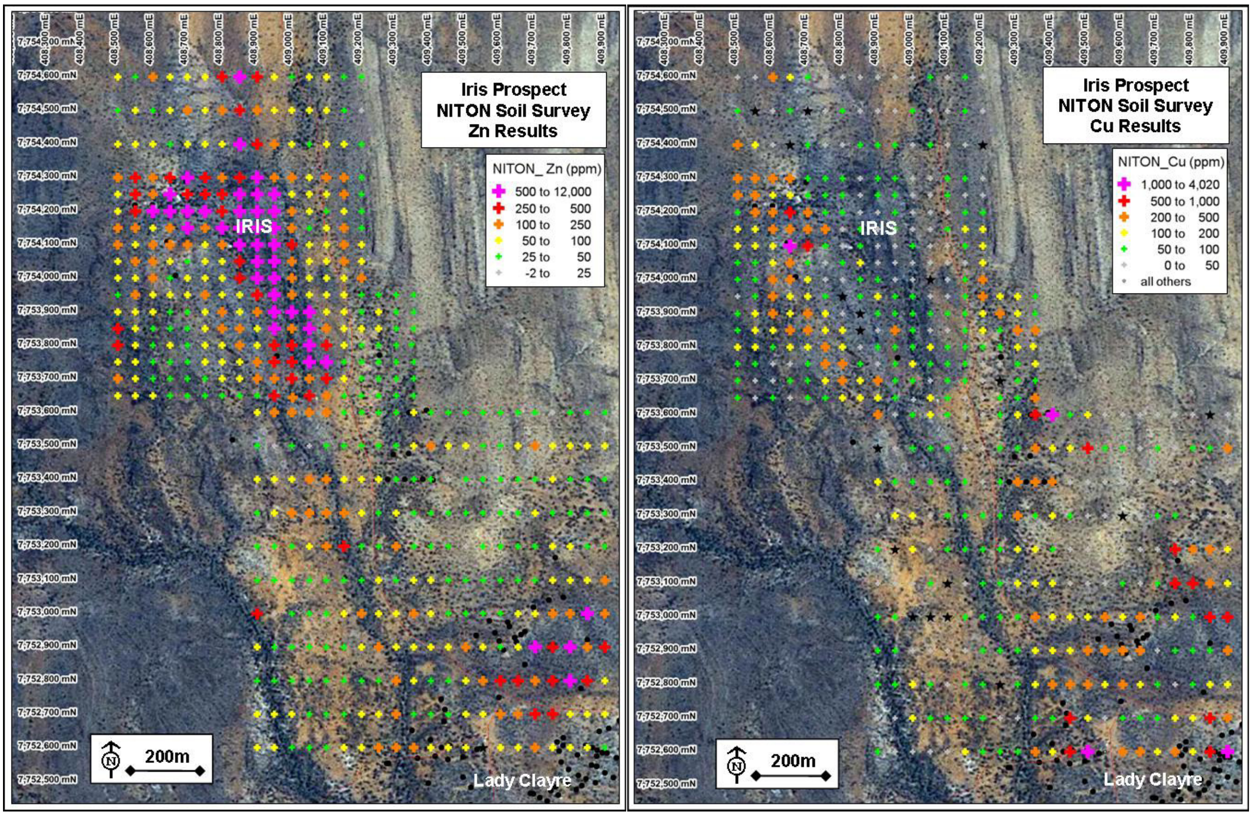

Figure 1.8. Soil geochemical grid in the Cloncurry region by fpXRF (Xstrata Copper Ltd, 2011); Zn left frame, Cu right; coherent Zn anomaly and Cu-Zn zonation revealed by spot readings of bootheel-tamped regolith amongst patchy low outcrop of Knapdale Quartzite and Corella Formation (SSW of Dugald River mine).

For detailed consideration of data quality, suitability for JORC reporting, instrumentation characteristics, field application and case studies the reader is referred to: a) Gazely & Fisher (2014), b) documents under the Seminar Presentations menu of the website of the Australian Institute of Geoscientists (November 2015) and c) the recent Mount Isa region case study by Gazely *et al.* (2017).

Chapter 2

Discrimination of gossans and ironstones

Overview

Chemical analyses, in the form of simple multi-element discriminants, can be used to distinguish gossan from weathered material with a sulphide-poor or sulphide-free precursor.

The first discriminant, termed the “regional filter”, is defined as:

$$\text{RegFilter}\mathit{10} = (\text{Cu+Zn+Pb})/150 + \text{As}/50 + (\text{Sb+Au})/15 + \text{Ag}/2$$

(for threshold value of 10)

This discriminant highlights weathered materials that developed from a broad range of mineralisation styles (sediment-hosted Pb-Zn and Cu-Pb-Zn, and shear-hosted Cu and Iron Oxide Cu-Au mineralisation). The filter is adaptable and its applicability probably extends beyond the Mount Isa region. For example, the addition of W/5 to the calculation accommodates the distinctive magnetite-hosted Au-Cu mineralisation of the Selwyn area without affecting the discrimination results for other mineralisation types.

The second discriminant, termed the “Isa filter” is defined as:

$$\text{IsaFilter}\mathit{10} = (\text{Cu+Pb})/200 + \text{As}/50 + (\text{Sb+Au})/20 + \text{Ag}/2$$

(for threshold value of 10)

This discriminant excludes Zn, and is useful for rock units where extensive pyrite and low-level Zn mineralisation, such as that in the Mount Isa district, produces numerous distracting signals as measured by the “regional filter”.

The discriminants provide a measure of the likelihood that a specific sample of weathered outcrop developed from a mineralised and/or sulphidic precursor. The level of confidence in achieving a successful discrimination probably exceeds 90%, but individual discriminant ‘scores’ are *not quantitative* measures of sub-surface mineralisation potential.

Applicability to rock chip samples

In common with a single element assay, a discriminant score will only be as effective and representative of a given outcrop, or prospect, as the original sample is. Therefore, diligence is required in their application to rock and regolith data that lack supporting information about the material sampled and the sampling procedure and area of coverage. Recommended sampling tactics and analytical methods are provided for the acquisition and assessment of new project data.

Potential applicability to soil samples

The issue of representativeness is generally less critical for soil samples. Therefore, the discriminants could reveal previously unnoticed trends and metal associations in compilations of open-file, historical soil geochemical data.

General applicability

The filters apply to surficial, ferruginous materials in a spectrum from saprock, with clear relict litho-fabrics, through to massive hematite. They appear to be effective with silica- and/or clay-rich material, except in cases of compositional extreme (*e.g.*, silcrete or well-developed saprolite).

Refinement of the filters and wider applicability could be achieved with more data for gossans from Au-dominated systems and the availability of high-resolution data for trace metals such as Bi and Sn. The interrogation of national datasets, including those of CRC-LEME and state governments, could facilitate specific adjustments for application of the filters to other regions and metallogenic provinces.

Introduction

In the Mount Isa region, extended periods of weathering have produced widespread ferruginous assemblages dominated by iron and manganese oxides, clay, carbonate minerals and silica, in a range of morphologies and landscape settings that can challenge the interpretative skills of the most experienced of mineral explorers. Many different types, irrespective of setting or mode of formation, have been shown to contain metals or 'pathfinder elements' from mineralisation (Anand, 2016; Anand *et al.*, 2002), and therefore continue to be favoured sample media, particularly for broad area reconnaissance ('greenfields' investigations).

In the special case where sulphide mineralisation is exposed by erosion, the process of weathering is intensified by acid leaching to produce *gossan*. Gossans have bulk mineral assemblages like those of ironstone (*i.e.*, rich in Fe, Mn, Si, and Al), but are vertically zoned (Figure 2.1) and display greater compositional and textural variability over smaller areas and volumes, particularly if eroded. Beneath the leached cap (Figure 2.1), the gossan profile is characteristically associated with colour variability and the presence of a hydrous iron oxide-silica mineraloid termed limonite, both in massive habits and as boxworks with metal sulphates after original sulphide grains/masses (*e.g.*, Blanchard, 1968; Taylor, 2016). However, these features are not always present or easily seen in outcrop, where resistive hematite and quartz accumulates in the leached cap in response to Fe-Si flooding as the weathering profile advances and matures.

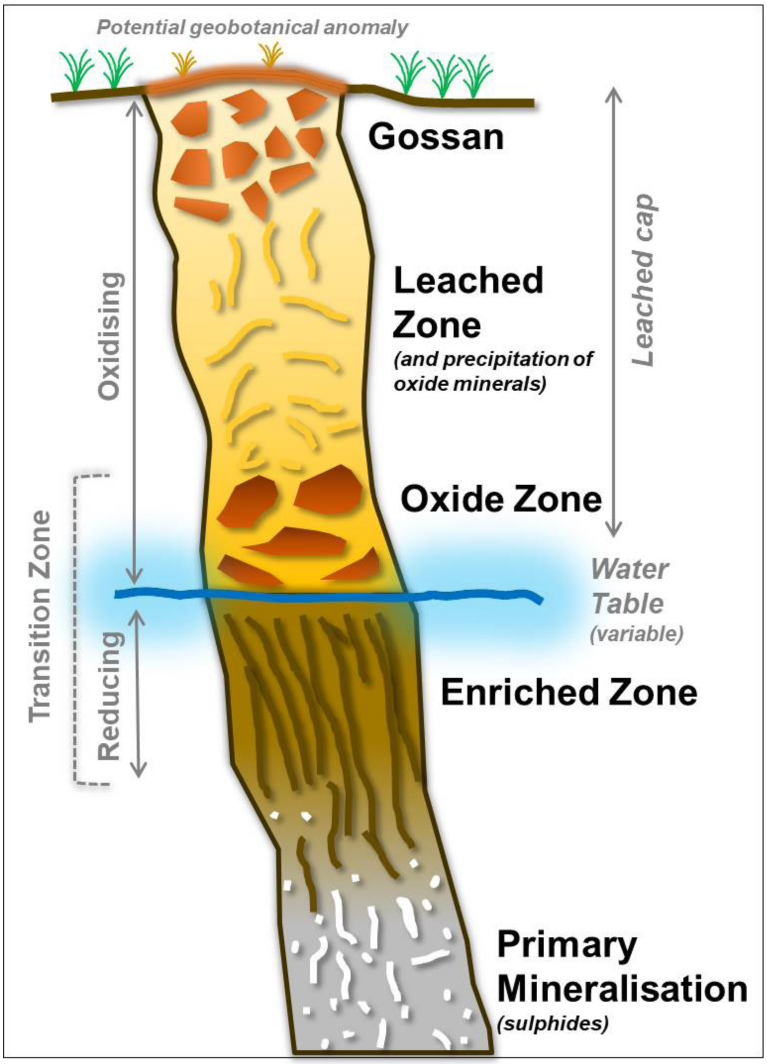

Figure 2.1. Schematic and idealised cross section of the internal structure of a gossan profile (after Taylor, 2016; Butt et al., 2005, Scott et al., 2002).

Ferruginous weathering products within bedrock, but not within or on primary mineralisation, are traditionally referred to as *ironstone*, and by some practitioners as ‘false gossan’. Bedrock ironstones recorded in the Mount Isa region include BIF, massive magnetite bands, oxidised pyritic sediments, and weathered mafic igneous and Fe-carbonate-bearing sedimentary rocks.

Other types of ferruginous materials present in the regolith of the Mount Isa region and shown to relate to their history of formation (Anand *et al.*, 2002), include:

- lateritic duricrusts, nodules and pisoliths
- ferruginous veins, along bedding planes and faults
- ferruginous bands, as water table-related redox fronts in saprolite and/or cover sediments
- ferricrete and seepage ironstones at breaks of slope, watercourses and swamps
- mottles in recent colluvial-alluvial cover.

Most have the potential, subject to location in the landscape and distance from source, to host or ‘accumulate’ metals derived from mineralisation, as generalised in Figure 2.2, and illustrated schematically for the area of the Lady Loretta Pb-Zn-Ag deposit in the Western Fold Belt (Figure 2.3).

The aim of this chapter, therefore, is to identify simple chemical criteria to recognise gossan, as distinct from variants of bedrock ironstone and other ferruginous materials not derived from mineralisation (mechanically or chemically). The chemical approach presented builds on the earlier findings and principles established by previous investigations, such as that for Mount Isa region Pb-Zn-Ag gossans and ironstones, by Taylor & Scott (1982), and the review work of Taylor & Thornber (1992). Whilst it is intended to instruct and encourage use in other regions and metallogenic settings, it should only complement, not supplant, practised field and mineralogic observation.

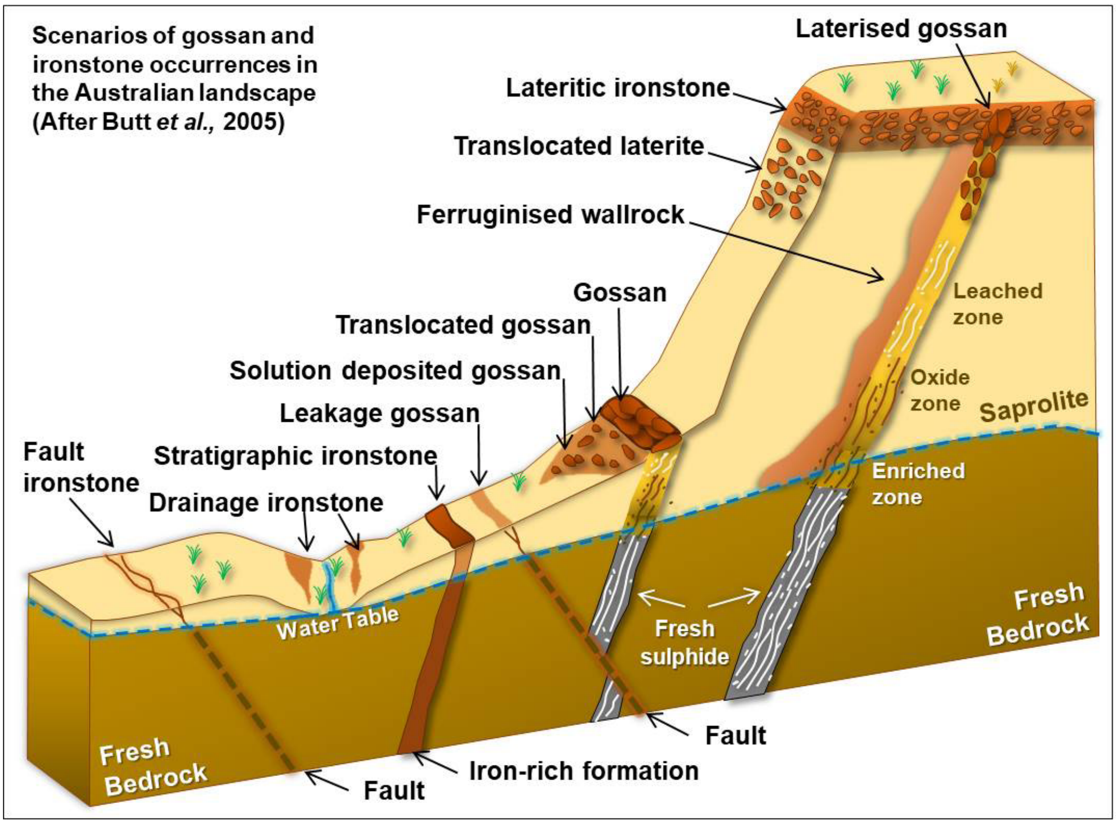

Figure 2.2. Scenarios of gossan and ironstone occurrences in the Australian landscape (modification of Butt et al., 2005).

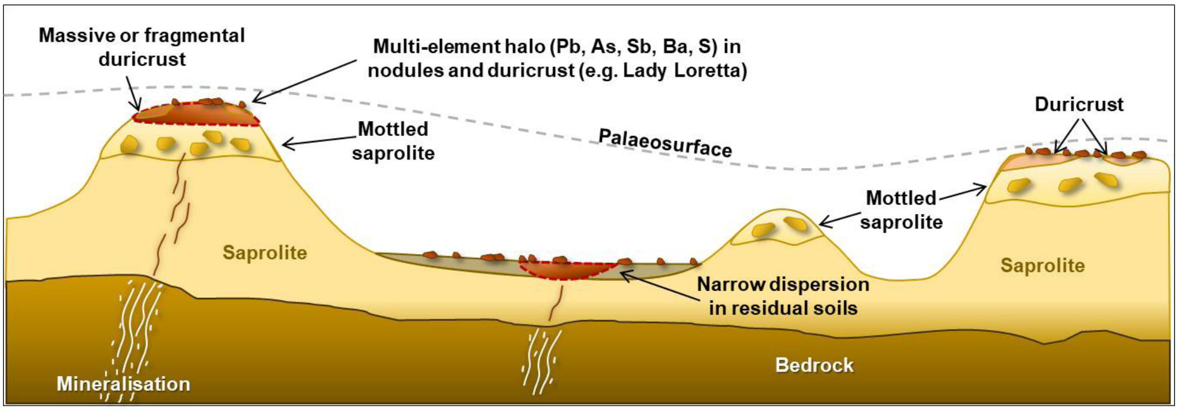

Figure 2.3. Schematic depiction of gossan and ironstone occurrences in a landscape setting typical of the Mount Isa Inlier (from Anand et al., 2002).

The chemical criteria are derived from an analysis of gossan and ironstone data for collections put together by MIM Exploration Ltd in the early 1990s and specified below.

Regional Gossan Collection

- Rationale—to establish a database of Mount Isa Inlier gossan analyses to assist with the recognition of mineralisation, and variants thereof, in strongly weathered and iron-rich outcrop
- assembled between April 1991 and September 1993
- samples collected by several geologists during routine field campaigns
- assays for 175 samples from 124 sites, primarily in the Western Succession (Figure 2.4)
- chemical analyses completed by AMDEL Laboratories of Adelaide (now Bureau Veritas)
- major elements by Li Borate fusion, ICP-OES (code IC4, LOI included)
- Ag, As, Bi, Co, Cr, Cu, Zn, and V by aqua regia digestion, ICP-OES (code IC2E)
- Sb, Bi, Ba, Y, Zr, and Nb by XRF (XRF3)
- Se, Te, Tl, Sn, W and U by 4 acid digestion, ICP-MS
- Au by aqua regia/AAS (dl=2ppb) or 50 g fire assay (dl=1 ppb)
- Pd and Pt by 50 g fire assay (FA3)
- S not analysed
- root data file is an excel spreadsheet named MimexGossan (supplied).

Mount Isa District Ironstone Collection

- Rationale—to sample all processed Fe anomalies as indicated by classification of satellite imagery (TM bands) covering the Mount Isa district
- assembled between July 1992 and September 1992
- samples from 69 sites (dark brown filled circles of Figure 2.5)
- assays for 102 samples from the 69 sites
- samples collected by BSc Honours student under supervision (K. Hannan, staff Project Geologist)
- chemical analyses completed by AMDEL Laboratories, Adelaide
- Ag, As, Ba, Bi, Cd, Co, Cu, Fe, Mn, Mo, Ni, Pb, Sb, Tl, V, Zn and Zr by 4 acid digestion, ICP-OES (unverified)
- Au by aqua regia/AAS (50 g, dl=20 ppb)
- original collection intact (Exploration Group of Glencore, Australia (Oban Rd., Mount Isa)
- root data file is an excel spreadsheet named IsaDistrictFestones (supplied).

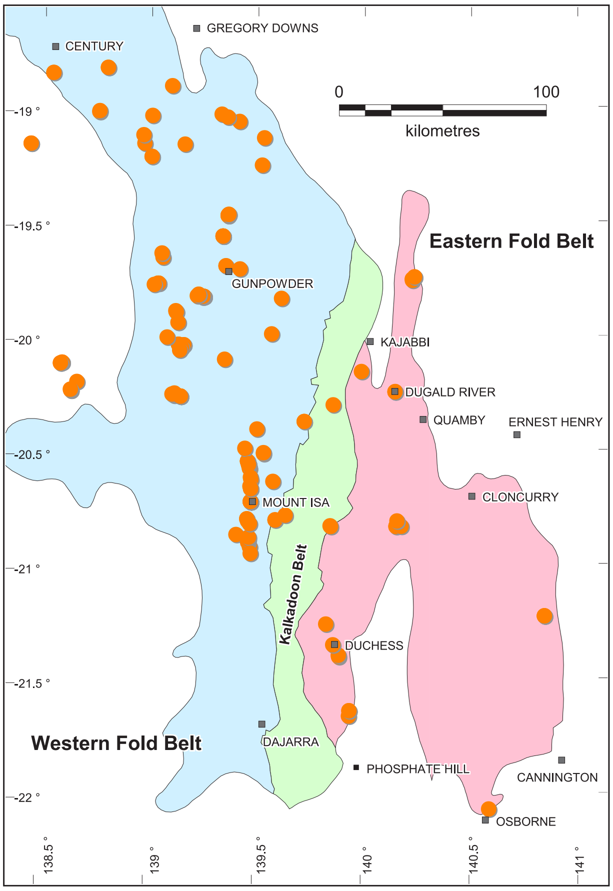

Figure 2.4. Locations of MIMEX Gossan Collection samples on regional-scale geologic base with selected towns and mine sites.

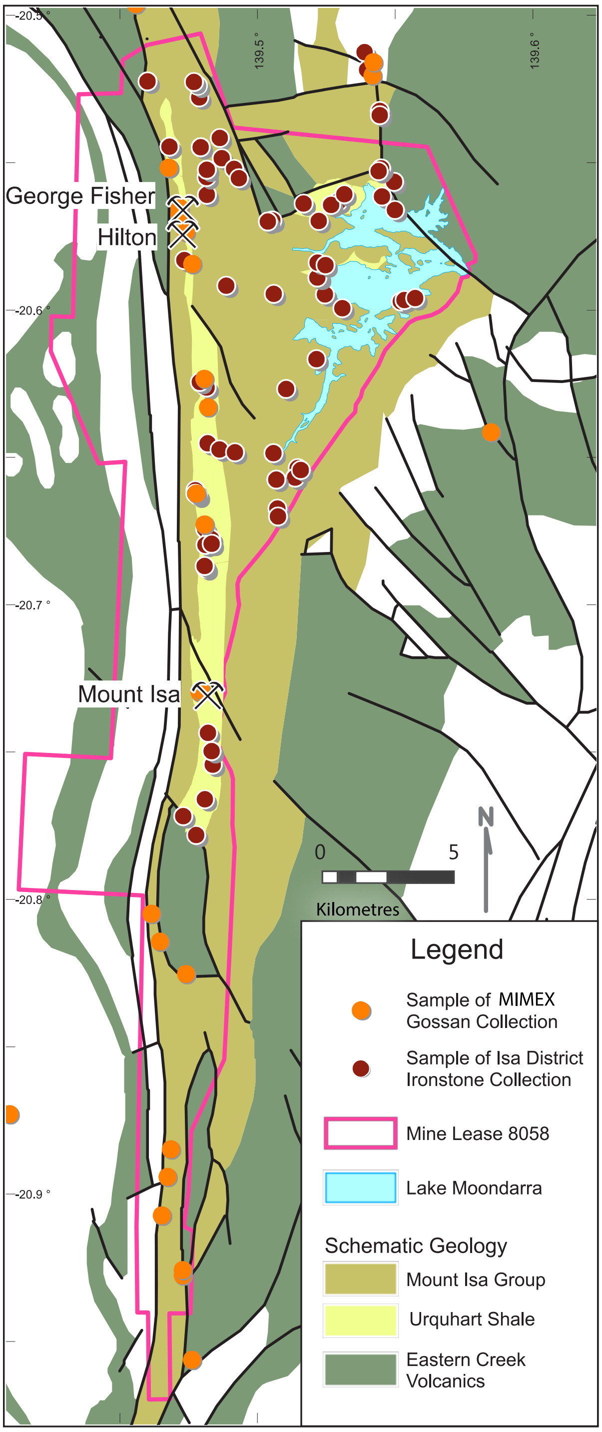

Figure 2.5. Locations of Mount Isa District ironstone collection samples (and relevant MIMEX Gossan Collection samples) on simplified geology.

Construction of the filters

Primary classification of sample collections

The combined datasets are summarised according to regional setting and sample site setting in the bar charts of Figure 2.6. Thus, for example, 100 samples were collected from locations within the Western Succession (which excludes the Mount Isa district). Of the 100 Western Succession samples, 60 were classified as originating from a prospect, 29 from a location not named or considered to be a mineral prospect (hence the term ‘reconn’), and a further 10 from a recognised deposit (upper left chart). In the case of samples from the Mount Isa district (upper right), the bar labelled as ‘Mount Isa deposits’ includes all gossan samples from Novit, Mount Isa Mine, Hilton and George Fisher.

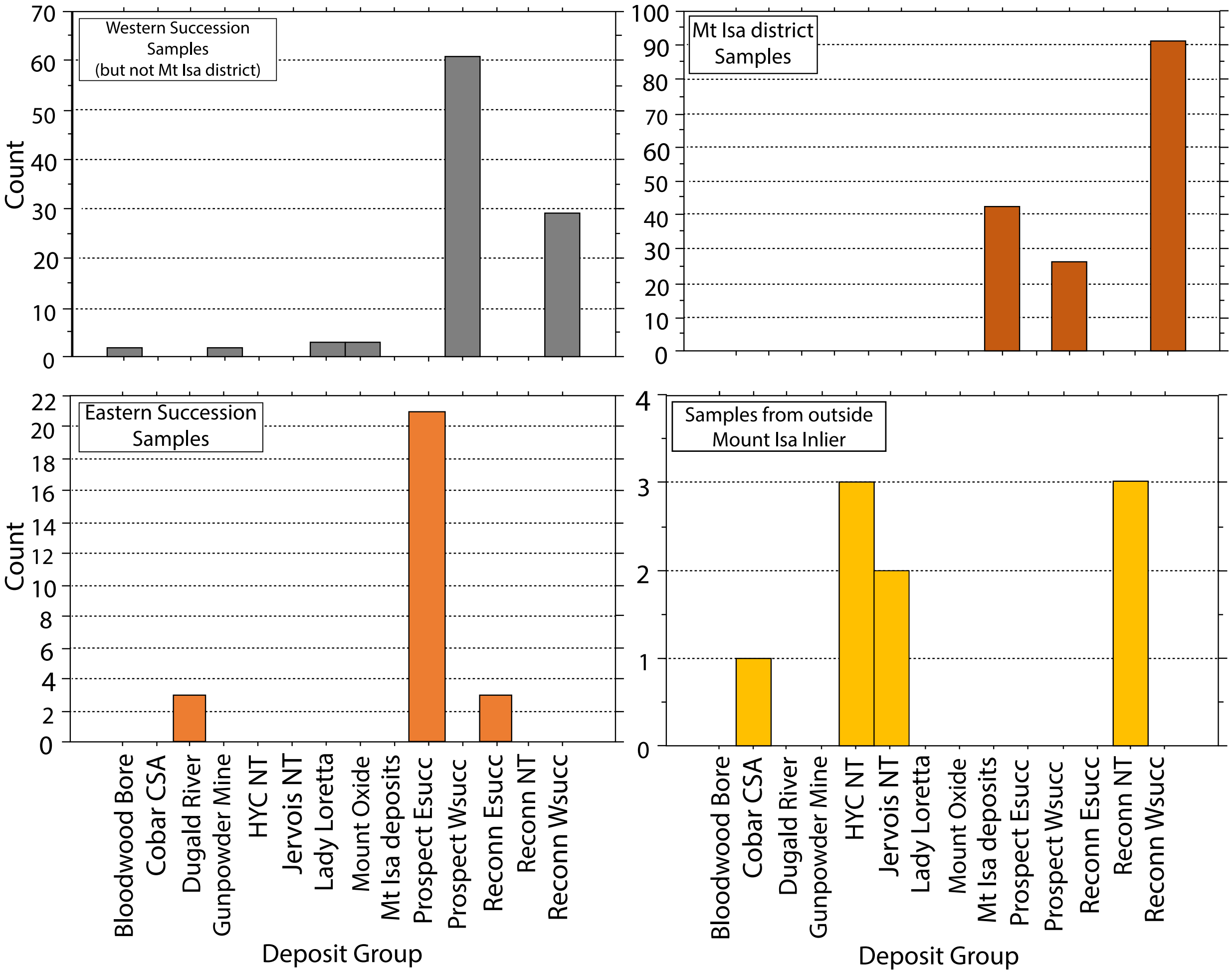

Figure 2.6. MIMEX Collection gossans and ironstones classified by regional setting (4 graphs) and sample site group (deposit, prospect or reconnaissance).

Classification of individual samples

In the case of the MIMEX Gossan Collection, 121 samples were initially classified as one of 4 subgroups, *viz*., Cu, Cu-Au, Pb-Zn, or Cu-Pb-Zn gossan, as they originate from recorded mineral occurrences (*i.e*., prospects). The 54 samples not from prospects (*i.e*., ‘reconn’ samples) were initially defined as unmineralised rock or ironstone, by default. In the case of the Mount Isa District Ironstone Collection, all 102 samples were classified initially as ironstone.

Then, the frequency distributions of iron content (Fe_2O_3T of both the ironstone subgroup of the Gossan Collection and the samples of the Isa District Ironstone collection were examined and found to have similar population breaks, corresponding to four, visually distinctive subgroups:

- Festone_aRk: $Fe_2O_3T < 10.3$ wt.% (effectively a rock)
- Festone_low: Fe_2O_3T between 10.3 and 17.4 wt.% (Fe-flooding but litho-fabric visible)
- Festone_med: Fe_2O_3T between 17.4% and 31.7% (litho-fabric strongly modified)
- Festone_stg: $Fe_2O_3T > 31.7\%$ (typically recorded as massive hematite).

Note that the total iron values are simply ICP Fe readings, by 4 acid digestion, recalculated as Fe_2O_3T.

The sub-grouping provided a pragmatic framework for iteratively graphing and testing the relationship between individual pathfinder elements and weathering induced ferruginisation (*i.e.*, supergene Fe_2O_3T and/or MnO enrichment). After initial data processing and confirmation of field setting, 12 of the Isa District ironstones were confidently reclassified as gossan. By contrast, 9 of the MIMEX Gossan Collection were reclassified from gossan to ironstone. A few of the Gossan Collection have extremely high Mn contents and were classified as Fe stone_Mn to highlight their presence on graphs. The classifications, prior to back-testing with the finalised discriminants, are depicted in Figure 2.7.

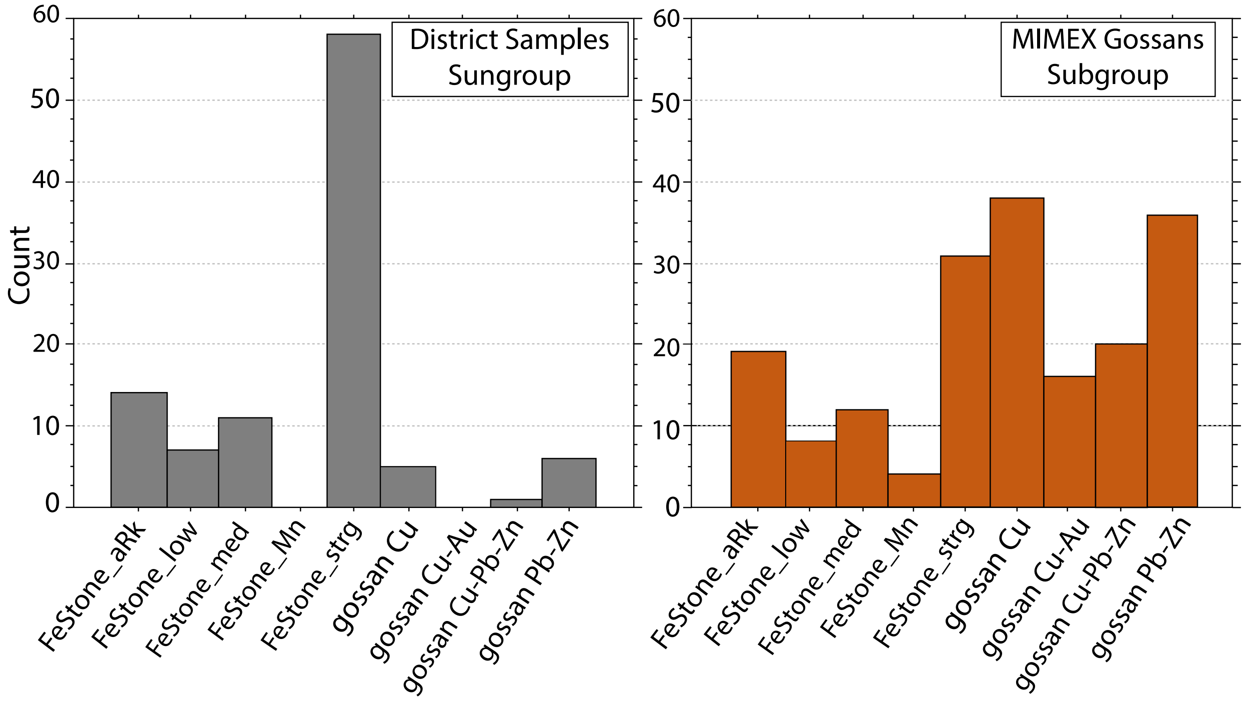

Figure 2.7. Classifications of District Ironstone Collection (left chart) and MIMEX Gossan Collection (right chart).

The basis of the filters

In the search for a multivariate factor, or discriminant, to separate gossan from ironstone and weathered rock, numerous graphs were generated to examine the relationships between individual metals and different classification variables (in effect, a stepwise or manual form of *discriminant analysis*). Three are discussed, below, to illustrate the process.

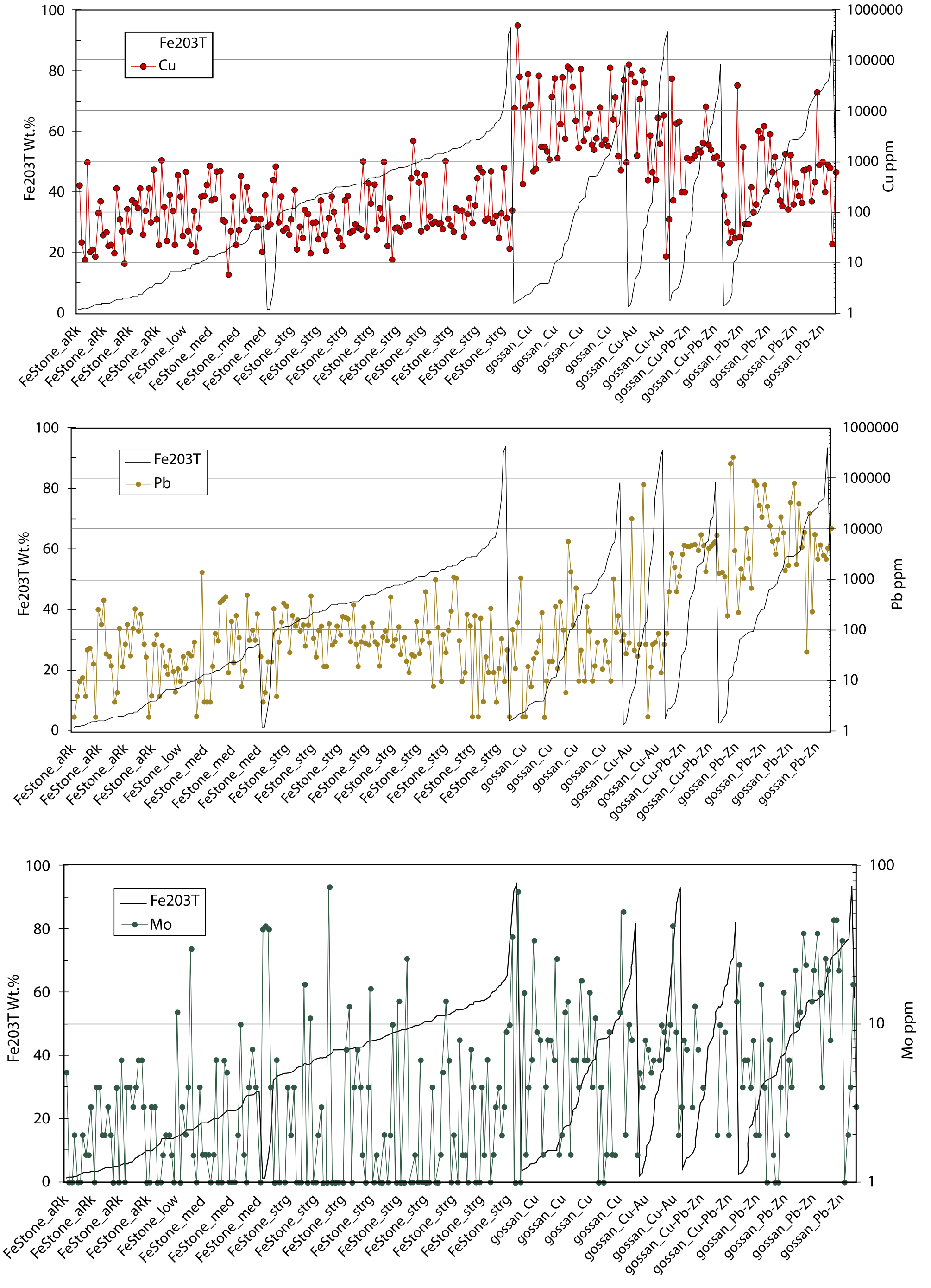

Figure 2.8. Cu, Pb and Mo versus ordered Fe_2O_3T in samples of the MIMEX Gossan Collection.

In each of the graphs of Figure 2.8, samples of the MIMEX Gossan Collection are plotted from left to right according to their final rock-type classification, and within each subgroup the samples are ordered from lowest to highest Fe_2O_3T content. The graphs clearly demonstrate a full range of iron content, expressed as Fe_2O_3T, within each ironstone and gossan subgroup. Cu, Pb, Mo are recorded on the right-hand Y axis of the upper, middle and lower graphs, respectively.

The potential of Cu to be used in any multi-element discriminant is clear (Figure 2.8, upper graph), given that most Cu, Cu-Au and Cu-Pb-Zn gossan samples have much higher Cu levels than the ironstone subgroups. Similarly, the ability of Pb to highlight most of the Pb-Zn gossans at the expense of ironstones implies that Pb, too, must be considered for any discriminant (middle graph). By contrast, it is evident that Mo has little potential to be used in a discriminant, because Mo levels do not occur at distinctive levels within any rock-type grouping (lower graph).

The graphs of 23 elements were inspected before selecting Cu, Pb, Zn, As, Sb, Au and Ag for detailed testing. Others, especially Bi, Sn and W, and perhaps Pd and Se, show promise, but insufficient ICP-MS data is available in the combined collections to confidently include them in a regional discriminant. Of the remaining elements, Co is potentially useful for district scale application (Cu and Cu-Au systems), whereas Mo, P, Tl, Ni, Mn, Cr, V, Ba, U, Ti and Zr are demonstrably unsuitable.

The relevance of metal-scavenging and the need for two filters

Although there is some evidence for the “scavenging” of some metals associated with weathering-induced Fe-Mn enrichment, the process does not explain the chemical profiles of most samples in the two collections, particularly at Fe_2O_3T levels above about 10 wt.%.

The Zn-rich character of ferruginous outcrop developed in formations of the Mount Isa Group is well known and demonstrated in the upper box-plot chart of Figure 2.9, which compares the Zn distributions, by sub-group, of the Isa District Collection ironstones with the samples classified as ironstone in the MIMEX Gossan Collection. Note how Zn ‘enrichment’ is not evident in the ‘regional’ ironstones (box median maxima of about 200 ppm). The lower box-plots emphasise that, unlike Zn, the level of Cu in progressively higher Fe-material does not increase in Mount Isa district samples (box medians < 70 ppm) as they do in the ‘regional’ samples (box medians 100–250 ppm Cu).

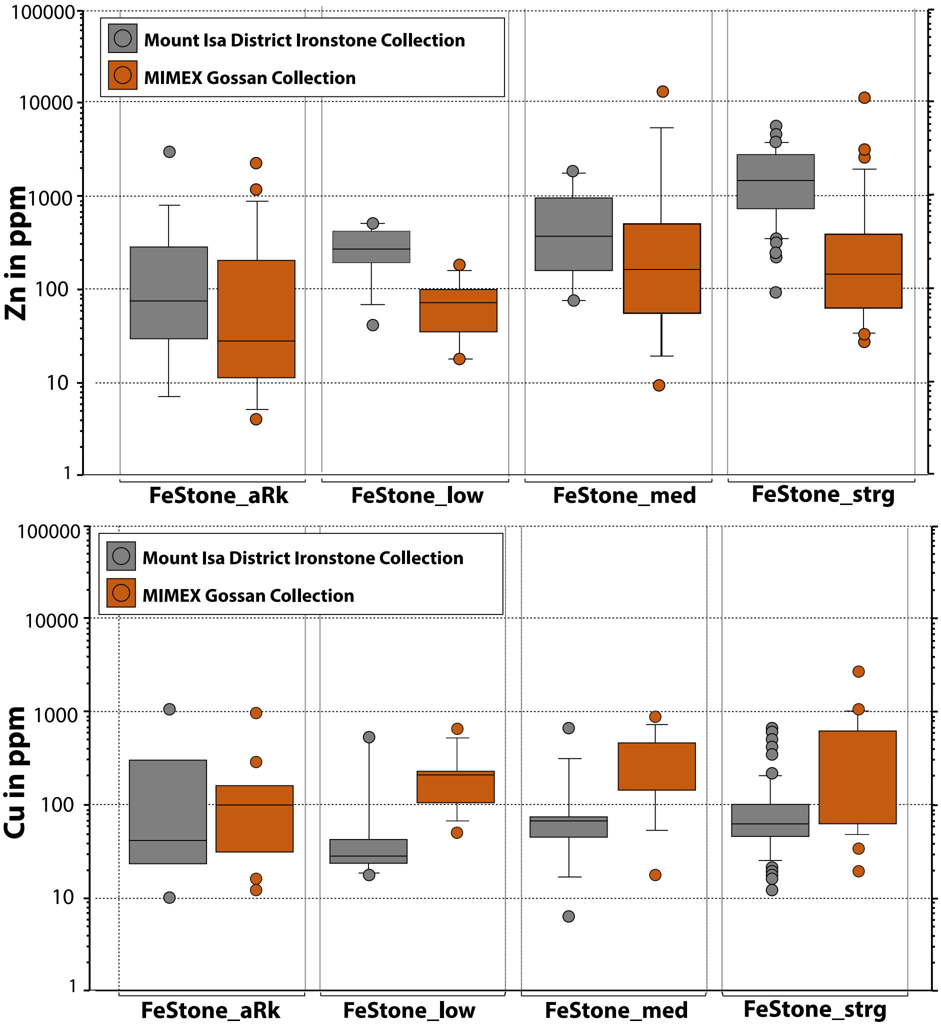

Figure 2.9. A comparison of Zn and Cu abundances in ironstone subgroups of the Isa District Ironstone and MIMEX Gossan Collections.

If "metal-scavenging" during weathering-related Fe-enrichment was the primary control, then the Fe-Zn correlation observed in Mount Isa district samples should be evident in ironstone-classified samples of the MIMEX Gossan Collection. Furthermore, two elements normally associated with metal scavenging by hematite and goethite, V and Co, do not display a systematic enrichment in the higher-Fe ironstone subgroups.

Thus, precursor bedrock control is paramount. The Zn-rich (and Cu-poor) character of the Isa district ironstone collection reflects widespread sulphidation (as pyrite) and associated weak Zn-Fe mineralisation of the host original rock units; and the relatively Zn-poor and Cu-elevated 'regional' ironstones reflects the mafic igneous parentage of many samples. An important implication is that, whilst Zn is an appropriate discriminate from the perspective of, say, a reconnaissance rock chip programme designed to detect evidence of large sediment-hosted base metal systems, it does not contribute to a diagnostic signal *within* such a system. This finding implies the need for a Zn-free discriminant for assessing the possibility of pyrite-enveloped SEDEX systems, of the Mount Isa, and perhaps Century and HYC types, as distinct from one for higher temperature systems featuring Cu and Au.

Identifying and back-testing the filters

By focussing on elements with contrasting abundance distributions between the sub-groups of ironstone and gossan, factors were determined for each metal to ensure that distribution heterogeneities were captured as equal contributions in derived additive combinations, or discriminants.

Regional filter

A combination of seven metals was found to best separate the classified gossans and non-gossans (ironstones) of the MIMEX Gossan Collection. With the sum of individual contributions (as population median values) factored to centre on a separation value of 10, the resulting formula, defining the regional filter is:

$$\text{RegFilter10} = (\text{Cu}+\text{Zn}+\text{Pb})/150 + \text{As}/50 + (\text{Sb}+\text{Au})/15 + \text{Ag}/2$$

The upper graph of Figure 2.10 shows that apart from one sample, the pre-defined gossans have filter values of greater than 10. The 'failed' sample is from a pod of quartz (SiO_2 = 92 wt.%) within the gossan of the George Fisher Zn-Pb deposit. Significantly, two samples from the surrounding ferruginous domain have filter scores of about 26 (with Fe_2O_3T ~58% wt.% and relict bedding).

By contrast, 21 of the 74 pre-defined ironstones 'pass', with filter scores above 10. All are from historically explored sites near Mount Isa and most 'pass' because of elevated Cu ± Zn levels. They include 12 from the sporadically Cu-mineralised Redie Creek Fault and Buckley River areas, north of Mount Isa, two from Doolans Hope (near Mount Isa), and two from an unusual Mn-rich and baryte-bearing locality, with anomalous Co-Zn-Ag-Tl, some 115 km northwest of Mount Isa. Evidently, this group was mis-classified, particularly the 13 samples with regional filter scores >15.

The lower graph of Figure 2.10 shows the regional filter scores for samples of the Mount Isa District Ironstone collection, many of which, as expected, plot in the gossan field due to consistently high levels of Zn (refer to Figure 2.9, upper graph). Unlike the small group of

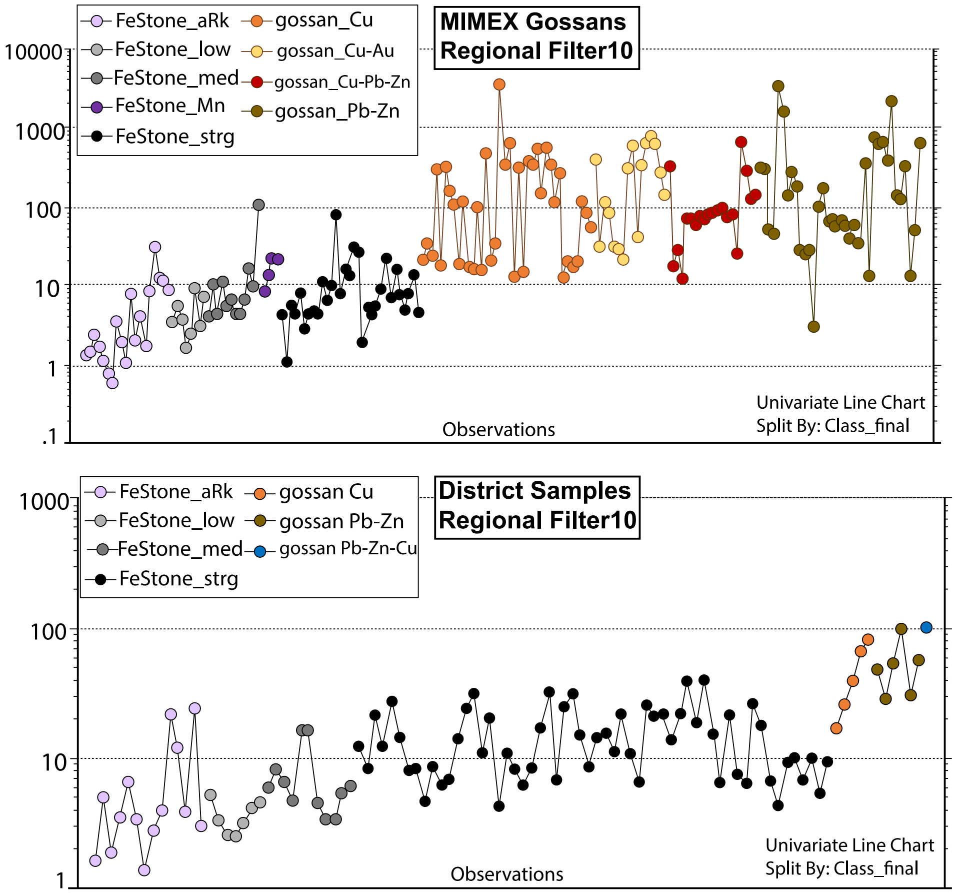

Figure 2.10. Application of the 'regional' filter to samples of the MIMEX Gossan (upper graph) and Mount Isa District Ironstone Collections (lower graph).

confirmed gossans in this collection, most of these samples are from localities without extensive soil or RAB geochemistry anomalies and if drilled, not associated with noteworthy bedrock mineralisation. What is abundantly clear is that the regional filter is ineffective for assessing ferruginous outcrop from different localities and prospects *within* the district of Mount Isa, especially those within units of the Mount Isa Group.

Isa filter

By excluding Zn, and slightly adjusting the relative contributions of Cu-Pb and Au-Sb, the following combination was found to best separate the classified gossans and non-gossans (ironstones) of the MIMEX Gossan Collection. With the sum of individual contributions (population medians) factored to centre on a separation value of 10, the resulting formula, defining the Isa Filter is:

$$\text{IsaFilter10} = (\text{Cu}+\text{Pb})/200 + \text{As}/50 + (\text{Sb}+\text{Au})/20 + \text{Ag}/2$$

The upper graph of Figure 2.8 shows how this discriminant has decreased the "signal" of many of the 21 contentious 'ironstone' samples of the Gossan collection to less than 10 (*c.f.*, Figure 2.11, upper), whilst maintaining the elevated scores of most of the pre-defined regional gossans, albeit with 3 Pb-Zn 'fails'. However, when applied to the Isa District Ironstone Collection (Figure 2.7, lower) the effect is a clear separation of pre-defined gossans (scores >25) and ironstones, most with scores of <10 (*c.f.*, Figure 2.11, lower). Accordingly, the Isa Filter is the preferred variant for Mount Isa district.

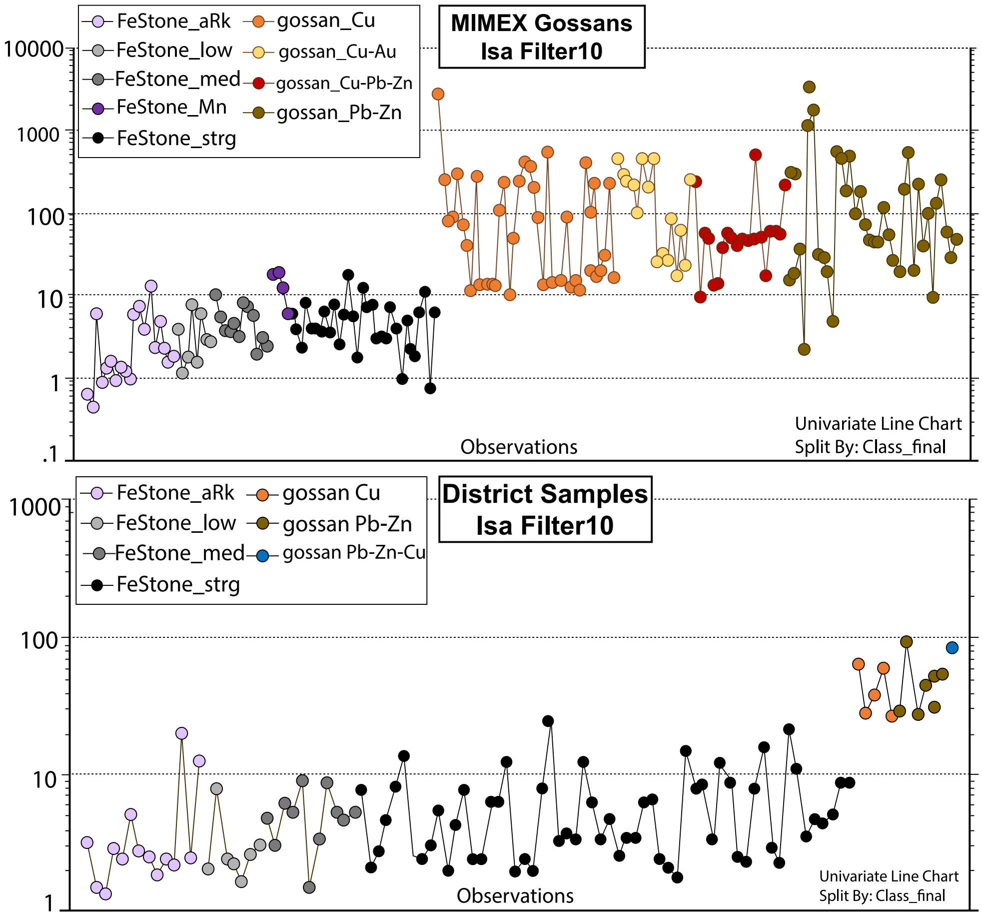

Figure 2.11. Application of the Zn-free 'Isa' filter to samples of the MIMEX Gossan (upper) and Mount Isa District Ironstone Collections (lower graph).

A similar process is feasible for so-called 'false Cu gossan', associated with mafic rock units, such as amphibolite and metabasalt, throughout the region. Though not presently verifiable, reducing the influence of Cu in the regional filter may be all that is required to distinguish ferruginous assemblages which developed by the weathering of Cu-bearing Fe-Mg silicates, to produce 'false gossan', from those after disseminated pyrite and/or chalcopyrite, to produce the hundreds of small copper prospects in the region which are demonstrably associated with gossan profiles (though generally thin and relatively immature).

Application of the filters

Example from the Western Succession

Hilton area case study

In the combination graph of Figure 2.12, Regional and Isa Filter scores, together with Pb, Zn and Fe_2O_3T, are plotted for several ironstones that outcrop as elongate pods within the Breakaway Shale some 1000 m to the east of the Hilton-George Fisher 'line-of-lode'. The pods lack relief, have strike-lengths of 10s to 100s of metres and are up to 25 m wide. Despite moderate to strong ferruginisation, bedding is generally preserved.

With anomalous Zn abundances of several hundred to low thousands of ppm, they are typical of weathered pyritic horizons within Mount Isa Group sediments that otherwise lack Pb or Cu mineralisation. A few exceed the regional filter threshold, with scores of 20–30, but none of the samples from this area pass the Isa Filter (threshold score of 10).

For contrast, samples of gossan collected from ridges at, and along strike of, Hilton and George Fisher Mines are graphed in Figure 2.13. All samples pass the threshold of the two discriminants (note change of Y-axis scales from previous graphs). Despite a strong topographic expression

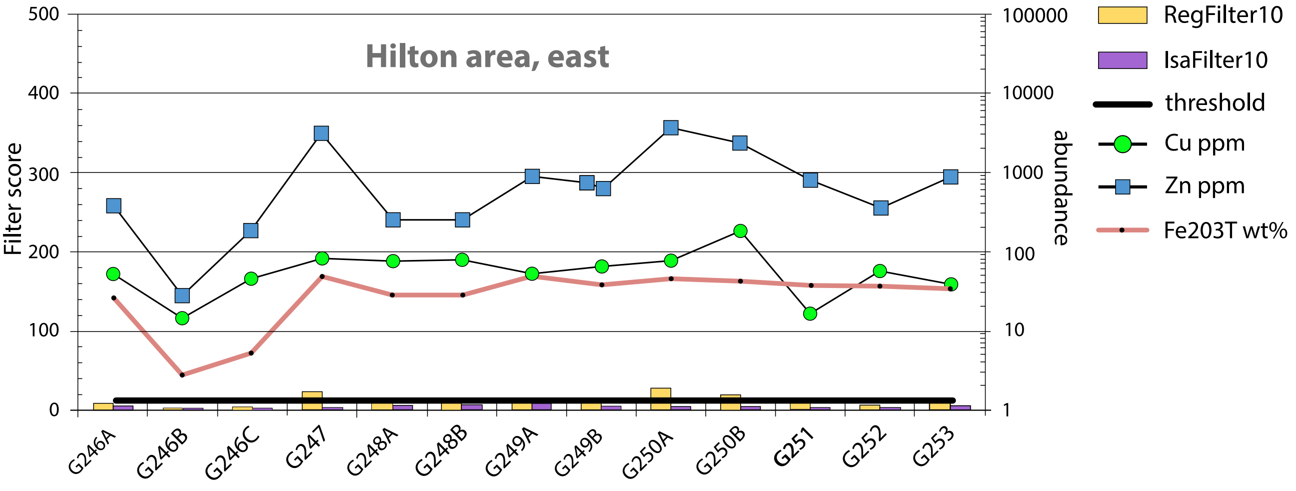

Figure 2.12. Application of the discriminants to samples from east of the Hilton-George Fisher line-of-lode (graph) and photos of site G247.

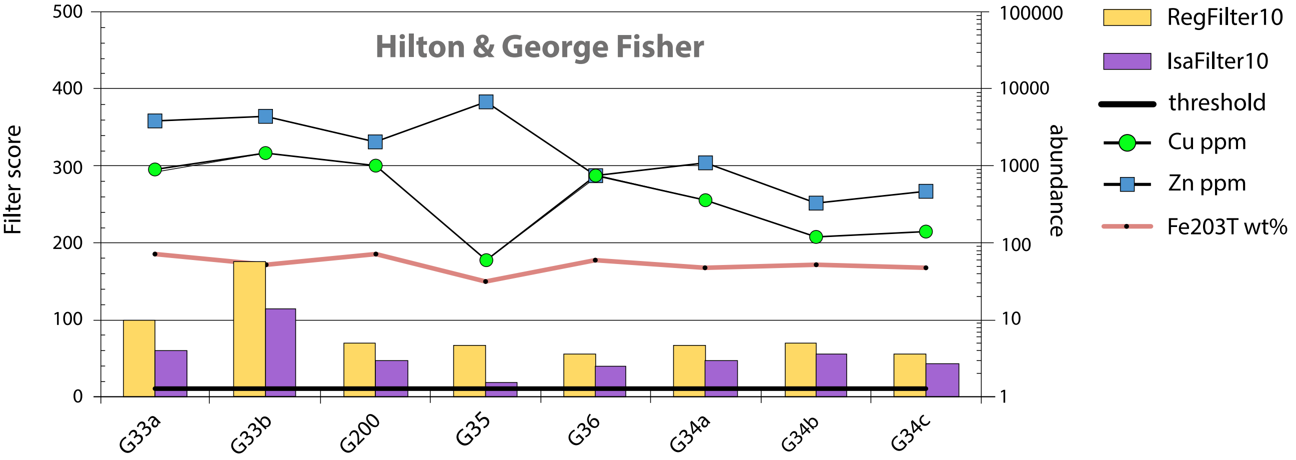

Figure 2.13. Application of the discriminants to samples from outcrops in the Hilton-George Fisher line-of-lode (upper graph).

and the presence of solution breccias and boxworks (photos), they probably developed in sub-economic mineralisation. Hypogene ore, now mined-out, was relatively deep and accessed by underground development. In contrast, some of the surface gossans at Mount Isa developed in ore grade Pb-Zn mineralisation and have filter scores in excess of 500.

Examples from the Eastern Succession

Ore deposits and major prospects

Figure 2.14 displays the Regional and Isa Filter scores, together with Pb, Zn and Fe_2O_3T, for gossans associated with the significant mineralisation of several Eastern Succession prospects and ore deposits (upper graph). All samples have regional filter scores above, including the Fairmile deposit sample that is partly obscured by the threshold marker line (regional score 13.5).

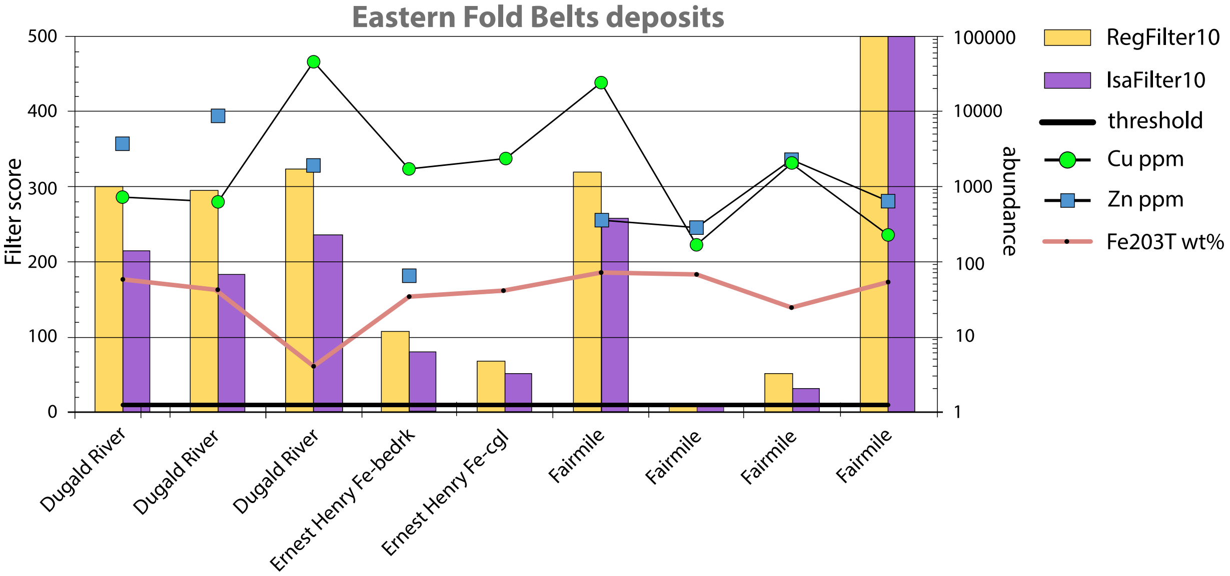

Figure 2.14. Application of the discriminants to samples from Eastern Succession deposits (upper graph).

The high scores of samples from the Dugald River and Fairmile deposits are consistent with gossans developed in high grade mineralisation. In the case of Fairmile, a polymetallic and sub-economic prospect of the Broken Hill Type of mineralisation, the signal is dominated by Ag (up to 160 ppm). The two results for Ernest Henry, a Cu-Au-Co-U deposit of the IOCG type, apply to drilled ferruginous material at depths of 30–40 metres on the Cretaceous palaeo-surface directly above Au-rich supergene ore.

Selwyn Au-Cu District magnetite-hematite gossans and ironstones

The regional filter is applied to samples of weathered outcrop of two ore lenses of the magnetite-hosted Selwyn Au-Cu deposit and samples of ‘barren ironstone’ exposed 1 km to the east, in the upper graph of Figure 2.15. Clearly, the two groups cannot be distinguished at filter values < 10. However, by accounting for the tungsten-anomalous character of the Selwyn ores (evident in the W plot of Figure 2.16), and adding 0.5W to the filter algorithm, a good separation is achieved with minimal overlap at the threshold level of 10 (lower graph, Figure 2.15).

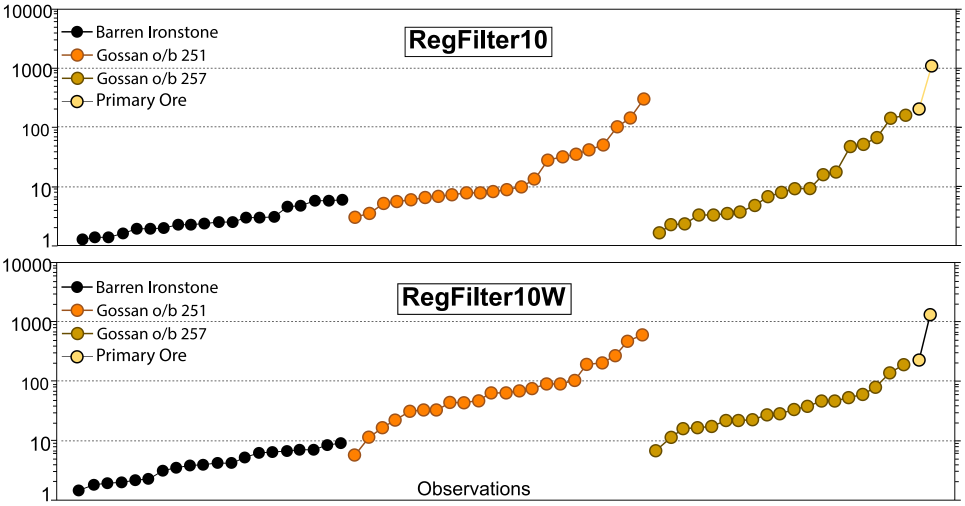

Figure 2.15. Comparison of Selwyn district gossan and barren ironstone regfilter10 (upper graph) and regfilter10 values adjusted for tungsten (lower graph).

Clearly, the two groups are distinguished by the elevated Mn and Ba, and sub-20 ppb Au of the ironstones, as concluded by the original investigator (Wildman, 2001) and shown in the Au frame of Figure 2.16. However, this example demonstrates that the regional filter, developed as it was from data heavily weighted to base metal systems, is easily adapted, and its metallogenic reach extended, by the addition of an appropriately weighted pathfinder element—in this case to relatively sulfide-poor magnetite-hosted Au-Cu-W mineralisation.

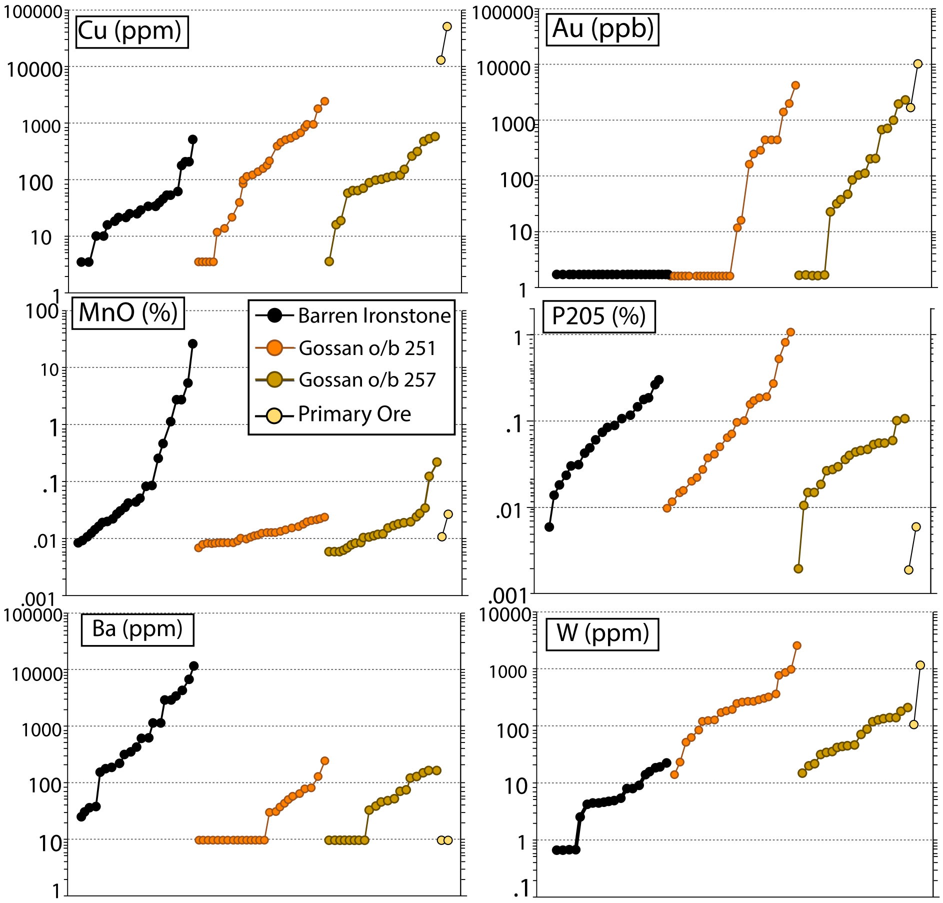

Figure 2.16. Abundance distributions of W, Cu, Au, Ba, Mn and P for Selwyn district gossan and ironstone (legend as for Figure 2.15).

Field and laboratory guidelines

Recommended sampling tactics

- Random sampling of outcrop fragments within recognisable mineralogic/textural ‘niches’; iron oxide dominated niches should have priority over siliceous or clay-dominated niches.
- At least two samples per 25 m^2 locality for small occurrences (outcrop area 50–250 m^2; each sample to weigh 2.5–3 kg.
- For large occurrences, several samples from 2 or more equidistant localities is suggested.

Recommended analytical tactics

- Minimum cost option is aqua regia or fire assay for Au (1 ppb) and aqua regia digestion for Fe, Mn and other metals, determined by ICP-OES (most elements, including S) and ICP-MS (for Ag and Sb and other trace pathfinders like Bi, Cd, Mo, Tl, Sn and W). The resulting data is sufficient for gossan filter calculations but of limited utility for lithogeochemical assessment. Estimated current cost of $45–$55.
- Dual purpose option, for both lithogeochemical characterisation and gossan filter calculation—the major elements by Li borate fusion/XRF (including S), trace elements by 4 acid digestion (for resistate mineral dissolution) and ICP-OES/MS finish, Au by aqua regia dissolution or fire assay. Estimated current cost of $75–$90.

Chapter 3

Use of the Pb-Pb isotope method for base metal exploration

Relevance to pre-discovery exploration

1. The largest base metal deposits, such as Cannington and Dugald River of the Eastern Fold Belt (this article), and Mount Isa and Century of the Western Fold Belt, contain Pb derived from a consistent bulk crustal source in a major initial event followed by later additions during orogenesis. The typical result is a tight cluster of Pb isotope compositions corresponding to the primary event ($^{206}Pb/^{204}Pb$ range of <0.04), and a second 'overprint' population, generally as texturally later sulfide, with younger compositions spread up to 0.15 units of $^{206}Pb/^{204}Pb$ along the relevant growth curve.
2. From point 1, the Pb isotope compositions of a few exploration samples can be used to eliminate likely sub-economic prospects, or 'barren' occurrences with otherwise anomalous base metal levels, if the results are either clearly displaced from the relevant regional growth curve or they lack a component of 'major event' Pb. An important caveat is the possibility of major deposit-like patterns on a previously unrecognised growth trend (see point 8).
3. Exploration samples with as little as 200 ppm Pb, and background U levels (< 3 ppm), have a high probability of retaining initial (syn-mineralisation) Pb isotope ratios.
4. Pb isotope signatures are retained during weathering and gossan development. Therefore, gossan with growth curve-coincident Pb isotope ratios is likely to have developed from mineralisation associated with a significant metallogentic event. Accordingly, Pb isotope analysis offers a means of prioritising 'broad-acre' surface geochemical results, such as those produced by multi-element discriminants like the RegFilter (Chapter 2). The diagnostic potential of the method extends to other sample media, such as groundwater and vegetation.
5. As a corollary of point 1, and with reference to exploration in the Eastern Fold Belt, reconnaissance sampling and Pb isotope analysis of individual prospects should enable the exploration geologist to distinguish Pb-rich systems that contain pre-Isan Orogeny Pb (*e.g.*, Soldiers Cap Event) from those without (*e.g.*, Monakoff and Casablanca).
6. The available data indicates that Pb isotope analysis is unlikely to contribute significantly to the understanding or evaluation of very low-Pb occurrences, such as Cu-only or Cu-Au mineralised systems or prospects. However, there is limited scope for determining the metal reservoirs and approximate mineralisation ages from secondary isochrons generated by the radiogenic decay of U in low-Pb Cu-rich prospects.
7. Inferences about system size, continuity or grade cannot be made on the basis of spatially restricted data typical of a pre-discovery exploration campaign. The task is impeded somewhat by a regional Pb isotope database that is underpopulated with critical support information (*e.g.*, Pb and U assays and sample site detail). Enhancement of the diagnostic potential of the Pb isotope is expected if future emphasis is given to the double-spike procedure, which dramatically improves the precision of $^{207}Pb/^{204}Pb$ determinations, *and* the dedicated reporting of sample and sample-site attributes.
8. At a regional scale, the distribution of Pb isotope compositions of significant Pb-rich occurrences are attributed to distinct hydothermal epochs or metallogenic events

affecting favourable stratigraphic packages within discrete structural blocks or terranes. The contrasting systematics of mineralisation associated with the Soldiers Cap event and posited Kuridala event in the southern part of the Eastern Fold Belt is one example examined in this document. The distinct crustal sources evident in the characteristic signatures of several major Western Fold Belt base metal deposits provides another. It follows, particularly in the case of drilled targets in areas of thick cover, that Pb isotope data can complement geophysical methods for terrane mapping and developing refined metallogenic models to guide further exploration.

Introduction

Pb isotopic compositions provide a means of direct comparison of base metal mineralisation in weathered outcrop (as gossan), or in drill hole samples (containing sulphide), with that of known major deposits, which are known to lie upon regionally relevant 'common Pb-Pb' growth curves. This fundamental relationship is illustrated at the global scale in Figure 3.1, where data for stratabound deposits of widely differing ages, geologic character and geographic settings conform to a generalised growth curve for a single stage event and assumed reservoir U/Pb (*viz*., a source region with U^{238}/Pb^{204} ratio of 9.1).

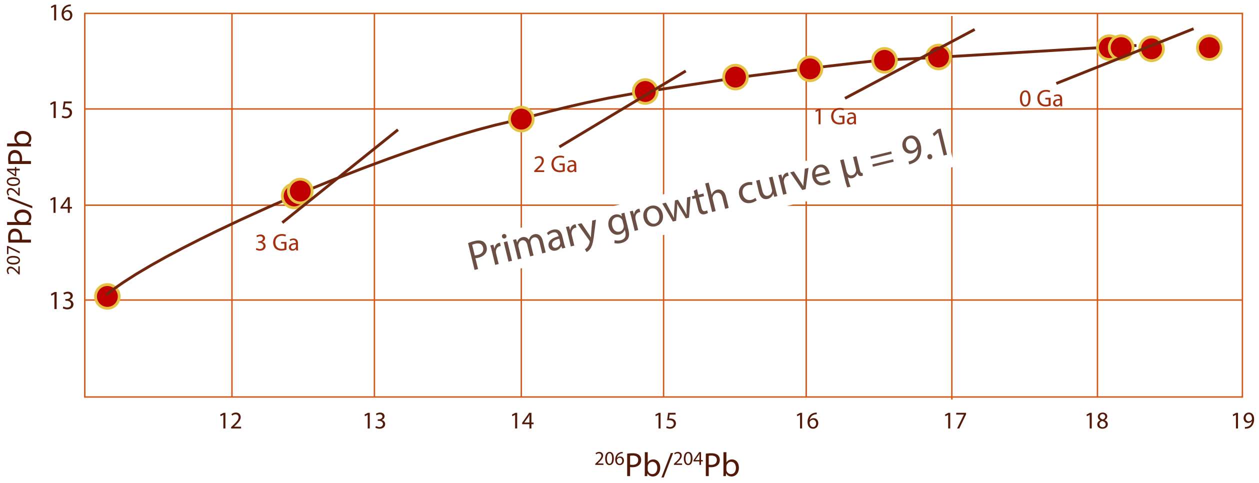

Figure 3.1. Pb isotope data for stratabound ore deposits (from data in Albarede & Juteau, 1984).

Indeed, it had become recognised by the mid-1970s that for a region with many deposits, those with Pb isotope compositions closest to the primary growth are generally larger, and consistent with derivation from a well-mixed source in a single event, whilst those with 'anomalous' compositions are smaller and formed by multi-stage accumulation, with Pb from more than one source (*e.g.*, Doe & Stacey, 1974)

In the case of the Mount Isa region, AMIRA Project 480 researchers developed separate 'common Pb' growth curves for the Eastern and Western Fold Belts. The fields of data for some of the major deposits are shown in relation to the two growth curves in Figure 3.2. Critically, it was concluded that exploration samples that do not plot on these curves are unlikely to represent major mineralisation (Carr *et al.*, 2001).

In detail, the Eastern curve was derived from Pb-isotope determinations on feldspar in gneiss units, Wonga granite, and significant Pb occurrences (Pegmont and Cannington deposits). The Western curve was derived from high precision 'double spike' data from major deposits (Mount Isa, Hilton, Lady Loretta, Century, MacArthur River). Ultimately, the curves are interpretative and subject to refinement, particularly the EFB, because a spectrum of bulk crustal Pb contributions is evident in the Pb isotope data of Eastern Succession Pb deposits and prospects. Nevertheless, they provide an invaluable frame of reference for the interpretation of exploration Pb isotope data.

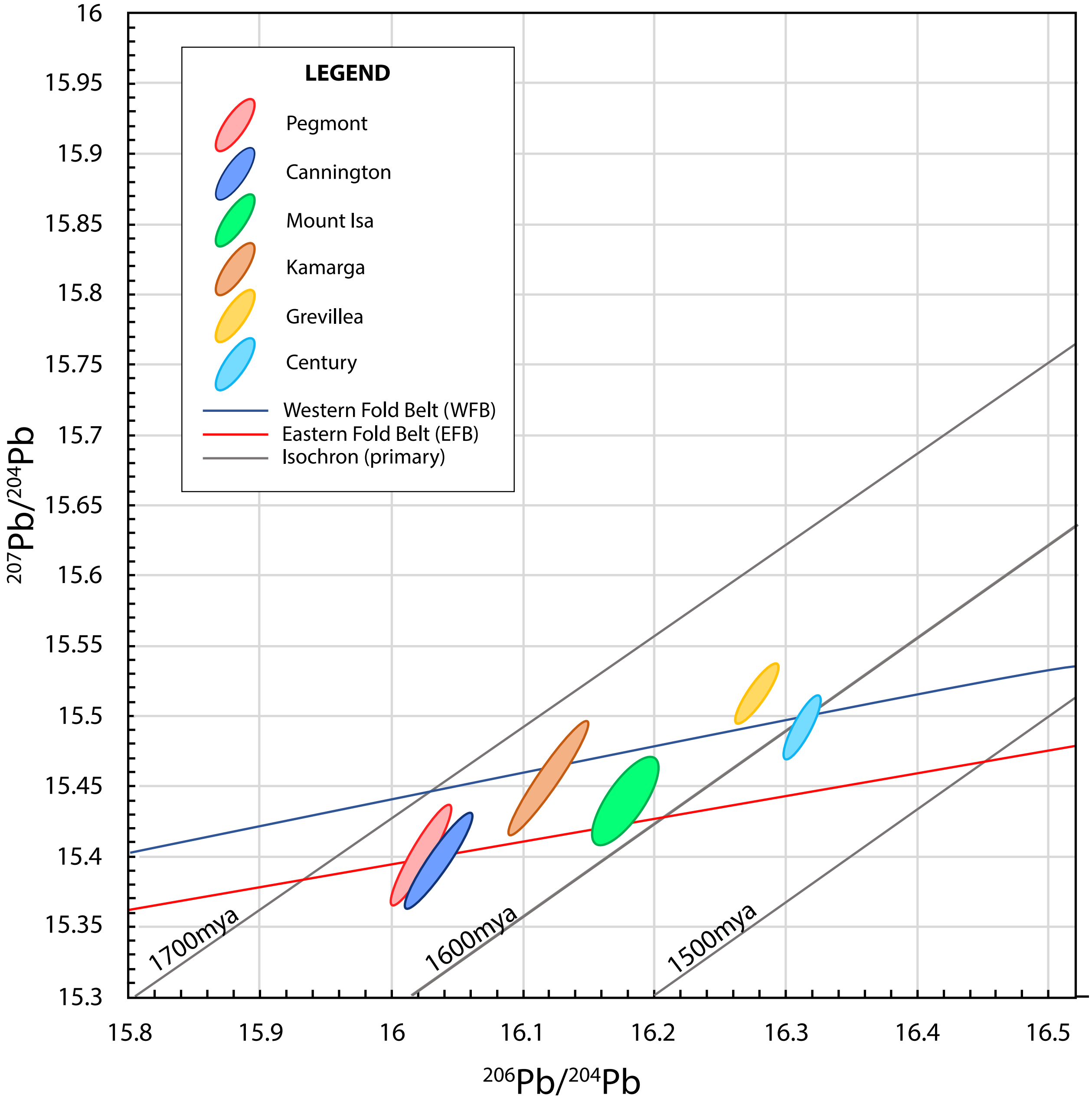

Figure 3.2. Conventional Pb isotope plot with regional growth curves and primary isochrons showing containment ellipses for samples of main-stage sulfide of Mount Isa region base metal ore deposits and significant prospects (from the database and graphs of Carr et al., 2001).

The AMIRA P480 report (*op. cit*.), is a comprehensive record of the state-of-play at 2001 and remains so. The database (copy supplied), especially, provides a basis for comparative assessment by explorers with newly acquired Pb isotope data. Yet, few explorers leverage the diagnostic potential and cost-effectiveness of the method or are aware of the relative simplicity of the required sampling and analytical procedures.

It is hoped that by reviewing the AMIRA P480 work and providing examples of how the Pb isotope method is applied, and the data interpreted, that this shortcoming can be addressed to some extent. Specifically, this document uses graphical summaries to both capture the essential characteristics of the numerous Pb isotope data and to provide a simple framework for distilling the considerable body of the AMIRA report. Much of the review component is derived from a draft consultant's report to Xstrata Copper, as a former sponsor of AMIRA P480 (*viz*., Hannan, 2004).

Pb-rich systems, Eastern Fold Belt

Preamble

The earliest mineralisation of the 'economic' Pb-rich systems of the Eastern Fold Belt is referred to as population 1 (pop1) and is distinguished from subsequent mineralisation classified as population 2 (often described as vein- or breccia-hosted galena). Pop1 is directly associated with the so-called Soldiers Cap Event at about 1662 Ma. Figure 3.3 demonstrates how the Pb isotope ratio distributions of pop1 for Soldiers Cap Group-hosted Cannington and Pegmont deposits are essentially indistinguishable. Those of the Corella Formation-hosted Dugald River

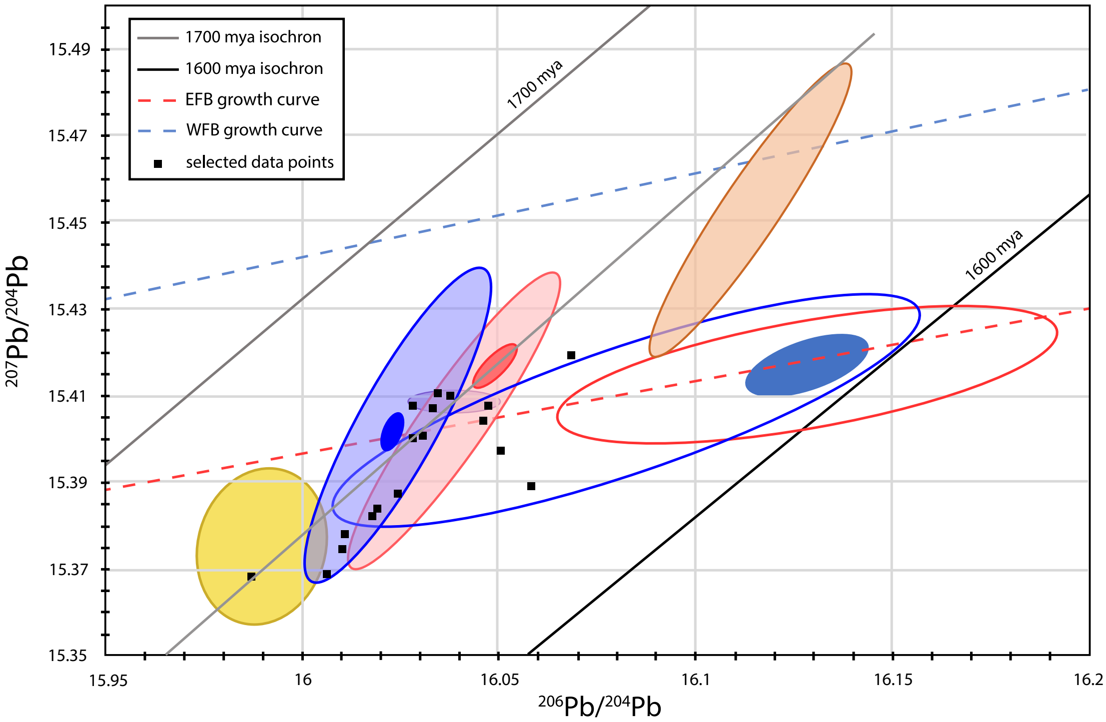

	Mainstage Soldiers Cap Event (about 1665 mya)	
●	Cannington ore deposit	'population 1', paragenetically early galena (19 samples)
	Pegmont deposit	'population 1,' paragenetically diverse galena (44)
	inetrior ellipse	double spike (DS) results (4)
●	Dugald River ore deposit	'population 1', paragenetically early galena from 5 drill holes (13)
	red interior ellipse	Dugald River DS results (2)
	Interpreted Isan orogeny overprint event(s)	
○	Cannington	'population,2' Isan orogeny overprint (9)
	interior ellipse	Cannington 'population 2' DS reults (5)
○	Dugald River	'population 2', late galena (5), including 3 vein samples with 900 ppm, to 5% Pb
	Fairmile large prospect	4 galena samples, 5m interval of DDH FD7
	Maronan large prospect	10 galena samples, 'cross-cutting', 4 drill holes(?)
●	purple interior ellipse	Fairmile and Maronan DS results (4)
	Low μ event (amphibolite association, about 1660 mya?)	
●	Killer Bore	3 samples drill hole coarse gn-py-sph
	Jasper Ridge prospect	3 surface samples with about 0.2% Pb, 1 sample repeated by DS
	Mainstage Mount Isa District Event (about 1655 mya)	
●	3 major Pb-Zn deposits	'population 1' with DS point data
	1 large prospect	

Figure 3.3. Conventional Pb isotope distributions, as 95% contain ellipses, of major Eastern Fold Belt Pb-rich deposits; showing main stage and orogenic overprint populations, fields of double spike data and other detail discussed in the text.

deposit differ from Cannington and Pegmont by having only marginally higher $^{206}Pb/^{204}Pb$ values (up to 0.03 units), consistent with a slightly younger age of mineralisation. For reference, the 95% containment ellipse is also shown for pop1 of Western Fold Belt deposits of the Mount Isa district (Mount Isa, George Fisher and Hilton mines and sub-economic Mount Novit).

Noteworthy characteristics of the largest deposits and prospects

1. The discriminating potential of double spike (DS) determinations is exemplified in Figure 3.3 by the spatially separate fields of DS data for the Dugald River (small red interior ellipse) and Cannington and Pegmont deposits (small blue interior ellipse). These data, though few, imply slightly differing ages of mineralisation *and* differing bulk ore fluid U/Pb ratios (source regions), with Dugald River DS data plotting distinctly above the Eastern Fold Belt growth curve. Therefore, DS analysis, by virtue of superior precision, is probably the most efficient way of establishing the fingerprint or pedigree of mineralisation in exploration samples.

2. The blue and red unfilled ellipses of Figure 3.3 apply to a small number of texturally cross-cutting high Pb ‘pop2’ samples from Cannington and Dugald River, respectively. Such compositions, with $^{206}Pb/^{204}Pb$ ratios extending to 16.2, are explained by the mixing of older, Soldiers Cap Event Pb with younger Pb that evolved in essentially the same bulk reservoir up to a time of about 1500 Ma. The P480 report identified Isan Orogeny events D2 (1585 Ma) and/or D3 (1530–1490 Ma) and associated intrusive activity as likely driving mechanisms. Such overprinting is evident in most deposits of the region that were, or have become, economic. A spread in $^{206}Pb/^{204}Pb$ ratios of up to about 0.2 is typical. Thus, evidence of niche-controlled, but growth curve-tracking isotopic spread for large areas or volumes of mineralisation, is a favourable characteristic from the perspective of the pre-discovery explorer.

3. Most of the drill hole data for the sub-economic Maronan and Fairmile deposits fall within the ‘pop1’ fields of Cannington and Pegmont (Figure 3.3, black squares). The Maronan samples are recorded in the P480 database as texturally cross-cutting galena and are not given a ‘population’ designation. The implication is that galena in texturally late settings with the early, Soldiers Cap Event Pb isotope signature is a comparatively unfavourable characteristic, consistent with a time-limited, single pass system. As such, veins and breccias are vital sample niches for system evaluation in the absence of significant wall rock mineralisation.

4. As a corollary of Points 2 and 3, DS data for cross-cutting mineralisation may reveal discrete overprint events, as suggested by the cluster of DS results within the Cannington overprint ellipse (Figure 3.3, blue fill polygon centred at $^{206}Pb/^{204}Pb$ ~16.13).

5. The available Maronan and Fairmile DS data occupy a narrow, but almost growth curve-parallel field between those of Cannington-Pegmont and Dugald River (Figure 3.3, interior purple ellipse). The spread of DS $^{206}Pb/^{204}Pb$ with minimal variation in $^{207}Pb/^{204}Pb$ is strongly suggestive a sequence of fluid inputs of uniform origin over a discrete period. However, it is argued that such a pattern for a *restricted distance or volume* of mineralisation implies a relatively weak or intermittent plumbing system and limited economic potential. The Maronan example contrasts with the greater spreads in DS $^{206}Pb/^{204}Pb$ observed over large distances (volumes) within high grade giants like the Mount Isa 650 copper orebody and the Century Zn deposit (see later). More, well attributed DS data for individual ore deposits and prospects is required to test this argument.

Examples relevant to pre-discovery exploration

Results displaced from a recognised growth curve

The yellow-fill ellipse of Figure 3.3 is somewhat interpretative and based on 3 samples of Pb mineralisation from two prospects hosted by the Kuridala Formation, 10–20 km southwest of the Pegmont deposit. These data are suggestive of a source with a distinctly lower bulk U/Pb ratio, such as a crustal volume dominated by mafic igneous rocks. An implied 'Kuridala' event possibly occurred at about the same time as the Soldiers Cap Event, because a pseudo-isochron that bisects the DS data points of Maronan and Fairmile and Dugald River can be extended to intersect a double spike analysis of galena from the Jasper Ridge prospect, which is hosted by the Kuridala Formation (indicated by a faint line, Figure 3.3).

All the high-Pb sample data for base metal prospects within the Kuridala Formation are plotted, by prospect name, in Figure 3.4. The total spread at first glance is discouraging, but the few results for the Killer Bore (Zn) and Jasper Ridge (Cu) prospects, some 11–15 km southwest of Pegmont, are not. In the absence of other considerations, such results are worthy of follow-up by an explorer. Killer Bore, for example, is a buried Zn-Pb occurrence with a Zn intersection of 258 m @ 0.15% drilled by BHP/Aberfoyle in the mid-1990s (note, it is erroneously identified as simply "Kuridala" in the P480 database). Similarly, one of only two data points for the Anitra Cu prospect, located 7.5 km to the south of Killer Bore, plots amongst the DS data for the Dugald River deposit and is therefore of interest; but those of the Jolimont Cu occurrence, a few kilometres to the east, lack evidence of both Soldiers Cap and Kuridala event Pb.

For contrast, the large spread evident in the data for outcropping gossan with 0.1–1.8% Pb at the Venture Cu-Pb-Zn occurrence suggests an unfocussed system comprising multiple Pb sources.

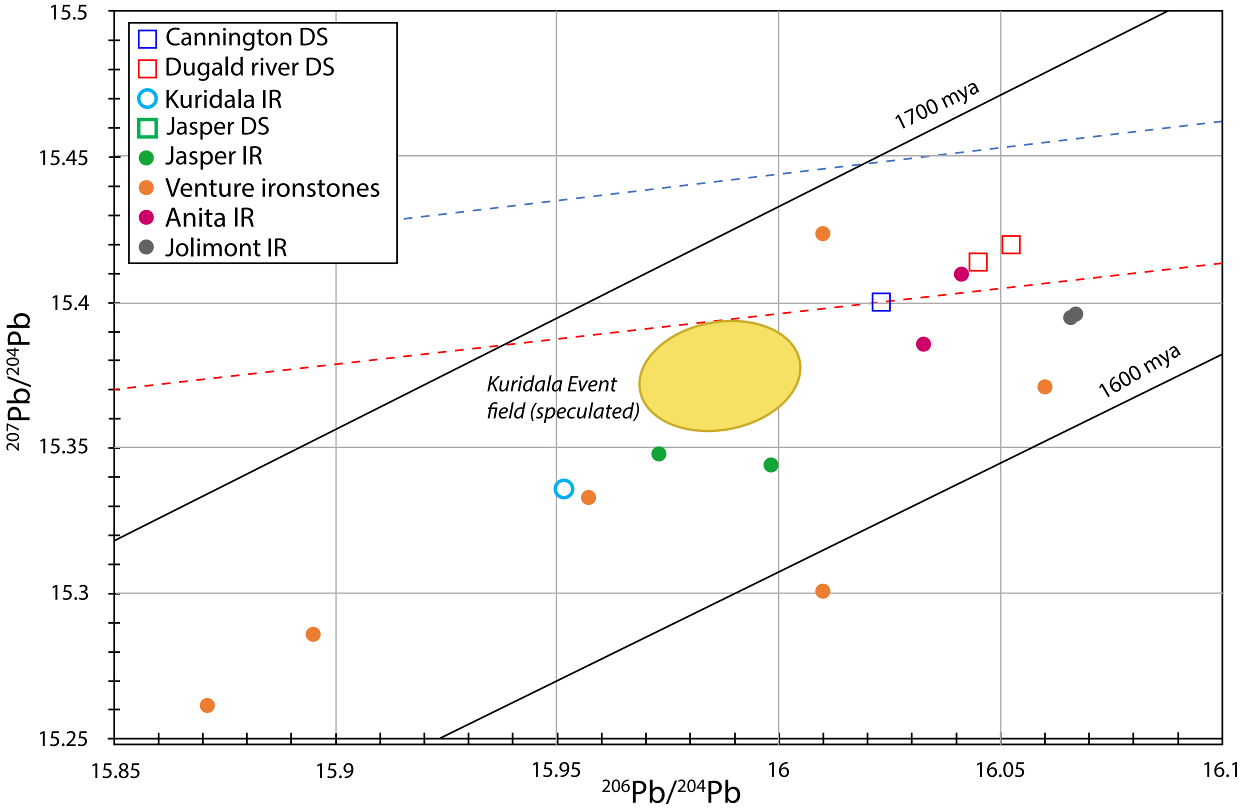

Figure 3.4. Conventional Pb isotope plot of high Pb samples from prospects hosted in the Kuridala formation or Answer Slate, showing the sub-EFB growth curve field of the posited Kuridala Event.

Surface sample results with single source and multi-stage characteristics

Figure 3.5 applies to the data for high Pb surface samples of BIF from the Fairmile prospect (0.4–7.2% Pb). This is an instructive data set because it further exemplifies the mixed origin of the largest Pb occurrences in the Eastern Fold Belt, but also the importance of obtaining several samples, with representative outcrop coverage, to avoid drawing wrong conclusions about the potential of a prospect, or area, based on reconnaissance Pb-isotope determinations.

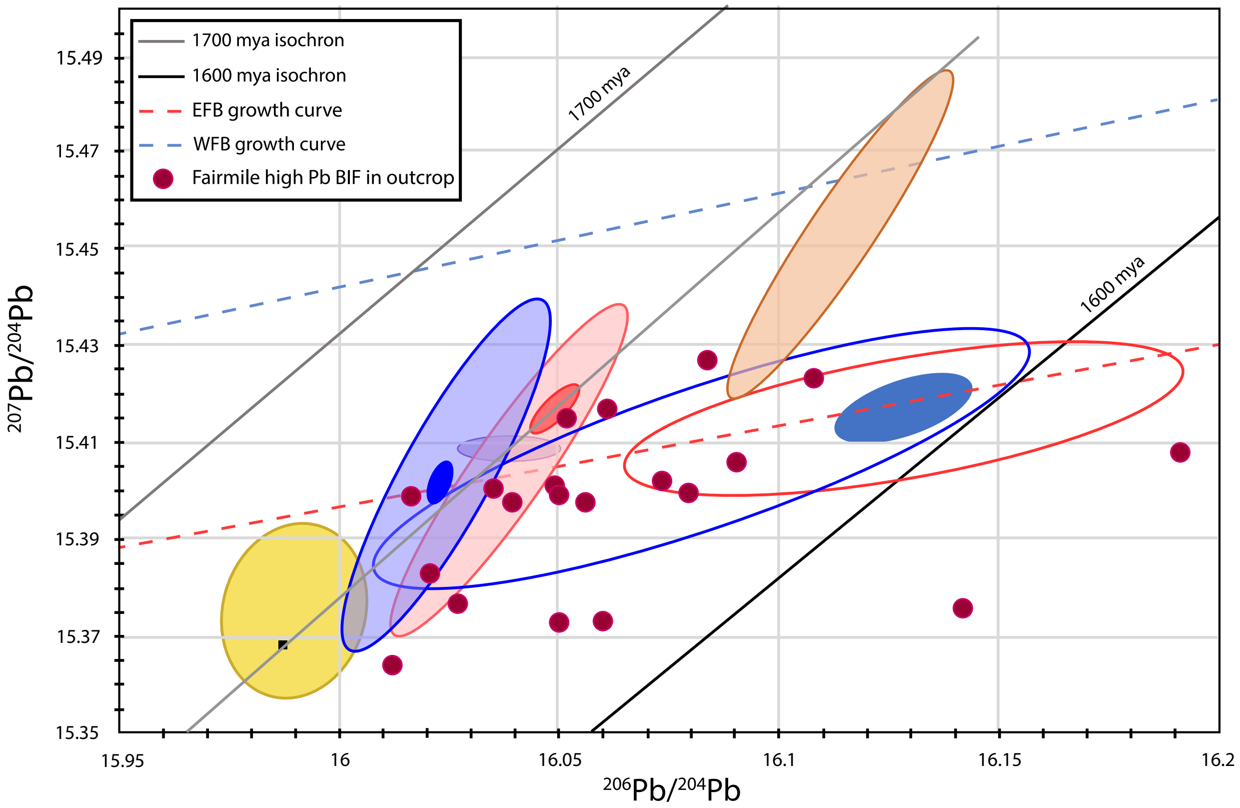

Figure 3.5. Conventional Pb isotope plot of high Pb BIF samples, in outcrop, from the Fairmile Zn-Pb deposit, in relation to enclosure ellipses of major deposits and their Isan Orogeny overprint fields (see legend of Figure 3.3).

Firstly, a reminder that the single double spike analysis of galena extracted from outcropping BIF plots very near the double spike data for Cannington and Pegmont, and drill hole galena samples plot in the mainstage Cannington/Pegmont/Dugald River ellipse (refer to Figure 3.3). Secondly, most of the conventional results for surface BIF samples, which probably should be referred to as gossan, plot in the general vicinity of previously discussed pop2/overprint ellipses. Therefore, the Fairmile gossans would be of fundamental interest to an explorer, in the absence of any drilling results, as they exhibit evidence of Pb introduced by both the Soldiers Cap Event and the Isan Orogeny. Interestingly, the relatively large number of data points appears to include a sub-population of five or six low $^{207}Pb/^{204}Pb$ which may indicate a contribution of a second, more amphibolitic or mafic rock-influenced source.

Surface sample results with initial ratios but lacking main event Pb

In the case of the distinctive Monakoff and Casablanca prospects (Figure 3.6), the high Pb samples plot within or near the ‘population 2’ ellipse of the Dugald River deposit. That is, they appear to contain only post-Soldiers Cap Event Pb, in contrast to the mixed Pb character of the previously discussed sub-economic deposits like Fairmile and Maronan. Furthermore, the spread of 0.15 $^{206}Pb/^{204}Pb$ units in the Monakoff data applies to texturally similar samples

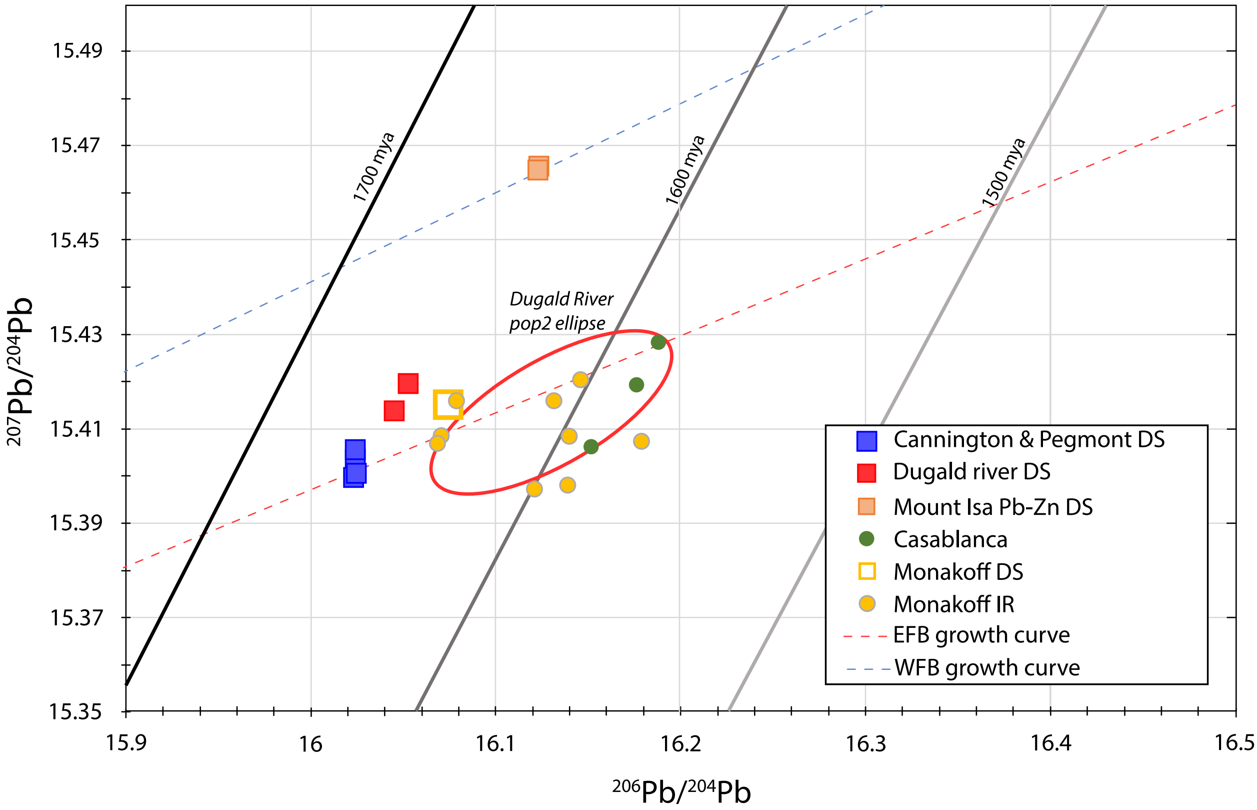

Figure 3.6. Conventional Pb isotope plot of Pb-rich prospects lacking evidence of a Soldiers Cap Event component.

within 5 metres of one another (according to grid references supplied with P480 data base). It is therefore reasonable to conclude that the distinctive Pb-rich Cu-Au mineralisation at Monakoff is the result of incremental hydrothermal inputs over a significant period *after* the Soldiers Cap event; that is, a product of the episodic Isan Orogeny. Multiple fluid sources are also likely but more, carefully located spike data would be required for confirmation.

How low can you go?

The question now asked is, what is the minimum level of Pb required in a sample to ensure that analysis will yield initial Pb isotope ratios? In Figure 3.7, the data for miscellaneous Eastern Fold Belt prospects with more than 950 ppm Pb are all interpreted as initial ratios (magenta-fill circles). They include previously plotted data for Monakoff (6), Casablanca (1) and Anitra (1), and data for Boorama (1), Blackrock (3), Cowie (1), Dingo (3) and Gidyea (1). Nearly all the samples plot within the pop2 fields of Cannington and Dugald River, suggesting an Isan Orogeny pedigree.

Prospect samples classified as “low Pb” and with a reported Pb assay of <200 ppm, or without a reported Pb value, are plotted as olive-fill circles (Blackrock 1, Camp Grid Gossan 4, Cowie 1, Monakoff 8 and Percy Bore 2). Most (15 of 16), plot beyond the pop2 fields of the major deposits, with $^{206}Pb/^{204}Pb$ ratios of more than 16.2, and within the extensive band of compositions exhibited by Eastern Fold Belt IOCG deposits and prospects. Any samples which plot within this band, indicated by the gold polygon (and extended in Figure 3.9), were probably ‘shifted’ from lower, Isan Orogeny ratios by the *in situ* radiogenic decay of contained U. For samples now with < 200 ppm Pb, measurable radiogenic shifts are easily achieved over 100s of millions of years without the need for above background levels of U (*i.e.*, less than 0.5–2.5 ppm for most rock types).

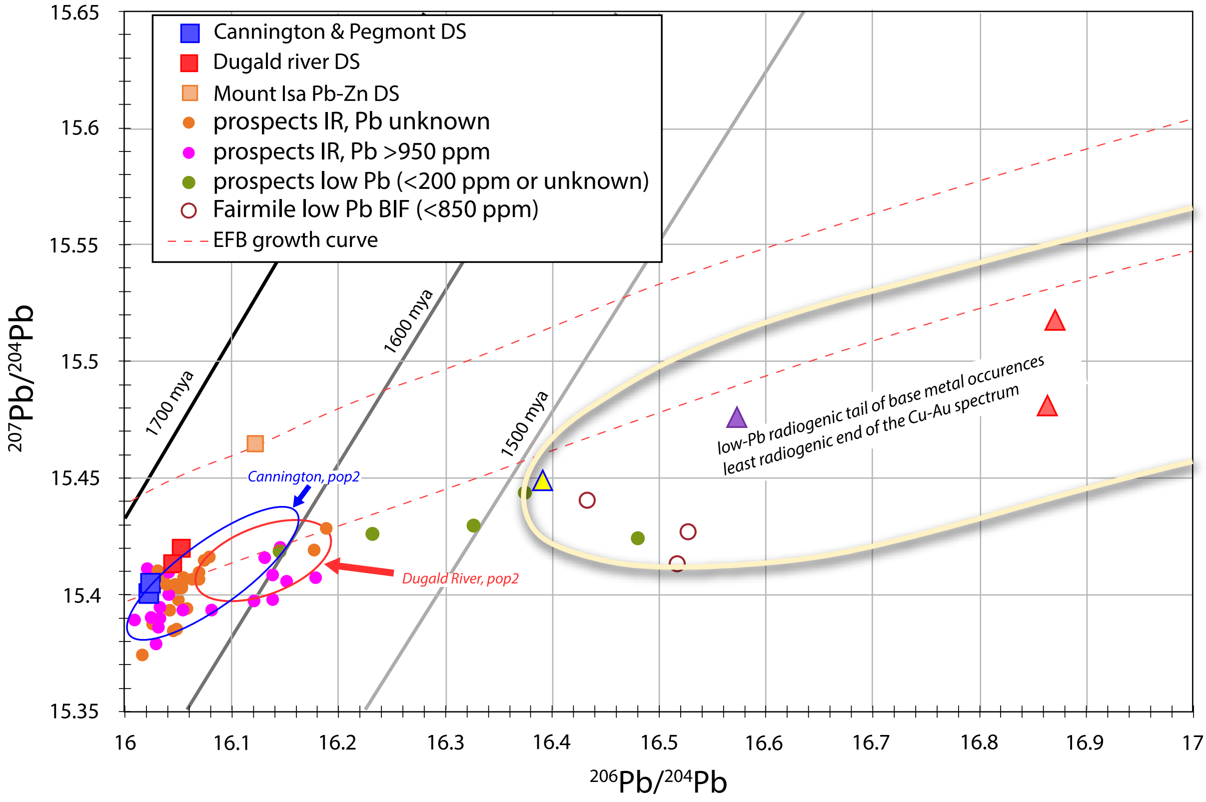

Figure 3.7. Conventional Pb isotope plot of grouped miscellaneous Pb-rich prospects: comparing high and low Pb samples, relative to the Soldiers Cap Event overprint fields (pop2 samples, major Pb-Zn-Ag deposits) and the beginning of the radiogenic Pb trend of IOCG deposits and prospects.

Fairmile samples classified as 'low Pb' (maroon rings), but with 400–850 ppm Pb, also plot in the radiogenic data trend of Figure 3.7 (and its extension in Figure 3.9). Modelling indicated that between 10 and 70 ppm U would have been required to produce the observed shift from initial mid-Proterozoic ratios. With background U abundances, these samples would probably have been shifted by only about 0.1 $^{206}Pb/^{204}Pb$ units, as demonstrated by the 750 ppm Fairmile "low Pb" sample in the Pb versus $^{206}Pb/^{204}Pb$ plot of Figure 3.8A. The clear inverse relationship between Pb content and $^{206}Pb/^{204}Pb$ in Figure 3.8B and the likelihood that the Fairmile BIF is U-anomalous supports the P480 researcher's interpretation (Carr *et al.*, 2001). For contrast, 'low Pb' *and* low U samples at Mine Isa Mine don't appear to exhibit evidence of radiogenic shift in samples unless they contain less than 200–300 ppm Pb (Figure 3.8B).

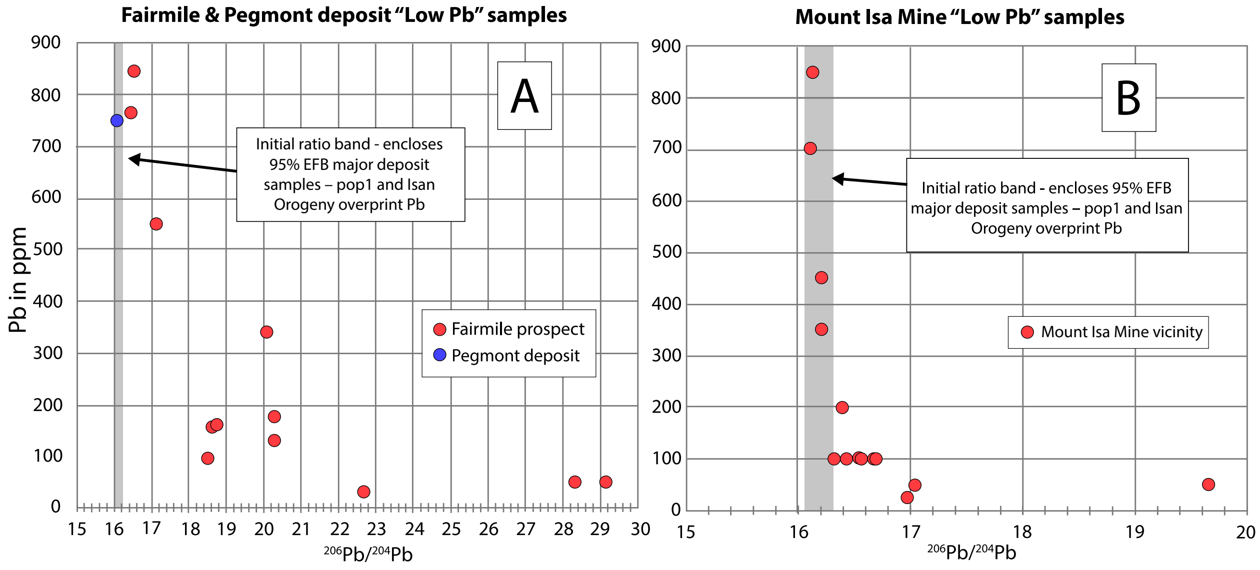

Figure 3.8. Pb content versus Pb isotopic composition plot of samples classified as 'low Pb' from Fairmile and Pegmont (A) and the vicinity of Mount Isa Mine (B).

Cu-Au systems, Eastern Fold Belt—an overview

All the available data for mineralised Pb-poor systems in the Eastern Succession correspond to samples with very low Pb contents (generally less than 50 ppm). Consequently, the identity or age of specific mineralisation events, or the age of last remobilisation, must be interpreted from arrays of *radiogenic* rather than *initial* Pb isotope ratios.

Thirty seven of the 115 data points are displayed in Figure 3.9, which extends to a $^{206}Pb/^{204}Pb$ ratio of 30. The remainder plot off-scale, but on the same trend with $^{206}Pb/^{204}Pb$ ratios of up to 100 or more. All the major deposits in the IOCG spectrum of the Eastern Fold Belt are represented, including Ernest Henry, Osborne, Starra and Eloise.

In the P480 Final Report of Carr *et al.* (2001) the results for individual deposits such as Ernest Henry, Starra and Eloise are examined in detail. To summarise, the data from several deposits can be modelled to fit reasonably convincing secondary isochrons, either by:

a. single stage Pb isotope growth initiated at a specific time in the Proterozoic (varying from 1511 Ma in the case of Starra data to about 1450 Ma in the case of Ernest Henry), or

b. two stage Pb isotope growth consisting of an array of data points on a steep slope, corresponding to early, perhaps multi-stage mineralisation and Pb-isotope growth (pre-1500 Ma) and a less steep array corresponding to growth since the last significant overprint event (1500 to 1000 Ma).

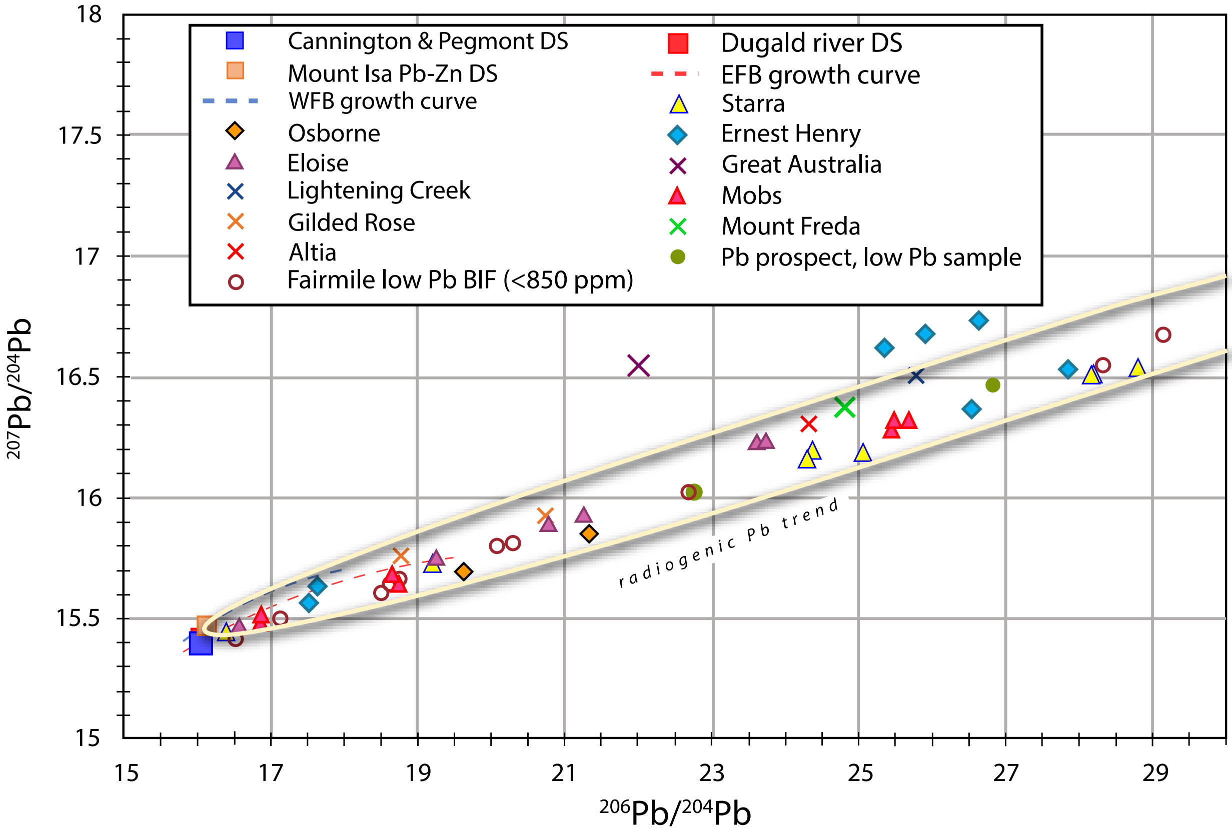

Figure 3.9. Conventional Pb isotope ratio plot of Eastern Fold Belt IOCG deposits and prospect samples in relation to a 95% enclosure ellipse referred to as the radiogenic Pb trend (which extends off-scale to $^{206}Pb/^{204}Pb$ values of 100 or more).

Some Pb in these deposits is estimated from the secondary isochrons to be older than Soldiers Cap Group rocks (*viz.*, 1750 Ma in the Great Australia deposit and 1670 Ma in the Osborne deposit). However, all the studied Eastern Succession Cu-Au deposits are interpreted, from Pb-isotope arrays, to have formed after the Soldiers Cap Event, during one phase or other of the Isan Orogeny.

From the perspective of an exploration geologist, there is little advantage to be gained from applying the Pb isotope technique to low-Pb target styles such as Cu-Au systems in the Eastern Succession. The most that can be gained is an approximate age of the most significant overprint event (*i.e.*, time of U addition or loss), and perhaps an indication of the age of mineralisation from the slope of secondary isochrons. In both cases, sufficient samples are needed to construct individual isochrons, which are subject to considerable uncertainty and subjectivity of interpretation.

Field sampling and laboratory analysis

Field sampling

Standard sampling practices for outcrop, including gossan, and drill hole materials are adequate for Pb isotope determinations. Contamination by petrochemicals and drilling muds must be avoided.

Laboratory analysis

Low precision analysis

The major mineral laboratory groups in Australia, such as ALS, SGS and Bureau Veritas, provide Pb isotope analyses by quadrupole ICP-MS. With this method, ratios such $^{207}Pb/^{204}Pb$ and $^{206}Pb/^{204}Pb$ are reported with precisions of about 1% (nominally accurate to 3 significant figures, usually the first decimal place). The isotopic analysis follows a standard whole rock analysis by 4-acid digestion with ICPMS finish (for a total price of about $50). The total Pb content, provided by the whole rock analysis, determines the level of dilution required for the separate Pb isotope measurement step.

This alternative is adequate for reconnaissance investigations, where the explorer is concerned with broad system fingerprinting rather than system mapping and dating. The analytical procedure is very sensitive and can be applied to samples with as little as 5 ppm Pb, though it should be remembered that ‘initial ratios’ are increasingly unlikely with decreasing Pb content. Data delivery is likely to take up to 4 weeks.

High precision analysis

High precision (better than 0.1%) Pb isotope analysis using Thermal Ionisation Mass Spectroscopy (TIMS) is not commercially available in Australia, but can be accessed at University facilities, such as the John de Laeter Centre (Curtin University, W.A,) or through ALS, which has a service arrangement with the semi-commercial facility at the University of British Columbia. Measurement costs of $300–$400 are expected, but preparation costs are dependent on Pb content and potential interfering elements such as Hg. Explorers should budget at least $700 per sample and expect data delivery to take 2–3 months.

Thermal Ionisation Mass Spectrometry (TIMS) provides the levels of precision discussed earlier in relation to the double spike procedure. Thus, it is appropriate for detailed prospect evaluation where a knowledge of spread along a growth curve and system longevity or complexity is sought.

Other high precision techniques, such as HR ICPMS (high resolution, multi-sector), MC ICPMS (multi-collector) and laser ablation ICPMS are available at various institutional analytical centres within Australia. The John de Laeter Centre also offers double spike Pb isotope analysis by MC ICPMS, in preference to TIMS, for $600 per sample and the option of reduced prices for collaboration with broader research programs.

Discussion and summary

1. The largest Pb deposits in the Eastern Fold Belt have almost indistinguishable Pb isotope systematics. The data are consistent with mineralisation during the so-called Soldiers Cap Event (well-mixed crustal fluids at about 1665 Ma.), and overprinting, to varying degrees, by younger Pb introduced during the Isan Orogeny (multi-phase, 1585–1490 Ma.)
2. Systematic variations in a small number of high precision, double spike Pb isotope determinations from each of the major deposits indicate that the Pb in each deposit was sourced from reservoirs with slightly different bulk U/Pb compositions.
3. The Isan Orogeny overprint is expressed in the major deposits by texturally late galena, and by an associated spread in observed Pb isotope values. The spread encompasses the range of compositions recorded for smaller and sparsely sampled Eastern Succession Pb prospects.
4. The only Pb-rich prospects that seem to completely lack Soldiers Cap Event Pb are the polymetallic occurrences of Monakoff and Casablanca (Isan Orogeny Pb and radiogenic Pb, only).
5. Pre-Isan Orogeny Pb, with distinctively lower $Pb^{207/204}$ ratios than those observed in known Pb deposits like Cannington and Dugald River, is evident in the galena of prospects hosted by the Kuridala Formation and Answer Slate. However, insufficient data is available to assess the implied possibility that a significant Pb-rich hydrothermal system affected these parts of the Mary Kathleen Group in the south of the Eastern Fold Belt.
6. Exploration samples with as little as 200 ppm Pb, and background U levels, have a high probability of retaining initial (syn-mineralisation) Pb isotope ratios. For typically uranium-anomalous IOCG mineralisation, a Pb content of less than 750 ppm is likely to be influenced by the addition of radiogenic Pb after the mineralisation event.
7. Interpretations of Pb isotope data for Eastern Fold Belt Cu-Au deposits are based on modelled secondary isochrons because initial ratios have been substantially modified by post-mineralisation U decay. All studied deposits and prospects are interpreted to have formed after the Soldiers Cap Event, during one phase or other of the Isan Orogeny.
8. The geologic, textural and spatial context of individual samples in the P480 database are recorded sparingly and inconsistently. Pb and U data are often absent. These shortcomings impair the user's ability to consider fundamental factors, like sample distribution and sample niche, in assessing, as an example, the comparatively few Pb isotope data for individual prospects with the numerous data for individual major deposits. To achieve maximum advantage from the Pb isotope method term, explorers and institutional researchers must ensure full data attribution, *viz.*, 3D locational coordinates, sample site and material context (scale, rock type, fabrics, mineralogy *etc.*) and essential chemical parameters such as U and Pb contents.
9. The lack of consistently attributed data, particularly with respect to location, limits an evaluation of the potential of Pb isotope analysis to reveal gradients or vectors to ore. A small subset of data for 'low Pb' samples from the vicinity of Mount Isa Mine suggests that radiogenic 'tails' do not offer encouragement in this respect.
10. Though not treated in this document, the metallogenic fingerprinting potential of Pb isotope analysis extends to other exploration sample media, including groundwater (*e.g.*, de Caritat *et al.*, 2005) and vegetation (*e.g.*, Carr, 2013), and even alluvium. The versatility of the method extends to the recognition of contamination in sample media most likely to be affected by human interference (*op. cit.*).

Chapter 4

Bedrock geochemistry: Stable isotopes carbonate O and C, sulphide S

Introduction

The stable isotopes of oxygen, carbon, and sulphur are typically used in the field of economic geology to identify the likely sources of ore-forming fluids and the temperature, Eh and pH of fluid-rock interactions leading to mineralisation. They play an important role in the development of ore genesis models which underpin the early, generative phases of mineral exploration programs. Stable isotopes are also actively used in exploration to (a) assess the implicit assumptions of models and adjust exploration tactics accordingly and, (b) 'vector' to ore, by mapping patterns and gradients (*i.e.,* haloes) in isotopic ratios as a record of the passage and intensity of hydrothermal fluid flow. The sulfur isotopes of sulfides are typically utilised for the former task and examples from the Mount Isa region are provided. Vectoring requires the preservation of physico-chemical gradients.

Oxygen, carbon and sulfur each occur as several isotopes in nature. For oxygen, the ratio of two of its isotopes, ^{18}O and ^{16}O, is expressed as a deviation or del (δ) in parts per thousand (per mil, or ‰), from that of mean standardised ocean water (SMOW). Thus, a sample with a $\delta^{18}O_{SMOW}$ value of 10‰ is enriched in the heavier ^{18}O by 10 parts per thousand relative to SMOW. Equivalent systematics are applied to specific isotopes of carbon (^{13}C and ^{12}C) and sulphur (^{34}S and ^{32}S), using relevant standards, and reported as $\delta^{13}C_{PDB}$ and $\delta^{34}S_{CDT}$, respectively.

Each of the three systems is responsive to temperature, pH, Eh and mixing (fluid-fluid or fluid-wallrock). Rock or mineral-replacive alteration and mineralisation is essentially a mixing effect, quantifiable in terms of water-rock ratios (W/R). For example, because they formed largely from seawater, unaltered limestones and dolomitic sedimentary rocks have a marine oxygen isotopic signature (*i.e.,* $\delta^{18}O$ values exceed 20 per mil). Most hydrothermal fluids are shown to have a 'lighter' oxygen isotopic signature (*viz.,* $\delta^{18}O$ values of less than 12 per mil). Thus, when such fluids infiltrate and exchange oxygen with a rock containing 'marine' carbonate, the host rock $\delta^{18}O$ value progressively diminishes as more of the 'lighter' fluid passes through. Provided enough fluid is available, the host rock will eventually reach oxygen isotopic equilibrium with the fluid. Even at this stage the host rock will not necessarily display obvious signs of recrystallisation or alteration. The key implication is that, assuming other parameters, such as temperature, fluid Eh, and fluid $\delta^{18}O$ are known (usually the case for major mining districts), the $\delta^{18}O$ values of the carbonate component of scout samples, *e.g.*, in spaced drill holes, could reveal direction-of-fluid flow and intensity of reaction information. Logically, the greater the difference between the oxygen isotopic composition of the fluid and the carbonate of the recipient rock mass, the easier it should be to recognise and 'map' the effects of mixing between the two oxygen reservoirs. The voluminous silica-dolomite assemblage surrounding the Mount Isa copper ore bodies provides the type example of how zoned oxygen and carbon isotopic ratios in hydrothermal carbonate over very large distances can be used to estimate both the direction and distance to high grade, Mount Isa-style Cu mineralisation.

Chapter 4

CIT—Carbonate Isotopic Technique

Background

The presence of measurable gradients in the distribution of O and C isotope ratios in carbonate within and above silica-dolomite masses surrounding the Mount Isa copper orebodies was established by Waring (1990). ‘Lighter’ ratios are recorded closest to syn-mineralisation faults and the quartz-rich, high-grade Cu ‘cores’ of individual silica-dolomite lobes. The isotopic ratios become progressively ‘heavier’ trending vertically and laterally away from the strongly veined and brecciated zone towards the well bedded replacive dolomitic siltstone rocks. Figure 4.1 depicts mine-scale raw data with interpreted $\delta^{18}O$ contours. Data were analysed from 5 m of ½ core composites which were crushed, pulverised, and subsampled for O and C isotopic analysis. The entire range of isotopic ratios within the silica-dolomite zone is collectively lighter than the Proterozoic marine carbonate background signature of the host Urquhart Shale (Figure 4.2). Furthermore, the silica-dolomite ‘trend’ extends into strongly altered and carbonate-altered metabasalts structurally beneath the Cu orebodies, which were both an ore fluid conduit (Hannan *et al.,* 1993) and Cu-source (Heinrich *et al.,* 1989).

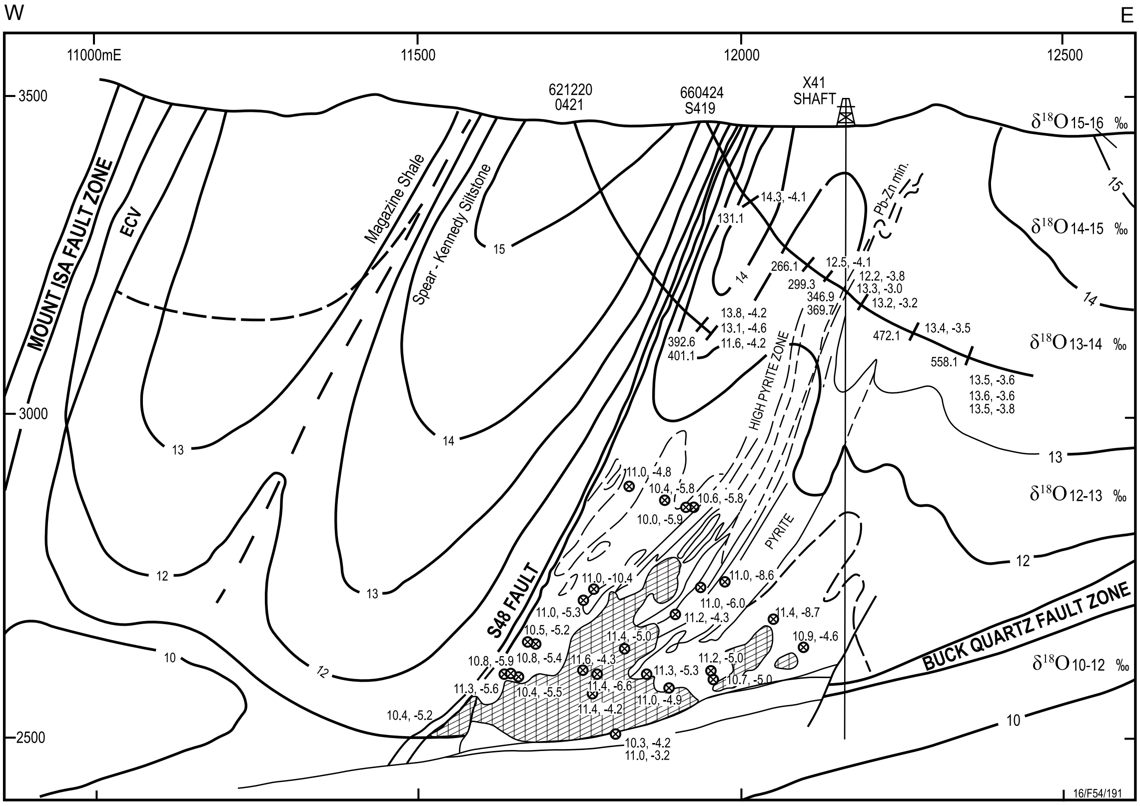

Figure 4.1. Composite cross section of Mount Isa Mine centred at 34200 mN showing carbonate O and C isotopic data along drill holes, interpreted $\delta^{18}O$ contours and the simplified geology (from Waring et al., 1998).

To ascertain that the observed gradients are a feature of the ore paragenesis and not simply fault-associated, MIM Exploration analysed the cores of a vent shaft scout hole (V334) from the surface into a lobe of the southernmost hangingwall of the 1100 orebody at a depth of 800 m (Figure 4.3). The drill hole transects a continuum of visibly unaltered and unmineralised Urquhart Shale, through increasingly veined wall rock, to well-developed silica-dolomite without the presence of Pb-Zn mineralisation and without disruption by major faults. The resulting carbonate isotopic data show an unequivocal trend of decreasing $\delta^{18}O$ (and $\delta^{13}C$), in both

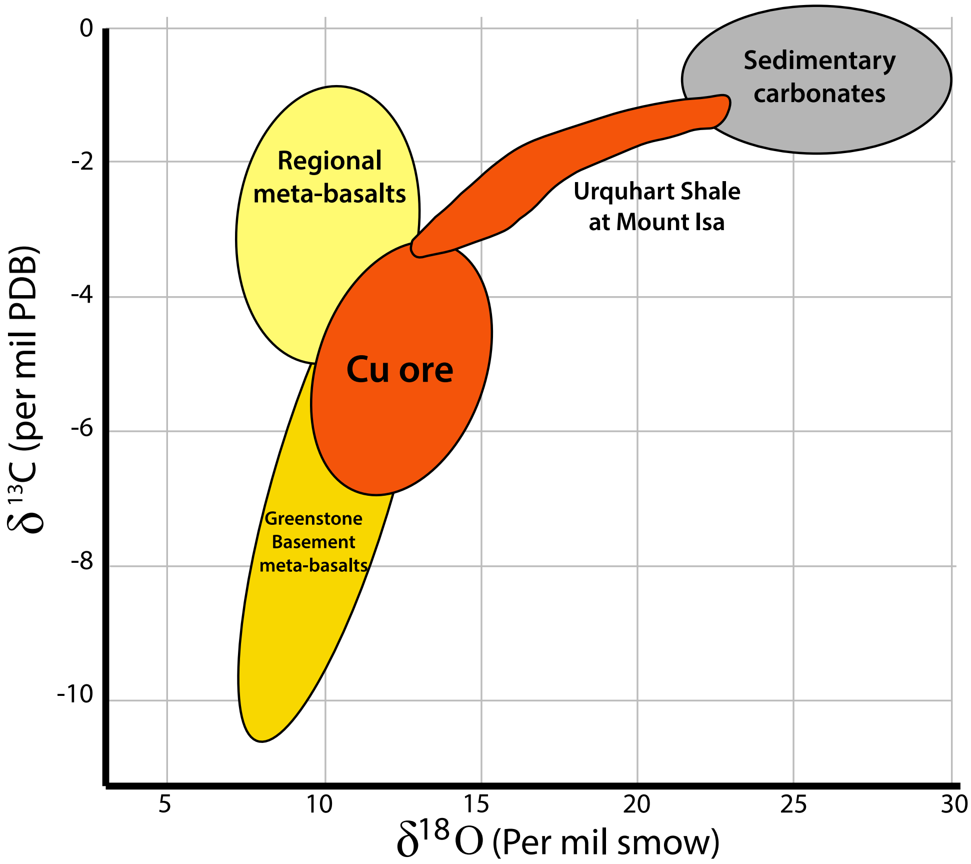

Figure 4.2. Summary of O and C isotopic compositions of carbonate in Urquhart Shale and Eastern Creek Volcanics, Mount Isa district (from Hannan et al., 1993, modified).

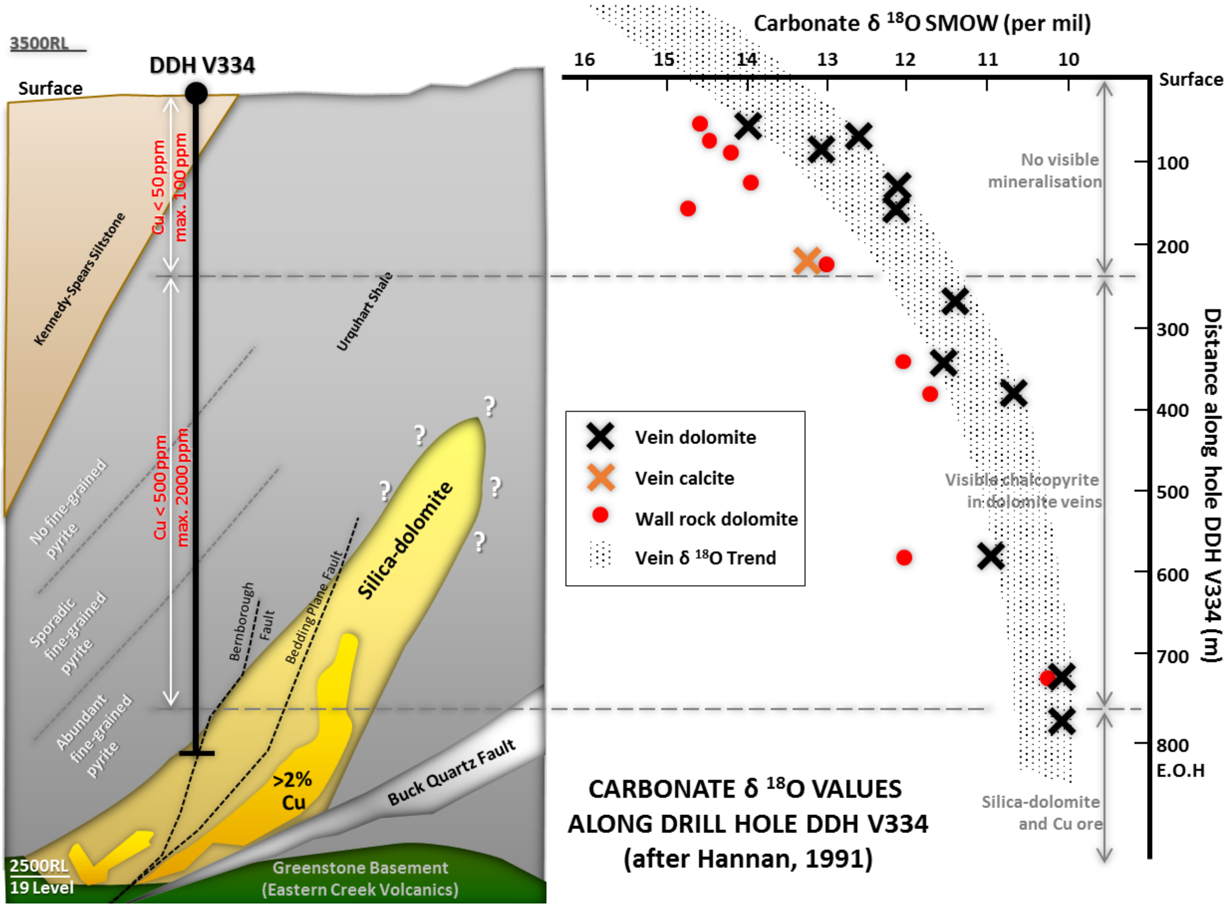

Figure 4.3. Left: cross section of Mount Isa Mine at 3340 mN with trace of drillhole V334 and simplified geology; right: carbonate (dolomite) O isotopic composition versus depth for DDH V334. (from Hannan, 1991)

wallrock and vein samples down the length of the drill hole. Samples consisted of 'spot' volumes of about 5 x 2 x 2 cm of core, in strong contrast to the mine-scale coverage.

Although Cu assays were never acquired, the labelled Cu abundance inferences in Figure 4.3 are based on the logs and assays of other mine drill holes. Decreasing $\delta^{18}O$ values are clear in the upper 200 m of core, where the Urquhart Shale is sparsely veined and without visible copper sulphide, affirming the potential of the carbonate isotopic technique (CIT) for detecting the distal expressions of Mount Isa style Cu "systems" in exploration drill holes in similar stratigraphic settings (Waring, 1991).

Based on the gradients observed at Mount Isa mine (22 Mt Cu metal), the cross-sectional dimensions of an $\delta^{18}O$-in-carbonate anomaly associated with smaller economic Cu targets can be estimated by simple scaling, with all other controlling parameters held constant. Figure 4.4 compares the $\delta^{18}O$ contours of a scaled 250 Mt orebody, like the 1100 Cu orebody at Mount Isa (5 Mt Cu metal at 2% cut-off), with those of a 30 Mt equivalent at the same depth (750 m). In practice, the interplay of fault orientations and bedding geometries affects the uniformly shaped reaction volumes and consistent gradients over large distances. However, the steepening of gradients with decreasing target size implicit in the models of Figure 4.4 is confirmed in practice, and provides a realistic interpretative framework for the explorer, as well as a guide for planning sample or drill hole spacings.

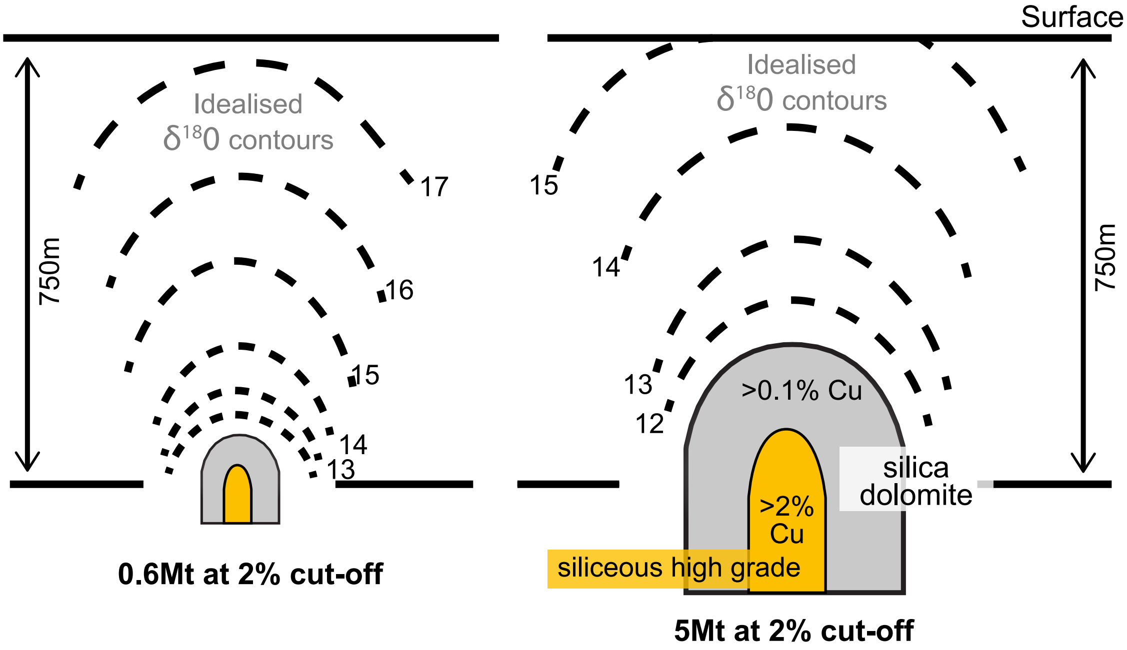

Figure 4.4. Cross sectional view of scaled and idealised $\delta^{18}O$ contours above two Mount Isa-style Cu orebodies (from Hannan, 1991).

Examples

The anomaly above the entire system of Cu orebodies is enormous, with a N-S strike length of at least 8 km, width of 1.6 km and depth extent of at least 1 km (Figure 4.1). $\delta^{18}O$ gradients around the silica-dolomite lobes of Cu ore at Mount Isa vary from about 0.4 to 0.7‰ per 100 m (*e.g.*, V334 and the 5 Mt model of Figure 4.4). However, broader gradients are present in the large volume of stratigraphically higher rock west of the S48, that lack a down-dip ore lode and large volume of silica-dolomite, even though weak Cu mineralisation and patchy silica-dolomite veining are present (Figure 4.5).

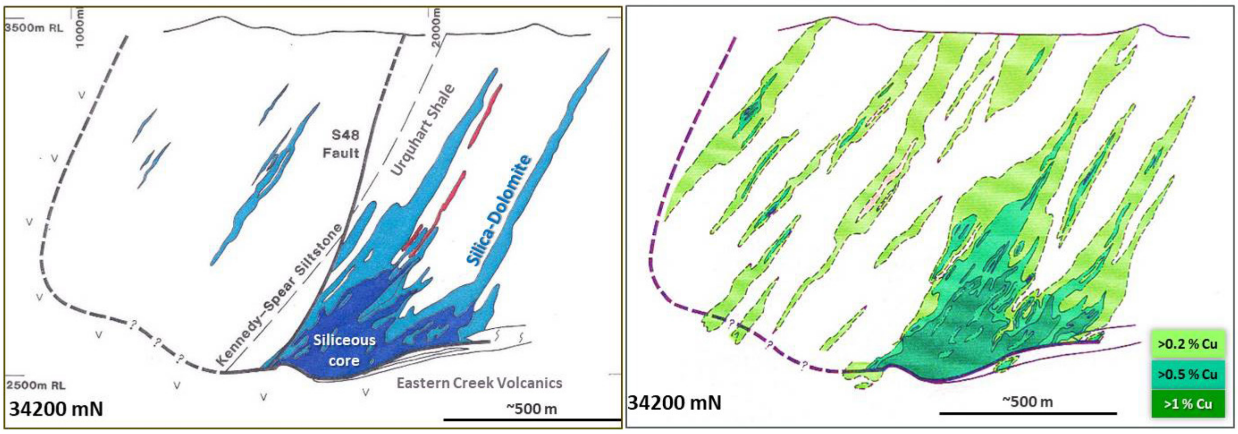

Figure 4.5. Summarised distributions of silica-dolomite (left) and copper grades (right) for a composite section of Mount Isa Mine centred at 34200 mN (from Hannan et. al., 1991).

The implication is that, without all the key 'ingredients' of the Mount Isa Cu ore system (*e.g.*, Perkins *et al.,* 2011), depletion halos without significant mineralisation are a possibility. For example, a hydrothermal fluid may be insufficiently saline, or the structural-geometric conditions for prolonged dilation to promote silica-dolomitisation and chalcopyrite precipitation may be absent. Thus, intersections of hundreds of metres in a δ^{18}O-depleted host with little or no decrease towards the anticipated target is an unfavourable outcome, especially if quartz-dolomite veining is weak or absent. This scenario was evident at the Buckley River copper project, 60 km northwest of Mount Isa, where large volumes of the Paradise Creek Formation (McNamara Group) were drilled by MIM Exploration in the mid-1990s to follow up fault-associated Cu mineralisation at the surface and a Mount Isa-like structural setting at depth (*i.e.,* a sub-horizontal structure at depth).

Much steeper δ^{18}O gradients, of more than 2‰ per 100 m, are observed at smaller Cu prospects where silica-dolomite alteration is confined to the vicinity of steep faults. There are also notable differences in the results for wall rock and vein pairs (>3‰) compared to those at Mount Isa mine (<2‰), consistent with less penetrative fluid-rock mixing and, perhaps, short-lived systems. The curvilinear Spillway Fault on the northwest shore of Lake Moondarra, 18 km NNE of Mount Isa, provides a clear example. As at Mount Isa mine, this 'old' fault separates Urquhart Shale and Eastern Creek Volcanics (ECV) (Figure 4.6A). Gossan along the fault trace is texturally consistent with a silica dolomite precursor. Two drill holes into the structure from the southeast, LA004 and LA007, intersected sporadic alteration and Cu mineralisation but have δ^{18}O-in-carbonate profiles which increase from 13–4‰ at the fault to almost background values of 18–19‰ some 250 m from the fault (Figures 6B, C). The steep gradient (2–4‰/100 m), lack of wall rock depletion to Mount Isa-like ore system levels (<12‰), and a difference of 3.6‰ between the wall rock and vein pair in LA007 (at 324 m), are all consistent with weak system and the absence of significant mineralisation within 1 km, or more, of the surface.

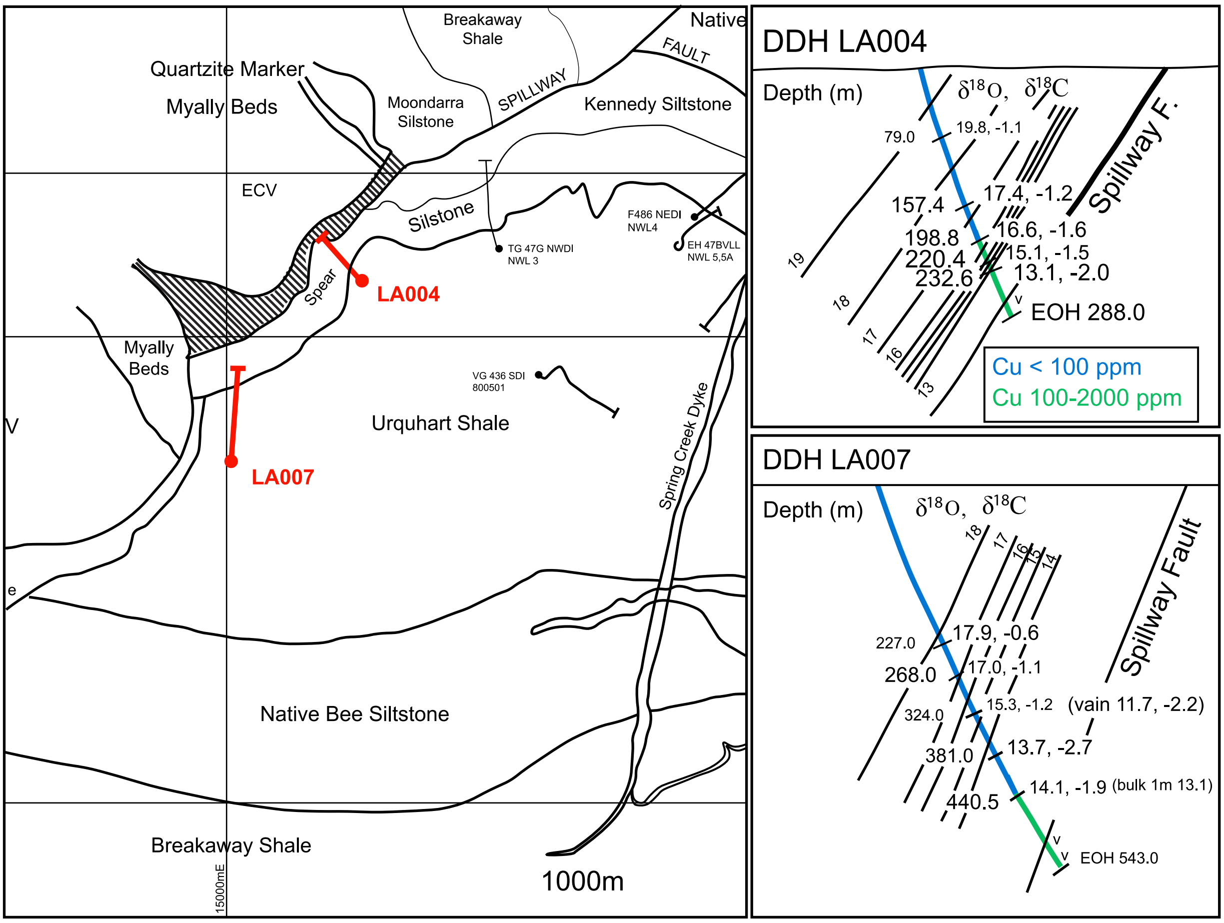

Figure 4.6. Northwest Lakes project area map and drill sections; A: geologic map with drill hole traces; B & C: distributions of carbonate $\delta^{18}O$ and $\delta^{13}C$ in 2 drill holes to ECV basement (from Hannan, 1992).

Applicability in the region

Western Fold Belt

An important premise of the CIT is that diagenesis and low-grade metamorphism had largely homogenised the O and C isotopic compositions of multiple generations of calcite and dolomite to produce a comparatively uniform reservoir for interaction and predictable isotopic exchange with later, syntectonic ore fluid. Mount Isa Group sedimentary rocks appear to meet this requirement, despite varying carbonate chemistries and modal abundances (Waring, 1991). However, other prospective and calcareous strata of the Carpentaria-Mount Isa 'zinc province' are generally sub-greenschist facies and it should not be assumed that the premise necessarily holds for specific formations of the McNamara and Fickling Groups in northwest Queensland, or the McArthur Group of McArthur Basin (N.T.).

Nevertheless, sufficient data is available to indicate that the CIT is appropriate in these settings if individual rock units are correctly identified and care is taken to maintain a consistent sample niche or 'facies' to maximise the likelihood of identifying an interaction gradient. Table 4.1 summarises the known carbonate O and C isotopic systematics of carbonate-associated Cu mineralisation in the Western Fold Belt and, for reference, Cu deposits near the HYC Zn-Pb mine in the McArthur Basin. Century domain occurrences are likely to display elevated $\delta^{18}O$ values (15–25‰), indicating proto ore-brines that probably exchanged with a reservoir of 'heavy' oxygen (*i.e.,* ^{18}O-rich) before mineralisation, most likely marine carbonate in the hosting basinal sediments (Jones, 1986). By contrast, occurrences in the Leichhardt River and

Table 4.1: Expected carbonate O and C isotope compositions and inferred fluid parameters for Mount Isa-style Cu systems in the Western Fold Belt and McArthur Basin.

Area	Structural domain	Carbonate component (wall rock and/or vein)		Rock-fluid interaction	Cluid	
	Stratigraphic position	$\delta^{18}O$ range	$\delta^{13}C$ range	Temperature	$\delta^{18}O$	$\delta^{13}C$
Mount Isa[1]	**Leichhardt River** middle Mount Isa Group	10.5 to 19‰	-7 to -1‰	325°C	5.5‰	-2.7‰
Buckley River[2]	**Mount Oxide** lower McNamara Group	12.5 to 21‰	-5 to 1‰	325°C	7.5‰	-0.2‰
Kamarga Dome[3]	**Century** lower McNamara Group	15.5 to 23‰	-6 to 0‰	325°C discordant Cu	10.5‰	-1‰
McArthur River[4]	**McArthur Basin** McArthur Group	18 to 25‰	-5 to -2‰	325°C discordant Cu	12.5‰	-2.8‰

Data sources: [1] Waring, 1991; [2] Hannan, 1993; [3] Jones, 1986 and Hannan, 1992b; [4] Rye & Williams, 1987

Mount Oxide domains of the Western Fold Belt are likely to show evidence of proto-ore fluid equilibration with some non-carbonate rocks, perhaps under metamorphic conditions, with $\delta^{18}O$ values between about 11 and 20‰.

Eastern Fold Belt

Calcareous metasedimentary rock in the Eastern Fold Belt is mostly restricted to the Corella and Doherty Formations of the Mary Kathleen Group and Stavely Formation of the Mount Albert Group. All these formations are scapolitic (Blake, 1982) and thought to have contained abundant evaporite before deep burial and metamorphism (*e.g.*, Warren, 2016). Though marine carbonate O and C isotope signatures are locally preserved, the three units are commonly intruded by mafic dykes and granites, metamorphosed to the amphibolite facies and extensively altered to calc-silicate assemblages, by scapolitisation and later albitisation (*e.g.*, Figure 4.7).

In the case of the widespread calcite pods, depicted in Figure 4.7, the isotope data suggest they are the product of infiltration of externally derived hydrothermal fluid, probably from crystallising magma, and that the L-shaped trend of the data on plots of $\delta^{13}C$ vs. $\delta^{18}O$ is indeed consistent with mixing (Oliver *et al.,* 1993). However, the transition between end-members corresponds to a visually unmistakeable assemblage of coarse grained calc-silicate (albite, amphibole, epidote, quartz) and there is no suggestion of a ‘cryptic’ halo extending into the finer-grained host metasediment (calcareous siltstone, granofels and marble of the Corella Formation).

In a major study of the carbonate O and C isotope systematics of the Eastern Fold Belt, which incorporated the Mary Kathleen Domain work discussed above, Marshall *et al.* (2006) showed that most data from the IOCG spectrum of Cu-Au ore systems lie within a three-end-member mixing grid comprising marine meta-carbonate rocks, graphitic metasedimentary rocks and sodic-calcic alteration of likely magmatic-hydrothermal origin. So, like the calc-silicate fringes of Mary Kathleen area calcite pods, the Cu-Au ore deposit data reflects varying degrees of equilibration between the fluid responsible for sodic-calcic alteration and demonstrably local metasedimentary rocks. A similar conclusion was reached in a separate and earlier assessment of silicate oxygen and hydrogen isotope data for the extensive sodic-calcic alteration system (Mark *et al.,* 2004).

For example, the data for the Ernest Henry deposit, hosted by the Mary Kathleen Group, indicate minimal involvement of carbonaceous strata (Figure 4.8a), in contrast to those of the Great Australia deposit, which is hosted by the shale-rich Soldiers Cap Group (Figure 4.8b).

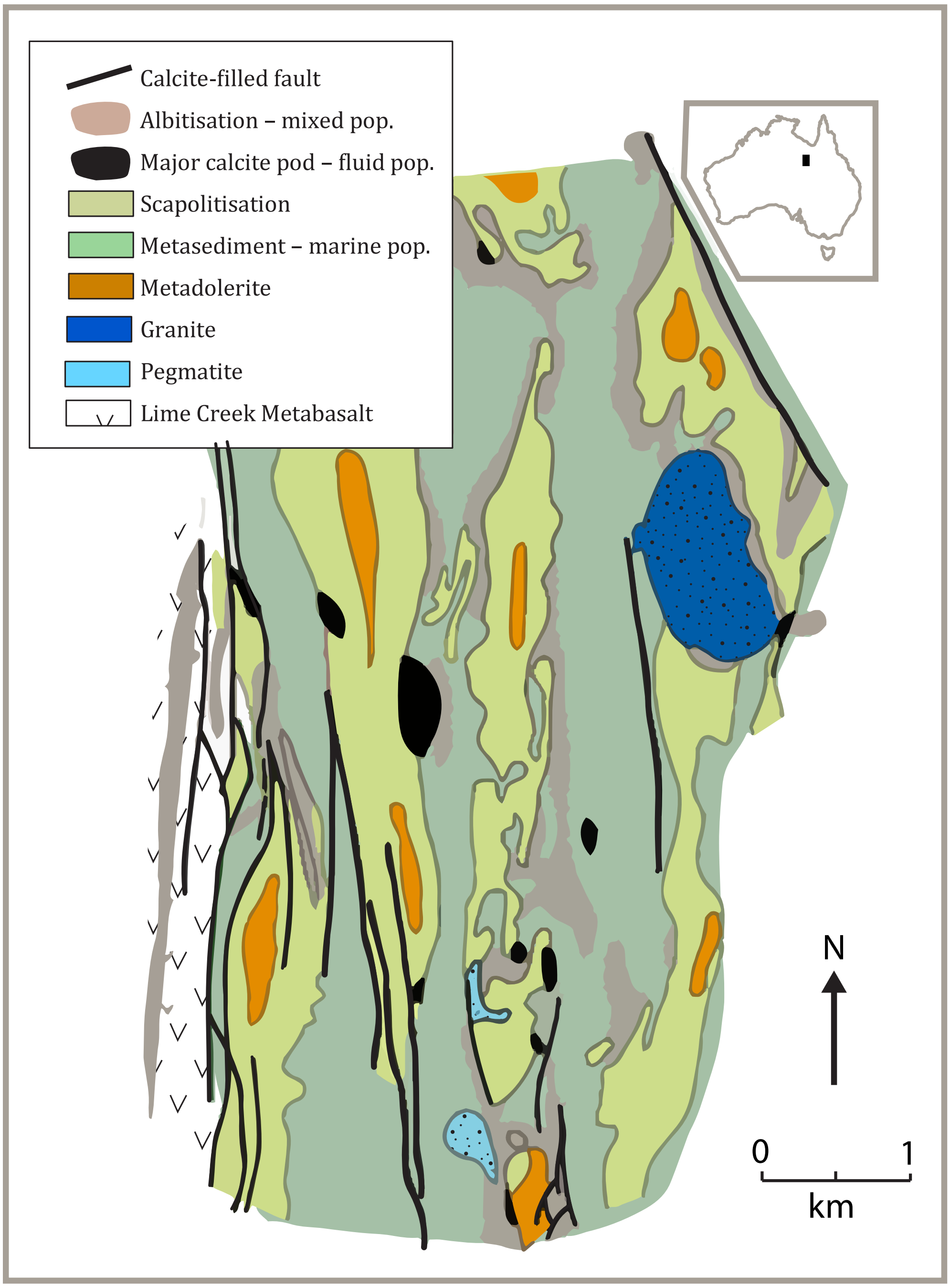

Figure 4.7. Geologic-alteration map of part of the Mary Kathleen Fold Belt, about 9 km NNE of MK, with carbonate $\delta^{18}O$–$\delta^{13}C$ populations (from Oliver & Wall, 1987, modified).

Not surprisingly, most of the Soldiers Cap Group deposits were found to contain carbonate with evidence of some organic carbon, including Eloise, Osborne and Mount Elliot (Marshall *et al.*, 2006).

Critically, there is no suggestion, or discussion, of the possibility of spatially extensive O or C isotopic gradients in any of the data. Rather, there seems to be an absence of zonation, suggesting a lack of end-member mixing at the actual site of mineralisation and alteration. The comprehensively overlapping $\delta^{13}C$–$\delta^{18}O$ ranges of carbonate from different parts of the Ernest Henry deposit paragenesis, including distal samples, are a case in point (refer to Figure 4.8a). Consequently, the effectiveness of the CIT in the Eastern Fold Belt is likely to be constrained and limited to the identification of sub-populations and contributing reservoirs. Apart from the Ernest Henry deposit (Fuss, 2014), there are no published accounts of stable isotope studies designed to measure gradients around economic mineralisation at a scale of interest to an explorer.

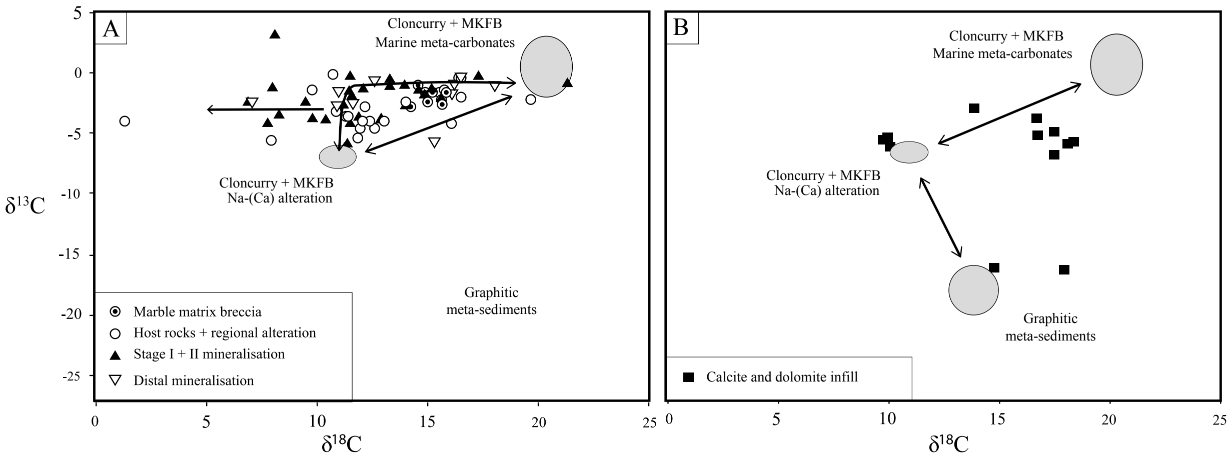

Figure 4.8. $\delta^{13}C$ vs. $\delta^{18}O$ plots for carbonate from the Ernest Henry deposit and environs (A), and the Great Australia Cu deposit (B); arrows refer to data trends, not model trends; 'MKFB' is the exposed part of the Mary Kathleen structural domain (also known as Wonga Subprovince) (from Marshall et al., 2006).

Sampling and analysis guidelines

The CIT can be applied at the target drilling stage of an exploration programme or earlier, where a grid of shallow drill holes is required in covered areas before deep drill targets are finalised. If weathering effects are minimal, it is possible to acquire isotopic data at the reconnaissance stage of exploration (*e.g.*, some areas of outcropping McNamara Group rocks in the Mount Oxide and Century structural domains of the Western Fold Belt).

Bedrock drill holes

For diamond core or reverse circulation (RC) drill holes, the sampling of carbonate-bearing core or RC chips at every 50–75th metre should reveal a $\delta^{18}O$ gradient if it is present. In the case of core, every second or third sample should include vein carbonate to help assess the size and 'effectiveness' of the hydrothermal system (*i.e.,* the approach to wall rock-fluid isotopic equilibrium). If evidence of zoned depletion is present, then subsequent drill holes could provide a three-dimensional picture of isotopic gradients and a 'vector' to ore.

Grid Rotary Air Blast (RAB)/Aircore surveys

Many prospective areas for Mount Isa-style copper mineralisation occur under thin cover (*e.g.*, black soil, alluvium, laterite, Tertiary–Cambrian sedimentary rocks). Widely-spaced isotope grids offer a means of identifying drilling targets at the prospect scale (*i.e.,* 1–10 km) if applied in conjunction with other exploration techniques. Line spacings in the order of 500 m and sample spacing of about 250 m, for grids covering several to 100 or more square kilometres, are feasible. The aim of an isotope grid is to establish a plan view map of fossil hydrothermal fluid flow (*i.e.,* horizontal vectors). Sampling involves the collection of the first fresh (unweathered) carbonate-bearing rock chips from bedrock below the unconformity from each hole. Air-core rigs are capable of penetrating 100 m or more in areas of thick, deeply weathered cover, and permit the sampling of vein-wall rock pairs.

Sampling and analytical procedures, and costs

Samples must be taken from below the weathered or carbonate leaching zone. Splits of 1 m RC intervals, or quartered core lengths of 10–20 cm, are sufficient for carbonate isotopic analysis, as less than a gram of material is required for analysis. All samples should be photographed (preferably halved core) for reference, particularly for intra- and inter-hole textural comparisons. Fifty to 100 g (*i.e.,* a handful) of chips is sufficient in the case of RAB samples. The use of weak HCL, a scribe and a hand lens will ensure that only carbonate-bearing samples are sent to the lab.

At the lab, the identity and relative proportions of carbonate species in each sample is first determined by chemical analysis, and XRD if necessary. Then, a separate sub-sample is dissolved and loaded on to a mass spectrometer for isotope measurement. The analytical data are then corrected in accordance with the quantity and fractionation factors of each of the carbonate species present. The total cost of analysis incurred at the laboratory is about \$100–\$150. Thus, a typical drill hole of 400m, sampled every 50 m, will cost about \$1000 for isotopic analysis. A 5 km x 2 km isotope grid, with drilling costs, will cost in the order of \$50,000 (average hole length of 30 m, RAB @ \$10/m).

Sulfur isotopes of sulfide

A regional overview

A large amount of sulfide sulfur isotope data is available for ore deposits across the Mount Isa Inlier. At the regional scale, it is evident that seawater was the ultimate source of much of the sulfur in Western Fold Belt ore systems, and that magmatic sulfur dominates mineralisation in the Eastern Fold Belt. This fundamental contrast is illustrated in Figure 4.9, which summarises the sulfide sulfur isotope systematics for each region and major metal association in relation to well established rock sulfur reservoirs. Both Cu and Pb-Zn-Ag sub-groupings of the Western Fold Belt are characterised by relatively 'heavy' sulfur, with sulfide $\delta^{34}S$ values generally between 13‰ and about 25‰, consistent with a major contribution by marine sulphate to the sulfur budget. The $\delta^{34}S$ values of Eastern Fold Belt chalcopyrite, galena and sphalerite range between about -5 and 9‰ and have statistically minimal overlap with the WFB populations.

The $\delta^{34}S$ ranges and population medians for most of the significant copper deposits of the region, together with non-ore populations of interest, are plotted in Figure 4.10. Although sub-populations are evident within individual deposits, most relate to differences between individual ore lodes (*e.g.*, Andrew *et al.,* 1989, Mount Isa mine), or differences between orebody data and

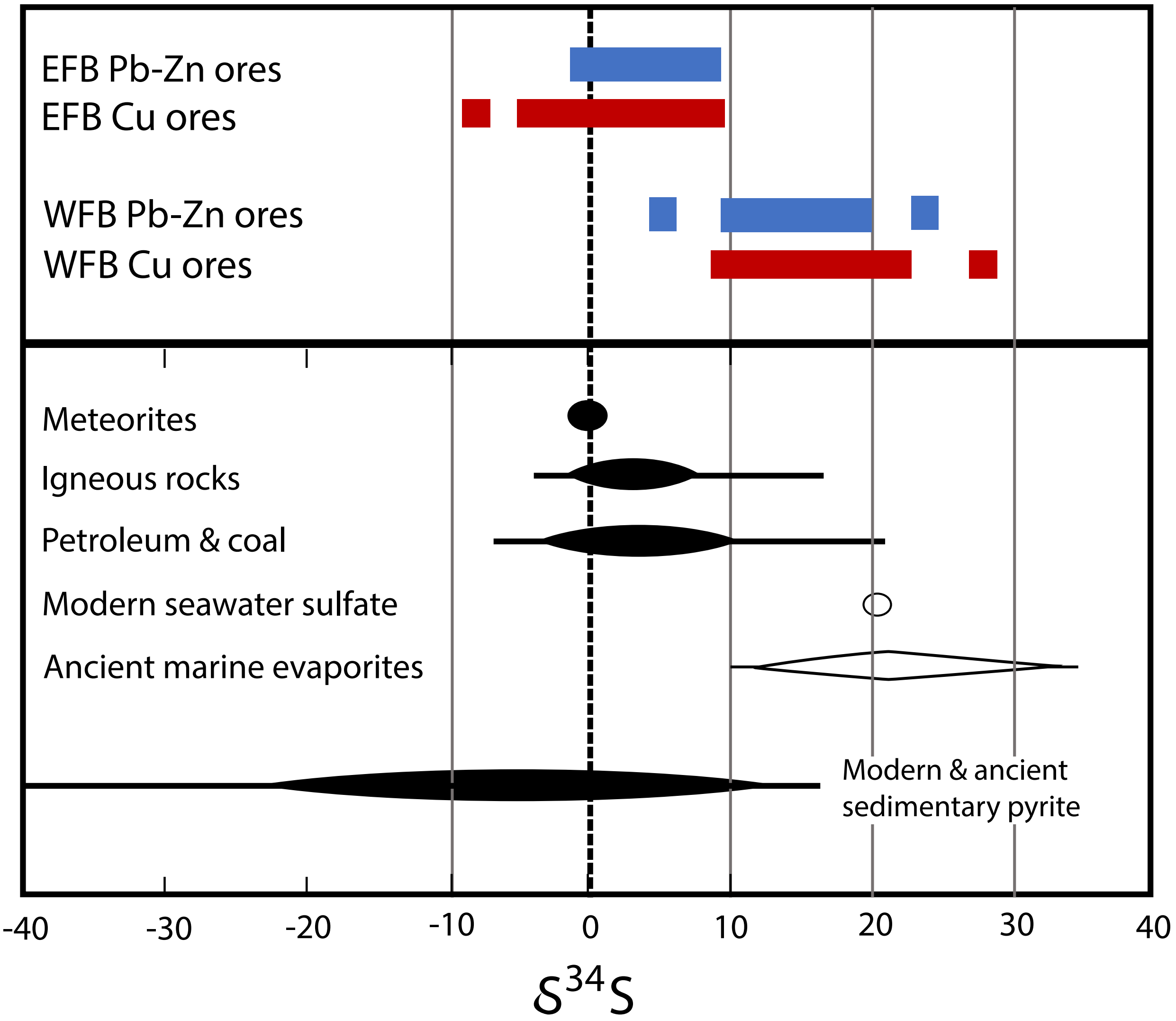

Figure 4.9. $\delta^{34}S_{CDT}$ distributions of Mount Isa Inlier ore sulfides compared to global sulfur reservoirs; red bars apply to chalcopyrite and blue bars to galena ± sphalerite (sources—Seal II, 2006; Davidson & Dixon, 1992; Case, 2016; Painter et al., 1999).

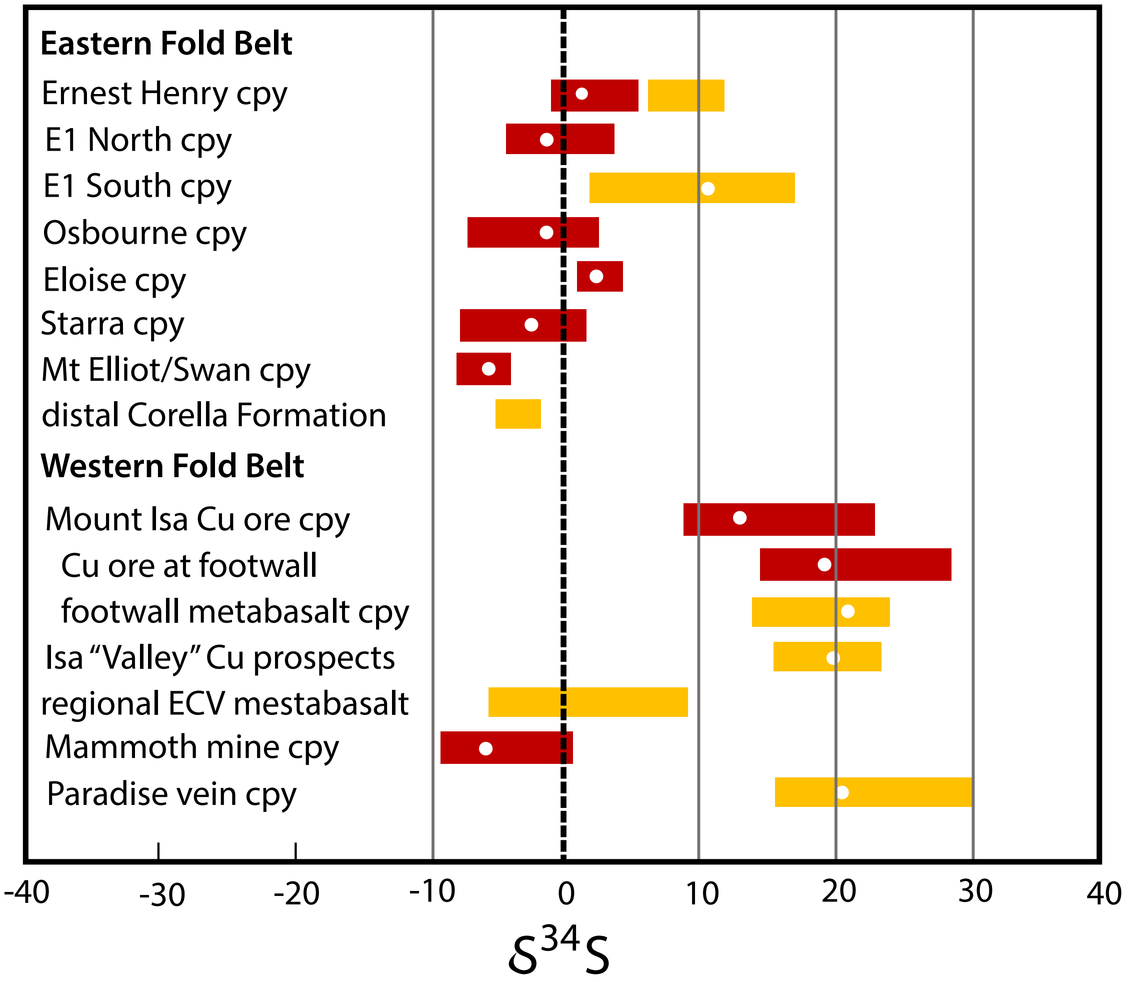

Figure 4.10. Ranges and medians of $\delta^{34}S_{CDT}$ values for chalcopyrite in Mount Isa Inlier copper ± gold deposits (red bars) and prospects (yellow bars). (sources—Case, 2016; Davidson & Dixon, 1992; Hannan et al., 1993; Painter et al., 1999).

proximal alteration assemblages (*e.g.*, Hannan *et al.* 1993; Mount Isa mine; Case, 2006; Ernest Henry). There are no reported gradients in sulfide $\delta^{34}S$ suggestive of a geochemical vector to mineralisation or ore.

Examples of discrete footwall alteration populations are indicated by the yellow bars for the Mount Isa and Ernest Henry Cu deposits (Figure 4.10). The Mammoth mine data are an exception for WFB copper deposits, with light chalcopyrite $\delta^{34}S$ values explained by derivation from local diagenetic pyrite formed under partially open-basin conditions of marine sulfate organic reduction (Scott *et al.,* 1985). The data for metabasalt within regional ECV, outside the major fault system which hosts the Mount Isa base metal deposits, is consistent with sulfur derived from within the volcanic succession—in strong contrast to the altered ECV metabasalt in the footwall of the Mount Isa Cu orebodies.

In the case of EFB Cu-Au deposits, discrete background populations which might permit the recognition of magmatic hydrothermal- and wall rock-sulfur mixing are not well defined. Moreover, a few samples of regional or 'distal' Corella Formation with traces of chalcopyrite are isotopically indistinguishable from EFB ore deposit chalcopyrite (Figure 4.10, data from Hannan, 1992c). Either the marine sulfate was never a significant constituent of EFB evaporites, or it was flushed from the sedimentary succession during diagenesis. The noticeably heavier sulfur of mineralisation at the small E1 South deposit, 1.5 km southeast of E1 North, is attributed to previously available local sulfate, as are the elevated $\delta^{34}S$ values of chalcopyrite in the footwall marble breccias of Ernest Henry (Case, 2006). For other deposits, where mixing

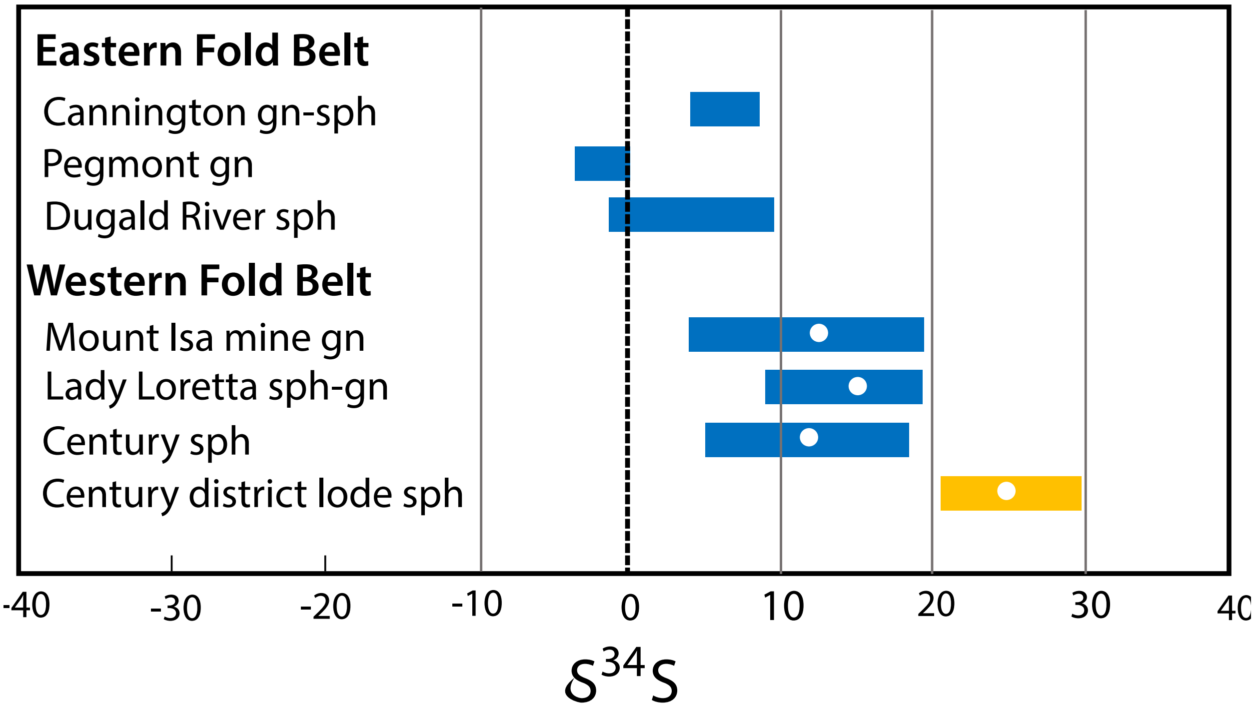

Figure 4.11. Ranges and medians of $\delta^{34}S_{CDT}$ *values for galena and/or sphalerite in Mount Isa Inlier Pb-Zn-Ag deposits (blue bars) and prospects (yellow bars) (sources—Davidson & Dixon, 1992; Broadbent et al., 1998; Painter et al., 1999; Walters et al., 2002).*

with the organic sulfur of local carbonaceous shale is evident, such as Au-dominated Starra and Mount Elliot (Figure 4.10, δ^{34}S values < -5‰), gradients are unlikely given the strong fractionations and departures from isotopic equilibrium implicit at sites of redox transition (*e.g.*, Seal II, 2016).

In Figure 4.11, δ^{34}S distributions are summarised for sphalerite and/or galena of the largest Pb-Zn-Ag ore deposits of the region. Again, a persistent statistical separation is evident between the Eastern and Western Fold Belts, and consensus in the literature is that of a marine sulfate versus magmatic/metamorphic sulfur source dichotomy. In the case of the lower temperature western systems, and the Dugald River deposit in the east, large volumes of pre-ore, fine-grained and bedded pyrite may have contributed to the ore sulfur inventory, but definitive trends in sulfide δ^{34}S values between ore zones and peripheral 'diagenetic' pyrite have not been demonstrated to date. The distinctively heavy sulfur of vein sulfide prospects in the district of the Century deposit is of interest, however, as another example of the capability of sulfur isotope analysis to reveal spatially defined sub-populations which provide clues to key system parameters and evolution. In this case, the likelihood is that the veins record an advanced state of closed basinal sulfate reduction and basinal structural adjustment after the primary ore forming event (Broadbent *et al.,* 1998).

In conclusion, the available data suggests that definitive gradients in sulfide sulfur isotope compositions in the critical transition from background wall rock to ore are either absent or yet to be recognised in the Mount Isa region. However, sulfur isotope analysis provides an efficient tool for the recognition and mapping of sub-populations at individual deposits, which relate to mechanisms of ore deposition and geometries of ore fluid pathways, and it provides a fundamental means of inter-deposit comparison and metallogenic evaluation.

Summary and conclusions

1. The ‘carbonate isotope technique’, or CIT, is used to assess the degree to which a carbonate-bearing rock has interacted or equilibrated with hydrothermal fluid; it provides an independent measure of Cu mineralisation potential of the Mount Isa type by direct comparison with the Mount Isa example; that is, the presence of an O- and C-isotope depletion halo in the carbonate component of the metasediments and silica-dolomite alteration assemblage surrounding the Mount Isa copper orebodies.
2. From an exploration perspective, the most significant feature of the halo is $\delta^{18}O$ depletion in visually unaltered Urquhart Shale without veining and with < 100 ppm copper hundreds of metres up-dip from the nearest mass of silica-dolomite.
3. Qualitative information about the size of the hydrothermal system is inferred from:
    a. the gradient in $\delta^{18}O$ values (*i.e.,* rate of change of $\delta^{18}O$ values with distance) and/or
    b. the relationship between vein carbonate and host rock carbonate $\delta^{18}O$ values.
4. Oxygen isotope gradients, in carbonate, at Mount Isa mine are typically less than 1‰ per 100 metres. By contrast, ‘steeper’ gradients of 2–4‰ are observed at small, fault-confined Cu prospects.
5. Significant deviations from the Mount Isa mine example, such as extensive $\delta^{18}O$ depletion, without gradients and/or evidence of silica-dolomite veining with Cu mineralisation, are indicative of barren hydrothermal events.
6. The CIT is appropriate for calcareous (dolomitic) units in the Western Fold Belt, with due consideration of structural domain-scale variation in end-member bulk host rock and hydrothermal fluid $\delta^{18}O$–$\delta^{13}C$ signatures.
7. The available data suggests the CIT is unlikely to be effective in the Eastern Fold Belt.
8. A review of the sulfur isotope compositions of Mount Isa region ore deposits indicates that spatially defined gradients are either absent or not yet measured. However, strategically applied sulfur isotope analysis during exploration will reveal sub-populations related to mechanisms of ore deposition and provide an informative means of inter-deposit comparison and metallogenic evaluation.

Chapter 5

Covered domain I: Transport mechanisms, sample media and analytical methods

Introduction

This chapter overviews the major themes and practical aspects of surface geochemical exploration in areas of transported cover. It provides introductory material for Chapters 6 and 7, which demonstrate the complex nature of surface chemical anomalies above buried ore deposits and how they are measurable in a variety of media.

The specific themes of this chapter are:

- mechanisms of metal and gas migration (from mineralised source to the surface)
- sample media and chemical analysis
- essential field sampling tactics and quality assurance (QA/QC)
- data processing and anomaly identification.

Each of the themes is fully referenced to support further investigation of the 'geochemical exploration through cover' principles. Familiarity with these issues is fundamental to its effective use and successful anomaly identification.

Mount Isa region perspective

Groundwater is generally encountered at depths of 20 to 80 metres in the Mount Isa region, which includes large areas of prospective Proterozoic bedrock beneath 150 m or more of transported cover. Therefore, metals and volatiles migration from deep mineralisation to the surface is dependent on transport mechanisms applicable to vadose conditions to traverse the upper few tens of metres of 'dry' transported cover. The interplay of fracture networks, barometric and seismic pumping, the generation of aerosols at the water table, and the action of deep-rooted vegetation are likely contributors. Secondary dispersions measured by weak leachants, soil-gas methods and vegetation sampling are chemically and spatially complex, and the extents and amplitudes of anomalies are governed by proximity to fractures. Anomaly profiles are expected to be spikey, irrespective of soil type and matrix characteristics, and their interpretation is strongly dependent on the recognition of patterns, trends and element associations.

The relevance of soil-gas techniques to covered domain exploration is compelling, but the analytical costs, demanding sampling protocols and the perceived risk of poor precision are impediments to widespread application. Moreover, it is not evident that soil-gas methods are superior to chemical leachants for anomaly identification in the semi-arid conditions. Therefore, soil-gas methods are probably more sensibly applied to areas where phreatic (saturated) conditions predominate and dispersion mechanisms are less dependent on near surface fracture distributions—such as concentration gradients (diffusion), electrochemical gradients (redox cells) and 'geogas' flux. Such conditions apply to the northern part of the region, where water tables rise towards the Gulf of Carpentaria, and periodically over a much larger area after monsoonal wet seasons.

In these conditions, the dispersions of deep, oxidising mineralisation are more likely to be mediated by indirect controls, such as redox cell geometries or hydromorphic gradients. Given the nature of the transport mechanisms, near surface anomalies might be expected to cover larger areas, with less spatial variability and lower signal/background contrast than fracture-mediated anomalies. Accordingly, soil-gas methods may be the appropriate option for regional scale and reconnaissance surveys, based on wide spacings intended for the evaluation of major structural trends or intersections. The same dispersions are probably accessible to the root systems of specific tree species and vegetation sampling may be a viable alternative if planned and executed with due regard to the need for appropriately scaled composite sampling and QA verification.

Transport mechanisms

Aspandiar *et al.* (2006) recognise two major metal transfer mechanisms in overburden and regolith—those operating below the water table, in saturated conditions (phreatic zone) and those above the water table (vadose zone). Table 5.1 and Figure 5.1 classify each known or hypothetical mechanism according to driving force and medium of transfer. The major modifying processes of microbial metabolism and regolith development are also treated, to produce a comprehensive account of secondary dispersion mechanisms pertinent to the Australian setting.

Table 5.1: Classification of upward metal transport mechanisms in overburden and regolith.

Zone	Mechanism		Force	Medium
Phreatic	Advective	Groundwater flow (hydromorphic)	potential energy	water
		Dilatancy pumping (along fractures)	Stress (e.g., seismic)	
		Convection	Heat gradient	
		Bubble transport	pressure/buoyancy	gas
	Non-advective	Diffusion	concentration gradient	water
		Spontaneous potential	electrochemical gradient	
		Redox gradient	electrochemical gradient	
Vadose	**Capillary action**		pressure/suction	water
	Gaseous	Diffusion	concentration gradient	gas
		Atmospheric pumping	Pressure gradient	
		Convection	Heat gradient	
	Plant uptake		Biological activity	water
	Bioturbation		Biological activity	regolith

after Aspandiar *et al.*, 2006, modified.

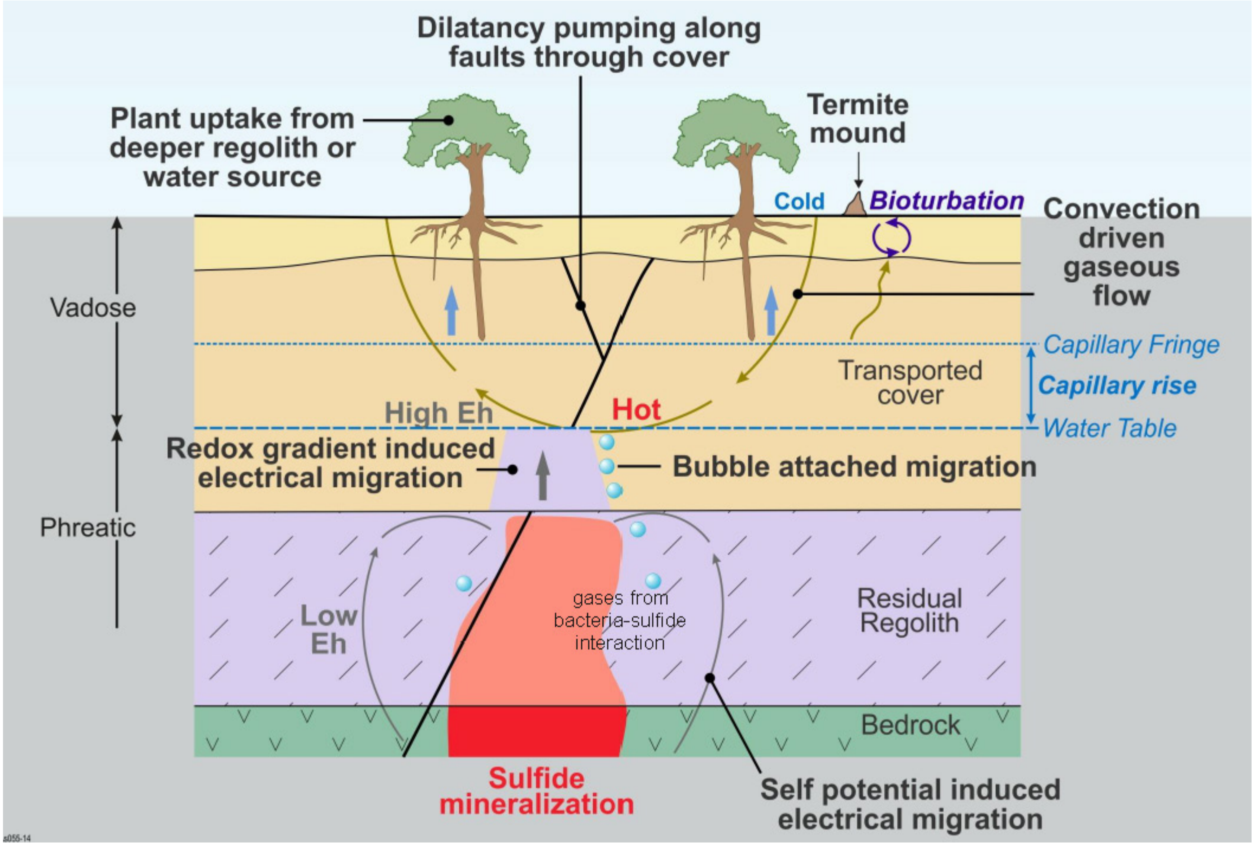

Figure 5.1. Schematic depiction of the range and scope of chemical transfer mechanisms in transported cover above sulfide-associated mineralisation in a typical Australian setting (from Aspandiar et al., 2006, modified).

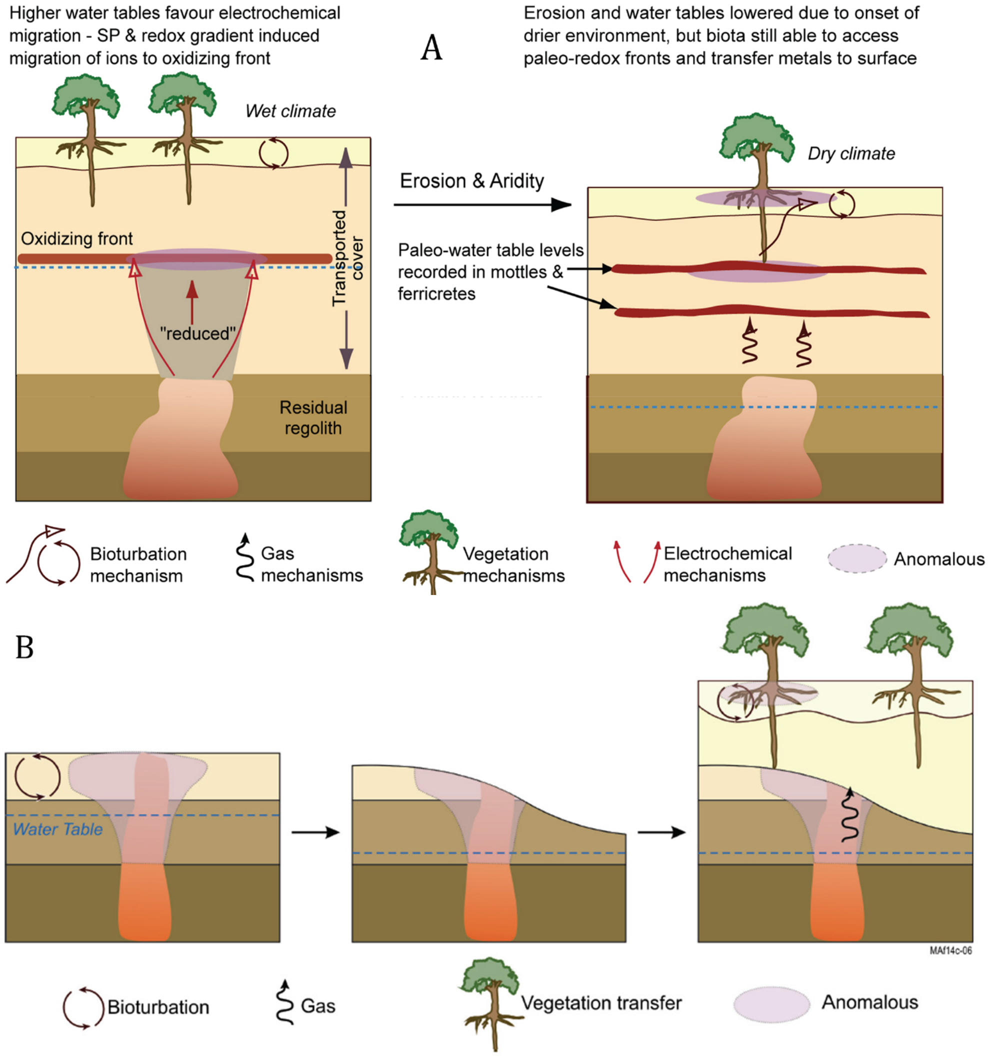

Figure 5.2. Schematic depiction of the dynamic nature of within-cover chemical anomalies in response to changing climate (A) and regolith evolution (B) (after Aspandiar et al., 2006).

Figure 5.2 alludes to the evolving and dynamic interrelationships between individual dispersion mechanisms. The resulting surface anomalies are characterised by compositional variability and larger spatial extents than the 'footprints' of source mineralisation.

In another major review paper, Cameron *et al.* (2004) first consider the theoretical and experimental framework for through-cover transport mechanisms, with emphasis on electrochemical and dilatancy/seismic pumping, then illustrate their relevance to ten project case studies in the contrasting geologic and physiographic settings of Chile, Nevada and Ontario. Anomalies were identified in the soils above mineralisation at all test sites, including the arid, low water table sites of Chile and Nevada. These outcomes, and the significance of time to the episodic and cyclic build-up of surface anomalies, are pertinent to the northwest Queensland setting. That is, semi-aridity and water tables depths of 10–80 metres are not an impediment to upward chemical transport, though it might be expected that the chemical signals will be more spatially and compositionally variable than those develop in saturated conditions (next section).

To conclude, an appreciation of transport mechanisms and dispersion models will assist the explorer to judge the effectiveness and success of a chosen sampling and analytical method. Without it, intrinsic risk increases, such as failure to differentiate negative results (no mineralisation present) from null results (inappropriate method, target not tested) and to recognise 'false' anomalies (Aspandiar *et al.,* 2006). All indirect exploration methods, chemical or geophysical, share these risks where applied with poor understanding or in isolation and without supporting targeting criteria.

Chemical leach methods

New chemical reagents and laboratory procedures were developed in the 1990s to isolate exogenic signals in the transported cover of known ore and sub-economic mineralisation. Most of the work was of an empirical nature (Cohen *et al*., 2007) but, critically, the routine availability of mass spectrometers permitted the quantification many elements to ultra-trace concentrations and some testing of conceptual pathways and transport mechanisms. Much more work is needed, however, to deepen our understanding of the mineralogical and environmental factors that control signal accumulation, and even how different reagents interact with similar mineral substrates.

Essentially, the weak reagents or leachants are designed to remove the loosely bound component of metals and trace elements in regolith, either on a whole sample basis or from specific and reactive secondary mineral phases known to co-precipitate with or attract elements in solution. The former is termed a “partial digestion” (*e.g.,* bulk cyanide leach), and the latter is referred to as a “selective extraction” (*e.g.,* EDTA, Enzyme Leach). Characteristically, the leachants produce solutions with much lower total dissolved solids than the strong acid combinations required to digest the ‘endogenic’ mineral substrate (*e.g.,* silicates and resistate minerals). Accordingly, individual solute concentrations are not masked by the lithogeochemical ‘background’ and are measurable by ICP-MS to very low levels of detection (Hall & Bonham-Carter, 1998; Cohen *et al.,* 2007).

The relationships between the most commonly used leachants (public and proprietary) and strong acids and the mineral substrate they target, or digest, are summarised schematically in Figure 5.3. For the characteristics of specific leachants, including composite techniques such as MOMEO, readers are directed to general reviews and references to dedicated publications therein (*viz.,* Wang *et al.,* 1997; Hall & Bonham-Carter, 1998; Thiede, 1999; Lilly & Hannan, 2016).

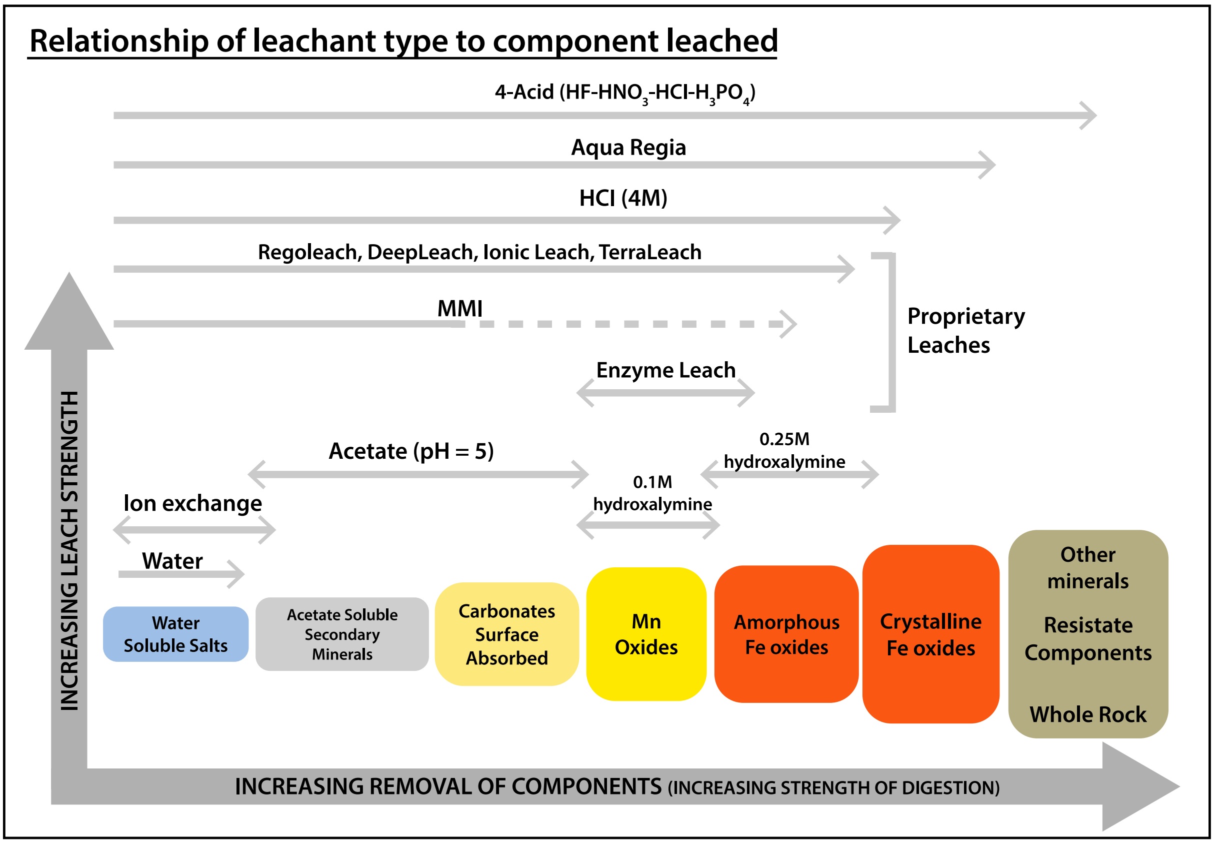

Figure 5.3. Relationships of leachants and strong acids to commonly targeted mineral substrates (from Rutherford, 2002, modified).

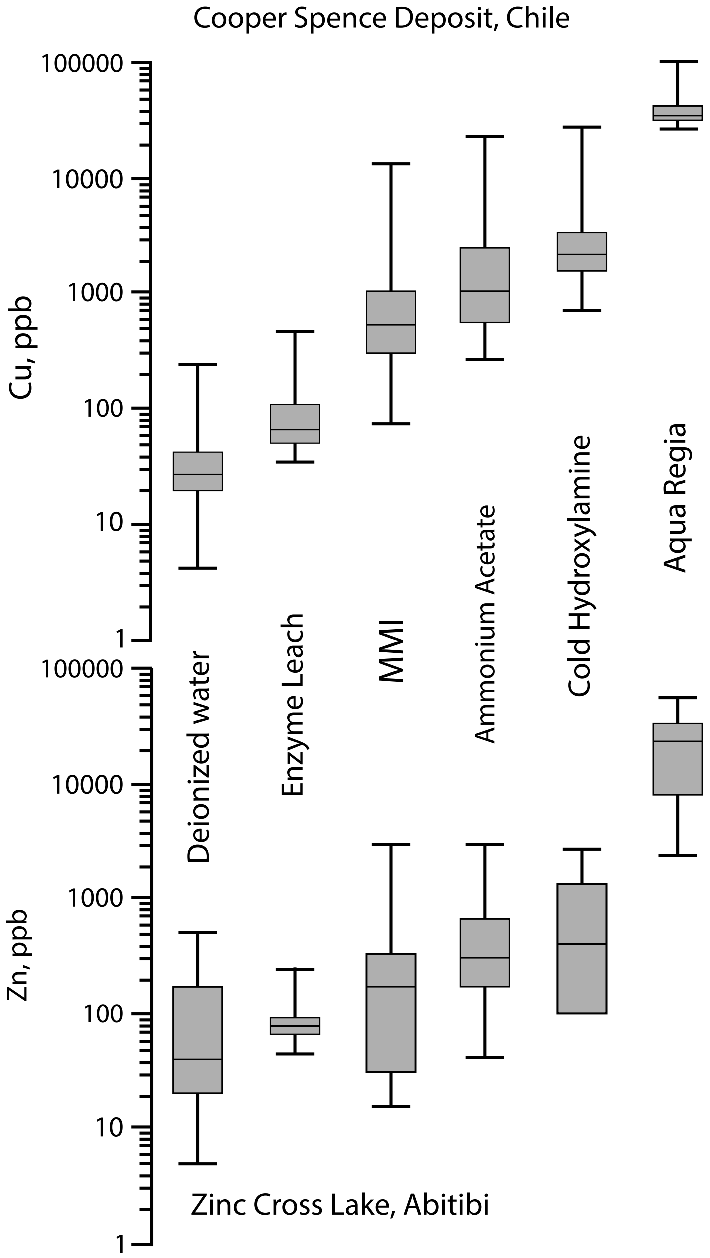

Figure 5.4. Box plots of extracted Cu and Zn by five chemical leaches and aqua regia in soil sampled across a buried Cu ore deposit and buried Zn prospect (from Cameron et al., 2004).

Of fundamental relevance to all leachants are the natural variables which determine chemical solubility in the weathering environment—these are examined in detail in Thornber (1992) and usefully synthesised in an Australian Laboratory Services newsletter (Rutherford, 2002).

The quantity of metals extracted by the different leachants varies enormously from a few ppb to tens of ppm (Figure 5.4). Reagents capable of digesting crystalline manganese oxide and amorphous iron oxide (Figure 5.3) will extract the highest proportion of 'total' metal available in given sample of regolith. With reference to Figure 5.4, and Mount Isa region experience, their 25th–50th percentile 'boxes' would most likely plot between those of aqua regia and cold hydroxylamine HCl if they were tested as part of the Spence deposit study.

The proprietary methods of Figure 5.3 have all been applied in the Mount Isa Inlier, either to investigate the secondary dispersions of buried ore deposits (see Chapter 6) and buried sub-economic mineralisation (Chapter 7) or as a primary exploration method (also Chapter 6).

Analytical considerations

Critically, the preparatory steps and conditions of digestion for each leaching method are strictly defined and require high levels of procedural consistency to achieve stable and repeatable extractions through time. Laboratories must also provide "clean" and well calibrated ICP-MS equipment to prevent contamination of the typically dilute leachates by the residues of strong acid digestions. Such requirements imply higher per sample costs than standard strong acid digestions, and impose longer job turn-around times and higher operational risks, especially for laboratories without dedicated facilities. Specific risks at the laboratory include:

1. sample preparation error, particularly drying temperatures above 40°C, which may promote the recrystallisation of amorphous phases and reduce the availability of originally loosely bound metals or trace elements
2. non-systematic procedural inconsistency, such as weighing errors and variations in the duration, agitation specifications or temperatures of extractions to produce analytical variability *unrelated* to sample matrices (*i.e.,* variability unrelated to major departures in the balance of adsorptive secondary minerals in specific sample)
3. batch-to-batch changes in analytical sensitivity from due to cumulative or systematic error (*e.g.,* reagent concentration, instrument calibration, interferences from inter-job contamination).

To clarify point 2, many leachants are designed to accommodate a range of sample matrices; for example, by using buffers to maintain a constant solution pH. However, extreme compositions often overcome the regulating mechanisms (*e.g.,* neutralisation by carbonate, resorption by organics or iron). Without corresponding strong acid determinations, only the explorer has the necessary support information (*e.g.,* imagery, regolith maps) and quality field observations to anticipate and account for the resulting unusual or unexpected data. The same support information is critical to the effective interpretation of the broader data set and the identification of secondary dispersions related to mineralisation (next section).

Data analysis and anomaly identification

The traditional approaches to anomaly definition are not appropriate for chemical leach data—especially for large area surveys of a reconnaissance nature without pre-defined targets. Subtle mineralisation signals are likely to be missed if the data for individual elements is treated statistically on a whole population basis, without regard to sample spatial context and the complex interplay of landscape setting, regolith type and the distribution of key secondary minerals (Cohen *et al.,* 2007; Riemann & Garret, 2005). For example, a discrete area characterised by unusual *variability* in one or more relevant metals or other measured parameters (*e.g.,* pH, Eh, volatile species), is likely to be of more interest than isolated extreme results or randomly distributed anomalous results in a regolith type predisposed to metal scavenging (analogous to false gossans in rock chip data). Such variability is an intrinsic feature (*e.g.,* Neuerburg, 1984) and is aptly demonstrated for a soil survey by Regoleach in central western NSW (Rutherford & Berkman, 1999) and a soil survey by Enzyme Leach in the Mount Isa region (Hannan, 1998).

The high degree of variability of chemical leach data over small distances (1 or 2 metres) was often attributed solely to the difficulty of maintaining stable leaching conditions, thereby bringing into question the viability of the practice. However, research and carefully executed orientation field studies in recent years has demonstrated both the spatial correspondence of

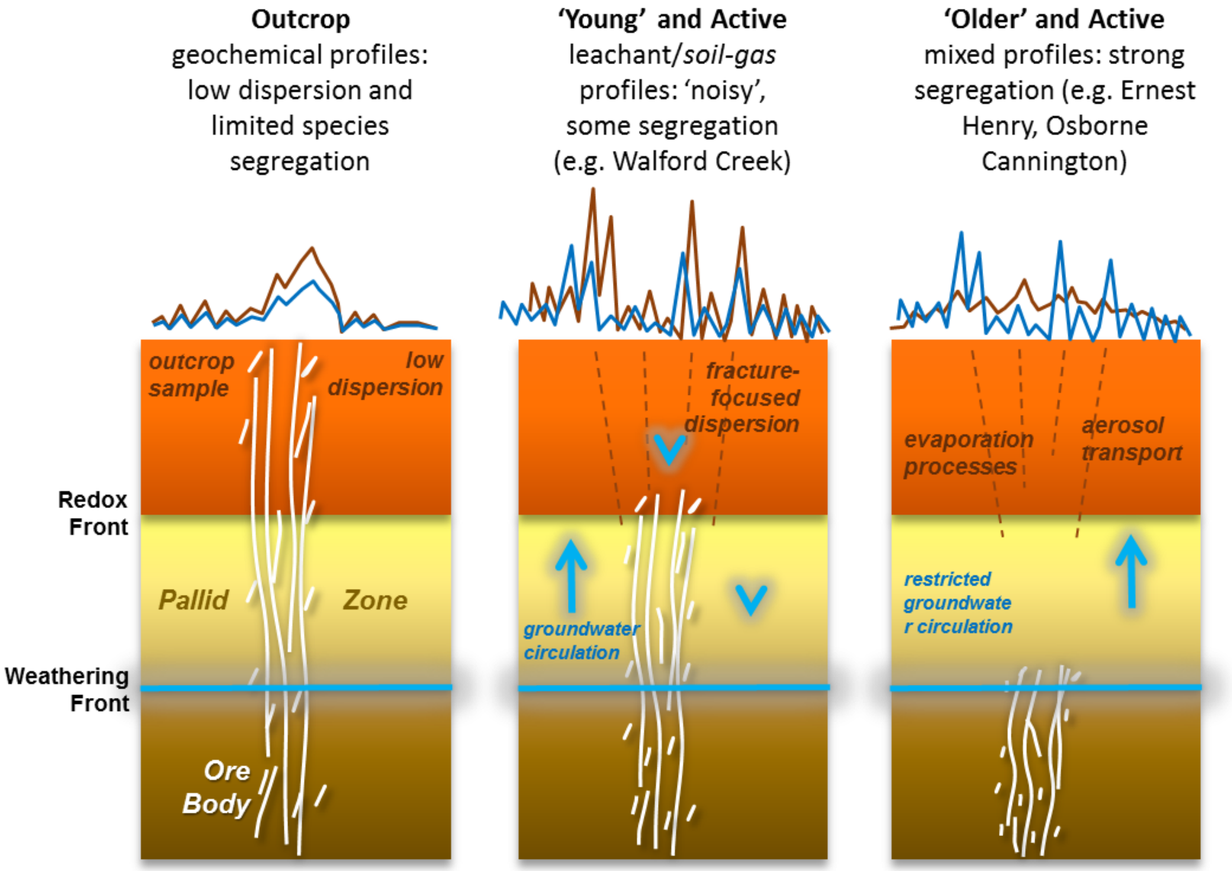

Figure 5.5. Schematic depiction of the shape and compositional variability of chemical anomalies above concealed mineralisation, with Mount Isa region examples (after Rutherford, 2018, modified).

chemical leach anomalies and fractures in transported overburden (*e.g.,* Rutherford, 2009), and the viability of fractures as the upward migration pathways for water and aerosols in the vadose zone (Klusman, 2009). Tellingly, soil gas data display similar spatial variability, as well as temporal fluctuations consistent with control of upward migration by fracture networks (next section).

These are important findings because they support the trend to pattern and variability analysis in anomaly identification (*e.g.*, Carranza, 2009) and provide the basis for an improved understanding of anomaly morphologies. For example, an actively forming anomaly might be expected to be spikey and to extend beyond the buried ore footprint, but subsequent aridification and redistribution by near-surface 'tertiary' processes, such as bioturbation or vegetative turnover, might produce a smoother, lower amplitude and less immediately recognisable feature (Figure 5.5). Similarly, smooth anomalies in certain metals or compounds, fringed or partly coincident with spikey anomalies in others, are expected as conditions evolve in the weathering profile (*e.g.,* the relative mobilities of cationic and oxy-anionic metal species in response to groundwater pH change).

To conclude, the interpretation of soil chemical leach and soil-gas data requires the availability of reliable control information, preferably shown with the data in stacked line profiles or maps, and an appreciation of the potential significance of areas and zones of enhanced signal variability for specific groups of metals or compounds. Without these fundamentals in place, 'false' anomalies are not easily recognised, and subtle, true anomalies easily missed. These risks are accentuated by the uncontrolled or blind processing of multivariate data—which invariably produces time- and resource-sapping artefacts.

Soil-gas methods

The collective term soil-gas applies to techniques which separate gases or mineral-sorbed compounds from the host regolith prior to chemical analysis. A 'free gas' classification implies the use of collectors to remove, from voids, *gaseous* species which *actively* flux from oxidising sources at depth; and the sorbed classification to the separation and chemical treatment of a fine silt or clay component which acts as an *in situ* adsorptive trap for miscellaneous volatile compounds.

This is a conceptually appealing but diverse and contentious class of surface chemical exploration methods. Three sub-types corresponding to major difference in field sampling procedures and logistics are briefly outlined:

1. Actively extracted 'free gas'—designed to capture either gaseous species (*e.g.,* metals and trace elements like Hg, As, Rn, He; sulfur gases like H_2S, SO_2, CS_2; hydrocarbons like CO_2, CH_3SH, CH_4) or microscopic particulates and aerosols transported in gas fluxes known to carry metal ions and complexes (*e.g.,* Oakes & Hale, 1987; Etiope & Martinelli, 2002; Klusman, 2009; Wan *et al.,* 2017).

   The pumping procedure of Metals in Soil Gas (MSG), shown in appendix A, exemplifies the latter variant. Whilst anomalous levels of analysed metal are attributed to oxidising and sulfidic point-sources (Wang *et al.,* 2008), the carrier is also attributed to earth-gas or *geogas*, depending on the scale of investigation. This contentious transport mechanism underpins a multi-kilometre sample spacing approach to locate entire districts or blocks of metallogenic interest and is measured by a sequential leach procedure (*i.e.,* the MOMEO procedure of Wang *et al.,* 1997).

2. Passively collected 'free gas' using static collectors to achieve a time-integrated average sample and reduce the influence of potentially significant local variables (*e.g.,* regolith porosity, air pressure, moisture content, level and type of biogenic activity). Collector types and procedures vary considerably (Thiede, 1999). The GORE^{TM} method, applied recently in the Mount Isa region (refer to Appendix A), provides an example of a broad-spectrum collection system for methylated organic and inorganic compounds, as well as other volatile compounds associated with the oxidative and microbial decomposition of sulfide minerals (Gore & Associates Inc., 2006). After about 30 days of *in situ* collection the modules are removed and sent off for thermal desorption and measurement by gas chromatography-ICPMS.

3. Chemically extracted sorbed volatiles from the clay or silt fraction of regolith—requiring only the excavation of representative soil/regolith in the field followed by physical separation of the adsorptive clay-rich component at the laboratory. As for GORE^{TM}, the broad gas spectrum and commercial aspects of these methodologies are outcomes of a focus on the oil and gas exploration sector. Well known variants include Soil Desorption Pyrolysis (SDP) and the currently available Soil Gas Hydrocarbons (SGH) method.

   SDP involves the high temperature pyrolysis of a 0.25 g sample and direct injection of the desorbed gaseous volume for determination by ICP-MS. Individual gas species are identified by the analysis of m/z peaks and partial pressures calculated after applying correction factors (Thiede, 1999). Reported compounds include the atmospheric gases, C1–C7 hydrocarbons ± S or halogens, several sulfur gases (H_2S, COS, SO_2 CS_2), F, HCl, H_2, He, NH_3, As and B.

   SGH, by contrast, is a hybrid method in all respects. Firstly, it involves a weak leach (aqueous) of the physically separated <0.18 mm fraction of each sample, followed by chromatographic separation and ICP-MS analysis; the data is provided as molecular weight

> groupings of 162 non-gaseous, semi-volatile hydrocarbon compounds in the C5–C17 carbon series. Experimental evidence indicates that some of the measured hydrocarbons are released by dying bacteria at sites of sulfide consumption, and it is argued that they subsequently migrate towards the surface in the associated electrochemical cell centred on the sulfide body (Sutherland & Hoffman, 2009). The varied and complex anomaly forms characteristic of SGH data correspond to the spatial clustering of groups of compounds with similar molecular weights, a feature attributed to the interplay of chromatographic effects and electromotive forces in the redox zone (Sutherland, 2011).

Mount Isa region examples

Except for the recently available GORE™ technique, most of the commonly known soil-gas methods are described and reviewed comprehensively in Thiede (1999). GORE™, a 'free' hydrocarbon collecting procedure, was tested at the Eloise copper deposit, together with MSG (Chapter 6). Sirogas, another 'free' gas, but commercially unavailable method, was trialled with positive results at the Osborne copper-gold deposit (also Chapter 6). Significantly, the leachant Regoleach® (Australian Laboratory Services) was developed in conjunction with, and as an outcome of, the Osborne Sirogas study (N. Rutherford, May 2018, personal communication).

Of the 'sorbed' gas variants, the commercially defunct Soil Desorption Pyrolysis (SDP) method was tested at the Ernest Henry and Osborne deposits (with mixed results, Chapter 6); and the currently available Soil Gas Hydrocarbon (SGH) method was tested at Eloise (also Chapter 6).

Nature of data and implications

As observed for chemical leachants, the anomalies of soil-gas methods exhibit high spatial variability or spikiness, which is attributed partly to the role of fracture networks as primary pathways of mass transport across the vadose zone to the near surface environment. Additionally, the concentrations of individual soil-gas compounds from a single site often display poor long- and short-term reproducibility. This is evidently an intrinsic characteristic, reflecting the complexity and transient nature of the processes which generate and transport the compounds rather than simply a function of sampling and analytical uncertainty.

The ability to discriminate mineralisation-related signals from the potentially 'false' geochemical anomalies associated with regolith compositional peculiarities is an argued strength of commercial methods such as GORE™ and SGH, and the formerly available SDP method. It is based on the premise that mineralisation is expressed by the anomalous behaviour of multiple compounds, the association and concentrations of which are collectively less influenced by local factors (*e.g.,* substrate grainsize, permeability, organic content) than individual species. Accordingly, processed data, such as compound ratios to reduce local "noise", or principal components analysis (PCA) scores to map the distributions of highly correlated compounds, are common deliverables of the commercial methods, including SGH. In the case of the SDP method, the concept of an ore 'template', derived from the ratioed data of a known ore deposit and the search for its presence in 'brownfields' exploration data was promoted strongly.

An example of the template concept, ambitiously extended to the fingerprinting of an entire ore class, is provided in Figure 5.6, where SDP data for soil samples over the buried Osborne copper-gold deposit were processed using the 'ore' template of a buried porphyry copper deposit in Chile. While it is evident that the densely sampled ore footprint displays extreme variability, it is equally clear that strong template signals are absent beyond about 100 metres of the footprint. Though conceptually appealing, the template approach never gained commercial traction and too few case studies are published to thoroughly assess its effectiveness and potential.

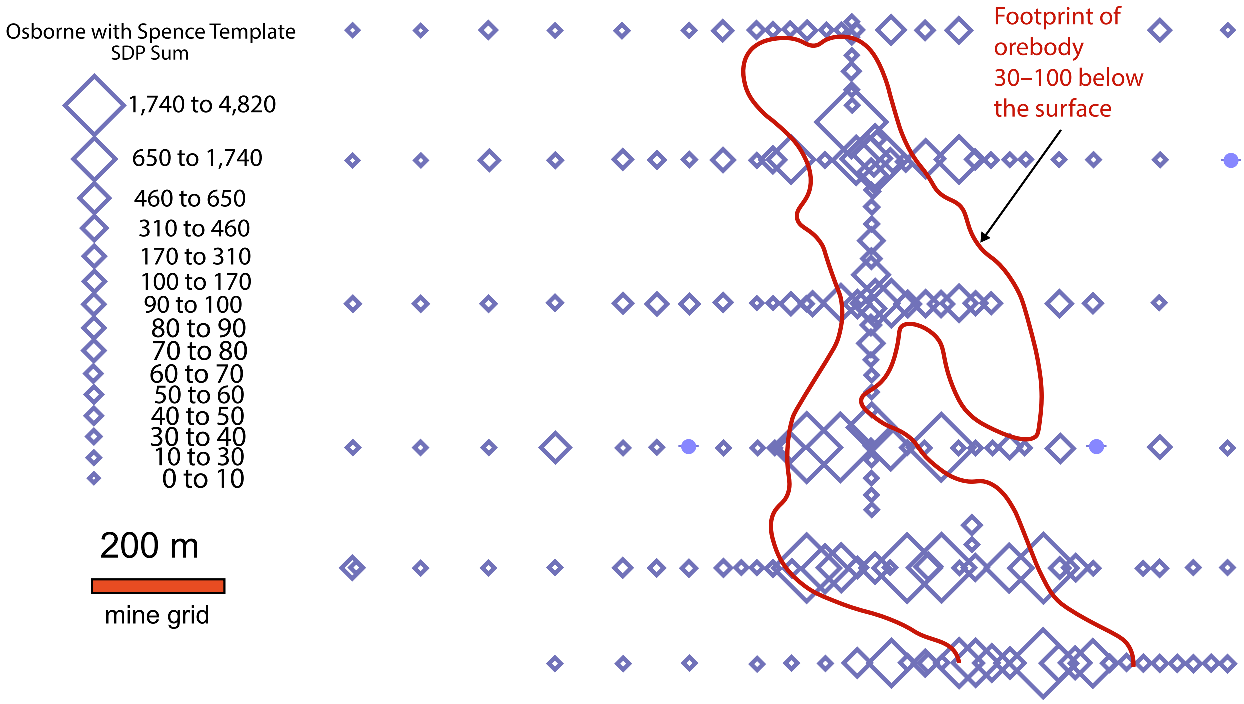

Figure 5.6. Osborne deposit soil sample grid showing the cumulative sum of anomaly/background ratios for compounds present in the ore template of the Spence porphyry copper deposit (modification of an SDP Pty Ltd presentation slide, circa 2002).

Biogeochemical methods

The coincidence of soil geochemical and vegetation chemical anomalies is well documented and attributable to the numerous ways in which plants take-up, recycle and redistribute metals and trace elements (Cohen *et al.,* 1999; Dunn, 2007). With due regard to the potential for contamination, both in the field and at the laboratory, the availability of high sensitivity analytical instrumentation makes the determination of the trace level concentrations involved a comparatively routine process.

Plants are an accessible surface sampling medium for the exploration of buried deposits because their root systems sample groundwater, regolith or rock. The root systems of woody plants in the water- and nutrient-stressed conditions typical of Australia commonly extend beyond depths of 10 m to reach local water tables (Figure 5.7). Absorption of solutes in groundwater and production of organic acids at root tips to dissolve minerals allow the plant to take up nutrient elements, as well as waste elements, that are subsequently segregated into various plant parts. Critically, the uptake of metals and trace elements is species-dependent, tissue-selective and seasonally variable.

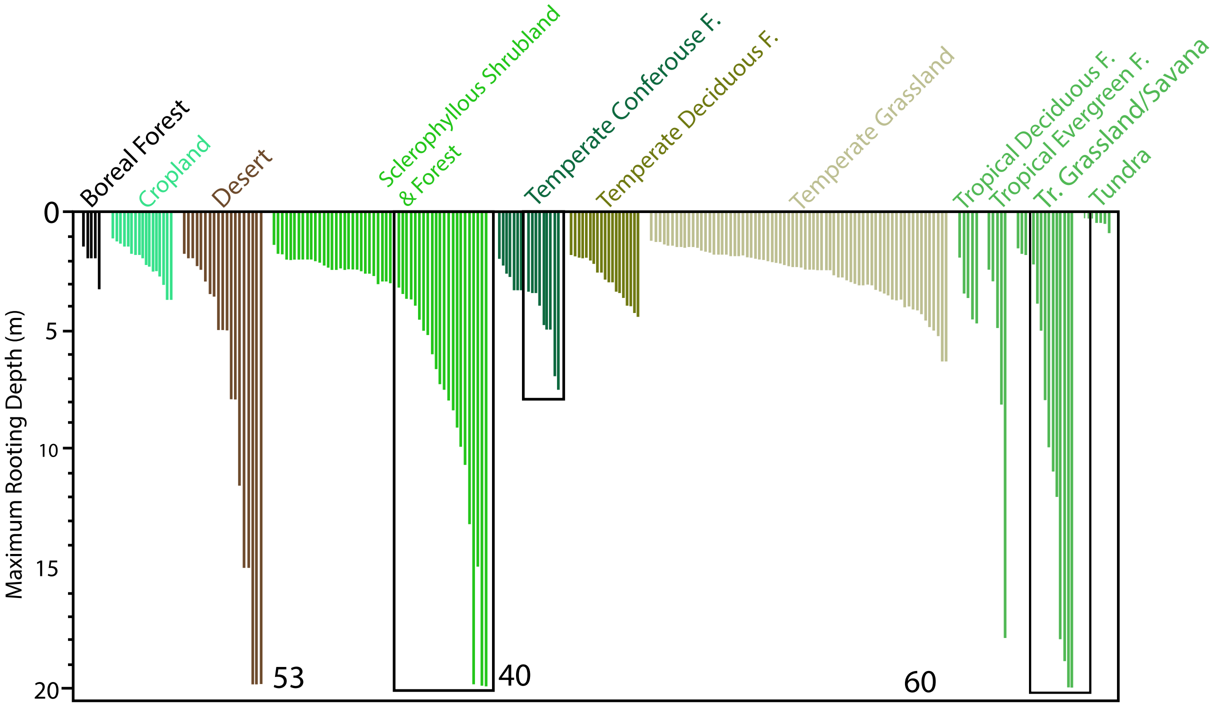

Figure 5.7. Bar chart of maximum rooting depths of reported species (Canadell, et al., 1996) grouped according to terrestrial biome. The boxed areas are dominated by data from Australia (after Aspandiar et al., 2006).

Biogeochemical sample collection is a relatively simple and low-impact process. Regularity of geographical distribution, tissue type and sample size need be considered before finalising which species are optimal for any given project (*e.g.*, Table 5.3). Material from different species must not be mixed within any given survey. Leaf material is generally considered the most suitable sample medium as it is less prone to contamination from soil and mineral particles (*e.g.,* plant roots), but it is important to select sample material from the same stage of growth on any given plant. As with any geochemical survey, a measure of sample site repeatability, by the preparation of replicates, should be factored in to the planning and budgeting of each biogeochemical survey.

The wide lateral spread of many root systems and the redistributive (cycling) capacity of the entire plant provides a compelling conceptual basis for vegetation as a suitable medium for broad area, reconnaissance investigations. Where the sampling of more than one species is needed to maintain the required sampling density, simple levelling of the analytical data by species may reveal coherency in elemental spatial patterns and anomalies that are not evident on a single species basis (Lilly & Hannan, 2016). For other semi-arid region case studies and the identification of favourable eastern Australian species for biogeochemical exploration refer to Cohen *et al.,* (1999); Hill (2004).

Chapter 5

Field sampling

Soil survey grid configuration

Pre-defined targets

Concealed and spatially discrete exploration targets are generally elongate, reflecting the importance of structural and stratigraphic criteria in their identification and selection. In these circumstances, square soil sample grids are not only expensive but not necessarily optimal for data interpolation. Line spacing/sample distance ratios of two or four are commonly used (*e.g.,* 50 m sample spacing along 100 m or 200 m spaced lines), with sample lines directed orthogonally to the primary controlling fabric. Ratios of ten or more may be appropriate for some target types (*e.g.,* large tonnage stratabound mineralisation).

Individual targets, including those within larger target zones or corridors, should be intersected by at least 2 sample lines and two or more samples per line. Line lengths should exceed the target width by more than a factor of five (ten is favoured).

Reconnaissance surveys

Grid specifications of 400 x 400 (*i.e.,* square) or 400 x 200 are commonly used for regional surveys which aim to locate new, large area targets (*i.e.,* up to the scale of porphyry systems).

Spacings of 1 km or more have been used in areas of thick, transported cover to evaluate the potential of large scale geophysical trends and structural domains, using methods such as MOMEO to measure the local metal signature of the *Geogas* flux (Wang *et al.,* 1997).

Sample site configuration

Conventionally, sample site selection is strongly influenced by the need to conform as closely as possible to the intersections defined by the line- and sample-spacing mesh (*e.g.,* the centre points of the yellow squares of Figure 5.8), and fractions thereof in the case of composites. However, a more flexible approach is desirable for reconnaissance chemical leach and soil-gas surveys to minimise the loss of data interpretability caused by the inclusion of atypical or unrepresentative sample material at potentially critical locations. This can be achieved by cell-based sampling, illustrated by sample points at varying locations within the contiguous blue squares of Figure 8. Such an approach remains amenable to pre-survey planning (*e.g.,* using high resolution regolith sensitive imagery to avoid subtle alluvial tracts), but ensures maximum sampler discretion ‘on the day’. It also provides a spatially flexible and directionally unbiased basis for composite sampling.

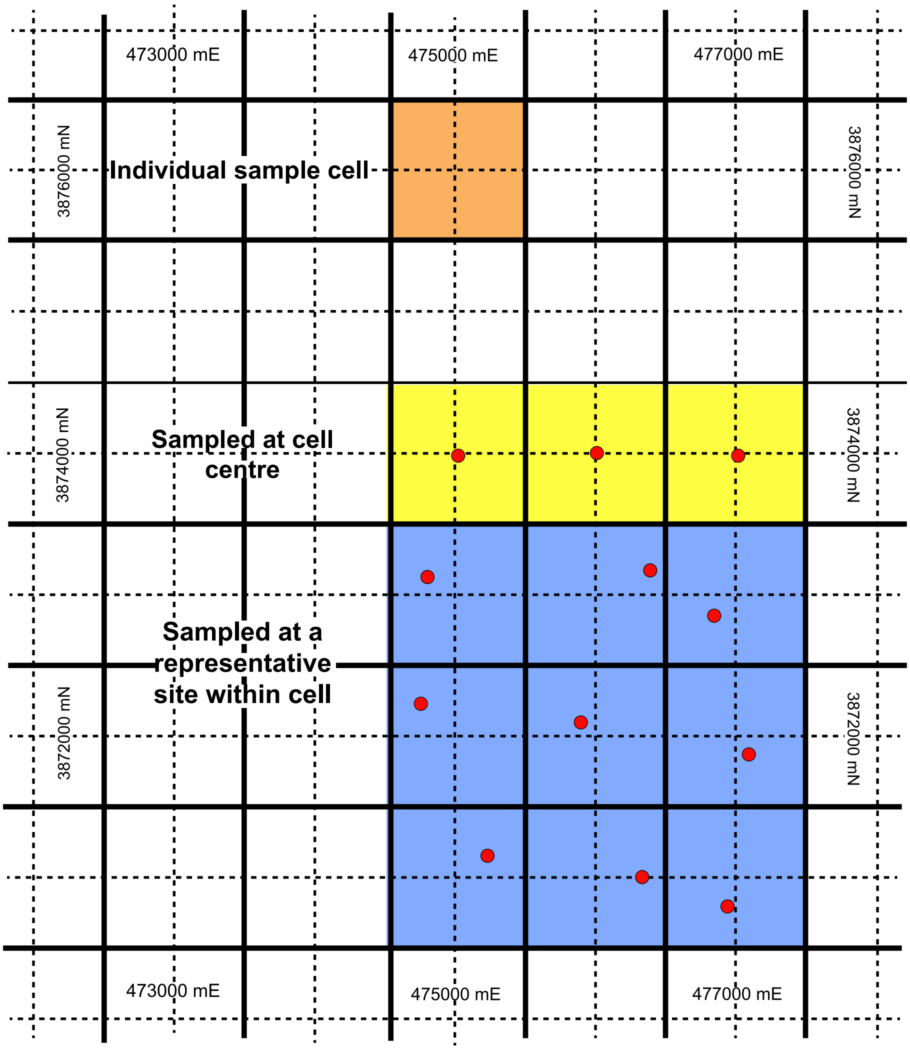

Figure 5.8. Conventional grid point and cell-based layouts for large area soil survey (from Rutherford, 2018).

Chapter 5

Sampling procedures

This section presents an overview of essential field sampling procedures for soil chemical leach, soil-gas and biogeochemical surveys in the Mount Isa region. Detailed procedures for each method are described in Lilly & Hannan (2016).

Chemical leachants

Abbreviated instructions for the sampling and analysis of soil samples by chemical leachant(s) are listed in Table 5.2. They are suitable for reconnaissance surveys and emphasise the processing of a consistent volume, area and depth interval of regolith.

Table 5.2: Field sampling procedures for chemical leach (and some soil-gas methods)

1. Scrape lag and surficial debris from an area of about 0.6 x 0.5 m, then photograph to record the prepared sample site and its immediate surroundings (a few metres).
2. Excavate an area of about 0.5 x 0.4 m to a depth of 10–15 cm, which normally exposes the top of the root horizon of grasses and/or corresponds to a colour change and the 'B' horizon.
3. Loosen the regolith within the primary hole to a depth of about 25 cm, taking care not to collapse the walls, then scrape into a central pile; place a scale bar with sample number label against the pile then take a close-up photo as a visual record of the raw sample material.
4. Measure and record the pile's pH then process the entire pile (12–20 L, or 14–25 kg) through the survey-specified sieve into a wide diameter tub/pan; use a gloved hand to nominally mix before sub-sampling.
5. Extract each sub-sample destined for analysis from the pan using a clean plastic trowel and pour into a numbered bag (generally zip-lock PVC); record the sample weight.
6. Back-fill the excavation

Soil-gas

For the GORE^{TM}, SGH and MSG methods refer to Appendix A, and for SDP, refer to Chapter 6 and Thiede (1999).

Vegetation

Abbreviated instructions for the sampling and analysis of tree leaves (*e.g.,* Gidyea) and grasses (*e.g.,* Mitchell Grass) are listed in Table 5.3. For detailed instructions refer to Lilly & Hannan (2016).

Table 5.3: Vegetation field sampling procedures

1. Photograph the sample site or area prior to sampling.
2. Where possible, samples to be collected from more than one plant of the chosen species, preferably at the same stage of growth and within a consistent area (sample spacing-dependent). Trees: collect leaves on twigs, from branches at about 2 m above ground level. Grasses: cut at the base of the leaf stem with clean shears.
3. Resample at a regular interval to produce an adequate number of field replicates for QA/QC.
4. Collect in calico bags and allow to air dry for up to 2 weeks, then remove all twigs.
5. After drying tree leaf samples should weigh 50–70g and grass samples 200–300g.
6. Typical lab process: samples are ashed and about 0.1 g is digested in aqua regia and measured by ICPMS for about $50 per sample (50–70 elements).

Quality assurance

QA Procedures

Systematic field and laboratory quality assurance procedures (QA/QC) underwrite the integrity and interpretability of soil chemical leach and soil-gas data. The following list sets out recommended QA sampling and QA data evaluation practices.

Routine precautions specific to covered domain surface geochemistry

Minimise contamination at the sample site by: removing jewellery, cleaning sampling equipment between sites, wearing gloves if sunscreen is in use, and using equipment appropriate for the analytical method (*e.g.,* paintless digging implements, plastic versus certified stainless-steel sieves).

Field replicates—high priority

A field replicate is defined as a second sample from a new excavation, near a designated original sample. Field replicates are strongly recommended to monitor and quantify total sampling precision. In conjunction with analytical QA data, replicate data pairs can be used to evaluate signal variability and other survey characteristics, such as the comparative performances or repeatability of different leachants. Field replicates should be collected at a constant distance, preferably less than five metres, from the original site.

The frequency of replication is survey size-dependent, but as a rule-of-thumb, about 12 samples is sufficient for small surveys (100–250 samples). To control QA costs on large surveys, which may extend across different soil types and landforms, replicate frequency can be adjusted to maintain 12-sample coverage for each major sub-population.

Field duplicates—low priority

A field duplicate refers to a second sample, or split, of the sieved material from which the original sample was extracted; the original and its duplicate comprise a ‘duplicate pair’. Field duplicate pairs provide a means to evaluate the compositional homogeneity of the target fraction of individual field samples. As such, they are of more relevance to orientation issues (*e.g.,* quantifying grain size influence on signal strength) than evaluating the significance of anomalies or patterns.

Laboratory repeats—high priority

A laboratory repeat or ‘check assay’, corresponds to the analysis of a second sub-sample of the same volume of pulp, or stock, from which the original sample was directly extracted for leaching and analysis; the original and the repeat comprise a ‘lab-repeat pair’. Most laboratories prepare and analyse lab-repeats routinely, ideally as a group at the end of analytical runs (batches) and supply the data to clients automatically.

Ordinarily, lab-repeat pairs are used to evaluate the homogeneity of sample pulps, but in the case of chemical leachants and soil-gas procedures, lab repeats also provide information about the stability of the digestion-analysis process where standards are not available.

Reference materials (standards)—high priority

Standards available for selective extraction or soil-gas methods generally lack certified true values and tolerance bands for individual elements; if available, multiple analyses provide a measure of accuracy and, by inference, the stability of the chemical digestion and analysis. However, a carefully prepared 'monitor' standard, comprising typical soil of the survey area, can be used for this purpose. If several monitor standards are used per lab job, at regular intervals in the analytical sequence (nominally 1/100), then within-batch analytical drift and systematic differences in leachant yield between batches can be monitored and quantified. For maximum control the standards should be preceded and succeeded in the analytical sequence by blanks.

QA data processing

Despite the inherent variability of chemical leachant and soil-gas data, explorers still need measures of data quality to demonstrate adequate laboratory performance and to assess the effectiveness of the chosen field sampling procedures. The following guidelines provide a robust and non-generic approach to the treatment and visualisation QA data.

Differences in the analyses of field-replicate pairs reflect variability at the scale of sampling (*i.e.,* 1–5 metres) and all sources of variance from that point forward (Thompson & Howarth, 1978). Each subsequent source of variance contributes additively to the total measure of spread in analytical data. Once the spread is quantified, as precision, the effectiveness or 'repeatability' of the chosen field sampling tactics can be compared with any other sampling procedure for which equivalent pairwise data is available.

Precision is conventionally expressed as a percentage. Bias, being a consistently directed deviation between two sets of results is easily deduced from the same sets of paired results. In the special case of differences between analyses of reference materials (standards) and their 'true' or 'expected' values, the pair-wise data permit the calculation of accuracy (correctness). For all three parameters, smaller differences between paired results correspond to improving bias, precision or accuracy (expressed as lower percentages).

Specifically, calculations of precision and accuracy follow those developed by Thompson & Howarth (1978) and Shaw *et al.* (1998) and are provided as step-wise instructions in Appendix B. The methodology is applicable to all stages of sample volume reduction and processing for many types of media, including drill core.

QA data evaluation

Table 5.4 provides a reference list of upper limits of precision suitable for resource modelling and public reporting of sampled mineralisation in Table 5.2 (most commodities). For comparison, the average precisions obtained at equivalent procedural steps are shown for recent soil surveys by aqua regia, chemical leachant and soil-gas data in the Mount Isa region (Lilly & Hannan, 2016).

Significantly, the average precisions of field replication and duplication for Terra Leach (TL) and the much weaker Mobile Metal Ion (MMI) are not dramatically inferior to those by aqua regia; by contrast, and as expected, matrix effects and analytical variance, represented in the lab repeats and accuracy averages, are higher in progressively weaker leachants, and higher still for soil-gas methods. Bar charts are easily generated in excel to show similar information for multiple extraction types (*e.g.,* Figure 5.9), whilst the detail for individual samples and multiple elements can be visualised on X-Y graphs (Figure 5.10). Discussion of these and other plots is provided in Section 4 of the GTC Project report (*op. cit.*).

Table 5.4: Acceptable and observed precision limits for selected QA parameters (chemical data)

QA Parameter	Mineralisation ('total' assay)	Control procedure	Soil by leachants	Soil-gas (MSG, SGH)	Soil by Aqua Regia
Analytical precision	≤ 3.5% (1–4 is typical)	*duplicate readings of the same liquor, XRF pellet etc.*	-	20%	-
Accuracy	≤ 5% (1–3 is ideal)	*certified reference materials*	7% TL 15% MMI	-	5%
Lab sample precision (Lab Repeats)	≤ 7% (5 is typical)	*1-in-15 digestions of a 2nd aliquot of pulverised stock*	10% TL 20% MMI	30%	8%
Pulping precision	≤ 10% (20%)[1]	*e.g., 100g split of 1–3 kg of pulp*	-	-	-
Crushing precision	≤ 20% (30%)[1]	*e.g., 1.5 kg split of 3–10 kg of core*	-	-	-
Field sample precision	≤ 40%[2] (50%)[1,2]	*field sample duplication*	20% TL 35% MMI	50%	15%
Field sampling precision	-	*field site replication*	40% MMI	60%	35%

[1] Ideal upper limit for coarse Au mineralisation (but often higher); [2] drill core and RC drill samples

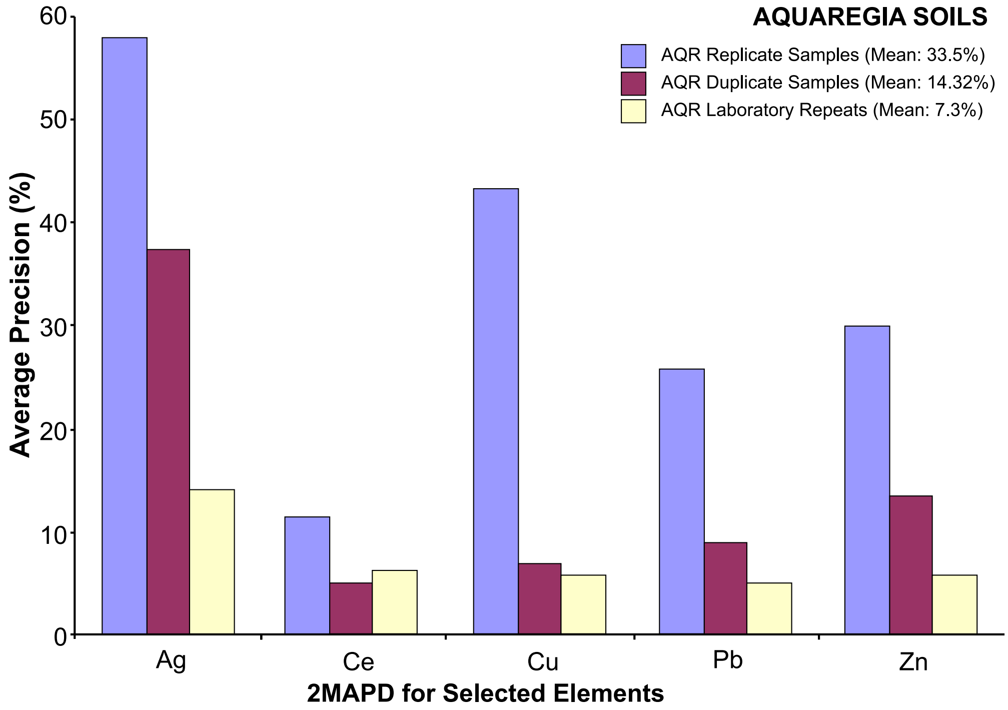

Figure 5.9. Bar chart of average precisions (2MAPD) for selected metals extracted by aqua regia from the <5mm fraction of soil sample field replicates, field duplicates and lab repeats (from Lilly & Hannan, 2016).

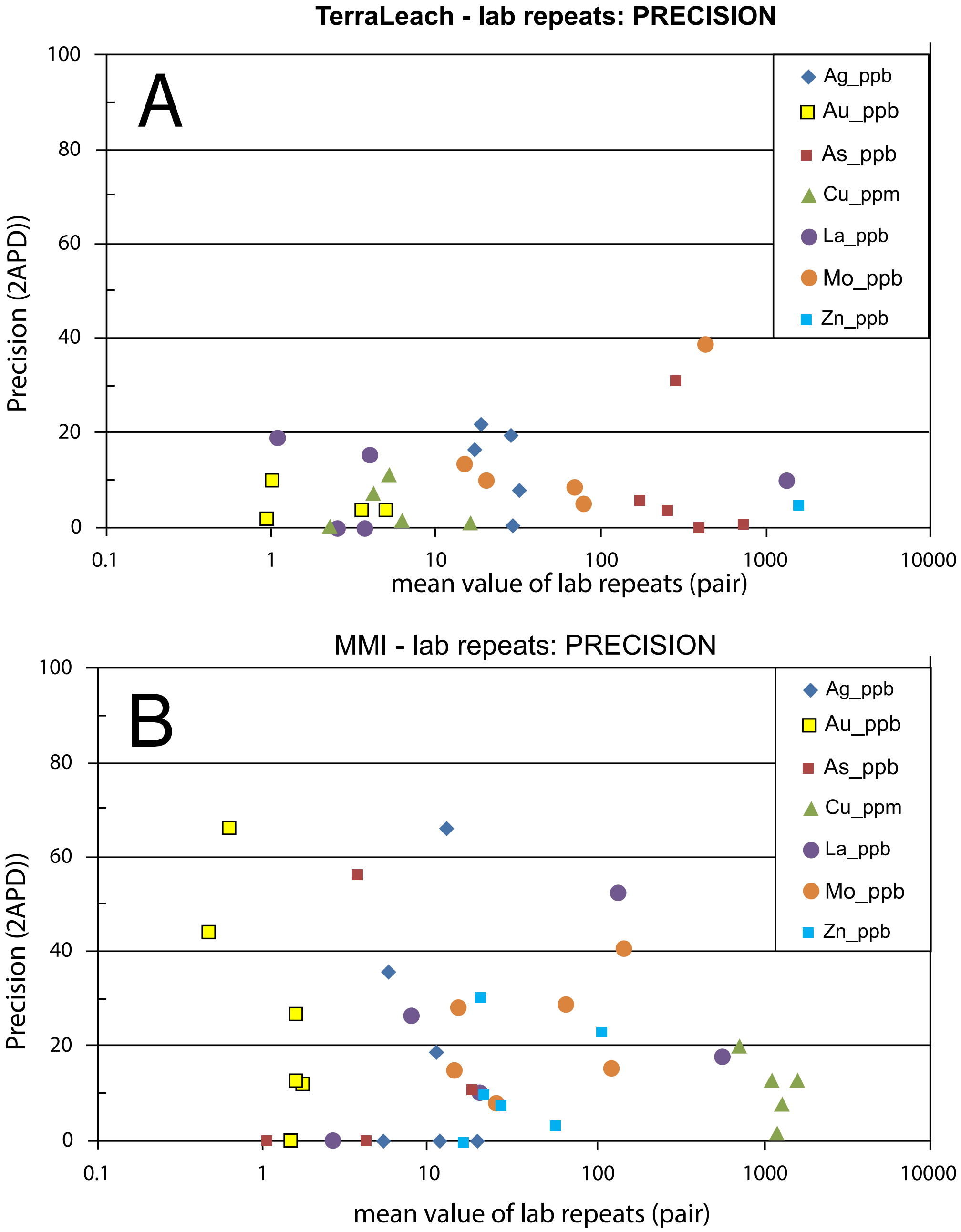

Figure 5.10. Precision-concentration X-Y graphs for selected metals extracted by Terra Leach (upper) and MMI (lower) from the <5mm fraction of soil sample lab repeats (from Lilly & Hannan, 2016).

Chapter 6

Covered domain geochemistry II: Secondary dispersions of blind ore deposits

Introduction

The theme of this chapter is the chemical detection of economic concentrations of base metals ± gold in the Mount Isa region through thin to moderate thicknesses of post-mineral cover (nominally 5–75 metres). All the significant discoveries of the last 35 years are confined to this domain and the result of drilling aeromagnetic anomalies—but it remains under-explored. With the cumulative experience and evidence brought to bear in this and supporting chapters, it is hoped that more explorers will develop the confidence and expertise to execute high quality chemical exploration programs in the covered domain—both for the pre-drilling follow-up of geophysically defined targets and, where appropriate, for primary target recognition.

The surface chemical data of four blind IOCG Cu-Au deposits (Ernest Henry, Osborne, Eloise and E1) and the blind Cannington Ag-Pb deposit are reviewed and summarised to provide a unique snapshot of the historical and somewhat spasmodic efforts to test and advance 'penetrative' chemical technologies for mineral exploration in the region. Each of the case studied deposits offers different insights into the controls of chemical anomalies attributable to deeper sources and, in some cases, the likeliest transport mechanisms. The results of 'failed' surveys are also discussed, as guidance for the challenge*,* inherent to all applied technologies, of distinguishing negative and null exploration results.

Ernest Henry Cu-Au deposit

Setting

The Ernest Henry iron oxide copper-gold (IOCG) deposit is located 37 km northeast of Cloncurry and is the largest of its type in the Eastern Fold Belt. It was discovered by Western Mining Corporation Ltd. and Hunter Resources Ltd. in 1991 by drilling a district-scale aeromagnetic anomaly in the grassy plains of the Carpentaria Basin (Figure 6.1). The pre-mining resource of 166 Mt at 1.1% Cu, 0.54 g/t Au was mined as an open pit operation between 1996 and 2013, and then as an underground operation with a resource of 87.1 Mt at 1.18% Cu, 0.60 g/t Au, from December 2015 (Lilly *et al.,* 2017).

The orebody is pipe-like in plan and long-section (Figure 6.2) and hosted in brecciated and K-feldspar altered andesitic volcanics that are dated at about 1740 Ma (Mark *et al.,* 2006).

An extensive suite of trace elements is associated with the hypogene Cu and Au mineralisation, including Ag, As, Ba, Co, F, Mo, REE, W and U. High abundances of all these elements occur at the Proterozoic-Mesozoic unconformity in contact with mineralisation, and most are recognised in the dispersion halos within the cover sediments (this chapter).

Pre-mining, the deposit 'sub-cropped' as a modest paleotopographic high under 25–40 m of moderately lithified Mesozoic and unconsolidated Cenozoic sediments of the Carpentaria and Eromanga Basins (*e.g.*, Figure 6.3).

Figure 6.1. Site of the future Ernest Henry mine (photographed mid-1994, K. Hannan).

A small area of gossan was originally excavated at the crest of the palaeo-knoll and relict paleosol and conglomerate with clasts of weathered ore mantled the surrounding Mesozoic–Proterozoic unconformity. The essential stratigraphic relationships are shown for the northern part of the deposit, where overburden is thinnest, over the basement paleotopographic-high, in Figure 6.3.

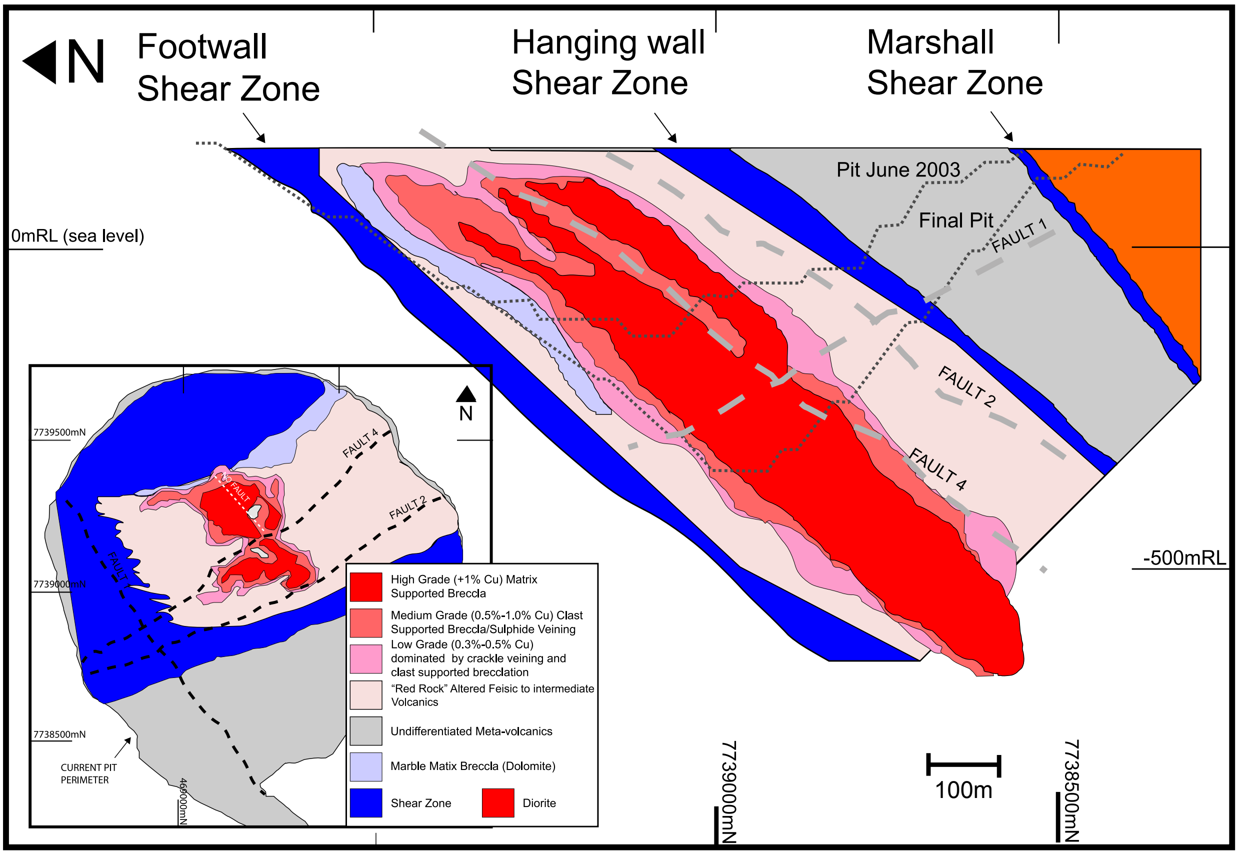

Figure 6.2. Geology and Cu-grade distributions of the Ernest Henry Cu-Au deposit—long section (upper frame), plan view (left frame, unknown RL) and legend (from Lilly et al., 2017).

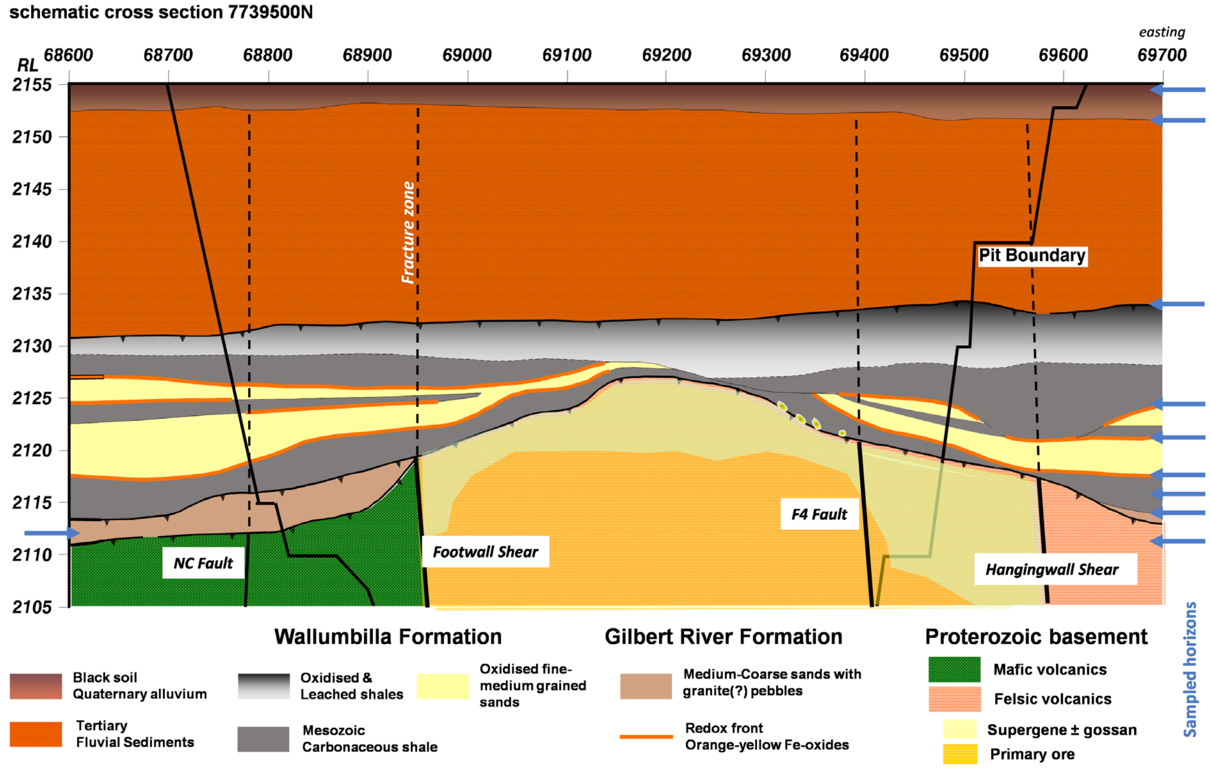

Figure 6.3. Cross section of the northern end of the Ernest Henry deposit, where paleotopographic relief is greatest and cover thickness the least (adaption of figure 4 in Sheppard, 2001).

The primary ore assemblage is dominated by magnetite, auriferous chalcopyrite, pyrite, calcite and quartz, and has an enveloping surface defined by two prominent shear zones which dip about 45° towards the SSE (labelled in Figure 6.3). Lesser shears penetrate the interior of the orebody and later, penetrative brittle faults locally displace it. These structures and their intersections controlled not only the formation and distribution of the original supergene resource, as conduits for groundwater access (Lewis *et al.,* 1994), but also the development of secondary chemical dispersions into the 25–40 m of late Jurassic – early Cretaceous and Cenozoic sedimentary cover (Hannan, 1994, 1995; Baker *et al*., 1995; Sheppard, 2001). Additionally, the vertically projected positions of the basement faults commonly coincide with changes in the RLs of cover unit surfaces which correspond to thickness changes (*i.e.,* not simply draping a lower surface). This critical finding is illustrated for the Tertiary (on Mesozoic) unconformity and the upper surface of the lower shale unit of the Wallumbilla Formation in Figure 6.4. It provides strong evidence that the basement faults were subject to reactivation and responsible for the propagation of fracture zones as the Phanerozoic overburden accumulated (depicted in Figure 6.3 as dashed lines).

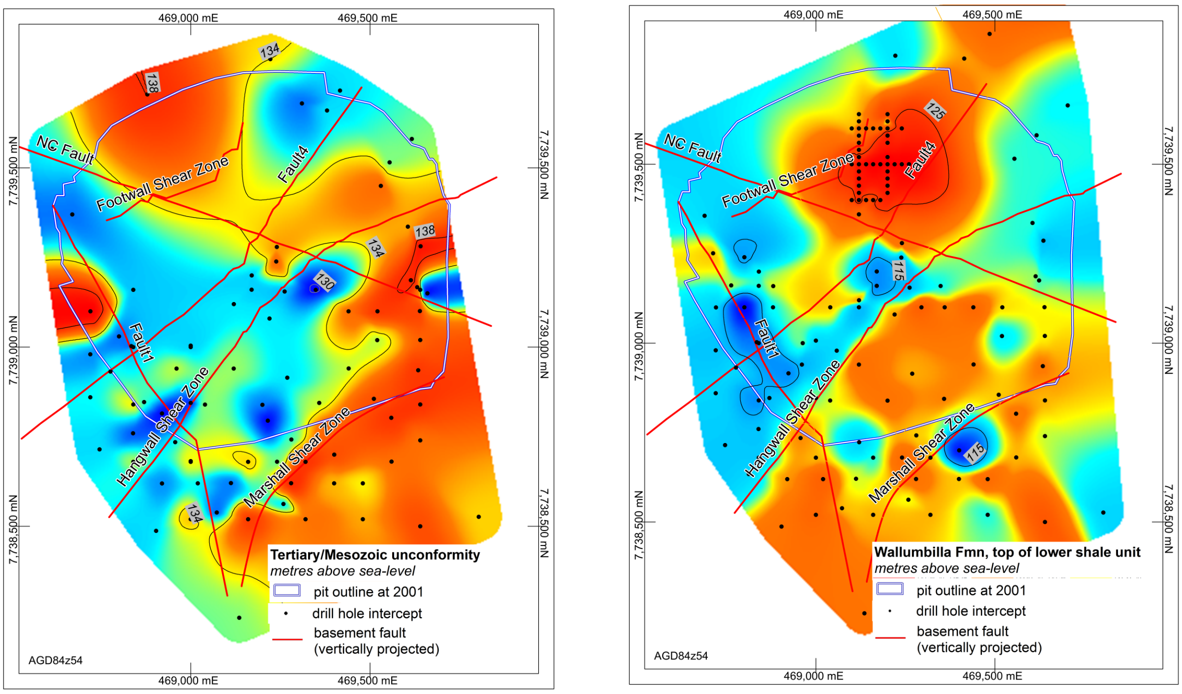

Figure 6.4. Relationship of major structures to the gridded intercepts of two paleosurfaces: left frame—Tertiary unconformity, right frame—top of the lower shale unit of the Wallumbilla Formation (modifications of figures 16 and 18 of Sheppard, 2001). The pre-mining surface RL was about 156 m (ASL).

Surface geochemistry

Three campaigns of orientation soil/regolith sampling were completed in the period between the supergene resource drilling program by MIM Exploration in late 1993 and the start of open cut operations by Ernest Henry Mining Ltd in late 1996. The survey lines are depicted in Figure 6.5. The surficial regolith of 1–2 m of smectitic, ‘cracking’ soil, or simply “black soil”, was sampled by pick and shovel from the 15–25 cm depth interval along Lines 1–3 and 7. A persistent, 1–2 m thick reddened horizon within the underlying Quaternary sand was sampled at depths of 3–6 m along lines 4–6 by RC drilling. The entire redox-affected profile is at least 8 m thick. Two selective extractions, enzyme leach (ENZ) and mobile metal ion (MMI), one soil gas extraction method (SDP) and one free-gas method (radon) were tested, in addition to characterisation by conventional ‘strong acid’ digestion.

Conventional (strong acid digestion)

Cracking black soil is a notoriously ‘opaque’ geochemical medium for the explorer. Table 6.1 provides a reference set of averages for local black soil and underlying sand, as determined by conventional ‘total’ methods (HF-assisted digestion of pulverised samples). Black soil Cu values are tightly constrained to a range of 19–21 ppm, the gold content is 1 ppb or less, and the U average is 1.3 ppm. The chemical uniformity is emphasised in the Cu and U line data of Figure 6.6 (left frames), noting that the off-line samples of 2001 are consistently elevated or anomalous, almost certainly by the settling of airborne dust from the mining operation. In short, there is no evidence of a mineralisation signal in the pre-mining, bulk chemical composition of black soil above the deposit.

Although the upper 10 m of underlying sand have 2–4 times the average levels of black soil Cu, As, Mo, U and W (Table 6.1), a lateral gradient is not obvious in either the mapped local data (*e.g.,* Cu and U, right frames of Figure 6.6), or in several distal pre-mining ‘sterilisation’ and

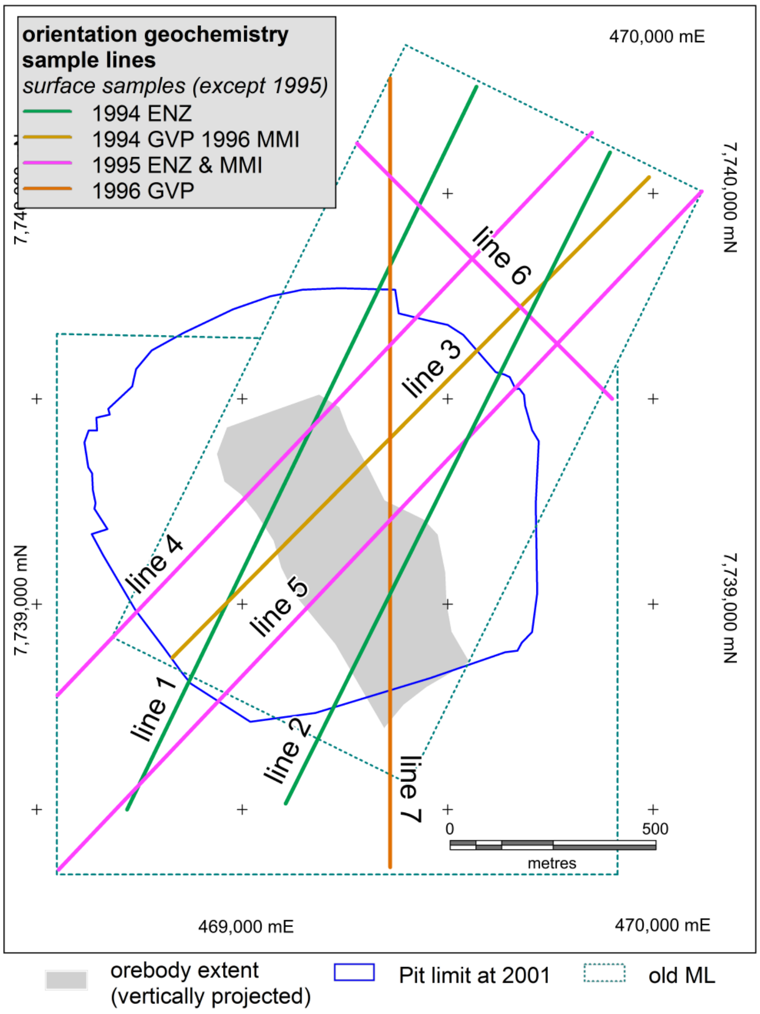

Figure 6.5. Locations and types of orientation soil/regolith geochemical surveys over the Ernest Henry Cu-Au deposit (pre-mining).

Table 6.1: Average compositions ('totals') of black soil and Quaternary sand at the Ernest Henry deposit.

Element	Soil (n=48)	Sand (n=189)	Comment (sand) (sands 1–10 m depth)
Au	< 1 ppb	1 ppb	range <1–4 ppb
Ag	0.27	< 0.5	max. 1.3 ppm (dl=0.5)
As	3.5	8	4–20 ppm
Bi	0.14	0.3	61 samples
Co	19	14	7–24 ppm
Cu	21	48	31–82 ppm
Fe	2.72%	5.0%	3.6–7.6%
Mn	925	570	310–1580 ppm
Mo	0.4	1.7	1.1–3.3 ppm, n = 61
Pb	15	14	8–25 ppm
S	47	250	100–450 ppm
Sb	0.3	1.1	61 samples
U	1.3	4.2	2.5–13 ppm
W	0.7	2.2	1–4.8 ppm, n = 61
Zn	27	40	17–62 ppm

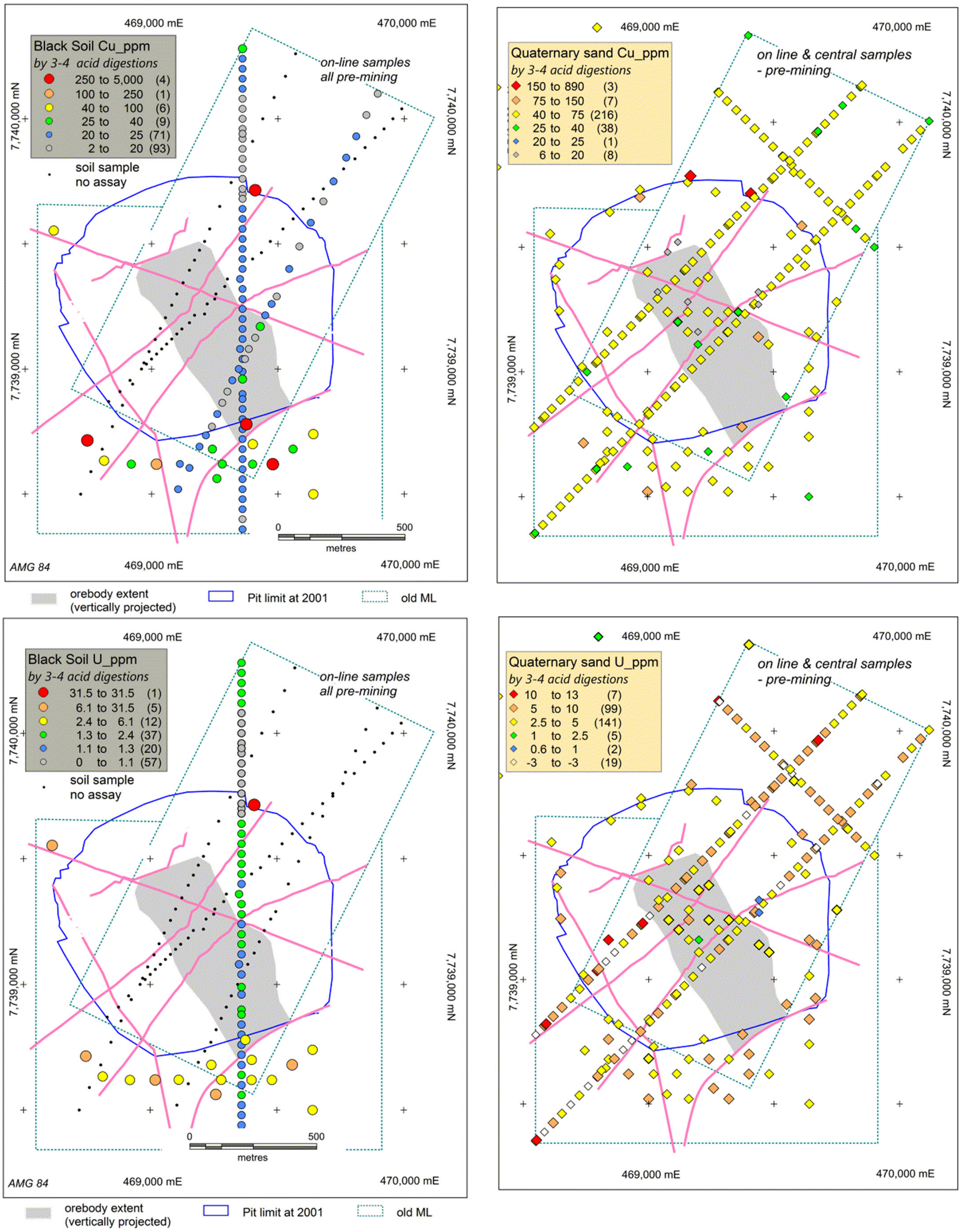

Figure 6.6. Total digestion Cu (upper) and U (lower) of black soil (left) and underlying Quaternary sand (right) in relation to original ML boundaries, 2001 pit, faults (pink lines) and projected position of the Ernest Henry orebody (sourced from the compiled data of Sheppard, 2001).

groundwater bores up to 3 km to the W, N and E of the deposit. However, sand in distal holes to the south of the deposit have metal abundances at the lower end of the tabulated ranges, so it is conceivable that interaction with groundwater has, over time, generated a plume as it passed northward over and around the rising and mineralised basement and metalliferous shales from the south, toward the Gulf of Carpentaria. The possibility certainly demonstrates the potential value of having a better knowledge of metal distributions in key post-Proterozoic strata across the region.

Enzyme leach and MMI

Black soil was bulk-sampled every 50 m along lines 1 and 2 (refer Figure 6.5) in mid-1994 and treated by a developmental version of the enzyme leach reagent at the WA Dept. of Mines. Despite clear evidence of analytical drift and a lack of resolution for some elements, the results for Cu, particularly on line 2 (Figure 6.7, upper-left), and the LREE on line 1 (Figure 6.7, mid-left), were considered sufficiently encouraging to persist with the possibility of low-level metal migration to the surface from mineralisation through 25–40 m of unconsolidated cover.

A few months later, in 1995, 50 m-spaced shallow RC holes were drilled along lines 4, 5 and 6 to target the known redox transition within the Quaternary sand as a potentially better chemical trap for migrating metals than the black soil. Field samples for enzyme leach and MMI treatment were passed through a 0.25 mm sieve and analysed at Australian labs recently licensed for the two methods. Field sample numbers were randomised to mitigate the lack of certified standards and drill hole duplication. Every 4th or 5th drill hole was sampled approximately 2 and 4 m below the first sample to test for profile variation (redox control) and as a measure of sample site repeatability.

The most promising and/or instructive results are presented in the right-hand column of frames of Figure 6.7. Despite analytical resolution and calibration weaknesses, reflecting the developmental nature of the extractions, Cu, Co and Ag repeatedly spike 3–5 times above local background levels, either above or proximal to the projected enveloping surface of the orebody. The profiles of total digestion Cu and Co are included for reference and contrast. In the case of total Cu, a 20 ppm ‘bulge’ above the 40-ppm background level is evident across the centre of Line 4, which is mimicked by the high amplitude MMI Cu trace. The MMI-total Cu pattern is a classic, though comparatively subdued, example of an apical selective extraction anomaly developed in a weak conventional soil anomaly (Mann *et al.,* 1997).

The somewhat peripheral setting of the two strong ENZ Co peaks of Line 4 (supergene ore) is matched by that for MMI Cd (not plotted) and is semi-coincident with strong peaks in MMI Ag. The effect is suggestive of metal zoning, reflecting differences in Eh/pH stabilities between elements, and the twin-peak anomalies predicted for divalent cations by electrochemical dispersion models (summarised and reviewed in Aspandiar *et al.,* 2008). In detail, evidence for the accumulation of the halogens and high charge cations, such as As, Mo, W, and U, as oxidative peripheral anomalies (Clarke, 1992) is weak or lacking—with only ENZ Br displaying a low amplitude shoulder at the SW end of line 4 and a broad, shallow trough above the ore zone (not plotted). However, stronger halogen anomalies are evident in the data of a later study (next section). Regardless, the accumulating salts of the relevant metals and halides would be subject to dissolution and redistribution through the regolith during the Gulf of Carpentaria’s monsoonal wet season.

Another explanation for the proximal metal anomalies is that they developed in networks of fractures vertically above the ore-confining and -cutting faults, which provided a direct and permeability enhanced route for metal- and gas-charged oxidation products to the water table (at a depth of about 20 m). Seasonally moderated capillarity could then have easily facilitated metal transport to the near surface environment (Mann *et al.,* 2005, Aspandiar *et al.,* 2008). In this regard, it is noted that the orebody limits, as displayed in Figure 6.7, are generalised for the Mesozoic unconformity from drill hole data available in 1996. Later publications show ore extending as much as 150 m further west along the Footwall Shear zone and Fault 4. That is, ore may have originally underlain the entirety of the black soil LREE peak (Line 1) and some of the strong MMI Ag anomaly on Line 5.

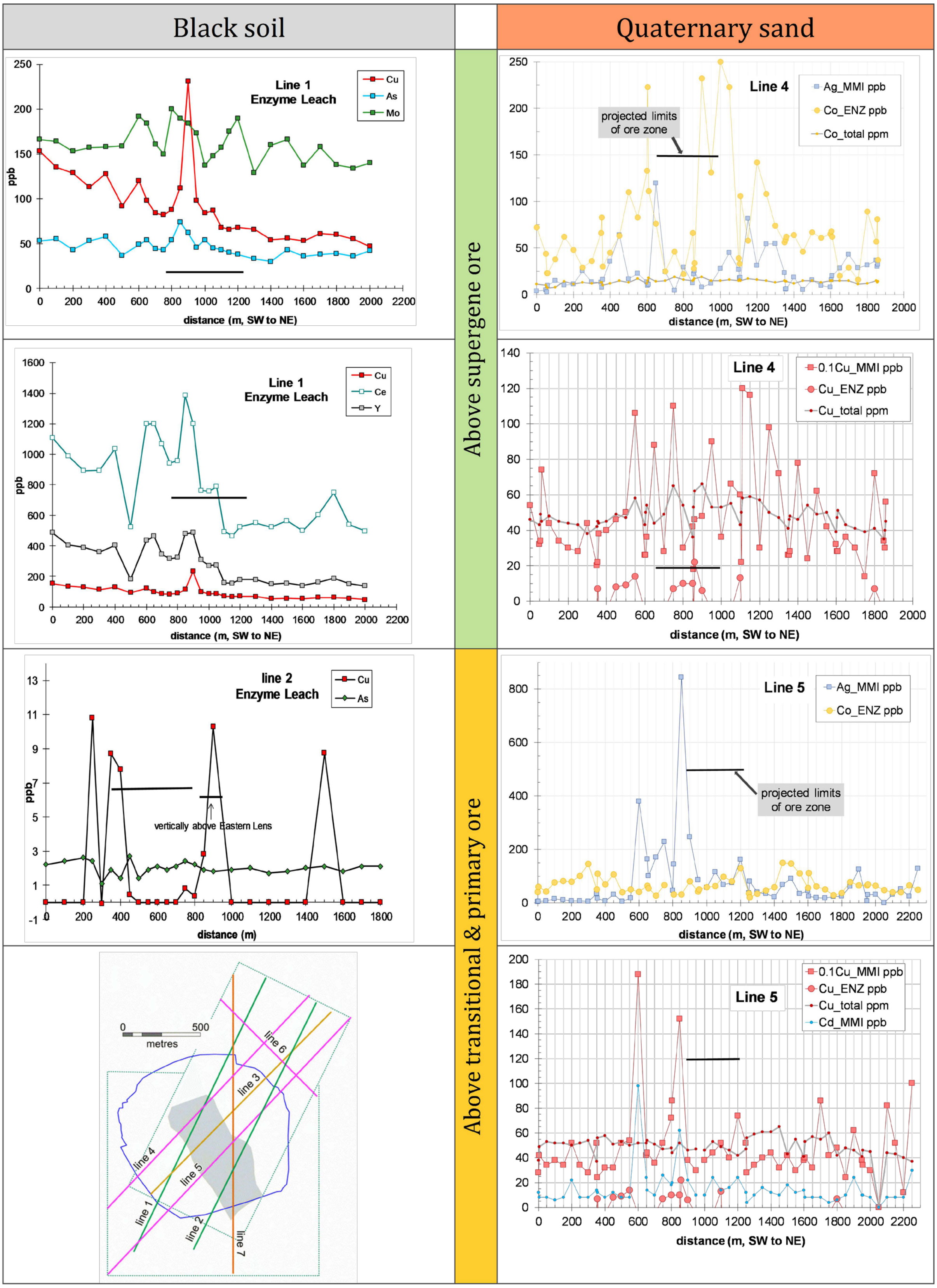

Figure 6.7. Line profiles of selected metals in black soil (left column) and near surface Quaternary sand across the Ernest Henry deposit (right column); (data from Sheppard, 2001).

The profile triplets correspond to samples at depths of 2–3, 3–4 and 4–5 metres, corresponding to mustard coloured, orange, and red-tinted pebbly sand, respectively. Below the reddened interval the colours transition to mid-browns through pale buff and greenish below 7 metres. The colour sequence varies little along the survey line and is consistent with an oxidation potential gradient. MMI-extractable Cu, Co, Ag and ENZ As and W levels are highest, by 1.5–2 times*,* at the reddened interval (4–5 m), and ENZ Mo, U, V, Br and Ce highest at the top of the sand profile.

Notably, total U (by XRF) is anomalously elevated in the upper profile samples, with an average of 10 ppm, dropping to about 4 ppm in the deeper samples. The significance of this feature can't be assessed until equivalent U data is acquired for distal localities.

In summary, the triplet results indicate that the detection and amplification of geochemical anomalies in commodity metals is favoured by sampling the reddened regolith, where adsorptive Fe and Mn oxyhydroxides accumulate at a transition from relatively oxidising to reducing conditions—as concluded in earlier reviews and case studies (*e.g.,* Butt *et al.,* 2005, Lawrance, 1999). Just as importantly, the strong zoning of elemental abundances in the redox profile emphasises the need to apply a strictly consistent sampling procedure for selective extraction geochemical surveys.

Orientation surveys with negative or ambiguous results

Soil desorption pyrolysis (SDP)

In 1994, black soil was sampled along Line 3 (see Figure 6.5) to investigate the effectiveness of the newly available technique known as GVP (Gas Vapour Phase) which had been developed for the oil and gas exploration to detect and map gas leakage zones related to blind reservoirs of hydrocarbons. The method is based on soil desorption pyrolysis (SDP), whereby samples are heated, and gases adsorbed by clay and silt particles are extracted and measured for a broad range of volatiles species. For mineral exploration, the focus of SDP are the gaseous products of sulfide oxidation (weathering), especially sulfur gases, such as CS_2, COS and SO_2, but also CO_2 (Aspandiar *et al.,* 2008) and spectrum of metal halide complexes and hydrocarbons.

Line 3 (Figures 6.5 and 6.8), served as a baseline survey for the calculation of a template, based on the GVP response of a subset of the samples located vertically above ore. The template is essentially a multi-variate statistical product, comprising modelled gas species ratios which best separate above-ore from all other survey samples. The template-defined results for Line 3 are plotted in the left frame of Figure 6.8. The statistical separation of above-ore samples is clear. Two years later, and still pre-mining, the template was tested on soil line 7. Sample

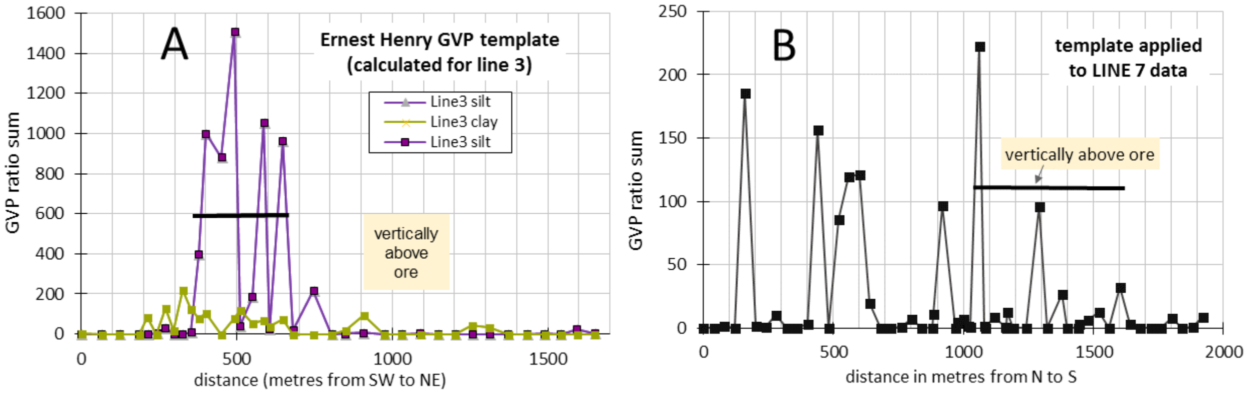

Figure 6.8. Soil desorption pyrolysis orientation survey results for Ernest Henry; left frame—optimised template based on the analyses of 6 above-ore and 6-background samples; right frame—template applied to randomised samples from a subsequent line of black soil samples.

numbers were randomised and the samples submitted for GVP analysis as bulk samples. The results, plotted in the right frame of Figure 6.8, display a spikey and decreasing trend, that best corresponds to an increasing depth to basement, from north to south (*i.e.,* from about 30 to 80 m). Alternatively, strong but deep mineralisation might underlay the coherent 450–600 m anomaly (an area sparsely drilled to only 150 m before utilization as waste dumps). An outstanding question, also, is whether the contrasting "ratio sum" amplitudes of the two surveys is a calculation, sample processing or even time-related artefact (*e.g.,* change in regolith moisture levels between the two surveys).

MMI trial 2

Archived splits of the black soil samples collected for the GVP template in 1994 (discussed above), were submitted for metal extraction by the MMI method in late 1996. The results were disappointingly uniform, without the slightest hint of elevated responses for any of the analysed elements over the projected position of ore (*viz.,* Line 3 of Figures 6.5 and 6.8). For example, Cu ranged from 360 to 500 ppb with an average of 425, and Ag from 4.2 to 7.3 ppb with an average of 5.3 ppb. The question remains whether two years of storage in periodically hot conditions could have led to the fixing of originally weakly bound metals into dehydrated and less soluble phases. Accordingly, this particular orientation survey is not regarded as a conclusive test of the MMI extractant.

Soil gas—radon

In November 1995, the Australian Nuclear Science and Technology Organisation (ANSTO) completed a survey of radon fluxes in pore air across Lines 4 and 5 (Zahorowski *et al.,* 1996). The aim was to identify sources of elevated U^{238}. Radon collection vials containing activated charcoal were installed at a depth of 50 cm in 30 of the RC holes drilled a month before to test geochemical responses (discussed above). After 2 hours of exposure in the back-filled holes, the vials were sealed and measured by a specialized scintillometer. The results are plotted in Figure 6.9.

Though superficially encouraging, with most elevated values close to projected known faults, the researchers presented modelling results which showed that the high levels of U present in Quaternary sand unit 1 or 2 metres below the surface, could easily account for the range of measured radon release, and would obscure signals from even ore grade sources of uranium at depths of more than about 10 metres (*op. cit.*). The general correspondence of the radon concentration patterns to U levels in the upper 1–2 m of the Quaternary sand probably supports this conclusion (compare Figure 6.9 and the lower right frame of Figure 6.6).

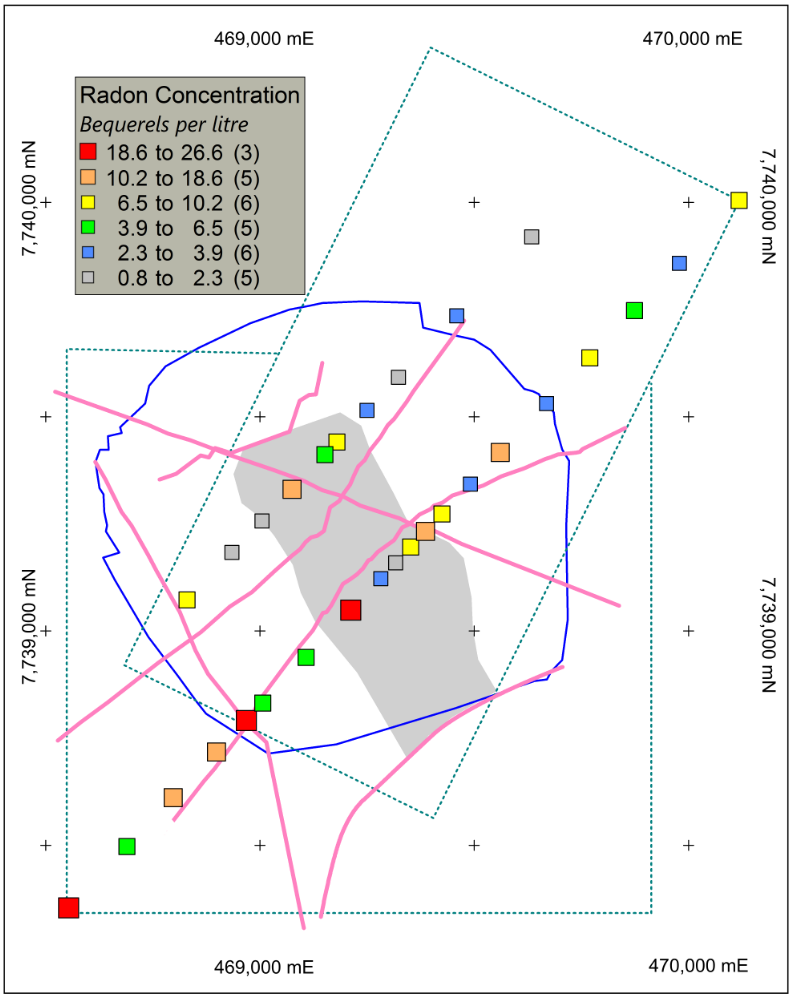

Figure 6.9. Radon concentrations measured at a depth of 50 cm across the Ernest Henry deposit (data from Zahorowski et al., 1996).

Within cover geochemistry

Background

As discussed in the Setting section, above, the presence of secondary dispersions at the Mesozoic unconformity and within the overlying upper Cretaceous and Tertiary sediments of the Ernest Henry deposit had been recognised before mining began in 1997. Figure 6.10 summarises the understanding at that time.

By 2000, MIM Exploration was able to access the mine site and execute the “Ernest Henry Cover Project” (Sheppard, 2001). The primary aim of the program of pit-wall and step-out ore-definition drill hole sampling, illustrated schematically in Figure 6.10 and photographically in Figure 6.11, was to quantify secondary geochemical dispersions in a 3-dimensional framework and develop a *predictive model* for further discovery. The 2000 program comprised 421 sample sites, from which a bulk sample was ‘totally’ digested, and splits of the <0.5 mm fraction were treated by aqua regia (Au), BCL (Au), Regoleach, MMI and Enzyme Leach.

Sample site locations for each of the sampled surfaces are illustrated in the map mosaics of Cu data in Figures 6.12 and 6.13. The coverage is restricted but sufficient to reveal some critical features. Copper was selected from a comprehensive set of mosaics (Sheppard, 2000) to demonstrate the contrasting distributions by different extraction methods and provide an example of vertically continuous and/or fault-proximal metal anomalies in the cover units above the orebody. The total digestion results for Cu are shown for each of the sampled surfaces or

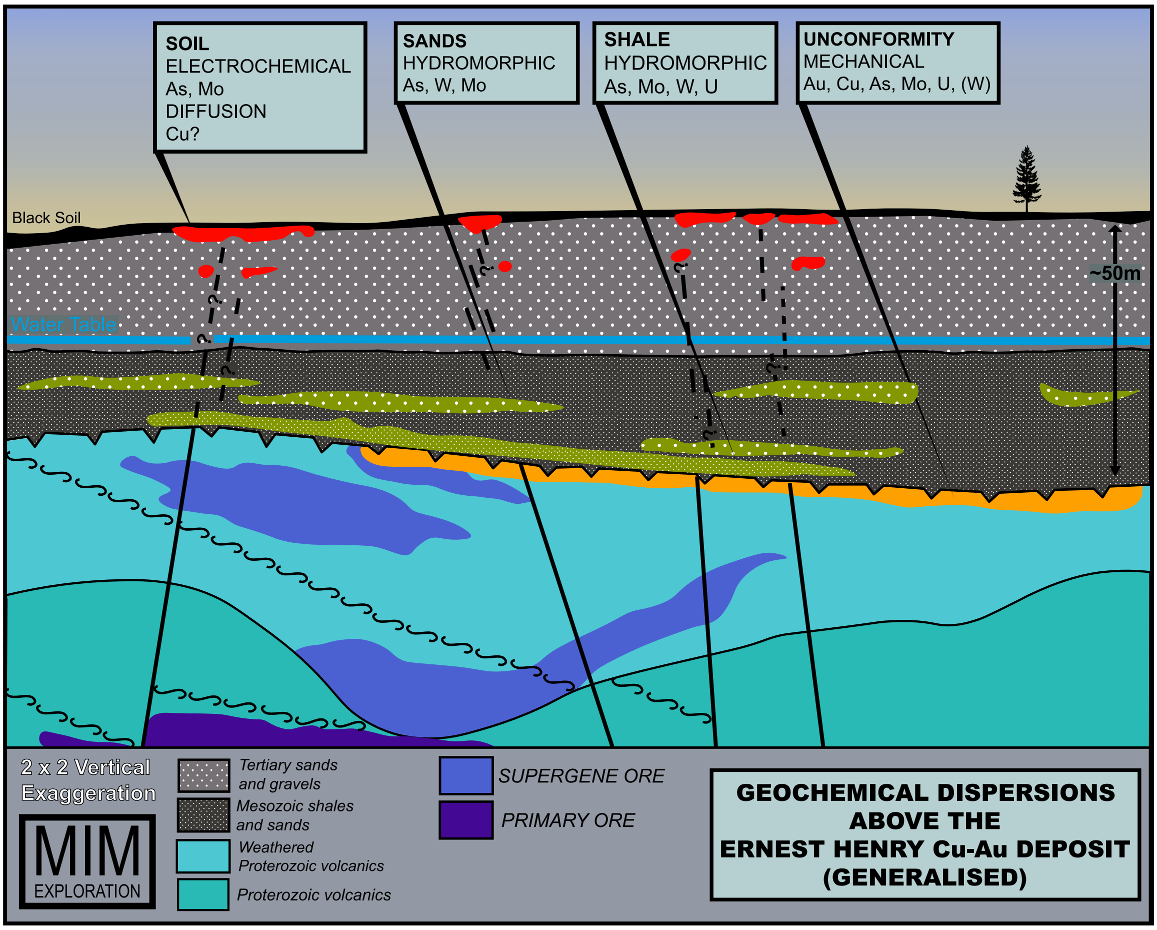

Figure 6.10. Schematic geology and secondary dispersions in cover units of the Ernest Henry deposit. (from Hannan, 1995).

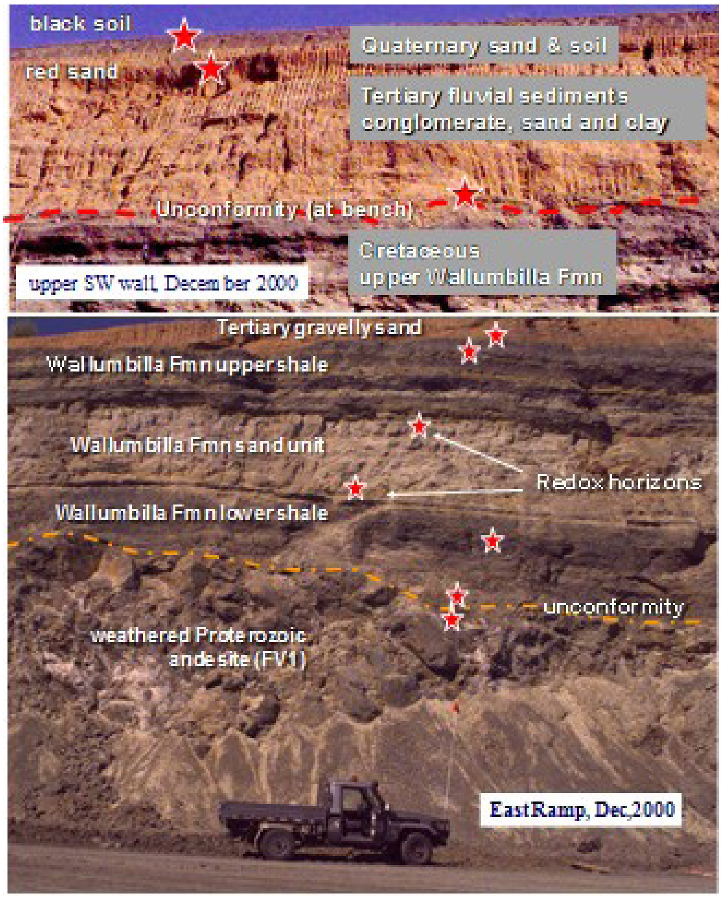

Figure 6.11. Overburden stratigraphy and Cover Project sample site horizons (from Sheppard, 2001, modified).

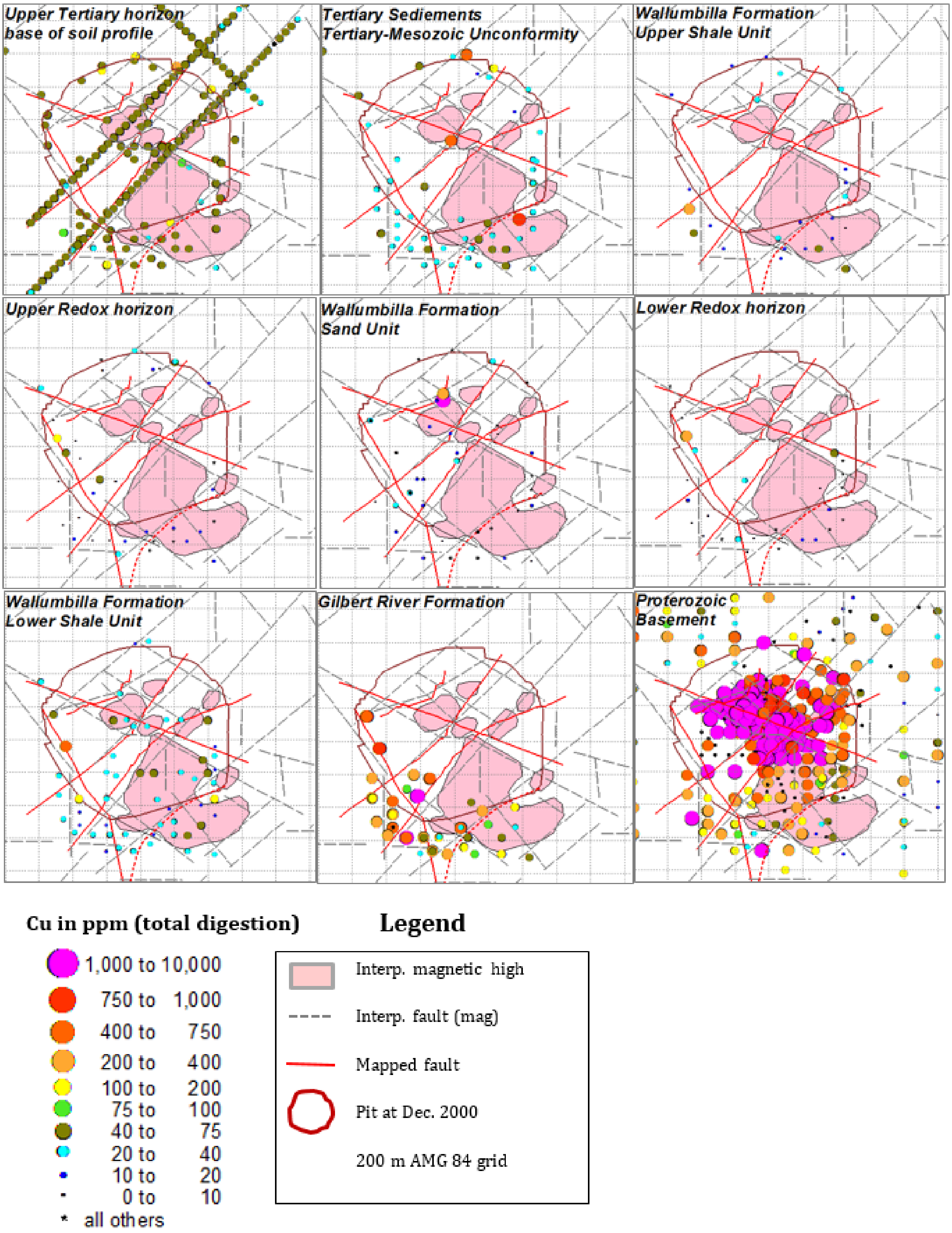

Figure 6.12. Ernest Henry overburden Cu distributions, by 4-acid digestion/ICP finish (from Sheppard, 2001).

units, excluding the surface black soil. Most of the plotted Gilbert River Formation samples are strongly Cu anomalous (100s to 1000s ppm). This, conglomeratic unit onlaps the basement paleotopographic high from the southwest and is known to contains clasts of weathered ore. Most of the project samples are located either downslope of subcropping ore or vertically above blind ore, south of the Marshall Shear Zone (refer to Figures 6.4 or 6.5). It is a clear example of an ore footprint enlarged by uplift, oxidation and erosion and preserved by subsequent burial and sedimentation. Gold and most of the Ernest Henry pathfinder metals are also anomalous in these

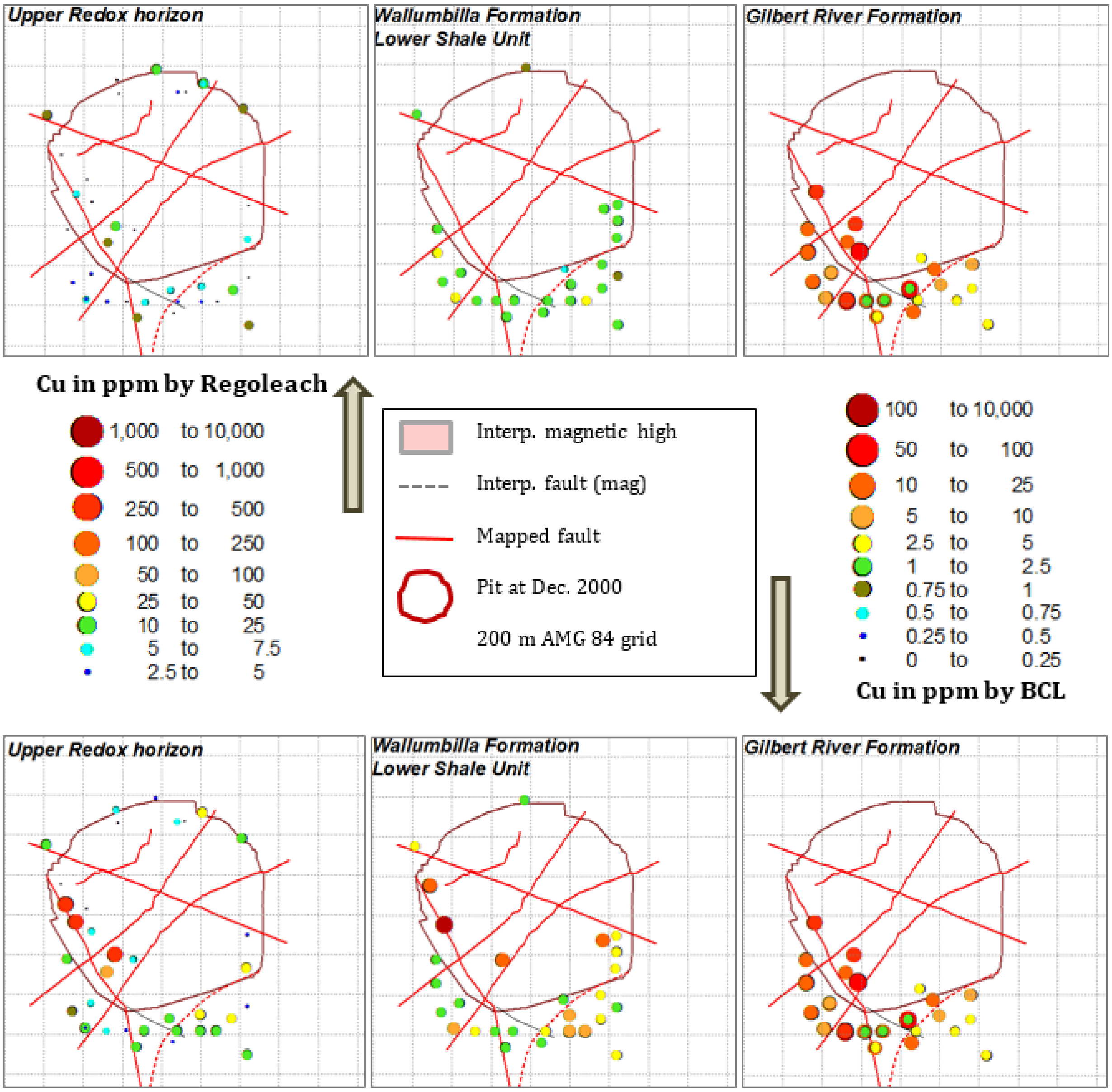

Figure 6.13. Ernest Henry overburden Cu distributions: upper row—by Regoleach; lower row—by bulk cyanide leach/AAS finish (modified from Sheppard, 2001).

samples. Higher in the profile, 'total' Cu remains at background levels except for the occasional 'spike' in the vicinity of one of the mapped faults or shear zones.

The frame for upper Tertiary (base of soil) results is a repeat of the Quaternary sands plot of Figure 6.6, and a reminder of the comparatively high levels of Cu (40–70 ppm) and U at a depth of 4–5 m across the entire area.

For comparison, the Cu results for extraction by Regoleach and the weaker BCL reagent are provided in Figure 6.13 for three reference sampling horizons. Regoleach Cu, like total digestion Cu, falls to background levels above the Gilbert River Formation (*i.e.,* from low 100s of ppm to <25 ppm, upper 3 frames). By contrast, elevated levels of cyanide-extractable Cu extend upward to the redox horizon at the base of the Wallumbilla formation sand unit, particularly near the projected position of the NNW-trending Fault1 (*i.e.,* above 5 ppm, lower 3 frames).

As described by Sheppard (2001), the two redox horizons are 20–30 cm thick and indicate where Fe^{2+}, possibly derived from the pyrite in the surrounding black shales, was oxidised to

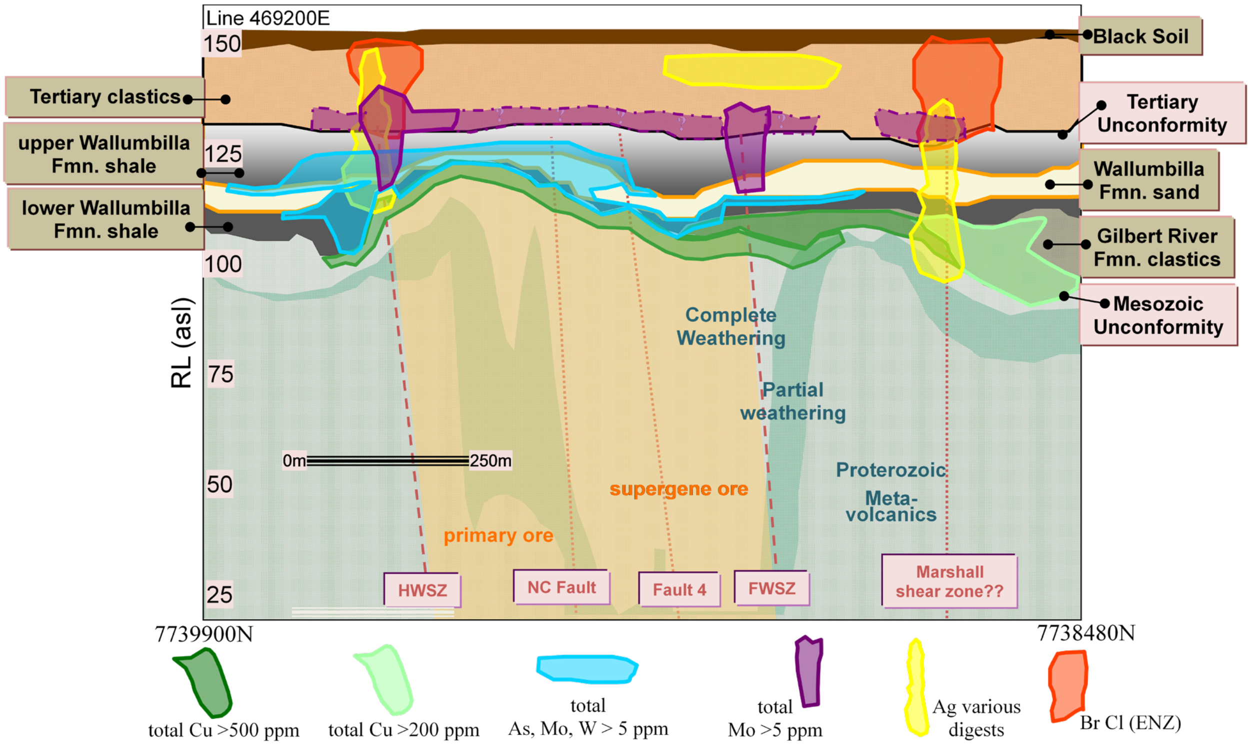

Figure 6.14. Schematic geologic long section and summarised geochemical dispersions in the overburden of the Ernest Henry Cu-Au deposit. (from a presentation, Sheppard and Hannan, 2001).

Fe^{3+} producing sesquioxides and less soluble Fe-oxides. Significantly, the sand unit is locally in contact with the paleo-weathered Proterozoic basement around the buried topographic high (see Figure 6.3). The oxidising groundwaters must have been in contact with both the sand unit and the underlying mineralisation, *after* the reducing conditions prevalent during the Cretaceous and shale deposition. That is, hydromorphic dispersion of pathfinder elements downslope, away from the paleotopographic high was a probable outcome, particularly as the Tertiary alluvials accumulated (the pre-mining watertable depth was about 21 m, generally below the Tertiary/Cretaceous unconformity). Significantly, the Wallumbilla Formation sand unit is completely reduced and without evidence of Fe-Mn oxides at its upper or lower contacts in an environmental monitoring hole drilled some 5 km ESE of the Ernest Henry deposit (*op. cit.*).

With the previous example as background to the scope and methodology of the Cover Project, an overview of its major findings follows. Each of the observation-based and/or interpretative findings is illustrated in the schematic long section of Figure 6.14 and the plan view maps of Figures 6.15 and 6.16 (which also depict sample site distributions. It is noted that the colouring of polygons for specific elements differs between the section and plans.

Mesozoic unconformity

Figure 6.14 shows schematically, and Figure 6.15A quantitatively, how the intensity and depth of weathering, as recorded by the logged BOCO surface (base of complete oxidation) is controlled by known major faults within the basement. Before extraction, supergene mineralisation was most strongly developed between Fault 4 and the HWSZ, south of the NC Fault, and extended up to 100 m below the Mesozoic unconformity.

Samples of basement at or just below the unconformity define a 500-ppm copper anomaly measuring 1000 m by 600 m (Figure 6.15B). This signal extends up to 400 m either side of the south-plunging orebody and is probably a mixture of supergene and hypogene mineralisation.

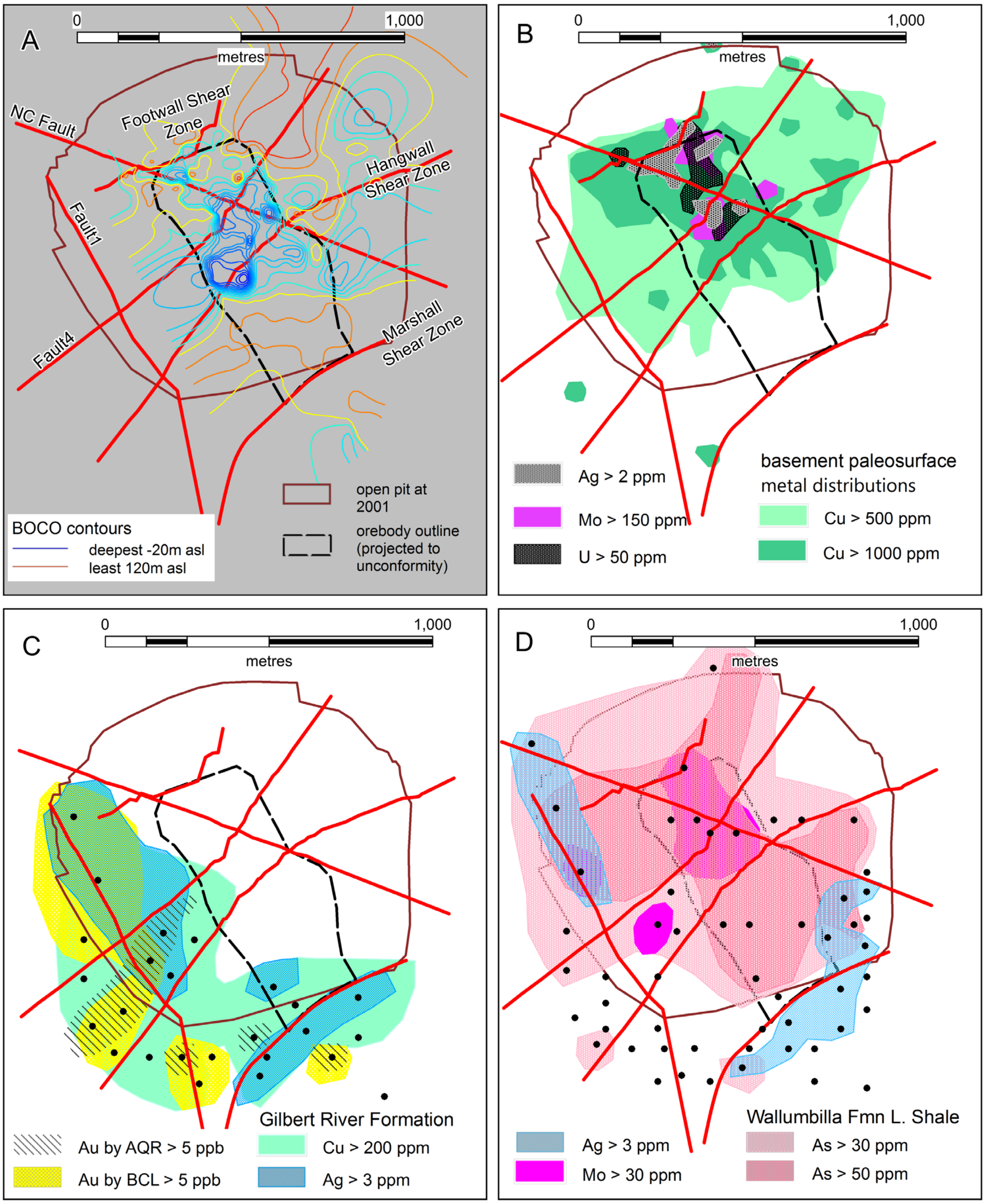

Figure 6.15. Plan views of the Ernest Henry Cu-Au deposit; A—'base of complete oxidation' contours & faults in Proterozoic basement; B, C & D—summarised geochemical dispersions at the 3 deepest sampling levels. (data from Sheppard, 2001)

That is, it should be regarded as a primary halo—some three times the area of the orebody's unconformity footprint. The inner, > 1000 ppm Cu signal (800 x 300 m) more closely matches the projected orebody limits, but its longest axis clearly tracks the NC fault. The ore suite of metals is also strongly anomalous in this area, with Au >30 ppb, As >50 ppm, and Mo >10 ppm (also Ag, Mn, and Co). Close to the faults, and within the weathered corridor, Cu levels reach 0.5% or more, Au > 5 g/t, As > 200 ppm, Mo > 150 ppm and U > 50 ppm. The relative enrichment of As and Mo above primary ore levels is consistent with the effects of acid leaching (metal cation removal, metal oxy-anion retention).

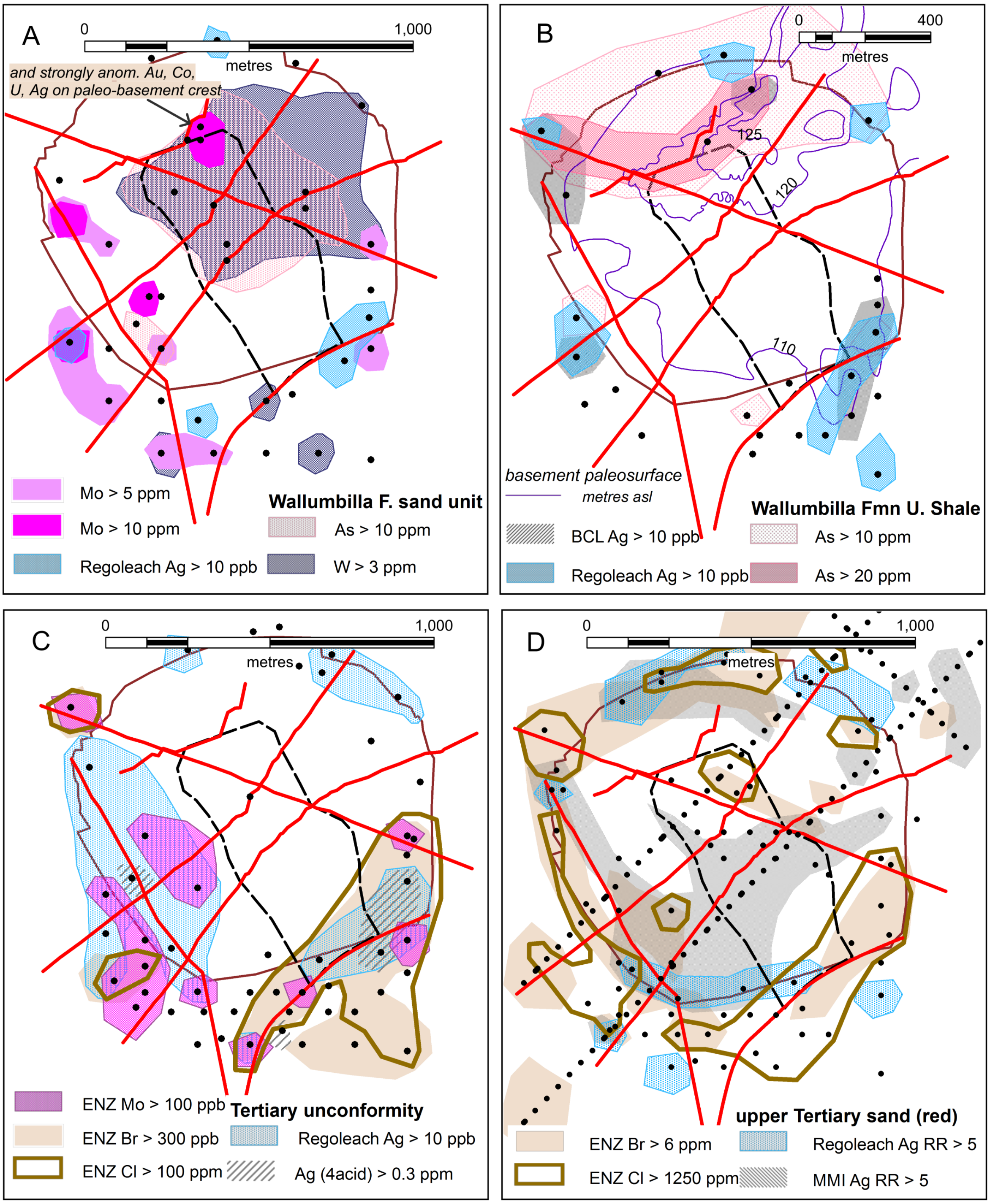

Figure 6.16. Plan views of the Ernest Henry Cu-Au deposit; summarised geochemical dispersions at progressively shallower levels (data from Sheppard, 2001).

Gilbert River Formation

A strong multi-element ‘conventional’ anomaly extends over an area of more than 1000 m by 700 m in the Gilbert River Formation on the southern side of the deposit (Figure 6.15C). The > 200 ppm Cu anomaly remains open to the south and southwest. Although mechanical dispersion directly downslope of the Ernest Henry deposit is the likeliest explanation, influence of the Marshall Shear Zone is also evident. Coarse clastics on a basement unconformity with paleotopographic relief is clearly a priority sampling target horizon for explorers.

Wallumbilla Formation

Broad As, W and Mo anomalies (> 30, 5 and 5 ppm, respectively), up to 1000 m by 1000 m, are interpreted for the shale and sand units of the Wallumbilla Formation and sand unit's redox horizons (Figure 6.15D and Figures 6.16A and 6.16B). Cu and Co anomalies are not evident in the Formation. Ag is consistently associated with the area above the Marshall shear zone and, to a lesser extent, the western Fault1. Significantly, the highest As and Mo levels occur in the lower shale unit above and on the basement paleotopographic high and decrease southward (Figure 6.15D), where they are 2–3x the abundance of average shale (15 and 3 ppm, respectively). The characteristic metal dispersions of the Wallumbilla Formation are attributed to the preferential solubility of As, Mo and W in a relatively alkaline and reduced groundwater regime as burial progressed during the Cretaceous period.

Tertiary unconformity

At the base of the Tertiary clastic unit, Ag and Mo distributions are like those in the underlying Wallumbilla Formation, but are somewhat weaker and broadened. A spatial association with mapped basement faulting and fracture zones in the cover is also still evident. At this level, a very strong coherent anomaly in Cl and Br by Enzyme Leach occurs spatially associated with the Marshall Shear Zone (Figure 6.16C), together with elevated total Ag and Mo (not shown, > 0.3 ppm and > 5 ppm, respectively), including Ag by Regoleach (Figure 6.16C) and MMI.

Quaternary sand

Abundance mismatches, or 'levelling issues' were noted in the combined mid-1990s data for Quaternary sand, discussed earlier in the chapter, and the Cover Project's 2000 data for the same horizon. Nevertheless Sheppard (2001), concluded that coherent anomalies are evident in the enzyme leach Cl and Br, and the levelled Regoleach and MMI Ag data (Figure 6.16D). The halogens appear to display an outer halo, with most anomalous samples located near vertically projected basement faults and along the western and northern margins of the pit. Ideally, sampling would have extended a further 1500 m in all directions to better define an annulus (in plan) or 'rabbit's ears' (in section). For now, it is sufficient to note a peripheral halogen-Ag association at both the base and top of the Cenozoic clastics (compare Figures 6.16C, D), and that such anomalies have been observed above the vertically projected peripheries of other buried ore deposits and attributed to the electrochemical dispersion (Chapter 5).

Discussion

The secondary dispersions observed at any given location within the overburden of the Ernest Henry deposit are influenced by:

i. the physical character of the host cover unit (*e.g.,* permeable clastics versus shale);
ii. position relative to mapped basement faults (projected) and fracture zones in the overburden;
iii. position relative to vertically projected limits of the orebody, where it subcrops and where it plunges beneath the paleosurface; and
iv. distance above the Proterozoic basement paleosurface.

That is, a complex array of chemical anomalies, or secondary dispersions, will be present in relatively weakly lithified Mesozoic and Tertiary strata above an undiscovered Ernest Henry look-alike. The implication is that that careful logging and evaluation of the cover sequence is required in drilling programs, especially where grid-drilling to basement is not feasible or commensurate with a drill target's priority ranking.

Accordingly, the following sampling tactics, identified in large part by Sheppard (2001), are recommended for the testing of exploration targets in areas with up to 75 m of non-lithified Phanerozoic cover:

a. An Ernest Henry-like deposit which subcrops directly beneath unconsolidated transported cover should be locatable by aircore or RAB drilling and sampling of the basement on 250–400m centres; this is a budget- and target status-dependent option and not exclusive of other sampling options.

b. Locally derived cover units like the Gilbert River Formation should be routinely analysed for evidence of eroded mineralised fragments from nearby or former topographic highs (the basement vertically beneath such secondary dispersions could be unmineralised).

c. Where grid-drilling to the basement is not possible (too thick or too expens*ive),* sampling of shale units below the Tertiary-Mesozoic unconformity and redox zones, both below and above the unconformity, could reveal elevated levels of pathfinder metals over hundreds of square metres related to deeper and oxidised Ernest Henry-style mineralisation.

d. The sampling of near surface clastics, below black soil, but at a consistent position in the redox profile, could reveal weak acid /selectively extractable, and perhaps transient, dispersions related to diffusion (along fracture zones) or electrochemical gradients in the cover above either:

   - blind but sub-cropping mineralisation (*e.g.,* north of the Hangingwall shear Zone)
   - or blind and buried mineralisation (*e.g.,* south of the HWSZ, Ernest Henry).

   Analysis by aqua regia/ICP-MS, and, in order of likely effectiveness, MMI (for metals and LREE), Enzyme Leach (for halogens and metals) or Regoleach (or equivalent) is recommended for this setting.

e. Based on the mid-1990s orientation results of MIM Exploration, the sampling of surficial smectic and strongly developed 'black' soil is the least favoured tactical option for mapping geochemical or gas fluxes through the cover. If black soil is poorly developed and the regolith of a clastic nature, then the more favourable scenario of option (d) still applies.

Based on the results of the Ernest Henry cover Project, a mineralised topographic high may be a prerequisite to generate the stronger and multi-metal dispersions recorded for the deeper Cretaceous sedimentary cover (Sheppard, 2001). Significantly, the pre-mining Mesozoic cover above the orebody was essentially reduced/alkaline and metal anomalism dominated by oxy-anion forming Mo, As and W, with Cu absent—conditions which contrast with those evident in the Mesozoic cover of the Osborne Cu-Au deposit (next section).

Chapter 6

Osborne Cu-Au Deposit

Setting

The Osborne iron oxide copper-gold (IOCG) deposit is located 158 km south of Cloncurry. Its discovery was the result of persistent exploration by multiple exploration companies. It began with the drilling of a strong aeromagnetic anomaly by a consortium of explorers in 1975 and an intersection of 2 m @ 0.13 g/t Au and 0.023% Cu. In 1985, Billiton Ltd and CSR Ltd drilled 11 RC holes and found quartz-magnetite ironstone with anomalous Cu and Au. Between 1985 and 1988 some 13,000 metres of RC and diamond holes had been drilled into 800 m strike-length of Cu- and Au-anomalous ironstone; but an ore-grade intersection was to wait until 1989, when Placer Pacific Exploration Ltd. drilled a coincident ground magnetic and IP high to reveal 32 m @ 5.8% copper and 3.23 g/t gold in distinctively ‘silica-flooded’ ironstone at a depth of only 98 metres. By June 1993, a 90 km drilling program comprising 475 holes resulted in a measured and indicated mineral resource of 11.2 Mt @ 3.51% Cu and 1.49 g/t Au (Adshead, *et al.,* 1998). Mining began in August 1995.

The ore deposit is dominated by two, 8–40 m thick, steeply NE-dipping lenses of quartz-magnetite-apatite ironstone west of the Awesome Fault (Figure 6.17). Primary ore consists of massive magnetite, pyrite, chalcopyrite and silica with lesser hematite and pyrrhotite up to 20 m thick, and is surrounded by a metasomatic assemblage of albitite, sillimanite gneiss and calc-silicates (Rubenach, 2001). Stratigraphically the Osborne deposit is hosted in pelites, psammites, quartzite, ironstone and amphibolite of the Mount Norma Quartzite (Soldiers Cap Group). Anomalous concentrations of Co, Mo, Ag, Se, Bi, Hg, Te, Sn, W, F, Cl, HREE, Y and Nb occur in the high-grade Cu-Au mineralisation (Adshead *et al.,* 1998). The upper supergene ore was rich in Cl (average 3400 ppm), a penalty element in the form of atacamite ($Cu_2Cl(OH)_3$).

Physiographically, Osborne and a smaller Cu-Au deposit to the west (*viz.,* Kulthor, discovered in 2001), lie beneath 30–100 m of strongly weathered and moderately lithified Mesozoic sedimentary rock on a west-sloping, lag-covered hogs-back some 278 m above sea level (Figures 6.18 and 6.19). The sedimentary rocks comprise basal grit of the Longsight Sandstone, and a fine sandstone-mudstone-claystone sequence of the Wilgunya Subgroup. Before the start of mining at Osborne mineralisation subcropped as siliceous gossan on a 20 m paleotopographic high in the Mesozoic unconformity at the northern end of the deposit (local grid 21,937.5 mN). Fragments of gossan were observed spread over the unconformity, as they were at Ernest Henry. An oxide zone with malachite, cuprite etc. transitioned to a supergene enriched assemblage about 5–10 m beneath the gossan, then to primary ore some 20–50 m deeper (Tullemans *et al.,* 2001). The Mesozoic cover thickens southward to 100 m, above the south-plunging ore bodies.

Truncation of the Proterozoic host rocks in lower saprolite, and the gossanous paleo-knoll indicate pre-Mesozoic weathering and erosion of the deposit (Lawrance, 1999), as noted for the Ernest Henry deposit. Marine incursion in the Mesozoic blanketed the entire area in reduced sediments (shale and siltstone). Subsequent uplift and weathering, produced a profile capped by up to 15 m of silcrete and ferruginous duricrust and a pallid zone (saprolite) which extends to a depth of about 30 m, overprinted by laterally extensive redox zones at depths of 12–18 m (a paleo-zone) and 25–30 m (active, perched water table), as shown in the cross section (Figure 6.20). A deeper redox front at 30–35 intersects the basement gossan and corresponds to shale/siltstone contact within the Mesozoic sequence.

Significantly, the Mesozoic cover is fractured and faulted and the duricrust is locally collapsed, brecciated and recemented with ‘root zones’ that extend several metres downward, locally as far the paleo-redox horizon (Rutherford *et al.,* 2005).

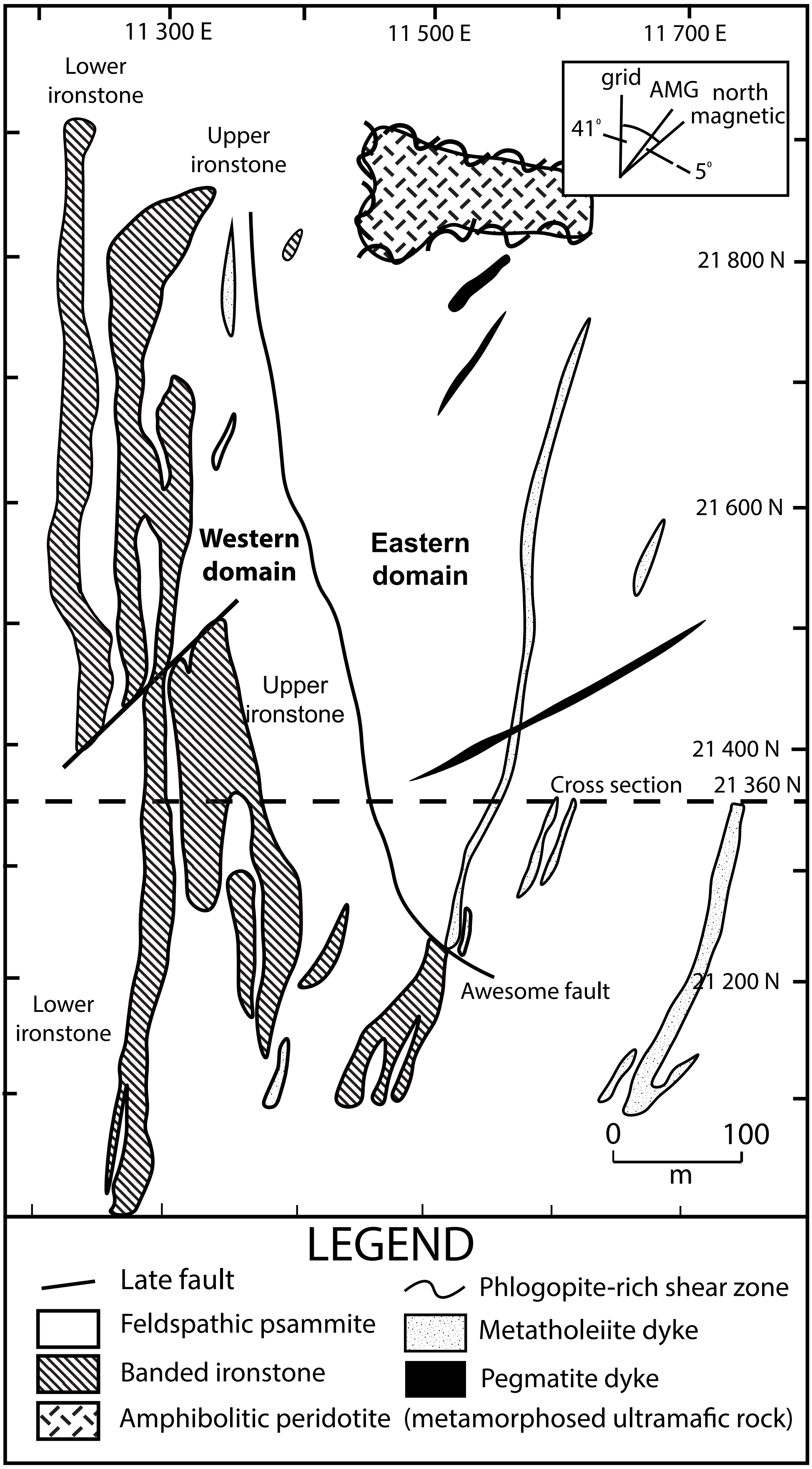

Figure 6.17. Simplified basement geology of the Osborne mine area (from Adshead et al., 1998).

Figure 6.18. Discovery site of the future Osborne mine (photographed in 1992, from Rutherford, 2009).

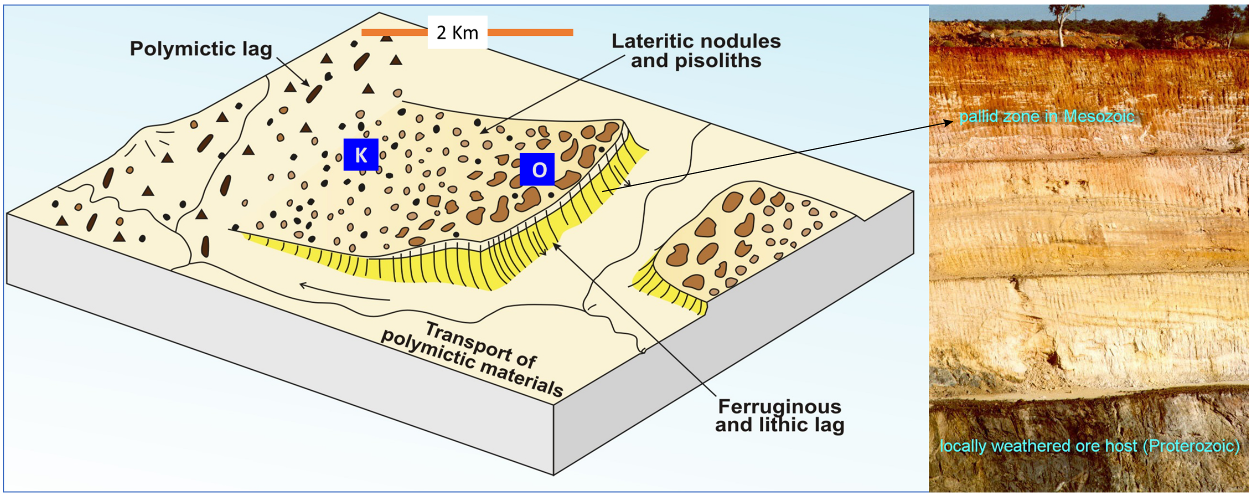

Figure 6.19. Landscape and regolith setting of the Osborne Cu-Au deposit; left frame—mine site on dipping plateau backslope indicated by 'O', Kulthor deposit by 'K' (from Rutherford, 2018, modified); right frame—view of pit wall with profile of weathered Mesozoic overburden (from Rutherford, 2009).

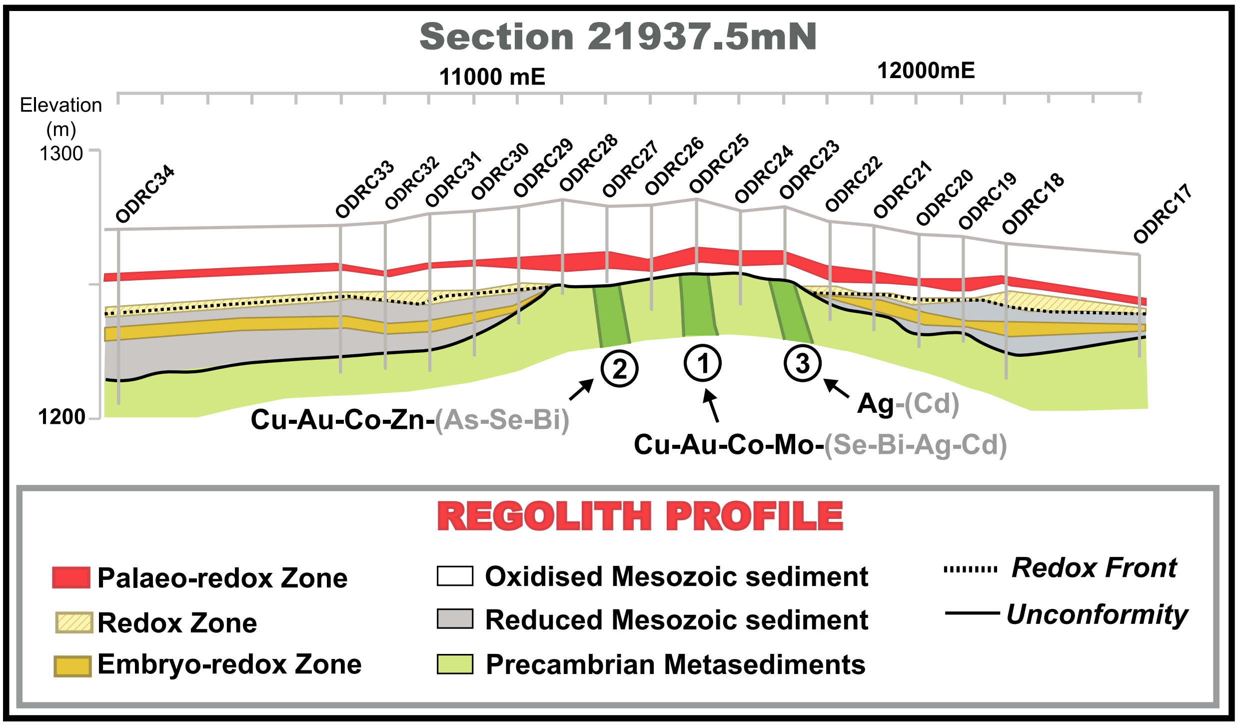

Figure 6.20. Sectional view of the regolith profile and geology of the Osborne deposit, at the site of the future open-cut (from Lawrence, 1999; modified).

Surface geochemistry

By 1993, the skeletal soil above the planned open pit had been the subject of several orientation surveys and tested by more than a dozen chemical and gas-in regolith extractive techniques. A review at that time, by Placer personnel and a consultant, found that a cold 0.1M HCl leach and pSirogas analysis produced the most distinct anomalies (Rutherford *et al.,* 2005). Other methods, including BCL, CHIM (a procedure developed in Russia), EDTA, weak nitric acid and total extracts, produced some elemental anomalies but with lower peak to background ratios (*op. cit.*).

The pSirogas procedure, based on the collection and analysis of condensates from streamed soil gas (Chapter 5), was tested in 1992 (an AMIRA project). The results for several major and trace elements are shown in Figure 6.21. The profiles are spikey, typical of selective extraction and gas-in-soil data, and presumably reflect the mode of their formation. In this case, clearly visible, near-vertical faults in the Mesozoic cover are the implied pathway of metals and gases to the surface because some extend to basement and are known to be chemically anomalous above ore, in the cover, as demonstrated for both Osborne and Ernest Henry (and later for Kulthor).

Anomalies in Cu, Bi, Cd, Ge, Hg and some REE are cited for the weak HCL extraction data (Rutherford *et al*., 2005), but total digestion analyses are not available, as they are for Ernest Henry, to eliminate the possibility of contamination by wind-blown drill hole spoil.

In the same year, three ‘Russian’ procedures were tested on three E-W (local grid) lines as part of the multi-client AMIRA P355A project. Two were essentially soil sampling methods (MPF & TMGM) and the third was a geoelectrochemical (CHIM) method. MPF extracted metals selectively from organic matter and results were reported as metal/C ratios; TMGM extracted metals selectively from Fe-Mn oxides. For CHIM, electrodes were installed along a traverse, a direct current was applied for a fixed period and the metals accumulated at the electrodes were measured at a dedicated, onsite laboratory. The composite results for Cu, Co and Zn, by CHIM are plotted for each survey line in Figure 6.22. The match with projected ore lenses is

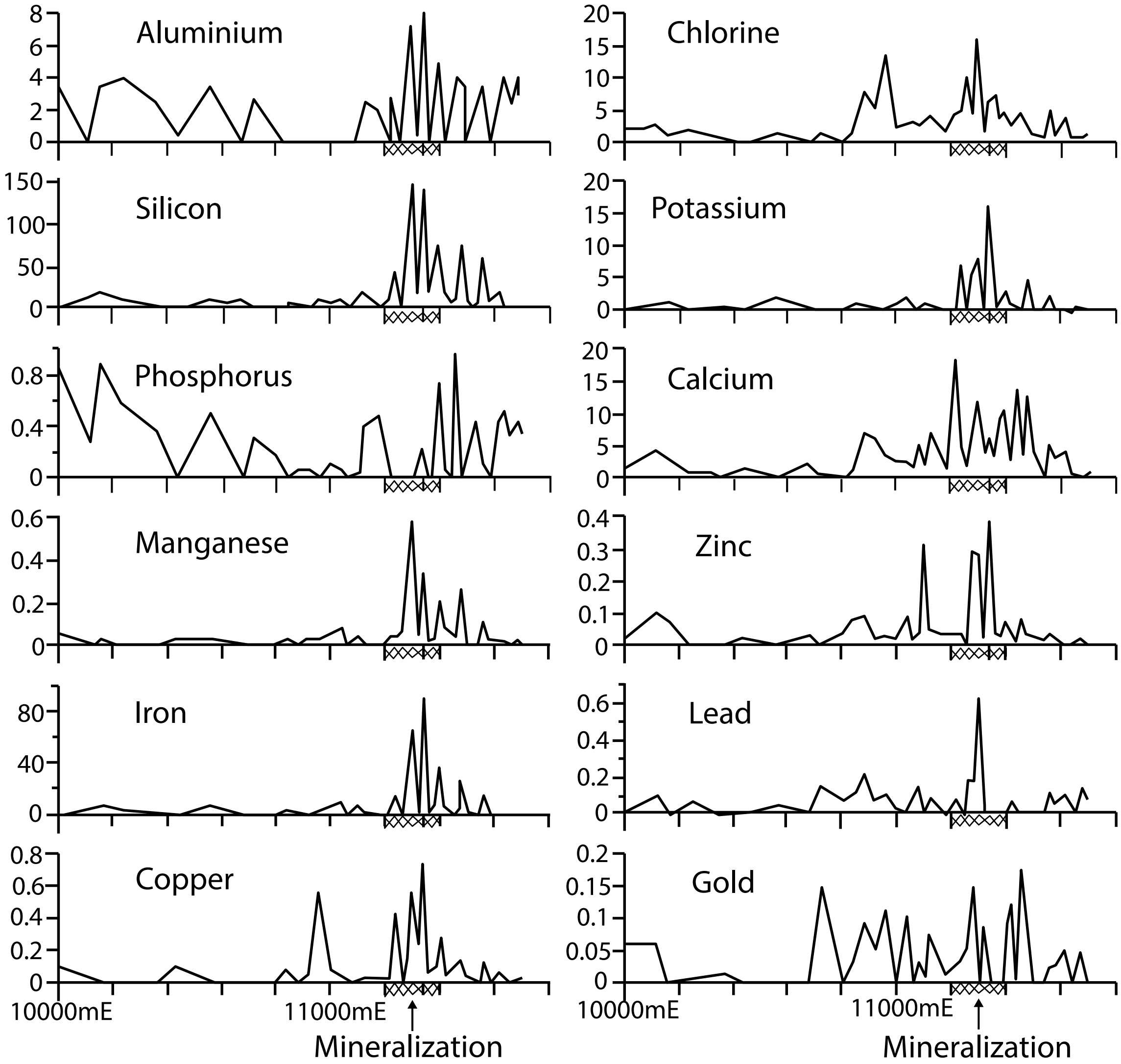

Figure 6.21. Pre-mining pSirogas profiles (in ppb) of Osborne mine open-cut area, Mesozoic cover 30 m (from Rutherford et al., 2005).

convincing. The 'western zone' is strongly indicated in the MPF results and coincides with the Cl and Cu spikes at about 10500 mE in the pSirogas profile (Figure 6.21)—its lower elevation suggests that it may be a seepage anomaly, down flow from the ore deposit. The TMGM profiles spiked in Cu and Co over ore on the middle line (SE of the eventual pit). Collectively, the survey yielded positive evidence of secondary dispersions through cover, but the logistical complexity of the 3-method suite was never viewed as a competitive alternative to single extraction methods also being developed.

The results of a subsequent soil Regoleach survey are shown for copper in Figure 6.23 (AMG grid, with survey lines at about 45 to the pSirogas and CHIM lines). This procedure, offered commercially within Australia, is a variant of the family of leachants selective for Fe and Mn mineral phases (Chapter 5). Both the date of the survey and the abundance intervals, as plotted, are unknown, but there is a clear correspondence of elevated results (red-and yellow-coloured points) and the surface-projected position of ore. Significantly, the NE extension of the geochemical anomaly (blue-dash polygon) was eventually drilled without a favourable result. Like the "western zone" feature discussed above, the Cu anomaly was reinterpreted as a downslope, lateral dispersion effect—generated by groundwater flow under silcrete layers and salt precipitation at erosional exit points Rutherford (2009). In the context of district scale reconnaissance, it is obvious that the regolith and landscape setting of such an anomaly would bear close attention to increase the probability of recognising a near-miss drilling result.

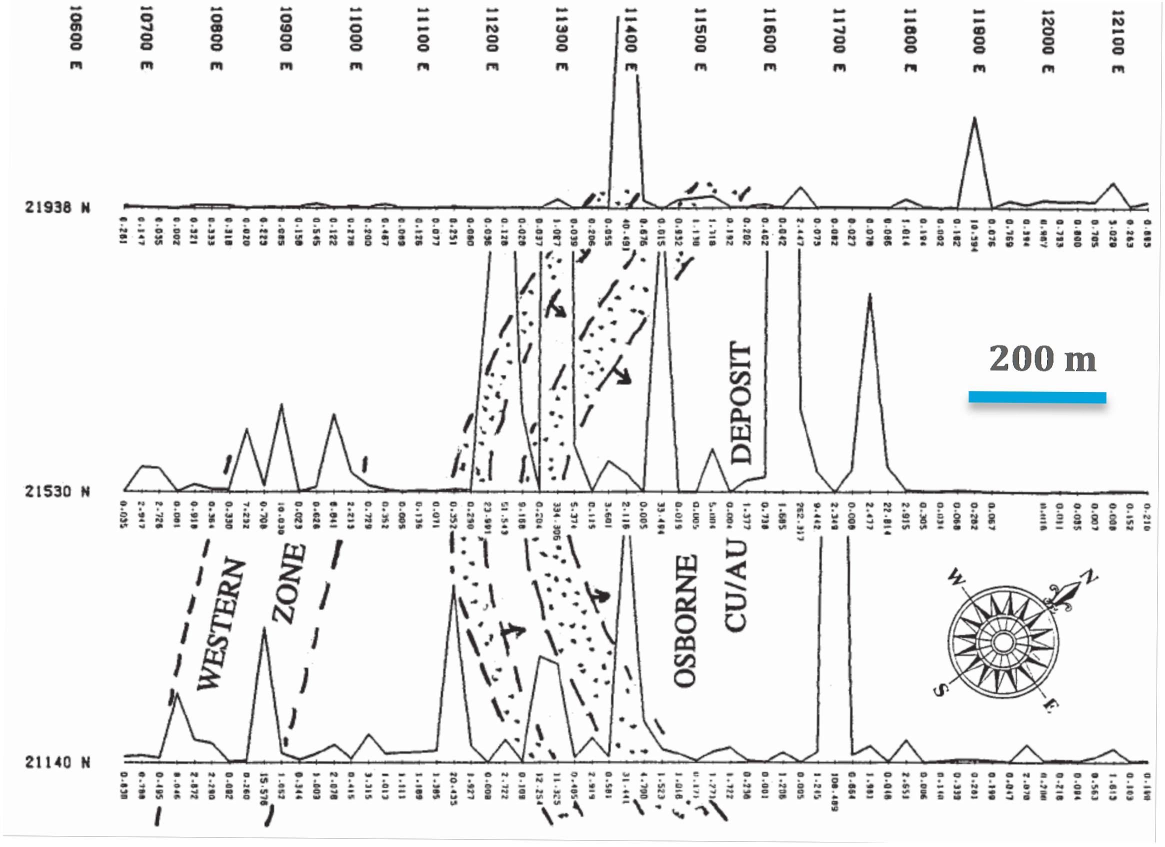

Figure 6.22. Pre-mining geoelectrical (CHIM) profiles of Cu x Co x Zn profiles of Osborne mine area, on local grid as for Figure 6.9 (from Ryss et al., 1992).

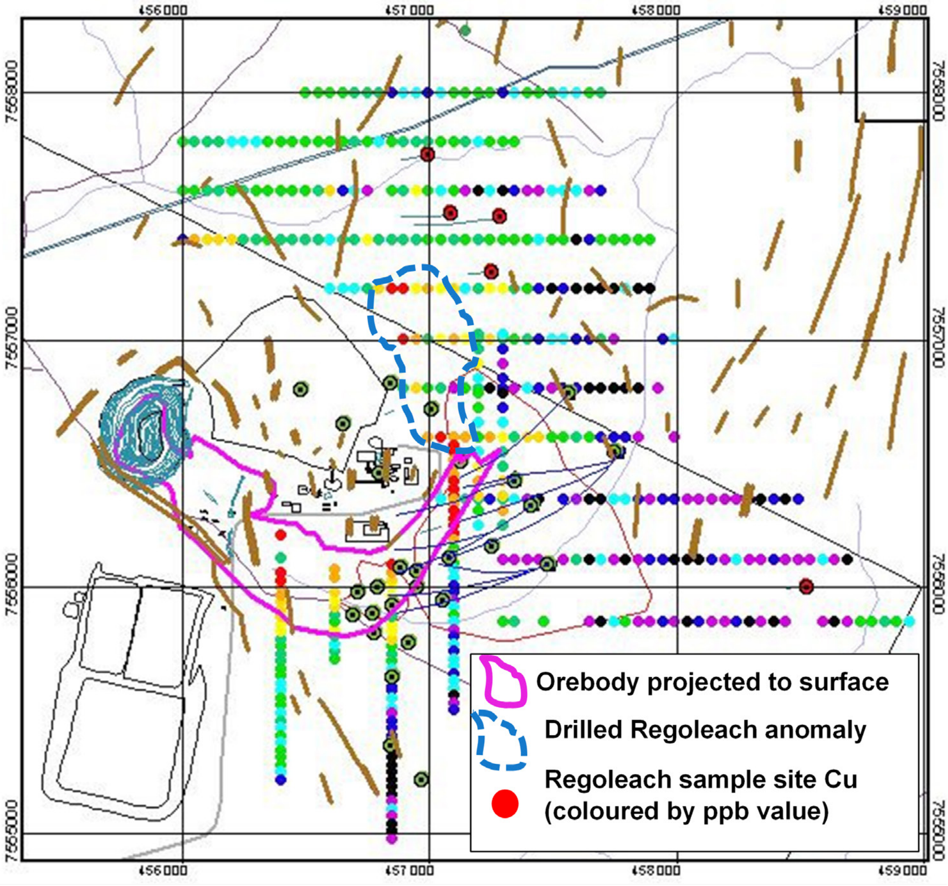

Figure 6.23. Soil sample Cu by Regoleach over the Osborne mine area, with pit shown at northwest termination of the ore trend. Abundances are colour coded from red (high) to black (low) (after Rutherford, 2009).

Within cover geochemistry

The line of drill holes across the deposit depicted in geologic and regolith-types section of Figure 6.20 were systematically sampled prior to open-cut mining to investigate geochemical patterns in the Mesozoic cover and upper basement (Lawrance, 1999). The results, presumably by a strong acid digestion and ICP measurement, for Cu, Au, Ag and Co in Figure 6.24 show:

- elevated Au, Cu, Ag, Bi, Se and Mo at/near the surface, coincident with ferruginous duricrust and a mottled zone (depths 0–5m)
- leached and metal-poor saprolite beneath the mottled zone (unspecified thickness)
- a 'plume' of elevated Au, Cu, Fe, and Bi in the oxidised Mesozoic cover directly above the mineralisation (present redox front is located on the basement paleotopographic high, as shown in Figure 6.24)
- elevated Au, Zn, Pb, Fe and Mn in the "perched" paleo-redox zone
- elevated Au, Cu, Ag, Zn, Cd, Pb, Co, Fe, Mn, Se and Mo in the "active" redox zone
- elevated for Zn, Cd, Pb, Co, Fe, Mn, and Se in the deeper embryo-redox zone (refer Figure 6.20) within the deeper and reduced Mesozoic cover.

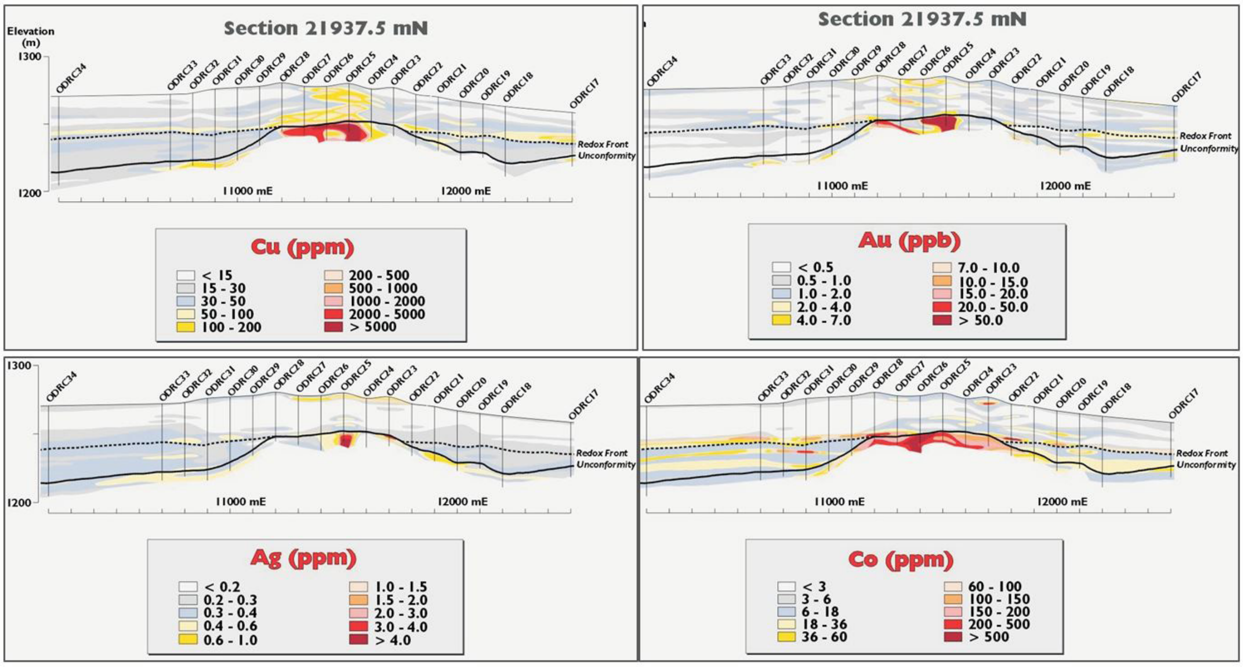

Figure 6.24. Distribution of selected metals in the variably weathered cover of the Osborne mine area (from Lawrance, 1999, modified).

In detail, the dispersions appear to form a stacked mushroom pattern above the subcropping orebody, especially for Cu (100–400 m wide, 50–200 ppm) and Au (50–200 m wide, 2–10 ppb). A coherent zone of elevated Fe, Cu, Co, Se and Zn extends over 1000 m to the limit of the section on both sides of the subcrop. However, much of the metal in this goethitic and active redox horizon, at about the level of the present water table, could be derived from local pyrite (see below).

Later sampling (circa 2000) of palaeo-redox zones, wall rock and fractures in the pit walls indicated preferential dispersion into the overburden through the discrete sub-vertical fractures and confinement of low order metal anomalies to the vicinity of the fractures (Rutherford, 2009). There also seems to be agreement amongst investigators that the redox zones only become anomalous if they intersect mineralisation (*i.e.,* intersect the basement) or structures in the cover that extend upward from mineralisation (*e.g.,* Rutherford *et al.,* 2005). Significantly, the strongest and laterally most extensive palaeo-redox zones were found to have developed in thin beds of pyrite-rich sediment, now present as botryoidal hematite (*i.e.,* locally sourced Co, Se, Zn and even Cu). The implication is that shallow palaeo-redox horizons in thick cover are unlikely to become dispersion hosts unless the present weathering and redox front intersects the basement and mineralisation. In the case of Osborne, this was achieved after a long period of aridification (Figure 6.25D) and the progressive downward redistribution of metal dispersions developed much earlier, at or soon after deposition of the cover sediments (Figure 6.25A–C).

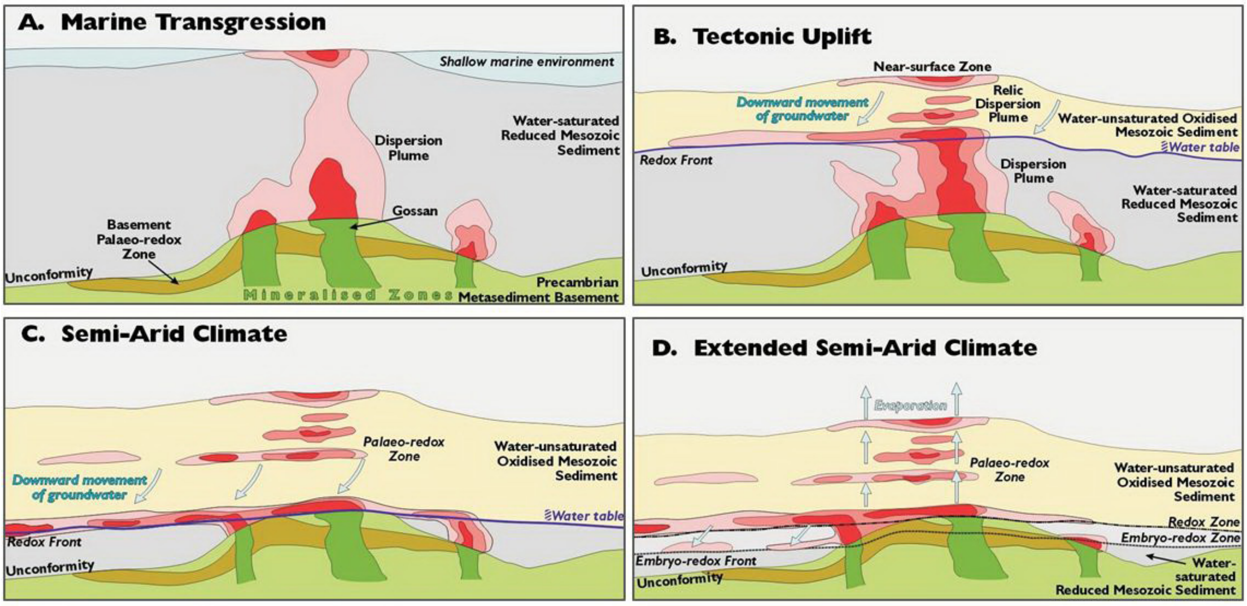

Figure 6.25 Time sequence model of trace element dispersion into 'post-mineral' Mesozoic cover above the buried Osborne Cu-Au deposit (from Lawrance, 1999).

Discussion

The exploration tactics identified for north of Cloncurry (based on Ernest Henry) can also be applied to the southern extremity of the Eastern Fold Belt, based on the results of geochemical investigations at Osborne. Although their secondary dispersions differ in detail, both have erosion-enlarged geochemical footprints at the Mesozoic-Proterozoic unconformity and both display evidence of pre-Mesozoic erosion and weathering of the enclosing Proterozoic host (*e.g.,* Figure 6.25A).

The vertical plumes of elevated Cu and Au in the oxidised Mesozoic cover above subcropping and oxidised ore on the basement paleo-crest distinguish Osborne from Ernest Henry. In contrast to Ernest Henry, the present water table and related redox transition are located deep within the overburden at about the level of the basement paleo-high, facilitating the dispersion of metals into the cover under acidic and oxidising conditions. The simplest, but unverified explanation for the contrasting pre-Tertiary conditions above the two ore deposits, leading to contrasting pre-Tertiary dispersion chemistries, is markedly differing environments of sedimentation.

There is strong evidence for lateral, hydromorphic dispersion to produce down-slope anomalies at relief-controlled exit points in the Russian MPF and Regoleach results, but not the pSirogas results. The contrast is consistent with the argument that gas-from-soil methods are much less susceptible than metal-in-soil methods to the generation ‘false’ anomalies above within-cover hydromorphic dispersions. Such features are documented for the Eastern Fold Belt (Phang, 2004) and are known to develop to multi-kilometre dimensions and grades of thousands of ppm in covered districts and structural domains of metallogenic provinces with high paleotopographic relief (Cameron *et al.,* 2004). Often the source is not located due to removal by erosion prior to burial by the younger sediments.

Though not treated in this document, regolith above the blind and ‘non-magnetic’ Kulthor copper deposit, 1.8 km west of Osborne, was also examined. The Regoleach, pSirogas and sulfur isotope (regolith gypsum) data all indicate upward dispersion of metals and sulfur near fractures within the transported cover (Rutherford, 2009).

Eloise Cu deposit

Setting

The Eloise Cu-Au deposit is located in pastoral alluvial plains some 60 km southeast of Cloncurry (Figure 6.26). It was discovered by BHP Minerals in 1988, by the drilling of a ground EM anomaly north, and along strike of, one of several strategically targeted aeromagnetic anomalies under thin cover in the Eastern Fold Belt (Skrzeczynski, 1993). The EM surveys were an outcome of the earlier discovery of subeconomic Pb-Zn mineralisation in banded quartz-magnetite and graphite schist at the nearby Altia prospect (Brescianini *et al*., 1992). When mining by AMALG Resources began, in late 1995, it had a reserve of 3.2 Mt at 5.8% Cu, 1.5 g/t Au and 19 g/t Ag.

The deposit is hosted by greenschist-facies metasediments and metabasic rocks of the Soldiers Cap Group - possibly its oldest unit, the Llewellyn Creek Formation. Mineralisation is associated with major retrograde shears and comprises an early assemblage of hornblende, biotitte and quartz, ore-stage chlorite, muscovite, pyrrhotite and chalcopyrite (± calcite and magnetite) and post-ore calcite, chlorite andquartz (±pyrite) in brittle faults (Baker, 1994). The essential geologic relationships are illustrated in the map and cross section of Figure 6.27.

Figure 6.26. Landscape vista of the Eloise mine area in 2009 (at an orientation survey site of Lilly et al. 2010).

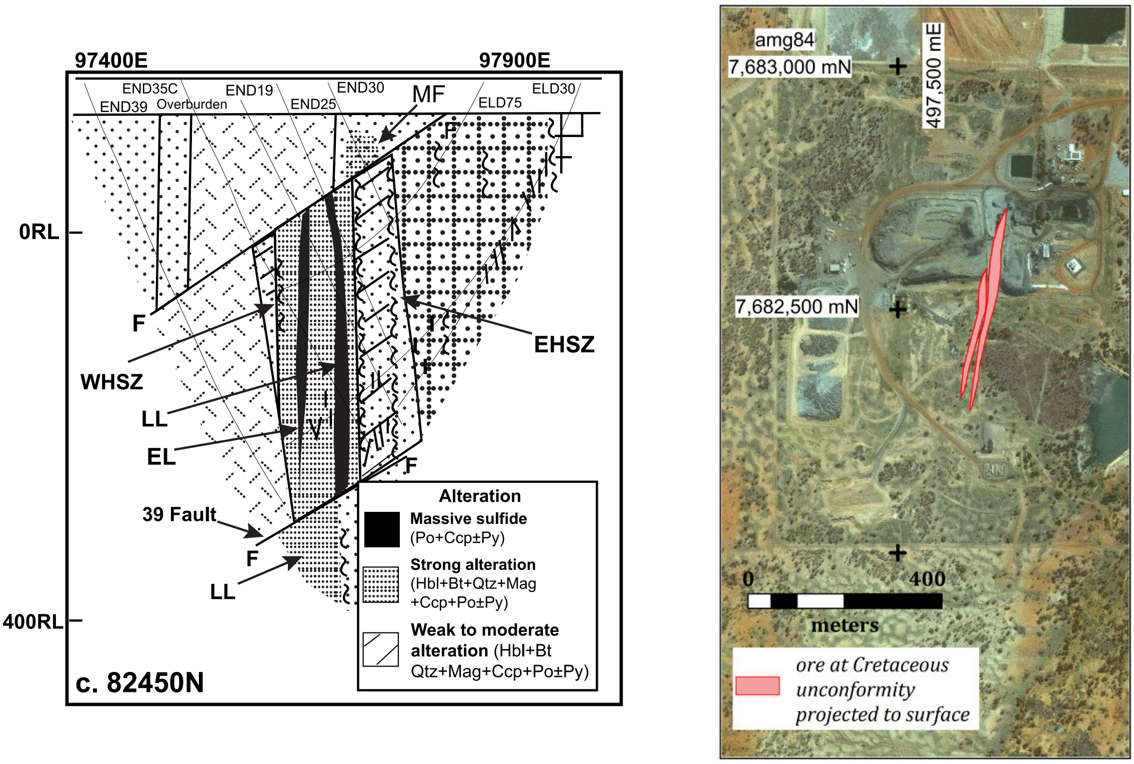

Figure 6.27. Geologic cross section of the Eloise deposit (left) and map of projected ore limits on aerial image of mine infrastructure at 2009 (from Baker, 1998, and Lilly et al. 2010, respectively, modified).

The Eloise deposit is buried under 50–70 m of late Mesozoic, Wallumbilla Formation mudstone and siltstone, and thin limestone beds of the Toolebuc Formation (cross section of Figure 6.28 upper). Much of the upper limestone unit was eroded and is capped by 5–7 m of Tertiary-Quaternary alluvium and sandy soil with patchy black soil development; topographic relief is generally less than 10m (Li Shu and Robertson, 1997). Exposures of Cretaceous rock in gullies and the base of alluvial terraces are saprolitic with an upper ferruginous zone. Thus, regolith types vary considerably over relatively short distances, as depicted in Figure 6.28 (A, B). Strong weathering, indicated by saprolite, extends to depths of 20–30 m (Figure 6.28, upper).

At the Mesozoic unconformity, which slopes comparatively steeply to the NE (*e.g.,* Figure 6.28 upper), the Proterozoic bedrock is only slightly weathered, but there are indications of mechanical, down-slope dispersion of Au, Cu, As and Sb for a lateral distance of a few tens of metres and the unconformity is marked by a thin layer of coarse conglomerate (Li Shu and Robertson, 1997). Furthermore, native Cu and bornite commonly occur with clay in weathered and vuggy quartz veins within the basement, up to 20–30 m below the unconformity (Baker, 1998). However, in contrast to Ernest Henry and Osborne, there is no reported weathering of the deeper levels of the Mesozoic cover and redox horizons appear to be absent.

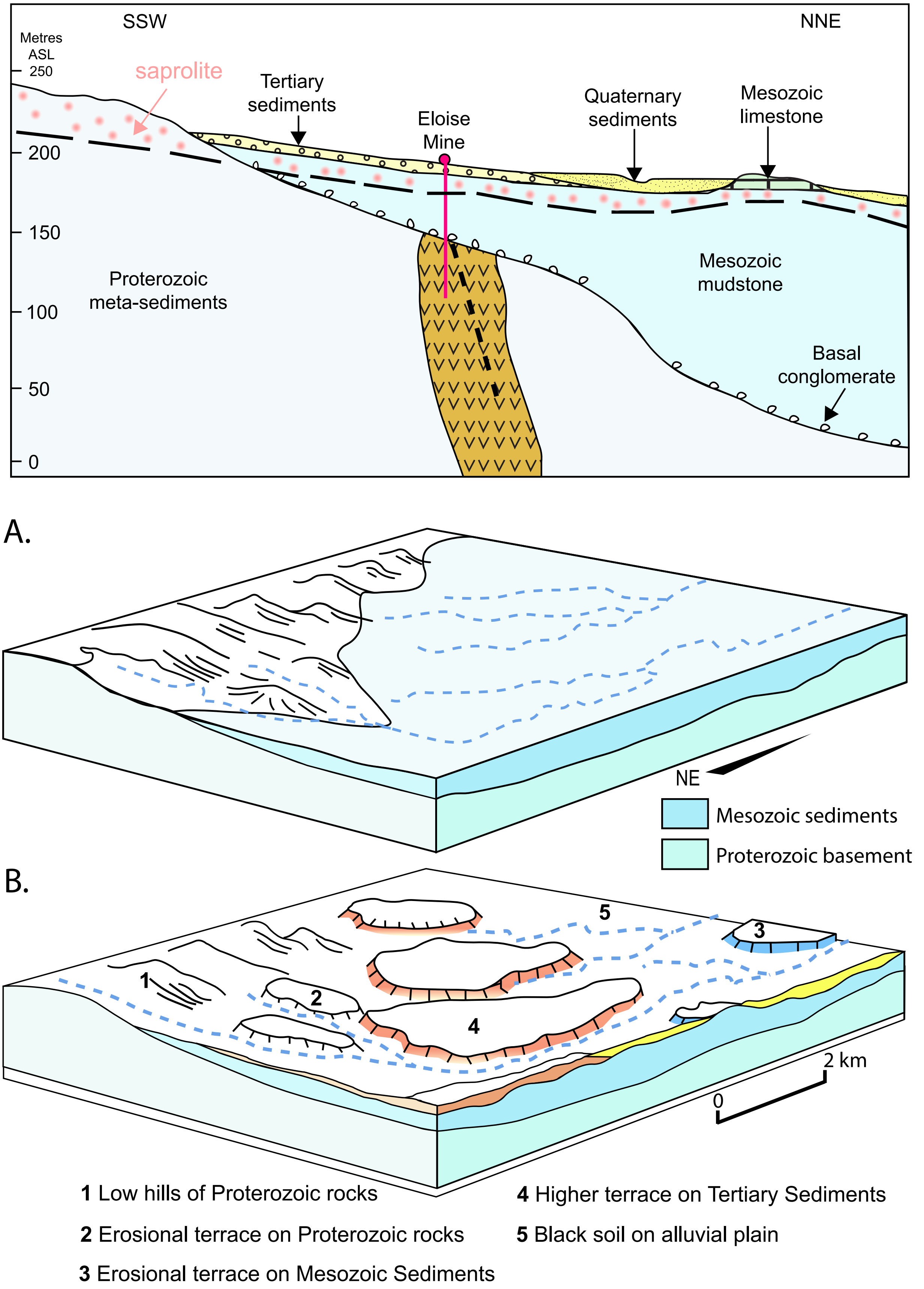

Figure 6.28. Schematic geologic cross section (upper) and landscape block models to illustrate stratigraphic relationships and the range of regolith types in the Eloise mine district (modified from Li Shu & Robertson, 2002).

There are no published grid-sampled surface geochemical data for Eloise that can be used to characterise the landscape and regolith of the district and test the possibility of secondary dispersions into the Cretaceous cover.

The only published data for local regolith apply to 32 widely distributed samples of soil, and eight orientation pits excavated about 500–1000 m north of the deposit, and on the trend of mineralisation. The data are 'totals' analyses measured by INAA and XRF for the full suite of major and trace elements, including Cl, S and selected REE (appendices of Shu & Robertson, 2002). In the case of the pits, 3–5 samples taken from surface to floor (3.5 m deep) were found to lack anomalous levels of commodity elements (*e.g.,* maxima for Cu and As are 55 and 62 ppm, respectively, in the same sample). Cl levels tend to increase with depth, from about 40 ppm to several hundred ppm (max. 1890 ppm), but the significance of the gradient cannot be definitively addressed in the absence of supporting field observations and comparative data from other locations. Lord's (2002) proposal that the elevated Cl might be a dispersive product from scapolite-bearing ore-host rocks at depth, based on 260–1770 ppm Cl values in unconformity samples from above-ore drill holes, compared to 110–570 ppm levels in distal 'background' holes, is of interest but tenuous.

In August–November 2009, Xstrata Copper Exploration completed a series of orientation soil surveys in the region which included a mining lease-confined grid of 40 samples over the Eloise deposit and its immediate vicinity. Underground mining had ceased at that time. The survey was regarded as high risk, given the multiple sources of potential contamination, including localised inundation by previously contained surface water run-off. However, some of the results provide strong evidence for soil-in-gas signals that are independent of regolith type or proximity to earthworks or man-made structures.

The sample sites are shown in relation to mine infrastructure in Figure 6.29, and surface-projected ore and intensity of primary alteration assemblages in the data maps of Figures 6.30 and 6.31. Most sample sites were in brown and dark grey smectitic soil ('black soil'), except the three samples in orange-brown sandy regolith at the western end of line 1 (discernible in Figure 6.29).

Standard aqua regia digestion with ICP-MS finish for many trace elements, was applied to the <5 mm fraction of the soil. A sample for Soil Gas Hydrocarbons analysis (SGH) was taken from the same excavation but prepared with only metal equipment (also < 5mm fraction). A specialised passive soil gas collector for GORE^{TM} analysis was installed into the regolith several days earlier, within 5 m of the soil excavation. The absorbent modules were inserted to depths of 45–60 cm and removed after 28 days for eventual analysis by ICP-MS. Later still, most of the sites were tested by the Metals in Soil Gas method (MSG). Details of the sampling procedures are provided in Appendix A.

The GORE® method targets free gaseous species (aromatics, oxygenated, inorganic and sulphur compounds) known to be generated at sites of reactive mineral oxidation and/or microbial activity, and which subsequently migrate to the surface (Chapter 5). The ICP-MS generated data are reported in the form of modelled species, in ppm. Like SDP, discussed earlier in the chapter, GORE^{TM} was originally developed for hydrocarbon exploration and environmental investigations. The SGH method targets adsorbed hydrocarbons (like the SDP method) of a lab-prepared minus 80 mesh fraction. The analytical procedure involves a weak leach and presumably low-temperature extraction of the accessible hydrocarbon component,

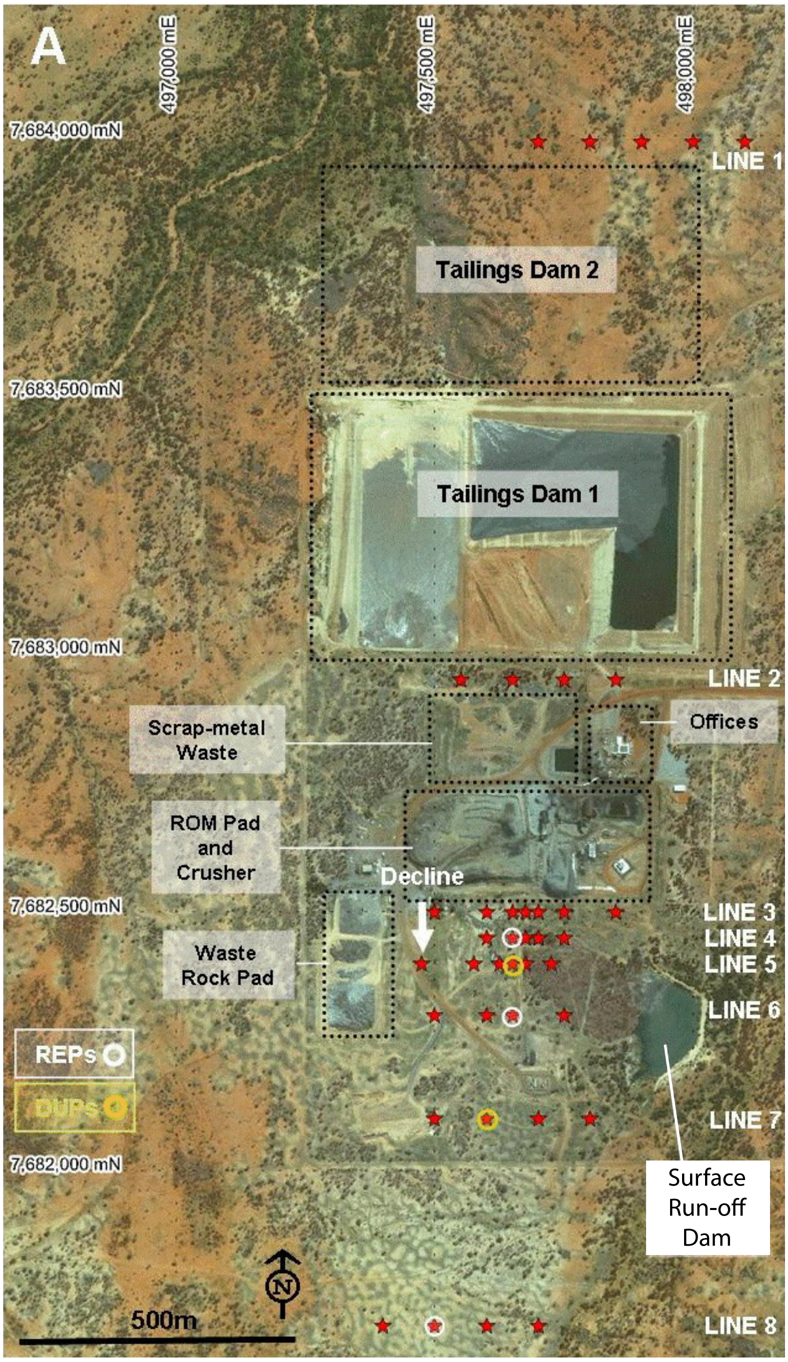

Figure 6.29. Eloise orientation soil samples in relation to mine infrastructure; QA samples indicated by circles (from Lilly et al., 2010, modified).

chromatographic separation and ICP-MS; the data is provided as molecular weight groupings (162 hydrocarbon compounds in the C5–C17 carbon series range). The MSG technique involves passing ‘geogas’ through an ultra-pure, weak acid collector (Chapter 5). The suite of elements analysed by MSG is mainly chalcophile metals, making it especially suited to metal exploration—under appropriate circumstances. Importantly, there is still some academic debate as to whether only gaseous species are sampled or whether a sub-0.45 ųm solid particle component is captured (Wang *et al.,* 2008).

It is stressed that the mapped results of Eloise in Figures 6.30 and 6.31, have colour-coded abundance intervals calculated for a larger population of samples. That is, an Eloise anomaly is anomalous on a multi-orientation site basis. The other orientation sites comprise prospects in the Cloncurry-Ernest Henry area and Mount Isa district (Lilly *et al.,* 2010).

Soil by aqua regia

The aqua regia digestion results provide a basis for evaluating contamination by wind-blown ore dust and general mine waste (particulate and in solution). The results for selected metals are plotted in Figure 6.30. The inset of each map shown is an enlarged view of the more densely sampled area directly above the orebody. Sample duplicates prepared by halving the material from one excavation are arranged vertically. Sample replicates, representing independent samples up to 5 m apart, are arranged diagonally.

The two soil samples at the foot of the wall of Tailings Dam 1 have distinctly elevated Ag, Bi and Ni and very high Cu levels (Figure 6.30). Other Eloise ore-associated metals, including Zn and Co, display a similar pattern. None of the pathfinders is evident in the remainder of the soil grid, including the two or three samples adjacent to, or in, the over flow zone of small dam used for the capture of mine site run-off (labelled as 'surface tailings dam' in Figure 6.28). Another of the three highest Cu results applies to a sample near the mine decline entrance (363 ppm). In contrast to the pathfinders, the Cu levels of 60–210 ppm in many of the central samples of the grid (Figure 6.30D) are well above those expected of typical smectitic soil in the region (10–20 ppm). Thus, it is suspected that Eloise soil, like Ernest Henry Quaternary sands and Osborne soils, has a uniformly raised background of soil Cu related to the incremental fluxing of 'mobile' Cu from depth.

Soil by GORE™ and SGH

The results for two 'channels' of GORE™ data, carbon disulphide (CS_2) propane (C_3H_8), are presented in the upper frames of Figure 6.31. These are probably the most spatially distinctive results of the dataset, though it is noted that several other channels reveal similar features, including:

1. a cluster of elevated responses above the up faulted block in which ore subcrops at the Cretaceous unconformity, and along a major fault in the down-faulted block to the south (*e.g.,* CS2, Figure 6.31A)
2. elevated responses confined to the southern, down faulted block, which is known to be altered but not economically mineralised at the Cretaceous unconformity (*e.g.,* propane, Figure 6.31B)
3. enhanced responses at 'along-strike' positions in the peripheral sample lines to the north and south
4. a lack of relationship between soil gas signal and recorded evidence of surface disturbance, surface run-off and particulate ore contamination.

The same features are evident, if not clearer, in the inter-channel correlation factors determined by multivariate statistical analysis (principal components). Figure 6.31C, for example, shows scores of the 2nd GORE™ factor, which capture the essential character of both the propane and CS_2 patterns. Additionally, the scores of duplicates and replicates match very well, indicating an improvement in precision over single channel QA results (*i.e.,* the multivariate factors are fit-for-purpose).

A similar process was undertaken with the SGH data, which on a single-channel basis are also imprecise relative to geochemical data (Lilly *et al.,* 2010). The 3rd SGH factor is shown to map ore block samples quite comprehensively (Figure 6.31D). Moreover, pairs of duplicated and replicated samples plot in the same 'natural break' intervals (legend and inset, Figure 6.31D). A detailed examination of the SGH data is not attempted for this document.

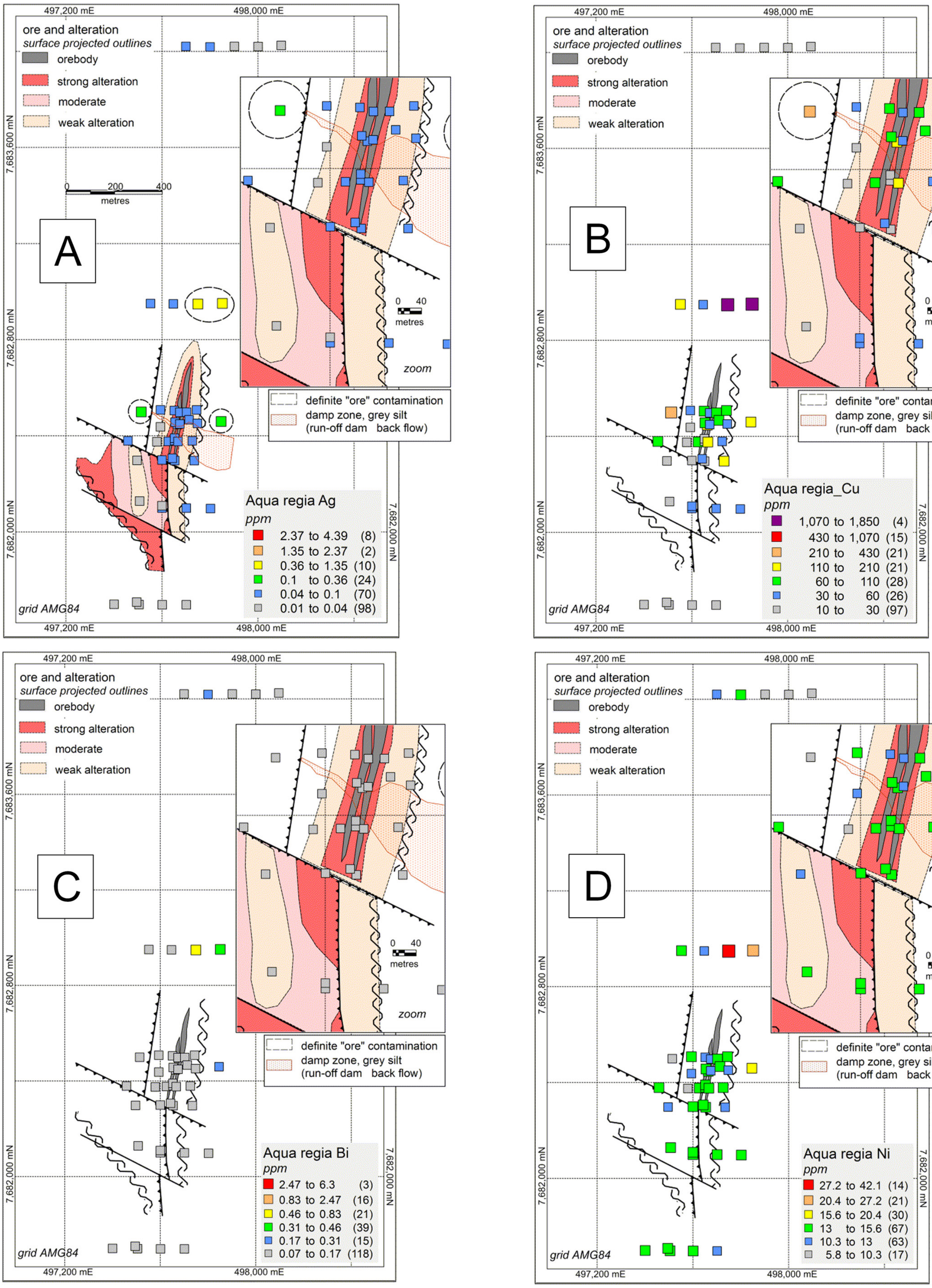

Figure 6.30. Distribution of selected metals in orientation soil samples around Eloise mine—aqua regia digestion (data of Lilly et al., 2010).

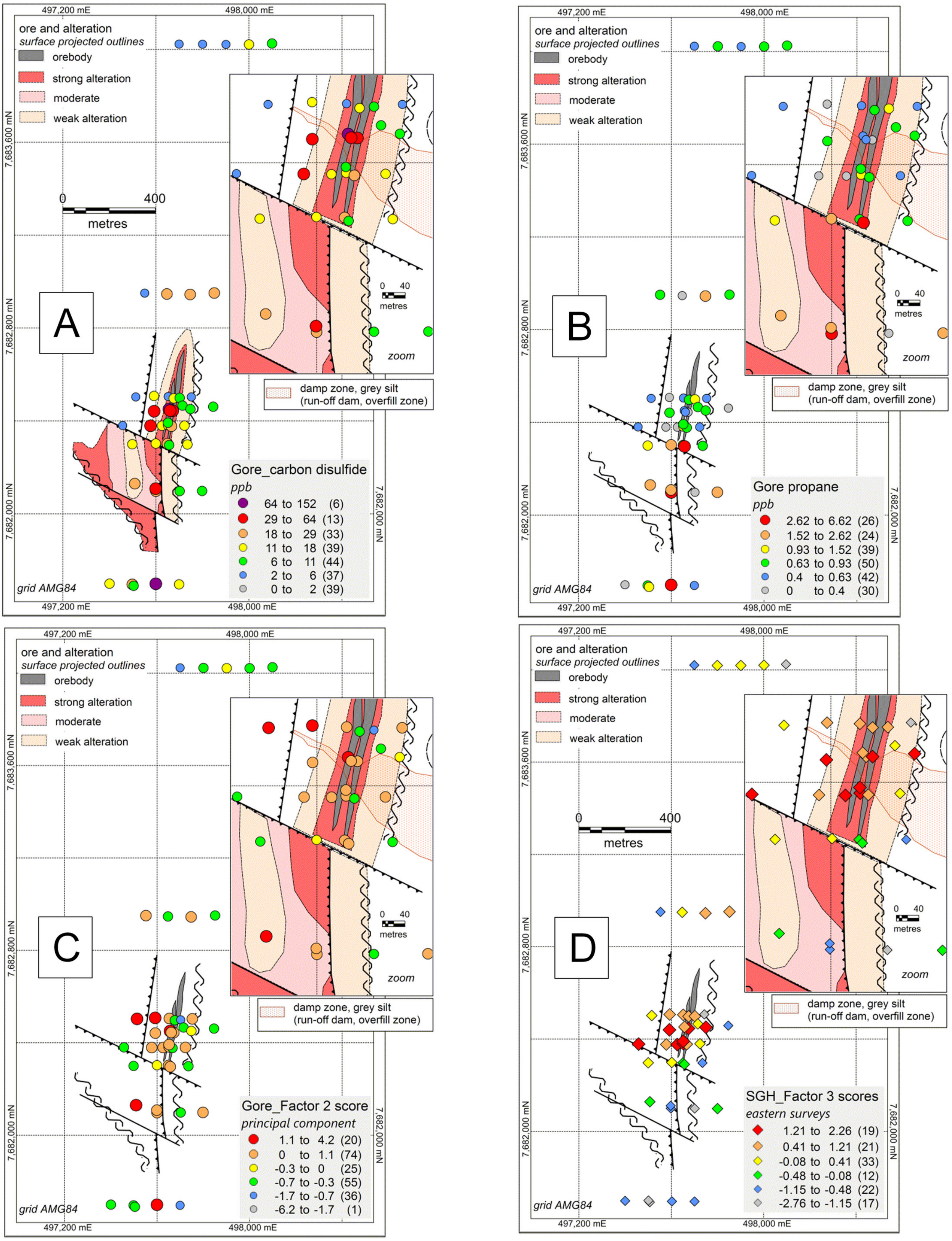

Figure 6.31. Distribution of selected hydrocarbons (A and B) and selected multivariate factor scores (C and D) for soil samples around Eloise mine—GORE^{TM} and SGH methods (data of Lilly et al., 2010).

Soil by MSG

The results for Cu and Zn by the MSG method are shown in Figure 6.32. The Zn result (Figure 32A), with two anomalous samples above the ore zone of the northern mine block, is the most encouraging of the survey (Zn is part of the ore metal signature). Coherent patterns are not evident in Cu or any of the other 47 analysed metals and elements.

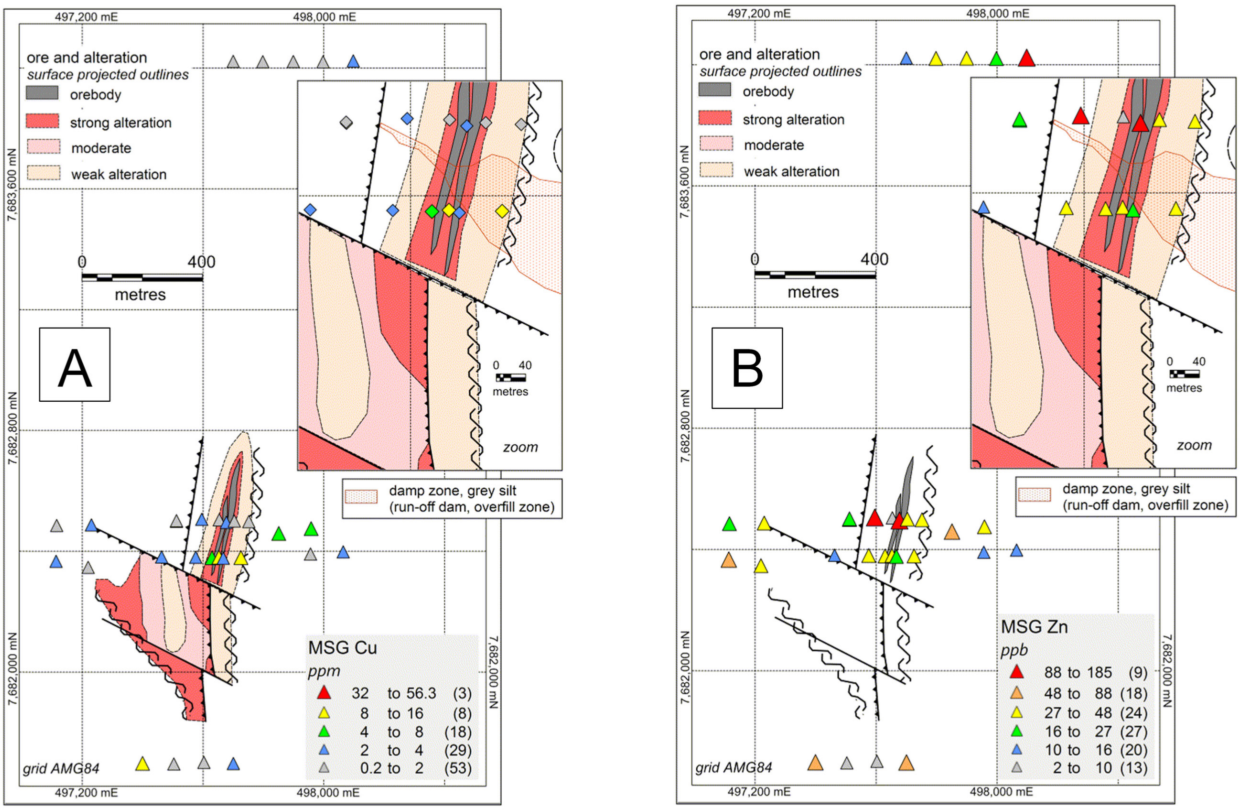

Figure 6.32. Distribution of Cu (A) and Zn (B) by MSG for soil samples around Eloise mine (data of Lilly et al., 2010).

The lower halves of two geotechnical drill holes to basement, but ending above the ore lenses (Figure 6.33), were sampled at 3–5 m intervals and analysed for a full suite of major and trace elements by a combination of XRF and INAA. Elevated levels of Au, Cu, As and Sb (up to 90 ppb, 75 ppm, 125 and 0.7 ppm, respectively), were evident only within 2 or 3 metres of the unconformity, mostly within gritty mudstone and basal conglomerate. These and similar results for samples of the overburden in the mine decline suggested that the argillaceous Mesozoic overburden was an effective seal to dispersion and therefore an unfavourable exploration sampling medium (Li Shu & Robertson, 1997).

Whilst clearly not an optimal sample medium, the Mesozoic cover at Eloise, like that at the Ernest Henry and Osborne deposits, is probably transected by a fabric of steep fractures, and that some fracture zones are hydrologically connected to basement structures or weathered ore. The soil Cu and soil-in-gas patterns at the deposit support this contention. Furthermore, the lower 30–40 m of overburden is not uniformly fresh and historically chemically inert, as implied, because 3–5 m thick saprolite is logged 10–15 m above the basement in the two investigated drill holes (*op. cit.*, Appendix 4).

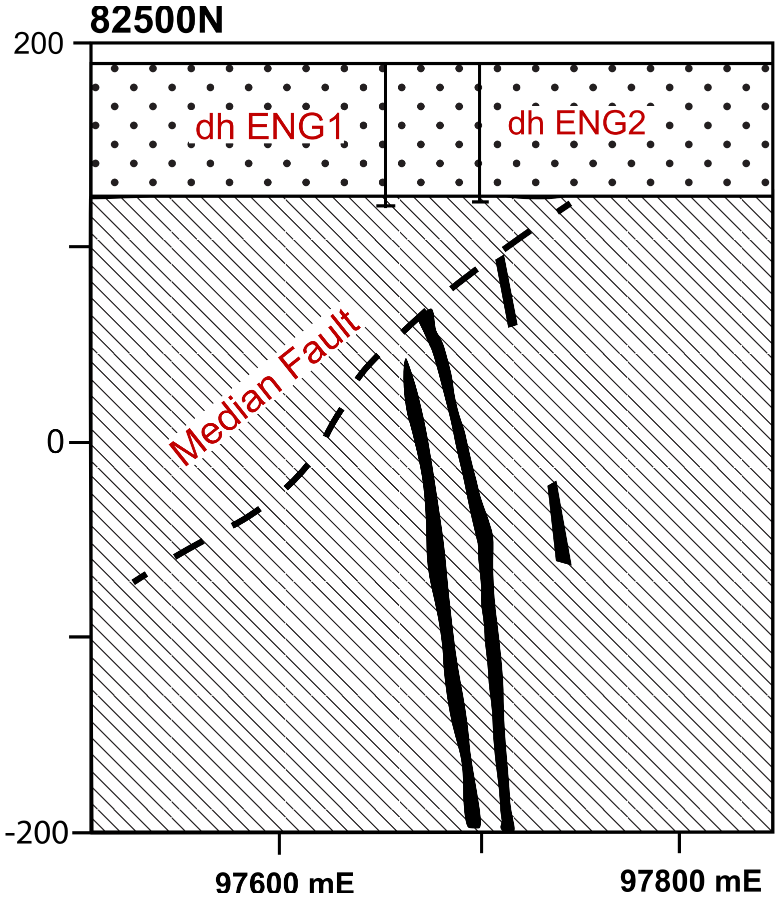

Figure 6.33. Cross section of Eloise deposit at 82500 mN with simplified geology and analysed lengths of drill holes in Mesozoic mudstone cover (from Li Shu & Robertson, 1997, modified).

Discussion

The Eloise setting is more challenging for geochemical exploration than Osborne and Ernest Henry, with thicker cover, an apparent lack of clastic interbeds and little preserved gossan or supergene alteration at the Proterozoic paleosurface. The results for Ernest Henry overburden showed that weak dispersions are indeed present and measurable where total digestion data indicate otherwise (demonstrated for Cu). Despite an even thicker shale- or mudstone-dominated overburden at Eloise, there is sufficient evidence to suggest that the overburden should not be ignored as a potential sampling medium, especially where fractured and/or oxidised.

The field QA data of the Xstrata Copper gas-in-soil orientation project confirm that both the active gas flux (GORE^{TM}) and the profile of adsorbed gas species (SGH) is inherently variable at a local scale (permeability/flux variations). The precisions calculated for duplicates and sample site repeats for individual gas species is markedly inferior to those for metals extracted by weak acids and other selective reagents, such as enzyme leach and MMI (Lilly *et al.,* 2010). It is also conceivable, in the case of the GORE^{TM} tubes, that non-systematic losses (or gains) of gases occurred prior to or post extraction. Nevertheless, the Eloise orientation survey data consistently show repeatable, multi-component adsorbed and free gas features located at the surface-projected positions of the blind orebody, its alteration halo and its confining structures. The results are a convincing argument for broader application.

GORE^{TM} and SGH produce similar results on a multivariate statistical basis, but it is difficult to identify and pair individual ‘channels’ for direct comparison.

The inconclusive nature of the MSG results is rather disappointing result given the conceptual simplicity of the method, and its success at the Mount Isa mine project site (Wang *et al.,* 2012). Large gaps in the sample distribution are partly responsible; as is the fact that the analyses were performed within Australia under somewhat developmental conditions, rather than at the University of Beijing’s established MSG facility.

The per-sample costs of free gas-in-soil surveys are comparatively high ($100s), and field collection requires considerable diligence and patience. Logistically and price-wise, the adsorbed gas techniques, such as SGH (or SDP), are better options but have their own disadvantages (Chapter 5). Presently, the authors are unable to favor one over the other in terms of effectiveness.

The challenges and opportunities presented to the Australian mineral exploration sector are clear though. Gas-in-soil methods offer a conceptually sound method for the detection of blind mineral deposits in areas of thick cover and low paleotopographic relief; that is, in areas where groundwater-related redox zones, historical or active, are unlikely to intersect basement and its contained mineralisation. Supportive evidence is mounting in the literature, but the potential, particularly in relation to the prioritising of geophysically and structurally defined exploration targets, remains under-appreciated.

E1 group of Cu-Au deposits

Setting

The E1 deposit is located 41 km NE of Cloncurry and 8 km east of Ernest Henry mine and comprises three distinct lodes with a total pre-mining resource of 47 Mt at 0.72% Cu and 0.21 g/t Au (Case, 2016). The only Proterozoic exposure is in a small hill 2.5 km to the southeast (Figure 6.34). E1 lies beneath 15 to 45 m of unconsolidated Mesozoic and Cenozoic sedimentary cover (Figure 6.35) in a flat, pastoral plain of variably developed smectitic 'black' soil in recent alluvial gravel and sand (also Figure 6.35).

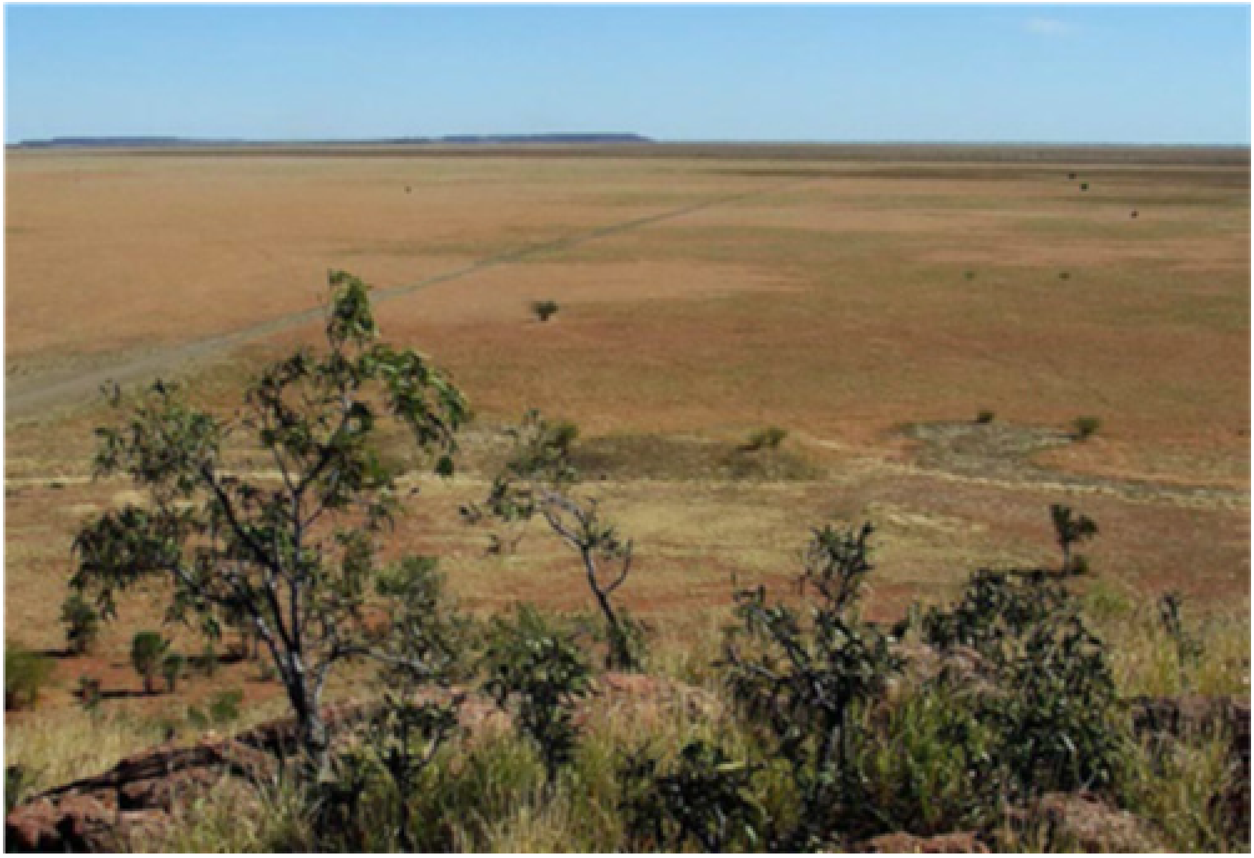

Figure 6.34. Landscape setting: view from Mount Margaret, 2.5 km to the SE of E1, west and across E1 toward the Ernest Henry spoil piles (from an Exco Resources ASX release, 2008).

It was discovered in 1995 by Western Mining Corporation with its first hole, drilled into an arcuate aeromagnetic feature of half the intensity of the Ernest Henry anomaly, adjacent to the geophysically prominent Mount Margaret Fault Zone. Exco Resources drilled three strongly mineralised areas in the 2000's and sold to Xstrata Copper/Glencore in 2011, who then mined E1 North between August 2012 and March 2014. E1 East and E1 South were only partially pre-stripped before operations ceased.

Mineralisation is hosted in a magnetite-rich sequence (Soldier's Cap Group, Cover Sequence 3) of steeply dipping, folded and locally brecciated metasediments and metavolcanic lenses stratigraphically below carbonaceous schist and above amygdaloidal meta-basaltic andesite (Case, 2016). Petrologically, the lower mafic volcanics are correlated with the Mount Fort Constantine Volcanics, which host the Ernest Henry deposit, and the metasediments may be Corella Formation equivalents (Foster & Austin, 2008). Chemically, the E1 lodes share the IOCG association characteristics of high Fe-Cu-Au-Ca-Ba-F-Mg-P-Mn and anomalous U-REE-Co-Mo-As. They also share an Ernest Henry-like paragenesis, but litho-types and

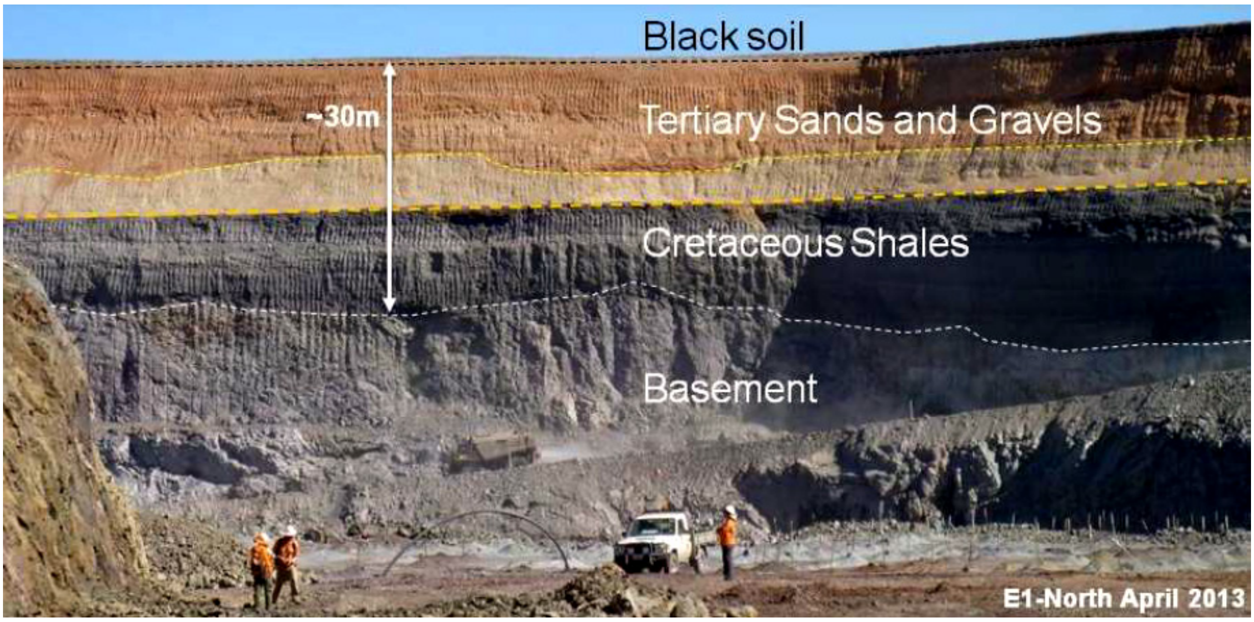

Figure 6.35. The E1 North pit at April 2013 (from Glencore/MIM).

mineralisation styles more closely resemble those of the Osborne and Starra IOCG deposits (Case, 2016).

The E1 North orebody extends more than 300 m down-plunge, southward, with widths of 20–100 m. Before its removal, a 'blanket' of supergene mineralisation straddled the base of oxidation and extended outward for up to 100 m with thicknesses of 15 to 65 m (Case, 2016). The mineralised ironstone lenses of E1 South and E1 East also subcrop at the Mesozoic unconformity but the presence of supergene mineralisation and pre-Mesozoic weathering of the basement at these localities is assumed rather than confirmed. Discrete paleotopographic highs are not obvious in the gridded basement depth data of Figure 6.36A, but a broad shelf in the paleo-surface is evident over the area of the eventual E1 North open pit, as the cover otherwise thickens to the north and northeast.

Surface geochemistry

In 2011, Xstrata Copper Exploration completed an intensive soil geochemical survey over the E1 group of deposits and two magnetic anomalies immediately to the south (Figure 6.36A). Samples from 15 cm depth (root horizon of local grasses) were sieved through a 5-mm mesh and analysed by aqua regia/ICPOES and the Mobile Metal Ion (MMI) procedure. The aqua regia digestions were completed on pulverised splits. The results provide a semi-quantitative measure of regolith geochemical variation and the likelihood of on-site contamination from the spoil of earlier drill holes (mostly RC). MMI extractions were undertaken on a 250-g split of the original < 5mm field sample.

A measure of soil type and regolith control is provided for this assessment by the availability of a 1997-vintage, natural colour Thematic Mapper satellite image (Figure 6.36B). This spectral product efficiently discriminates areas of smectitic 'black' soil (blue-grey hues) from sandy and gravelly clastics (white areas) and clastics coated with Fe oxide (orange-brown hues). Black soil and clearly demarcated areas of sand and gravel dominate the survey area.

The results for Cu (aqua regia digestion) are plotted in Figure 6.37A according to natural breaks in the population of 874 data points. Recalling the high drill hole densities over the three lodes (Figure 6.36A), it is reasonable to suspect that the five samples with more than 80 ppm Cu (yellow, orange and red) might have been contaminated with mineralised particulates (three

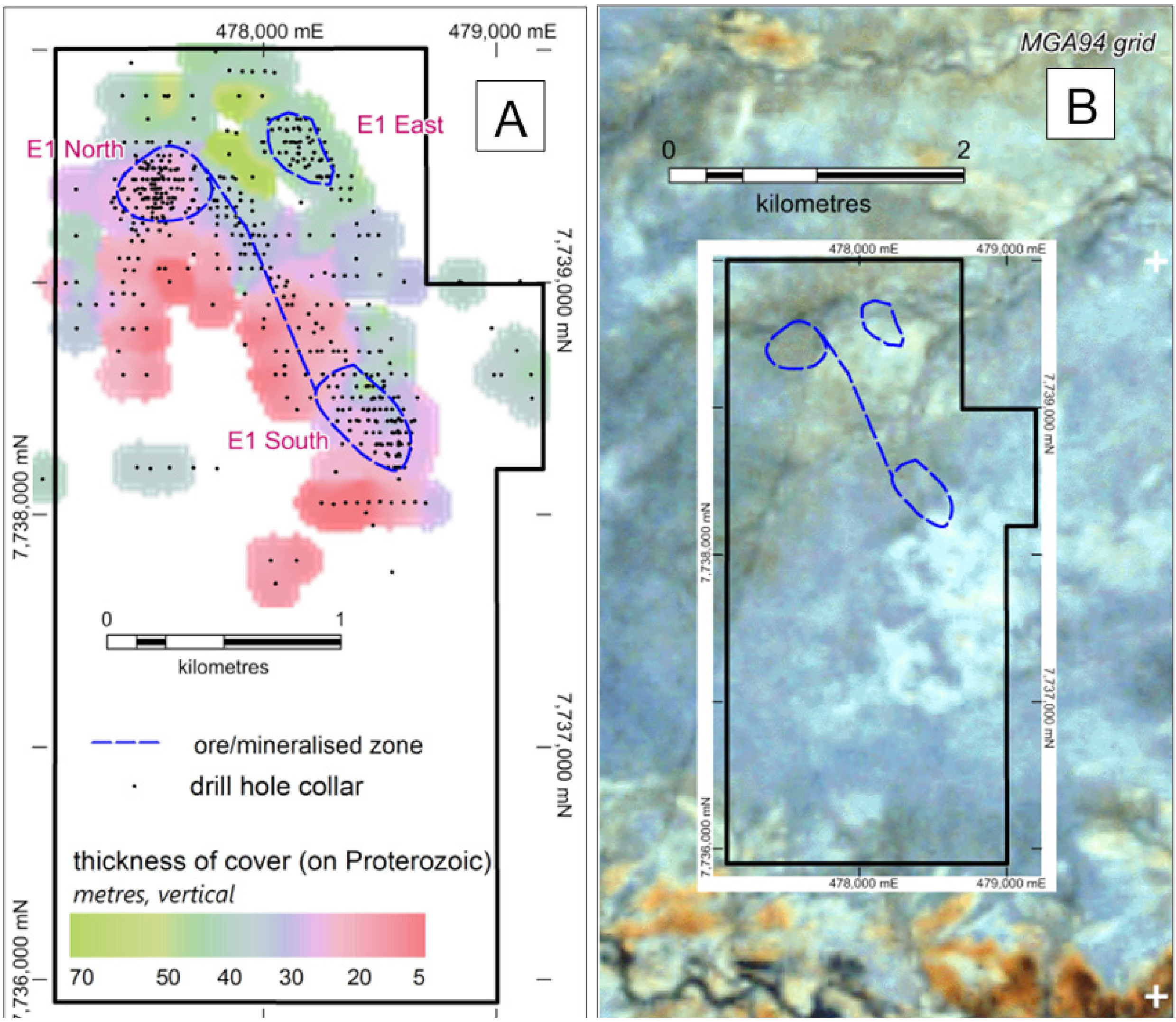

Figure 6.36. Outlines of E1 lodes and pre-mining soil survey limits on: A—grid of depth to basement; B—regolith sensitive satellite TM123 image (data of Glencore-MIM).

also have anomalous Mo and Co levels). However, most of the other sample sites within the lode polygons or located along the projected position of the mineralised structure between E1 North and E1 South, have less than 30 ppm Cu, in common with 98% of the survey's data. By replotting the same data with percentile breaks that approximate a log-normal distribution (Figure 6.37B), a >20 ppm sub-population is evident, which matches the northeast-trending 'sandy and moderately ferruginous regolith' between the two creeks that drain the area of E1 North and E1 East. An anomalous sub-population corresponding to the 95th percentile and above (*i.e.,* 23–90 ppm Cu, orange-fill circles), plots mostly within or near the three lode polygons. This group is analogous to the slightly elevated total digestion Cu backgrounds noted for surface samples above the Ernest Henry and Osborne deposits, and interpreted accordingly (*i.e.,* background Cu plus an exotic component, dispersed from mineralisation in the basement through overburden to the surface).

The MMI results for Cu are plotted with log-normal percentile breaks in Figure 6.38A. The upper 5 percent, corresponding to Cu levels of >1600 ppb (orange and red) lacks the regolith control evident in the aqua regia equivalent and is positioned over each of the lodes and between E1 North and E1 East. Whilst an encouraging result, there are only 4 samples, above E1 North, with MMI Cu signals more than 5 times the background level of about 1200 ppb. Moreover, there is little support from other pathfinders, such as U, Mo and Au, which only spike at the inferred contaminated sites (compare red-fill diamonds of Figure 6.38B with red-fill circles of Figure 6.37B).

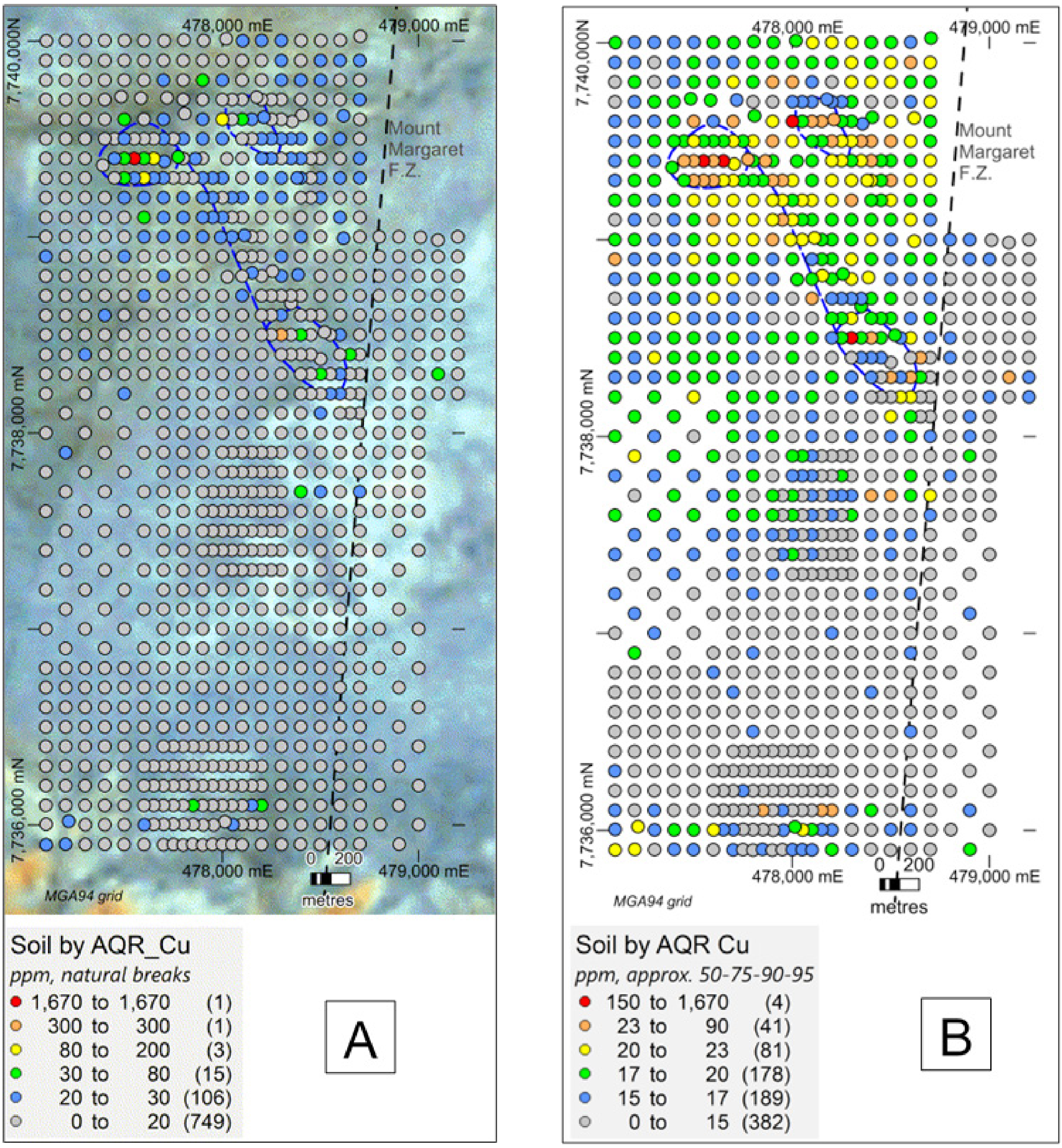

Figure 6.37. E1 area soil geochemical grid: A—aqua regia Cu with natural population breaks and TM123 backdrop; B—aqua regia Cu with pseudo logarithmic breaks (data of Glencore-MIM).

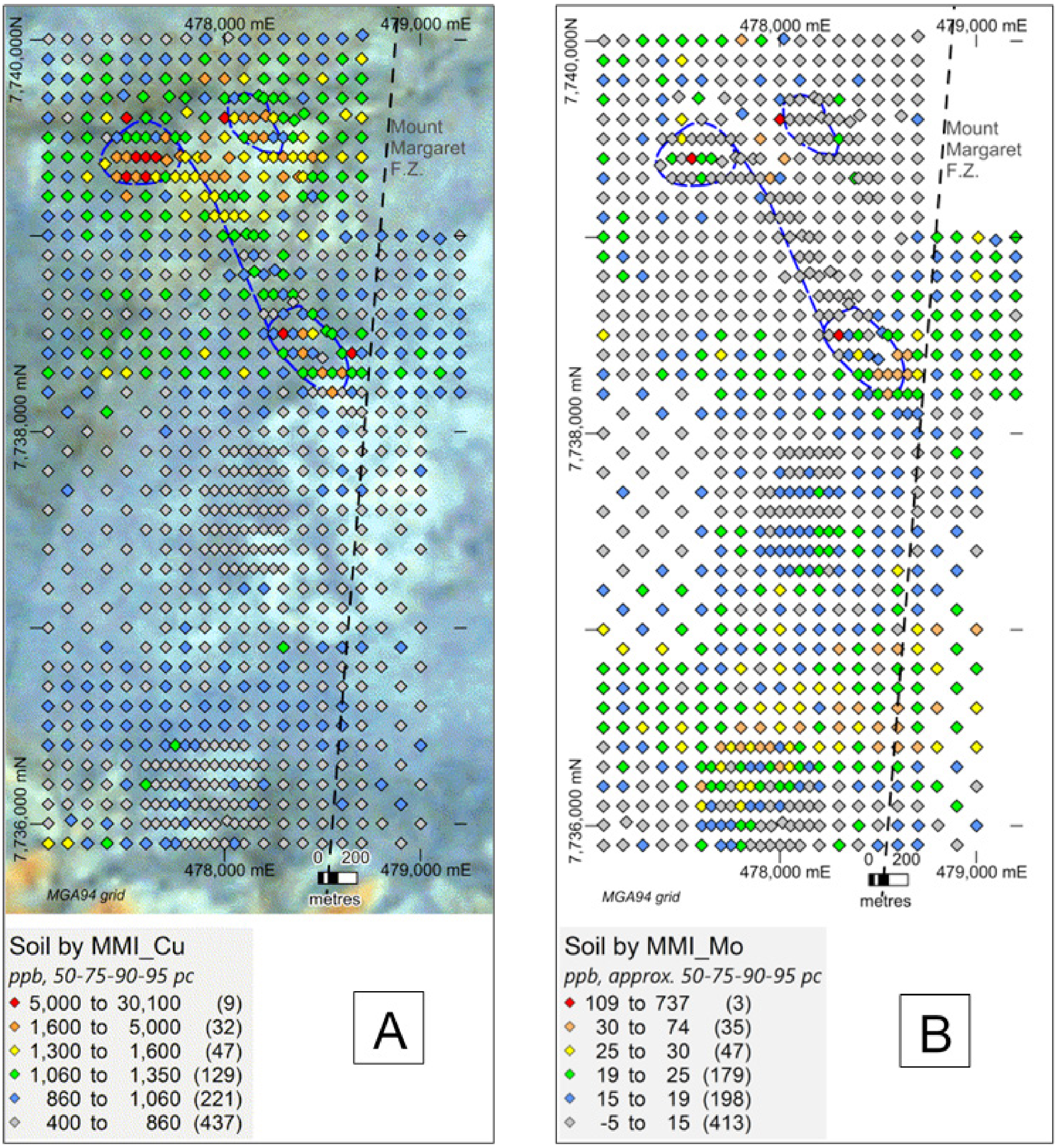

Figure 6.38. E1 area soil geochemical grid; A—MMI Cu on TM123 backdrop; B—MMI Mo (data of Glencore-MIM).

Discussion

Evidence for a surface geochemical signal related to the blind E1 IOCG lodes is strongest in the Cu by MMI extraction and Cu by aqua regia digestion results.

The aqua regia digestions were measured solely by ICP-OES. Thus, high resolution (ICP-MS) data for many IOCG pathfinders, including Ag, Bi, As, Sb and U, are not available to assess the extent of regolith contamination from drilling spoil, which was still visible in parts of the soil grid at the time of the survey. Fortunately, the strong acid data for Mo and Co are of sufficient sensitivity to indicate that only 3 to 5 of the survey samples are likely to be contaminated. Therefore, groups of samples with background Mo and Co but anomalous Cu are possibly areas of secondary Cu accumulation.

Though of modest amplitude, the Cu anomalies are located within and near to the projected outlines of the blind E1 lodes, suggesting direct and vertical dispersion of Cu from bedrock mineralisation to the surface. However, the extracted levels by MMI of the pathfinder metals, including Ag, Au, Mo, U, are very low and inconclusive. In this respect, the E1 results are similar to those achieved by MMI for the black soil regolith above the nearby Ernest Henry deposit. The following implications are evident:

- MMI reagent is not entirely effective for strongly developed smectitic regolith, except perhaps for Cu and where the substrate is comparatively sandy.
- As shown for Ernest Henry, a better sample medium for MMI, and stronger leachants such as Regoleach, is available at the horizon of Fe-oxide accumulation at a depth of 2–3 m, beneath the eluviated (bleached) zone of smectite development.
- More alkaline and/or oxidative reagents, such as Enzyme Leach or Ionic Leach, may produce more definitive results in surface samples at E1, as arguably demonstrated at Ernest Henry.
- The more logistically demanding soil-in-gas methods, such as those trialled with encouraging results at Eloise and Osborne, may be appropriate for the E1 and Ernest Henry setting, which apply to large areas with 10–70 m of unconsolidated cover north of Cloncurry.

Cannington Ag-Pb Deposit

Setting

The Cannington Ag-Pb-Zn deposit is located 150 km south of Cloncurry in a pastoral alluvial plain (Figure 6.39) and physiographic setting like that of the Eloise Cu deposit. It was discovered by BHP Minerals, in 1990, by drilling through about 50 m of recent and Cretaceous sediments to test a regional aeromagnetic anomaly in basement considered to be lithostratigraphically analogous to the Broken Hill deposit in NSW. Subsequent resource drilling revealed 10–70 m of Phanerozoic overburden, thickening to the southeast, and a lack of oxidation or weathering of Proterozoic bedrock at the buried unconformity (Walters & Bailey, 1998). By 1998, soon after underground mining began, the resource measured 44 Mt at 538 g/t Ag, 11.6% Pb, and 4.4% Zn, and in June 2017 total reserves of 23 Mt at 190 g/t Ag, 5.6% Pb and 3.5% Zn were reported to the ASX. Not surprisingly, it is regarded primarily as a world class Ag deposit, albeit with the geological and mineralogical characteristics of Broken Hill-type mineralisation.

The deposit is essentially stratabound, within strongly deformed biotite, sillimanite and garnet-bearing gneiss and associated amphibolite and pegmatite of the Soldiers Cap Group. Mineralisation tends to track the contact with ‘core’ amphibolite, which is relatively unaltered and occupies the axial trace of a south-plunging and east-dipping synform, as shown for the higher grade southern block in the cross section of Figure 6.40.

Typical ore is an assemblage of sphalerite and Ag-rich galena with hedenbergite, pyroxmangite, magnetite and fluorite as gangue (Chapman & Williams, 1998). Late structures with carbonate, micas and clay are often Mn, F, and Cl-rich (Walters & Bailey, 1998).

Figure 6.39. Landscape vista of the Cannington mine area, circa 2002 (from Jeffrey, 2002).

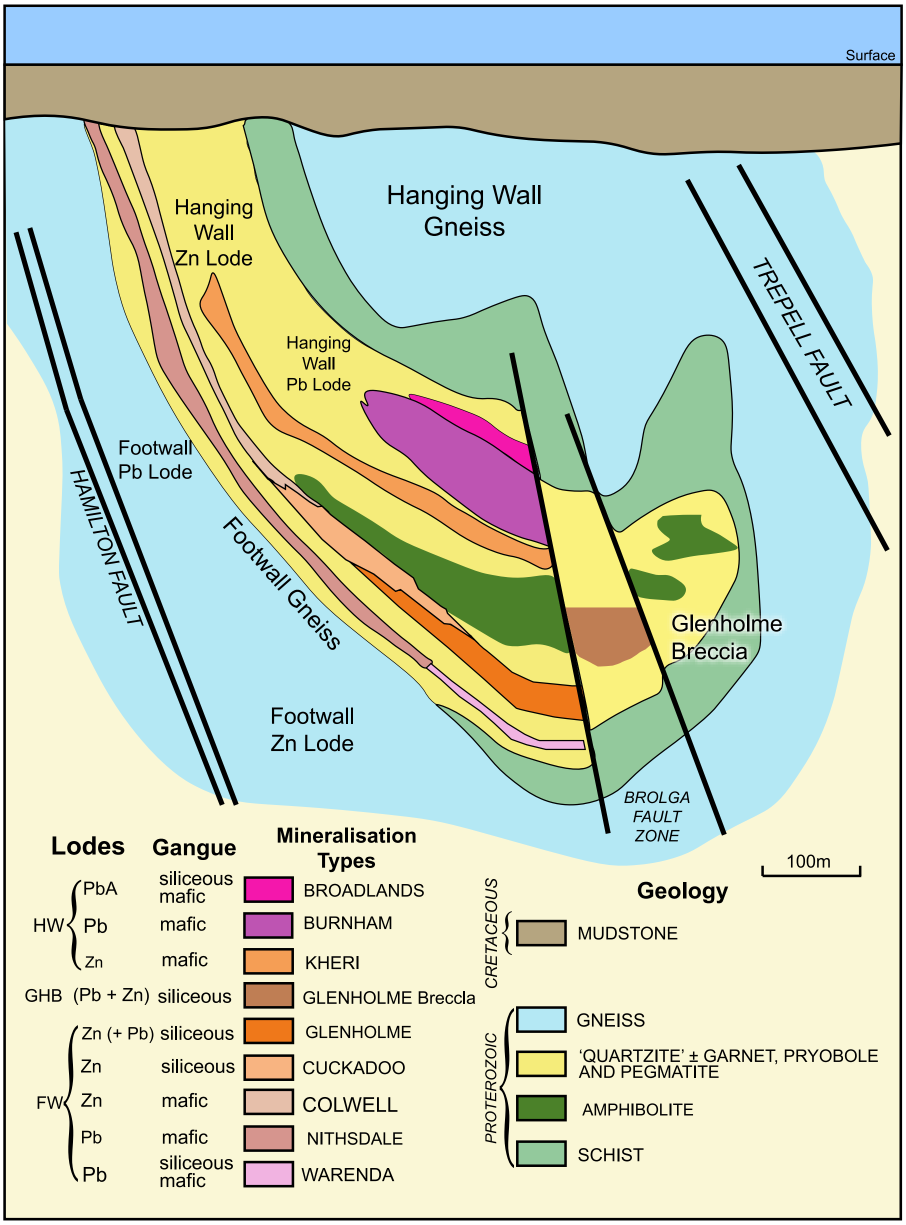

Figure 6.40. Simplified geologic cross section of the Cannington deposit (from Readford & Curypko, 2017).

Surface geochemistry

In 2001–2002, soil was sampled from three regolith types on an east-west line across the southern end of the deposit as part of AMIRA project P618 (Partial Isotopic Discrimination of Partial Leach Geochemical Anomalies in Covered Terrain). The location of the sample line is shown in relation to regolith type boundaries, landscape features, mine infrastructure and the projected limits of ore in Figure 6.41. In addition to Pb isotope analysis, the samples were tested by strong acid digestions and by several selective geochemical reagents. The results are discussed herein.

Regolith pH and grain size distribution measurements, plotted in Figure 6.42, provide a critical degree of control on chemical profile interpretations. The older alluvium between Hamilton River and Trepell Creek, and vertically above the ore zone, is moderately alkaline (probably due to the presence of minor pedogenic carbonate). Black soil east of Trepell Creek is not distinguishable by grain size modality.

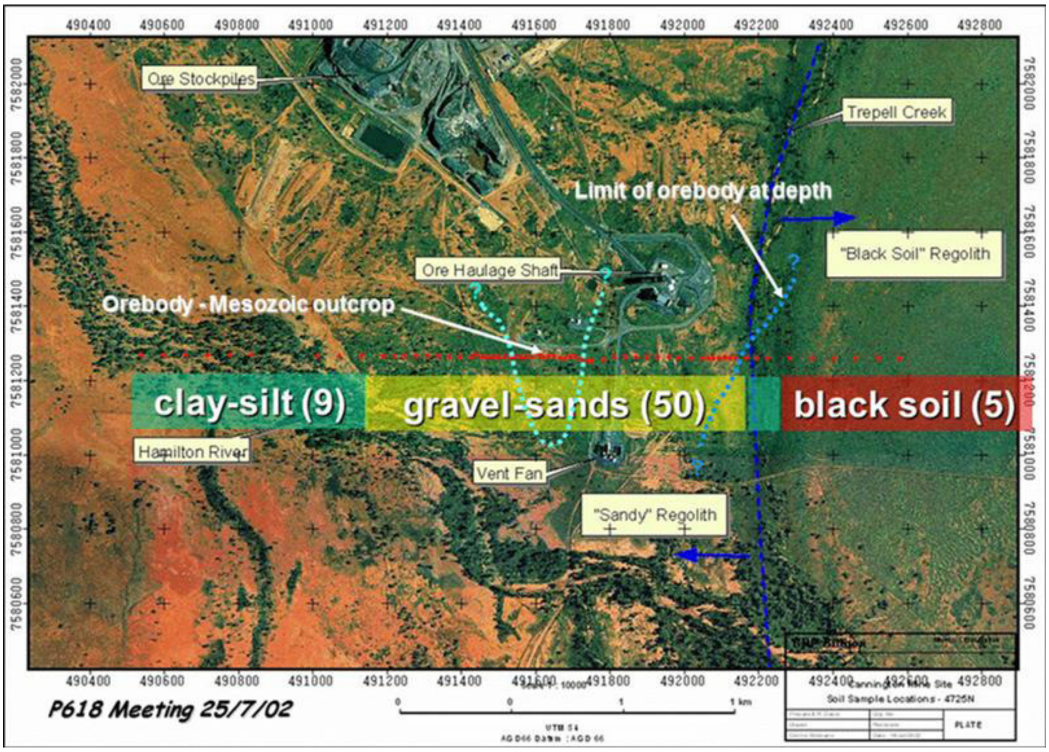

Figure 6.41. Cannington case study soil sample sites (red dots) on aerial image and vertically projected ore limits (from Carr & Denton, 2002).

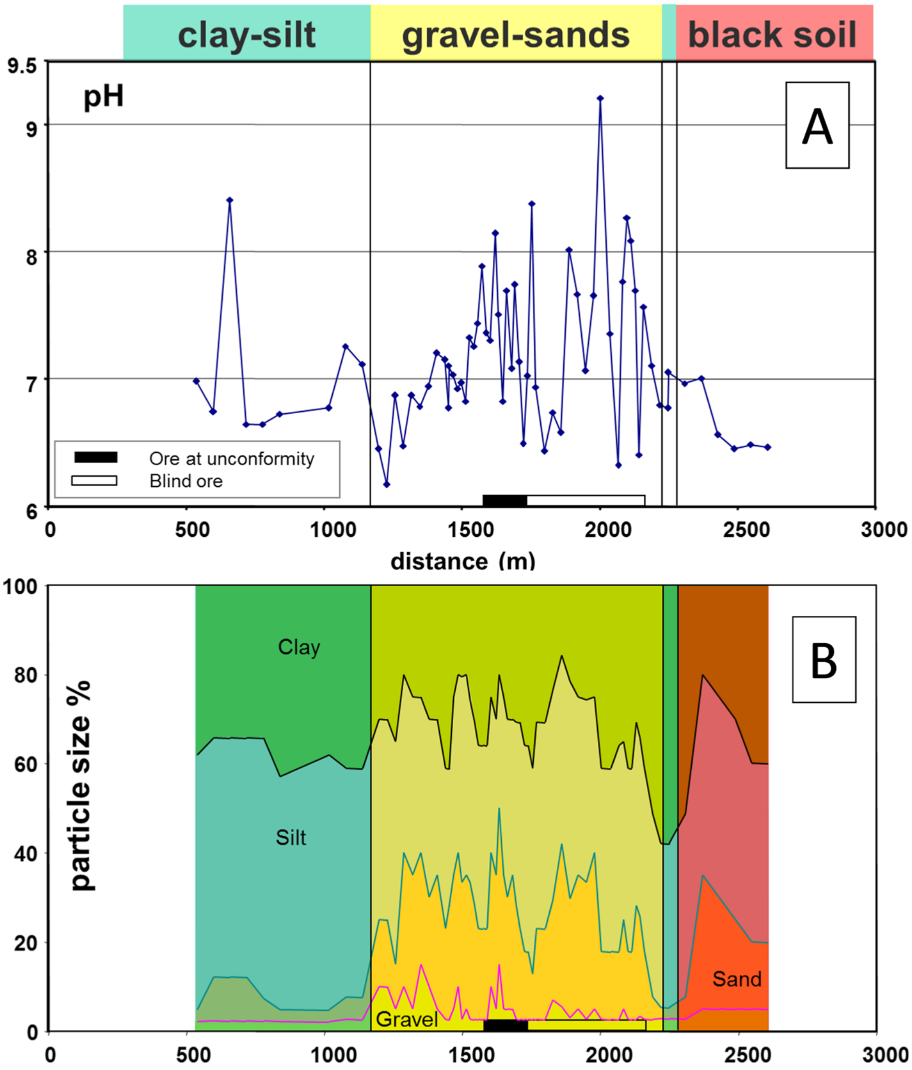

Figure 6.42. Soil pH (upper) and grain size distributions along the Cannington case study transect for P618 (from Carr & Denton, 2002, modified).

Three groupings of element distributions are evident and are discussed in detail.

Some regolith or minor pH influence

This classification applies to Fe, Mn, Cu, Zn and Pb by strong acid digestion, as illustrated by multi-acid and aqua regia digestion graphs of Figure 6.43. Fluvial dispersion of mine-related contaminants may be responsible for the elevated Zn levels by aqua regia (AR) adjacent to both Hamilton River and Trepell Creek (Figure 6.43D, 40–100 ppm). The divergent results of multi-acid (MA) and aqua regia digestions for Cu and Zn (and Fe) in black soil samples is probably due to the presence of an aqua regia-resistant Fe oxide phase in black soil. The elevated Pb values of gravel-sand samples which straddle the projected limited of ore beneath the Cretaceous unconformity is attributed to either mining-related contamination or ore-Pb sourced from depth—both because of Pb isotope signatures which approach that of typical Cannington ore (Carr & Denton, 2002). However, there is only one sample with more than 20 ppm Pb (off-scale at 92 ppm, Figure 6.43E) and it is located on the western shoulder of a strong MMI and BCL Cd anomaly centred on Trepell Creek (compare Figures 6.43E and F) and the western edge of a jump-up in regolith total Fe and Zn content (Figures 6.43A, C, D).

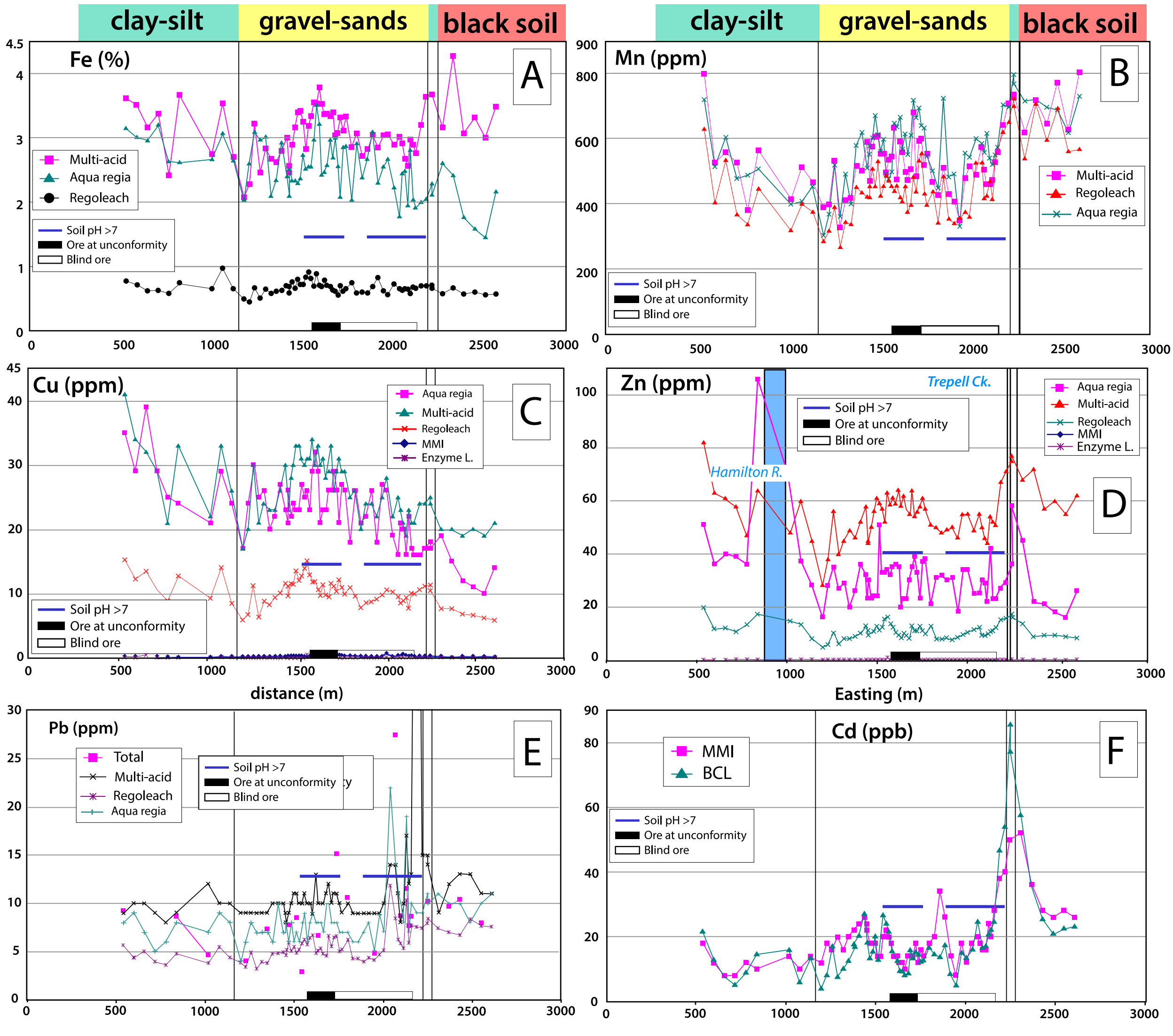

Figure 6.43. Cannington deposit line profiles of selected metals by strong acid digestions and Regoleach (A–E) and Cd by MMI and BCL(F) (from Carr & Denton, 2002, modified).

Strong pH or some regolith influence

This classification applies to the Ag, Co, Cu and Bi, by one or more of the trialled selective digestion methods. A twin peak pattern centred over the most alkaline samples is well developed for Ag, by MMI, Regoleach and BCL, at 2–4 times local regolith background levels (Figure 6.44A). Co and Cu by MMI also display twin peak patterns, though of lower amplitude (Figures 6.44B and C). Importantly, the detail of each of the profiles correlate approximately with regolith type and the indicated pH maxima of each graph (blue line segments), and the overall shape of each of the "anomalies", including the outer shoulders, best matches the vertically projected extent of the buried ore deposit. The Regoleach Bi profile shows transitional features, with weak twin peaks and a high black soil background, like the profiles of Mn and Zn (Figure 6.44D *c.f.*, Figures 6.43B, D). Though not provided, the profile of Mo by Enzyme Leach also shows a markedly elevated black soil background, but an antithetic relationship to soil pH.

No pH and no in situ *regolith control*

This classification applies to selectively extracted Zn and Cl. The MMI profile of Zn in Figure 6.44E features 150–300 m wide anomalies, 3–8 times background levels, which straddle the outer limits of projected ore. This is a remarkable feature, suggestive of dispersion controlled by fracture networks in the cover above ore-limiting basement faults. Anomalous Zn, further to the west, is likely to be related to Hamilton River alluvium (see Figure 6.43D). In the case of Cl, strong, multi-sample spikes are located on either side of projected ore subcrop (solid black bar), and at the eastern limit of buried ore. The extreme spikes of 500 and 1000 ppm at about 1250 mE apply to the two most westerly gravel-sand samples with anomalous Ag (*c.f.*, Figure 6.44A). Significantly, all the samples with anomalous levels of Cl, by Enzyme Leach, have distinctly elevated K abundances by an unspecified weak extraction, suggesting the possible presence of sylvite (KCl). The peripheral nature of the Cl anomalies is suggestive of an annular geometry predicted by the electrochemical model of dispersion.

Discussion

Despite the apparent absence of a weathering and oxidation effects at the Cretaceous unconformity (Walters & Bailey*,* 1998), neither variation in regolith type nor soil pH completely accounts for the distributions of several chalcophile metals and Cl along the test line over the southern termination of the buried Cannington Ag-Pb deposit. Presently, we are unable to confirm the veracity of the earlier claim and have no knowledge of the presence, or not, of weathering effects and redox horizons in the Cretaceous cover. In the authors' estimation, however, the Cannington data contain the clearest examples of surface geochemical anomalism above blind economic mineralisation available for the Mount Isa region.

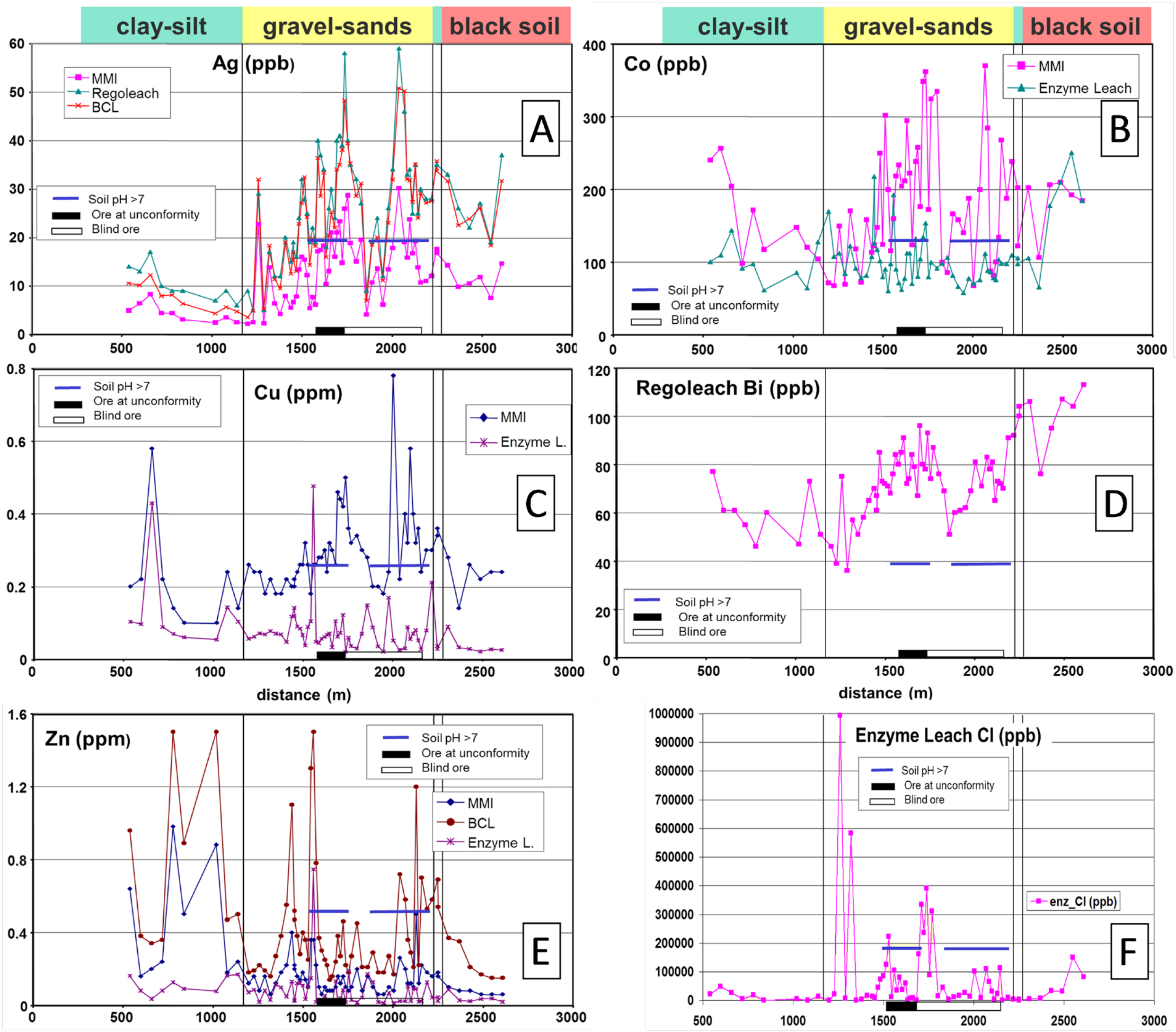

Figure 6.44. Cannington deposit line profiles of selected metals in soil by selective digestions by chemical leachants (from Carr & Denton, 2002, modified).

Conclusions and recommendations

1. Drilling to basement on a pre-determined grid to detect and measure primary or supergene mineralisation or paleo-slope dispersions in colluvium is still the most effective geochemical exploration strategy for covered areas. Standard sampling and chemical analytical methods apply to intercepts within 1 or 2 metres above the unconformity, and below; *viz.,* splits of bulk material and strong acid digestion with ICP measurement optimised for pathfinder metals (Ag, As, Bi, Cd, Mo, Sb, Tl, U, and W).

   A drill hole centre of 500 m is appropriate for an Ernest Henry look-alike, and 200 m x 100 m is probably sufficient for an Osborne deposit look-alike (500 and 200 ppm Cu thresholds, respectively). Reduced spacings, of 250 m and 100 x 50 m, respectively, are required if erosion-expanded ‘footprints’ at the Mesozoic unconformity are absent (*i.e.,* no paleo-relief).

2. The sampling of sedimentary cover units, particularly at unconformities (commonly Tertiary on Cretaceous), redox zones and fractured/weathered intervals (if visible) could reveal elevated levels of pathfinder metals over hundreds of square metres related to deeper and weathered mineralisation (*e.g.,* Ernest Henry and Osborne Cu-Au deposits), or large-area hydromorphic plumes in areas of marked paleotopographic relief.

High quality analyses of cover materials are also a strategic resource, for groundwater modelling and environmental monitoring.

Standard sampling methods apply (splits of bulk material) and aqua regia with optimised ICP measurement is an effective analytical minimum; additional analyses, by selective extraction methods such as Regoleach, MMI and Enzyme Leach may be appropriate in some circumstances, such as multi-hole drill hole campaigns not designed to reach basement and/or where persistent redox zones are present or the depth to basement from the point of sampling exceeds about 25 m.

3. Where grid-drilling to the basement is not possible (too thick or too expensive), the sampling of near surface clastics, below black soil but at a consistent position in the redox profile, could reveal weak acid /selectively extractable, and perhaps transient, dispersions related to diffusion (along fracture zones) or electrochemical gradients in the cover above blind mineralisation (demonstrated for Ernest Henry, reported for Osborne).

   Analysis by aqua regia/ICP-MS, and, in order of likely effectiveness, MMI (for metals and LREE), Enzyme Leach (for halogens and metals) or Regoleach (or equivalent) is recommended for this setting.

   Sample intervals of 100 m along appropriately oriented 200 m-spaced lines are suggested for discrete, > 50 Mt targets (*e.g.,* Ernest Henry and perhaps Cannington).

   Fractures zones are likely to correspond to geophysical discontinuities, extrapolated geologic trend, changes in soil mineralogy (evident in ASTER data), changes in soil colour (aerial photography), or changes in topography or drainage patterns. Selective drilling of such trends may increase the probability of locating secondary dispersions generated by concealed mineralisation.

4. Based on the Ernest Henry and perhaps the E1 examples, the sampling of surficial smectic and strongly developed ‘black’ soil is the least favoured tactical option for locating geochemical features at the surface which were generated by upward or lateral dispersion through the overburden. But, if black soil is poorly developed and the regolith is of a clastic nature, then scenario 3 is applicable (*e.g.,* Osborne, Eloise & Cannington).

5. Several gas-in-soil methods were trialled at Ernest Henry, Osborne and Eloise. The free-gas variant, pSirogas, which was developed in the 1990s but not commercialised, produced positive results over blind ore (Cu, Zn and U, and some major elements) and a null result over the known, downslope exit points of hydromorphic anomalies at the Osborne deposit.

   A test of an earlier version of soil desorption pyrolysis at Ernest Henry was inconclusive, and impaired by unsatisfactory I.P. constraints and a drawn-out field sampling programme. Similarly, a test of the metals in soil gas method (MSG), a free-gas variant, at Eloise was impaired by uncertainty with the choice of laboratory and incomplete sample coverage.

   Tests of soil desorption pyrolysis (SGH) and gas collection (GORE^{TM}) at Eloise produced repeatable, multi-component free- and adsorbed-gas features, respectively, at the surface-project positions of the blind orebody, it’s alteration halo and confining structures. Collectively, the results are a compelling argument for broader application. Logistically and price-wise, the adsorbed gas variant is the favored option.

Chapter 7

Covered domain geochemistry III: Exploration campaigns

Introduction

The purpose of this chapter is to record the distributions and summarise the effectiveness of surface geochemical exploration campaigns that targeted economic or tested presently uneconomic mineralisation beneath transported overburden in the Mount Isa region. The extents of both conventional (strong acid digestion) and leachant (selex) soil surveys are recorded in three sub-region maps. Surveys completed within covered areas of each sub-region are labelled (either individually or as groups) and paired with a tabulation of: 1) essential survey parameters, 2) primary outcomes as recorded in statutory reports ('CR' reports), and 3) where possible, a comment on survey performance or efficacy. Scrutiny of reported analytical data to assess the conclusions of individual companies is not undertaken.

The 2016 release of the Mount Isa region geochemical data compilation, discussed in Chapter 1, is the primary source of data for the maps. Secondary sources include proprietary data for the Ernest Henry district supplied by MIMRD and data released with the industry-GSQ collaborative Geochemistry Through Cover project (Lilly & Hannan, 2016).

The distribution of selex soil surveys across the Mount Isa inlier, symbolised by extraction type, is shown in Figure 7.1. In detail, the population comprises 7500 soil samples recorded in the open file compilation as sample type = "PD" (partial digestion), another 1000 samples found to be by selective extraction after checking relevant open-file company reports, and 220 vegetation samples from three biogeochemical surveys. The open-file report and laboratory file cross-checks also resulted in the reattribution of the extraction method to 'Deep Leach' for most surveys in the Lawn Hill region (replacing the ambiguous code 'PDMMI' used by some companies).

The most extensive selex surveys were undertaken within about 90 km of the Century Zn deposit using the Deep Leach reagent (Anglo American and Aberfoyle Resources), 60 km west of Mount Isa mine using Enzyme Leach (MIM Exploration) and within about 50 km of the Ernest Henry Cu-Au deposit using Enzyme Leach (also MIM Exploration). Much of the proximal margin of the Mount Isa Inlier, with as little as 5 to 10 and less than 100 metres of transported cover (Figure 7.1), remains largely untested by selex soil geochemical surveys.

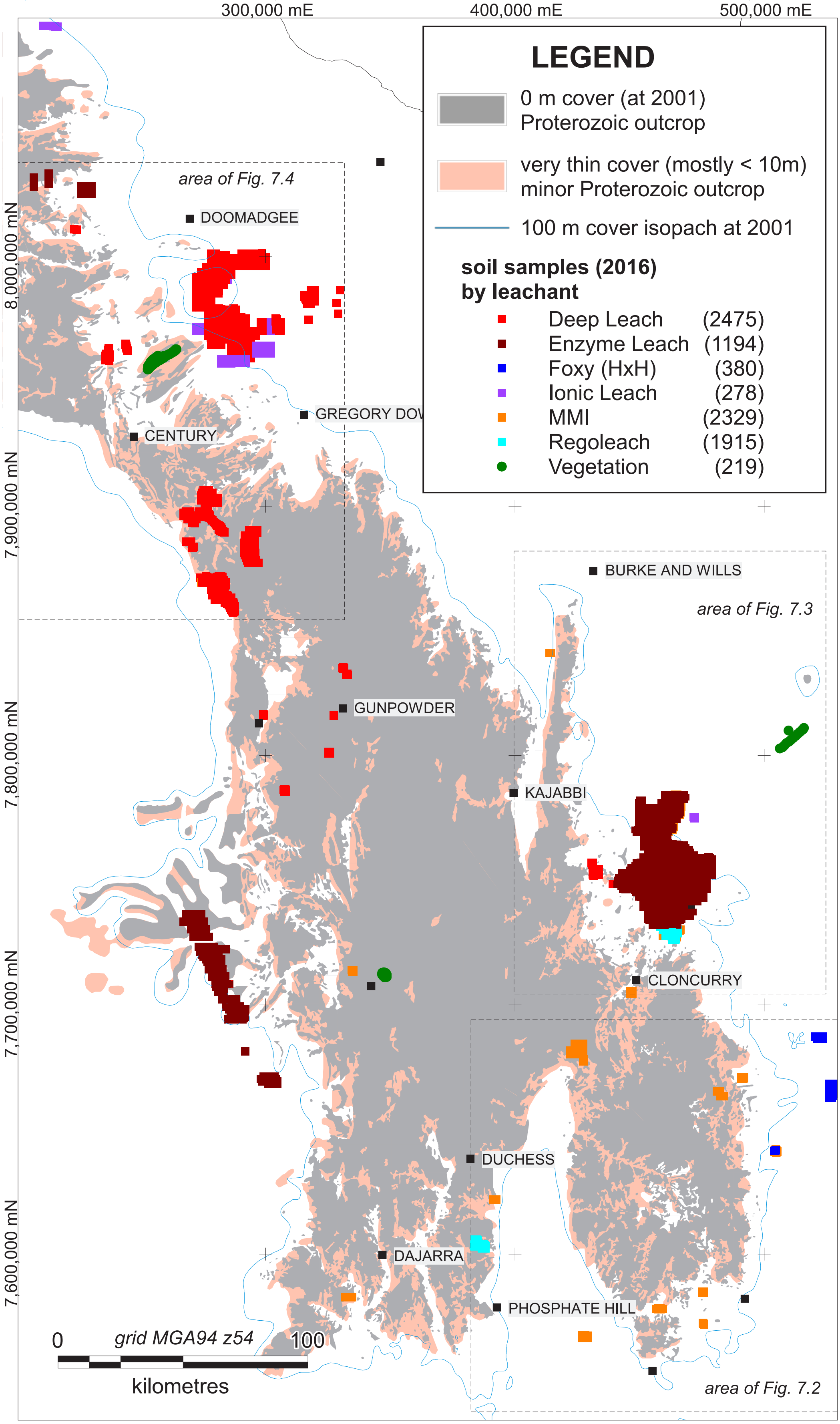

Figure 7.1. Distribution of Mount Isa region soil samples by chemical leachant (selex method) in relation to Proterozoic outcrop, very thin cover and the 100 m cover isopach of 2001.

Peripheral soil surveys—southeast

All soil samples compiled in the 2016 release of the Mount Isa region geochemical data compilation are plotted for the southern Eastern Fold Belt in Figure 7.2 and relevant surveys are summarised in Table 7.1. The map shows that very few selex surveys have been undertaken on the outcrop margins of this highly prospective region. Indeed, dedicated exploration reconnaissance grids have only been undertaken in areas of either:

- excessive cover (>250 m), such as the ‘Foxy’ extraction surveys of BHP at sites 1 and 2, and the Equinox Resources MMI survey, with more than 500 m of Cambrian overburden at site 9) or
- areas where conventional methods, such as aqua regia/ICPMS may have sufficed (*e.g.,* sites 11 and 12).

Elsewhere, orientation surveys at sites of known mineralisation with up to 80 m of recent unconsolidated and Mesozoic cover at Maronan (site 3), Strathfield (site 4, Lilly & Hannan, 2016), Brumby (site 7), and Killer Bore (site 8) prospects all recorded chemical anomalies interpreted as expressions of the buried mineralisation. Other surveys were either ineffective (site 6) or the results are unavailable (*e.g.,* site 4, BHP work).

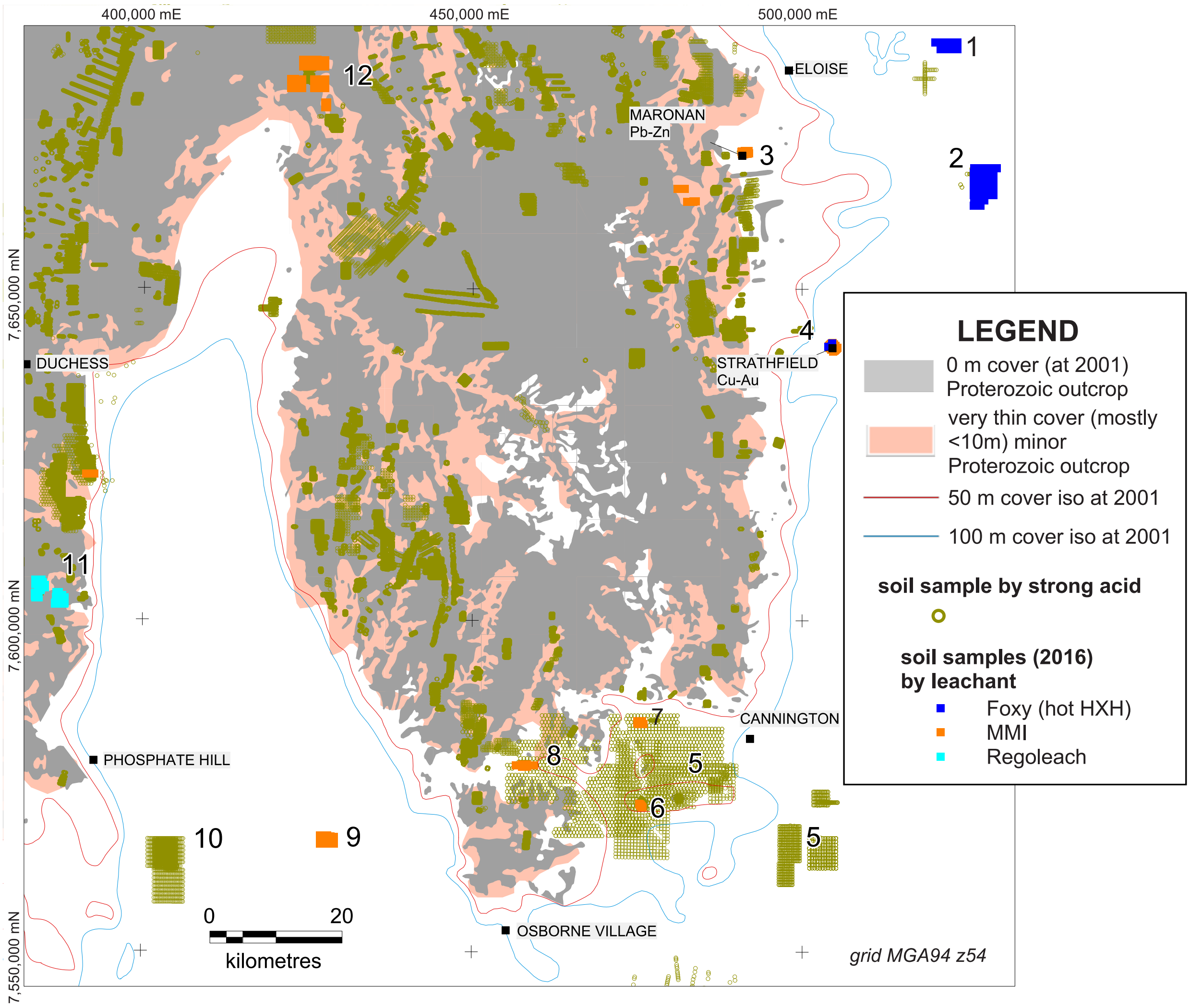

Figure 7.2. Distribution of soil samples in the southeastern Mount Isa Inlier in relation to Proterozoic outcrop, very thin cover and the 50 m and 100 m cover isopachs of 2001. Samples colour coded by digestion type.

Table 7.1: Selex and conventional soil surveys at the periphery of the southeastern Mount Isa Inlier.

Map code	Company	Cover (m)	Grid ID & fraction	Method[1]	CR report	Results ± comment	Support info.[2]
1	BHP	>250	Mayfields -80#	Foxy (hot HXH)	33605	Gravity - Broken Hill type Pb-Zn-Ag target; no anomalies recognised; no discussion.	good
2	BHP	~280	McKinley -60#	Foxy & SA	57237	Orientation over Breena Pb-Zn-Ag prospect; no anomalies reflecting mineralisation; regolith influence noted (consultant's report not in QDEX).	minimal
3	Acacia	40	Maronan -5 mm versus -80# (0.18 mm)	MMI & SA	28251	Orientation over Maronan Pb-Zn-Ag prospect; 1995, early MMI; 2-station Pb-Cu-Zn-Ag response ratio anomaly; some old RC spoil near one site.	adequate
4	BHP	1-10	Strathfield unk	MMI & Foxy	29421	Orientation (?) Strathfield Cu-Au prospect; data in DNRME 2016 geochemical compilation but CR report still confidential	minimal
4	EXCO GSQ	1-10	-5 mm -80#	multiple	NA	Collaborative orientation survey; MMI, Terraleach, Ionic Leach and vegetation; structure-related anomalies (Lilly & Hannan, 2016)	good
5	Glengarry BHP Aberfoyle	>30 <200	several -40# -2 mm -80# -10#	SA, BCL	24313 25522 30370 35653 35655 57670	Large conventional soil surveys in the covered areas of the Cannington-Osborne region; BCL and aqua regia/ICPMS results for areas with only recent cover probably the most effective (no Mesozoic cover).	adequate
6	BHP	<10	Spell Paddock unk, -80#, -120#	MMI BCL SA	29332	Orientation over magnetic Cu-Au intersection at 125 m depth; Zn, Cd, Ni, Au, Ag selex anomalies; short, 1-line survey not definitive.	minimal
7	Aberfoyle	20-70	Brumby -2 mm	MMI	25522	Brumby Cu-Au and Rustler Pb-Zn prospects; 1993 MMI; Pb, Zn, Cd elevated on Brumby mag trend; coincident elevated Ag at Rustler.	adequate
8	BHP	40-60	Killer Bore -2 mm -80#	MMI BCL SA	29398	Orientation over magnetic anomaly (pyrrhotite) and Zn mineralisation at depth of 100 m; 50–70 ppb Ag anomaly (MMI & BCL), also Cd and Co; BCL favoured.	very good
9	Equinox	>500	Mort River -5 mm? -80#	MMI DL SA	28770	Strong magnetic target under Cambrian cover, 300 m-wide multi-metal anomaly on northern line not repeated on follow-up.	adequate
10	Utah	n.a.	Mort River -80#	total	4143	1971 base metal search in Cambrian limestones.	n.a.
11	Cullen	0	Monastery N K-Ridge -2 mm	RL	31587	Regoleach soils for Tick Hill-style Au search in outcrop—chosen for enhanced sensitivity *c.f.* strong acid digestions.	good
12	QMC	0	Duck Creek 2–4 mm	MMI	53832	MMI survey in outcropping Marraba Volcanics; no discussion provided.	minimal

[1] SA=strong acid (either HF-assisted or aqua regia), RL=Regoleach; DL=Deep Leach, EL=Enzyme Leach, Foxy=hot hydroxylamine hydrochloride, MMI=Mobile Metal Ion, BCL=bulk cyanide leach, unk=method not recorded in CR report;

[2] As provided in CR report(s). 🟦 Positive result, known buried mineralisation

The group of large-area conventional soil grids on the inlier margin between the Cannington Pb-Ag and Osborne Cu deposits (site 5, refer Table 7.1) is noted as an example of a recognised area of high prospectivity with less than 100 m of cover that could reasonably be tested by selex soil geochemistry in the absence of comprehensive “first-basement” geochemical grid drilling. Only about 20% of the area is covered by grids of RAB and aircore holes and/or deeper target drillholes (refer to Appendix C for an equivalent map showing drill hole collar and selex survey distributions). The eastern margin of the Eastern Fold Belt between the Cannington deposit and the Eloise Cu deposit has been more intensively grid drilled to Proterozoic basement (also Appendix C) but there is still scope for applying selex geochemistry surveys, particularly for non-magnetic Cu-Au targets (sulfide- or hematite- rather than magnetite-dominant systems).

Chapter 7

Peripheral soil surveys—northeast

All soil samples compiled in the 2016 release of the Mount Isa region geochemical data compilation are plotted for the northern part of the Eastern Fold Belt in Figure 7.3. Most of those by chemical leachant are summarised by survey in Table 7.2. Apart from the enzyme leach surveys of the Mount Fort Constantine JV in the mid-late 1990s by MIM Exploration (sites 1 and 2), and separate MMI and Regoleach campaigns by Equinox Resources (sites 4 and 5, respectively), the outcrop margins of this highly prospective region remain comparatively under-tested. Large areas with less than 100 metres of unconsolidated quaternary/Tertiary and semi-consolidated Mesozoic sediment cover have not been tested by either targeted deep drill holes or 'first basement' drilling grids (refer to the matching map of Appendix C showing drillhole collars).

Table 7.2: Selex and conventional soil surveys at the periphery of the northeastern Mount Isa Inlier

Map code	Company	Cover (m)	Grid ID & fraction	Method[1]	CR report	Results ± comment	Support Info.[2]
1	MIMEX	20–150	ENZ1, 3 & 4NW -60# (0.25 mm)	EL	30357 39318 46125	Pre-ENZ4, local magnetic targets; EL, MMI & BCL all tested at target FC4NW, with buried mineralisation best matching the Ag results. All data available with GTK.	minimal
2	MIMEX	20–150	Mt Fort Constantine -60#	EL	39318 46125	large, 1 km x 1 km grid "ENZ4" (1997); 12 anomalies identified across large EPM (not reported); no discussion; sample spacing too ambitious? All data available with GTK.	minimal
3	Minotaur GSQ	145	-5 mm -80#	3 selex SA vegetation	NA	Collaborative orientation survey; aqua regia, MMI, Terraleach, Ionic Leach and vegetation; coincident anomalies, including a Ag-Zn selex and veg S-Se-Re feature; regolith effects quantified; (Lilly & Hannan, 2016)	very good
4	Equinox	1–10	Fort Constantine S. fraction?	MMI Regoleach	28894 30421	Separate MMI (1996) and Regoleach campaigns (1997); regolith effects quantified; four RL Cu-Ag-Co anomalies, two above subsequently drilled minor Cu-Au mineralisation (depth range 30–150 m).	good
5	Equinox	<50	Bony Creek fraction?	MMI	29549	5 lines of 10 to 20m composites over old Chevron holes; Cu, Co, Ni, Zn response ratio anomalies not followed up (Wik era).	minimal
6	Gryphon	n.a.	Cat Creek	vegetation	52357	Roll-front U search in Tertiary sediments; evidence of U and REE uptake in tree leaves over the U radiometric anomaly.	good
7	CRA Placer	1–10?	Dromedary -40# (0.425 mm)	SA	23447 24464 26721	Conventional soil grids in black soil and thin gravel cover to track structures, elevated Cu-Au results on flanks of some mag anomalies.	adequate

[1] SA=strong acid (either HF-assisted or aqua regia), RL=Regoleach, DL=Deep Leach, EL=Enzyme Leach, MMI = Mobile Metal Ion

[2] As provided in CR report(s); 🟦 positive result, known buried mineralisation; ⬜ positive exploration result

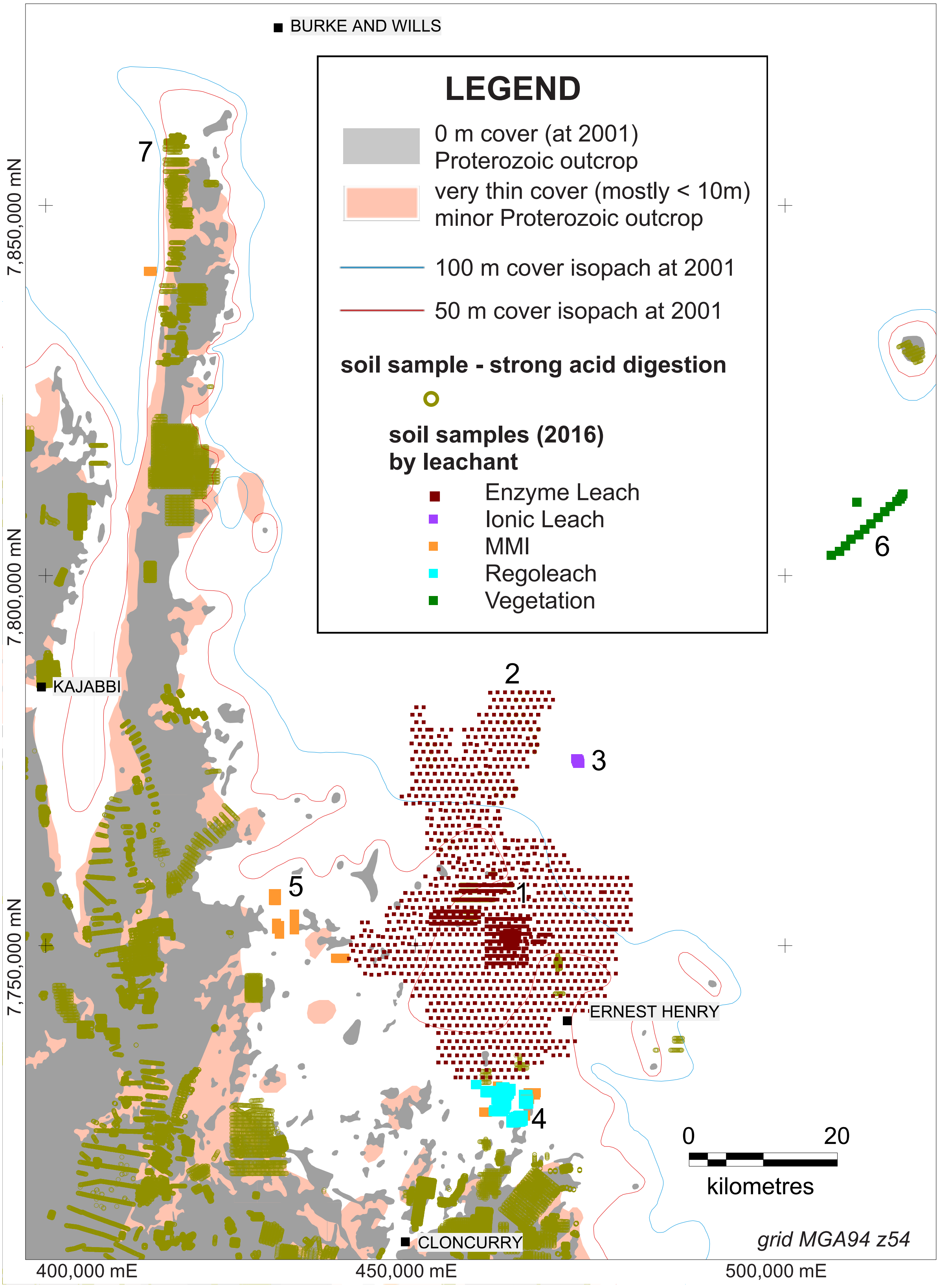

Figure 7.3. Distribution of soil samples in the northeastern Mount Isa Inlier in relation to Proterozoic outcrop, very thin cover and the 50 m and 100 m cover isopachs of 2001. Samples colour coded by digestion type.

The extensive MIMEX Enzyme Leach grid (Figure 7.3, site 2) was undertaken as an ambitious but cost-constrained attempt to achieve uniform geochemical coverage of numerous and varied magnetic features across a large tenement held jointly with Western Mining Corporation. Though several one- to three-station anomalies were identified and some subsequently followed-up, either by drilling or ground-based geophysical surveys, there was a clear understanding at the time that the one-km sample spacing was more appropriate for porphyry-scale systems than for resolving individual IOCG centres of mineralisation. Denser grids within the same tenement (Figure 7.3, site 1) were a direct outcome of the orientation work by MIMEX over the nearby Ernest Henry Cu-Au deposit (see Chapter 4). Particular mention is made of the northern three-line grid which tested Enzyme Leach, BCL and MMI responses over the drilled low-grade and extensive Cu-mineralised FC4NW target, and for which coincident Enzyme Leach, BCL and MMI Ag responses above mineralisation are recorded (Table 7.2). However, neither formal reporting nor reconciliation of the selex geochemical program with contemporaneous and subsequent exploration activity is evident in the open-file report system (QDEX Reports).

In this regard, it is noted that the Enzyme Leach grids depicted in Figure 7.2 are only partially reported under statutory obligation. MIMRD has kindly agreed to permit the release of all sample locations and assays with this publication.

A collaborative “blind” selex and vegetation chemistry orientation survey was recently completed at EXCO’s Cormorant prospect, some 35 km north of Ernest Henry and in an area with 145 m of Mesozoic and recent cover (site 3 of Figure 7.3 and Table 7.2). The results show two distinct features:

- a coincident vegetation Cd-Tl and regolith selex anomaly in multiple elements possibly sourced from pyritic beds within the 100 m of Mesozoic shale cover (Wallumbilla Fmn.)
- an association of elevated to anomalous vegetation S, Se and Re with a narrow selex Zn and Ag anomaly attributed to a potentially mineralised basement structure (Lilly & Hannan, 2016).

A dedicated vegetation survey at site 6, as part of a U search in Carpentaria Basin sediments (Table 7.2) provides another example of the potential of biogeochemical exploration in covered areas. Additionally, the positive results of CRA’s conventional soil grid in the thinly covered northern extremity of the Boomara Horst (site 7) affirms a primary theme of this document—that strong acid digestion, especially by aqua regia, of surface media, and chemical analysis by ICP-MS for pathfinder metals is an effective geochemical exploration tactic in areas of very thin, unconsolidated cover beyond the influence of major fluviatile activity (*i.e.,* erosional slopes and plains).

Peripheral soil surveys—northwest

All soil samples compiled in the 2016 release of the Mount Isa region geochemical data compilation are plotted for the northern Western Fold Belt in Figure 7.4. Most of those by chemical leachant are summarised by survey in Table 7.3; all targeted Mount Isa and/or Century-type base metal mineralisation.

The largest selex surveys were undertaken by Anglo American within tenements surrounding the very deep, extensive but low-grade Bluebush Zn-Pb occurrence (a project operated by Teck Australia). Field observation information and discussion of the Deep Leach results for these large soil surveys are not publicly available (*viz.,* CR reports listed in Table 7.3 for site 3). Later grid extension and infill sampling by Syrah Resources using Ionic Leach, a weak cyanide reagent, did not produce any reported anomalies (site 4).

To the north, MIM Exploration tested Enzyme Leach on two, four km-long lines at the sub-economic Walford Creek Zn deposit. Here, mineralisation in a strongly pyritic host dips southward from the Fish River Fault beneath 5 to 70 m of sandy alluvium (site 1). The eastern line, above the deposit itself, featured strong Zn and weaker Cu selex anomalies extending almost 1000 m from the fault. The equivalent profile for aqua regia Zn was essentially flat. No selex anomalies were evident along the “background” reference line six km to the west, nor within the subsequent exploration grid over the covered Nicholson Fault to the east (site 2, Figure 7.4 and Table 7.3).

The striking selex response at Walford Creek was attributed to groundwater interaction with sulfide mineralisation and hydromorphic dispersion. It was considered a favourable outcome for covered terrain exploration elsewhere in the Gulf of Carpentaria (Hannan, 1996).

MIM Exploration also completed a large Enzyme Leach soil grid much further south and about 60 km west of Mount Isa over the covered and inferred basin-controlling ‘Mongoona Fault’ (site 10 of Table 7.3 and mapped in Figure 7.1). Two Cu anomalies at the intersections of interpreted basement structures were identified for priority follow-up and narrow Fe-Pb and Cl-Mo (As) anomalies on groups of adjacent sample lines appear to trace the inferred position of the Mongoona Fault (Hannan, 1998).

The Deep Leach reagent was favoured at other exploration sites in the north western region by Aberfoyle/Pasminco and Coolgardie Gold (sites 6–9). Aberfoyle consistently applied both Deep Leach and strong acid digestions on grids to differentiate anomalies likely to be sourced in cover from those sourced at depth. An awareness of the potential of alkaline regolith to compromise the efficacy of the weak acid extraction was also evident with Ca levels above 2 wt.% flagged as sites with possible carbonate and compromised results (*e.g.,* Dronseika, 1998).

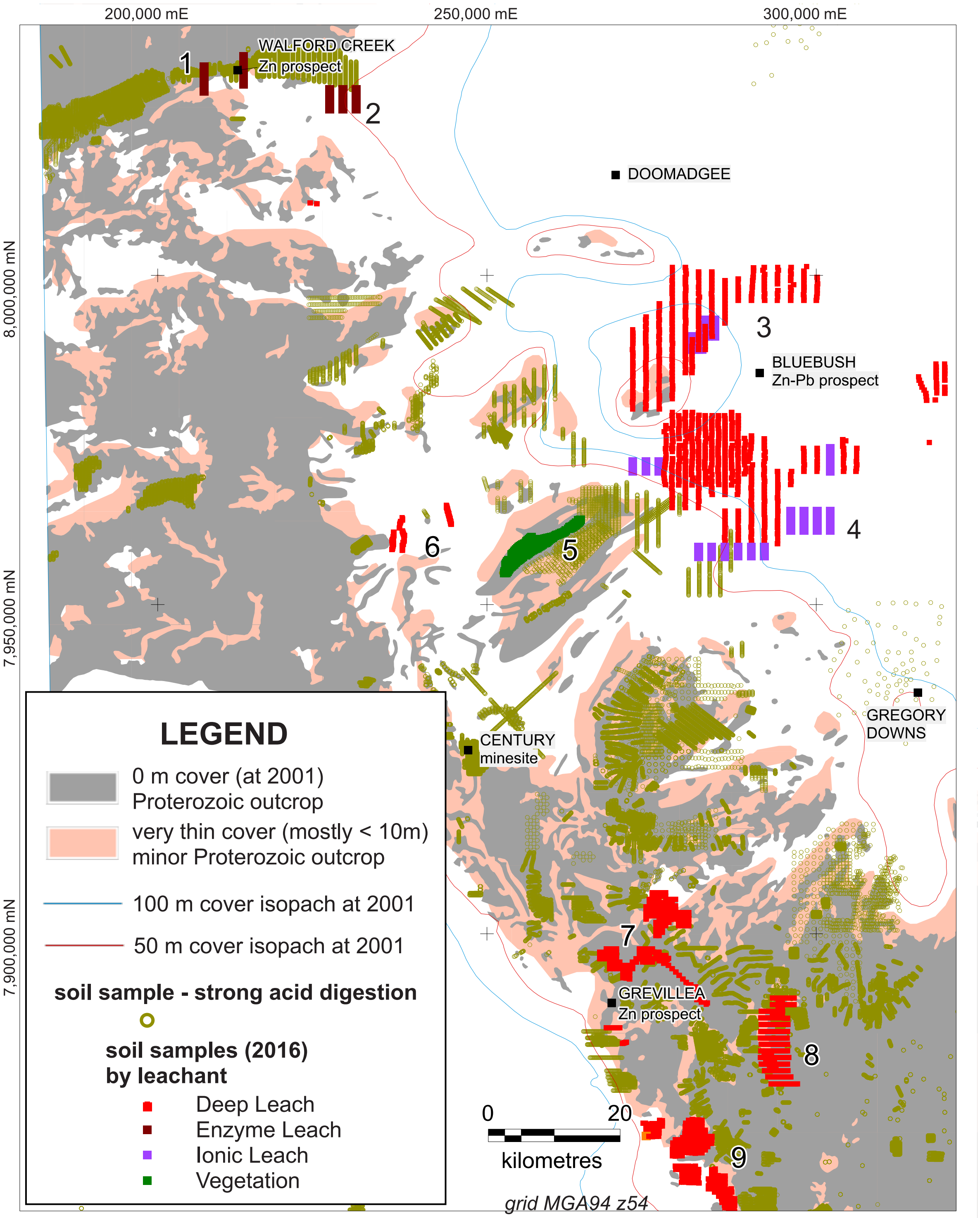

Figure 7.4. Distribution of soil samples in the northwestern Mount Isa Inlier in relation to Proterozoic outcrop, very thin cover and the 50 m and 100 m cover isopachs of 2001. Samples colour coded by digestion type.

Table 7.3: Selex and conventional soil surveys at the periphery of the northwestern Mount Isa Inlier

Map code	Company	Cover (m)	Grid ID & fraction	Method[1]	CR report	Results ± comment	Support info.[2]
1	MIMEX	5–70	Walford Creek -0.25 mm	EL v SA (HF)	n.a.	Orientation over Walford Creek Zn deposit; two 4 km N-S lines, 50 m spacing; EL Zn-Cu anomaly extends hundreds of m south of Fish River Fault—attributed to lateral or vertical hydromorphic dispersion (Appendix D).	adequate
2	MIMEX WMC	~50	Westmoreland -0.25 mm	EL & SA	27569	Nicholson Fault area covered Zn-Pb search; no recorded anomalies.	minimal
3	Anglo American WMC	50–200	Surprise Creek -2 mm	DL	33823 35932 38959	Sedex Zn-Pb-Ag target (*e.g.,* Bluebush); several large area DL soil grids (1-2 km lines x 500 m samples); no discussion.	minimal
4	Syrah	50–150	Surprise Creek -5 mm	Ionic Leach	58025	2008, a few extensions or infill lines of earlier Anglo DL grids; no anomalies identified.	adequate
5	Teck	<5?	McKenzie	Vegetation termitaria	79462	Zn-Pb-Ag search targeting Riversleigh siltstone in Mt. Caroline Anticline; boxwood leaves; no discussion of results.	minimal
6	Pasminco	<20?	Mount Oscar -2 mm	DL & SA	30374	Century-type target; 3 soil lines over alluvial tract; no discussion.	minimal
7	Coolgardie Gold	<5?	Rankin -20# (0.85 mm)	DL & SA	30635	Century type target; Cu & Zn anomalies at inferred structures, some discussion – *e.g.,* the 500 x 500 m grid was too coarse.	good
8	Aberfoyle	<0–20?	Police Creek -20#	DL & SA	29331 29924	Sedex target; fraction uncertain (-20# & -5 mm reported); DL v SA results compared—anomalies attributed to narrow structures.	good
9	Aberfoyle	10–50?	Limestone Gunsmoke -20#	DL & SA	29331	Sedex search; soil DL v SA results compared to rank anomalies, most attributed to minor mineralisation in Cambrian cover.	good
10 Figure 7.1	MIMEX	25–150?	Mongoona -0.25 mm	EL	30683	Mount Isa Cu or Pb-Zn system search along the covered Mongoona Fault; 1–3 km spaced lines x 250–500 m samples; 4 anomalies identified for drilling (Cu, Pb, or Zn); regolith effects accommodated by response ratios.	very good

[1] SA=strong acid (either HF-assisted or aqua regia), RL=Regoleach; DL=Deep Leach, EL=Enzyme Leach

[2] As provided in CR report(s); ■ positive result, known buried mineralisation; □ positive exploration result

Chapter 7

Summary and conclusions

1. Geochemical coverage of the periphery of the Mount Isa Inlier (*i.e.,* areas with up to approximately 150 m of post-Proterozoic cover) is confined to:
    - the environs of significant mines and prospects which were discovered by drilling strong magnetic (+/- gravity) anomalies (*i.e.,* were obvious 'brownfields' targets for deep drilling and/or unconformity geochemistry drill hole grids)
    - large-area soil grids by various chemical leachants in the districts of the Ernest Henry and Century ore deposits
    - small orientation grids over previously established basement mineralisation (*e.g.,* Killer Bore, Maronan)
    - conventional soil grids of the type normally associated with outcrop; most are located on the southern margin of the Eastern Fold Belt where cover thicknesses exceed 5–10 metres and the results are therefore of questionable utility
2. Several significant, but sub-economic, Cu-Au and base-metal prospects with as much as 70 m of cover have weak surface geochemical expressions. Exploration campaigns in areas with up to 150 m of cover have located similar, actionable features (*i.e.,* deemed worthy of follow-up).

    Anomalies are measurable in thin and unconsolidated transported cover (nominally, less than 5–10 m thick) by conventional 'strong' acid chemical digestion (*e.g.,* aqua regia), particularly if critical pathfinder metals are measured at low levels of detection (by ICP-MS) *and* the sampled regolith isn't recently deposited alluvium.

    For areas with thicker cover, where moderately lithified Mesozoic sediment is often present, anomalies have been measured by chemical leachants (or 'selex' methods) and vegetation analysis (biogeochemistry). Examples of gas-in-soil surveys for reconnaissance exploration are not available.
3. From the above, large areas of the covered periphery of the Mount Isa Inlier are appropriate for surface geochemical surveys using methods that resolve weak anomalies associated with buried sulfide mineralisation. Non-magnetic targets in areas with less than 70 m of cover present the greatest opportunity for explorers or projects where base of cover grid drilling geochemistry is not feasible or practicable.

Chapter 8
Groundwater chemistry case study: Ernest Henry mine and district

Introduction

Groundwater is a plausible sampling medium for geochemical exploration because of its reactivity with aquifers and sulfide minerals and, therefore, its potential to transport metal solutes considerable distances from ore bodies. Numerous published case studies demonstrate the potential of hydrochemical analysis to reveal gradients in metals abundances from concealed sulfide sources (e.g., Eppinger *et al.,* 2009, Leybourne & Cameron, 2010) and other rock-water interaction-sensitive properties, such as sulfur and lead isotopes (*e.g*., Caritat *et al.,* 2005).

Presently, groundwater analyses for northwest Queensland and northern Australia are being evaluated by the Geological Survey of Queensland and CSIRO, respectively, in anticipation of resampling programs to support and encourage the search for metalliferous resources in covered extensions of the known mineral provinces. Currently, very few metal data are available, at least publicly, for the large number of water bores in the Mount Isa region (Figure 8.1).

With the knowledge that some of the strongest secondary geochemical dispersions in the overburden of the Ernest Henry Cu-Au deposit are the product of a distinctive weathering history and palaeo-topography (see Chapter 6), MIM Exploration determined to test if groundwater chemistry might provide a more direct and active measure of interaction, especially at distances of more than 1 km from the orebody. Two investigations were carried out, seven years apart:

- the first in 1994, before mining began and restricted to drill holes within 2 km of the deposit
- the second in 2001, after many groundwater chemical analyses had been acquired by Ernest Henry Mining's environment monitoring scientists for:
    a) dedicated monitoring bores within about 10 km
    b) station windmill bores within about 15 km of the deposit.

This chapter presents the results and conclusions of each investigation. In the absence of comparable datasets and reports for other ore deposits in the region, a considerable proportion of this chapter is dedicated to the processing and discussion of the underlying data. The detail, much of it recorded in Hannan & Sheppard (2002), serves as both a record of process (for instruction) and investigation quality and effectiveness.

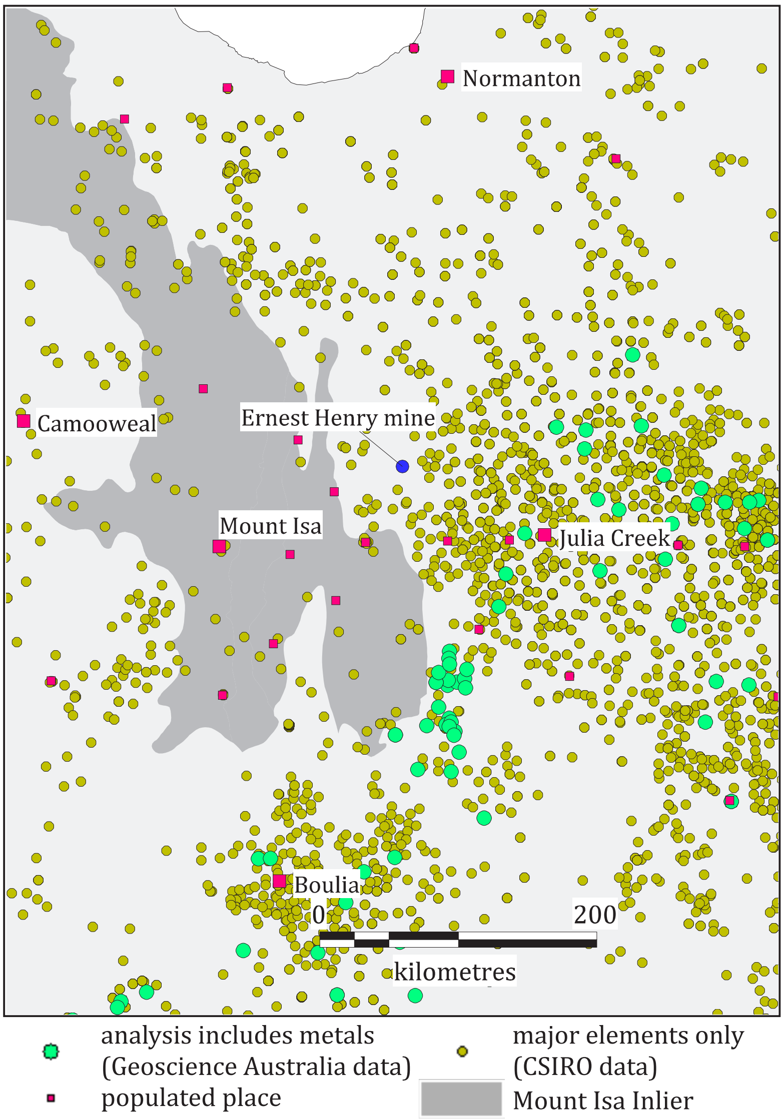

Figure 8.1. Distribution of northwest Queensland water bores with hydrochemical analyses; large green-filled circles indicate those with metal data.

Hydrogeologic setting of Ernest Henry district

Several aquifers were recognised by PPK Environmental and Infrastructure PL in their 1995, pre-mining investigations. A summary of their characteristics follows.

Tertiary aquifer

An ephemeral aquifer occurs at the unconformable base of alluvial Tertiary sediments, where they overly either the Mesozoic Wallumbilla Formation or Proterozoic basement. At the Ernest Henry mine site it is seasonally dry but this aquifer is probably the major source of groundwater accessed by the windmills along the Cloncurry and Corella River systems west of the deposit. Unfortunately, the geologic logs of many windmill bores are of insufficient quality to determine whether the groundwater is sourced from Mesozoic or Tertiary strata.

Mesozoic aquifers

The most extensive aquifer near the mine occurs directly above Proterozoic basement and is principally hosted by Cretaceous sands of the Gilbert River Formation. Draw-down data from the mine dewatering process indicates deep water flow from the south and southeast of Ernest Henry. It is not hydrologically connected to a deeper, artesian aquifer in the Gilbert River Formation east of the Mount Margaret Fault, some 10 km east of the Ernest Henry deposit. Another, separate Mesozoic aquifer is also evident north of Ernest Henry mine which is confined by a palaeo-topographic ridge beneath the northeast-flowing Cloncurry River.

Proterozoic aquifer

The fracture-controlled basement aquifer at the Ernest Henry mine site seems to have limited primary capacity but is hydrologically connected to the overlying Mesozoic aquifer. Groundwater access to the major faults and breccia zones within the orebody has resulted in deep weathering and supergene mineralisation development since at least Cretaceous times. Today, precipitation of carbonates along the fracture zones indicates that they remain open to groundwaters.

Chapter 8

Ernest Henry deposit area investigation (1994, pre-mining)

Specifications

The first investigation, in early 1994, comprised professionally collected samples of water from six resource drill holes, four mine-planning cover thickness drill holes and two water bores, all within 2 km of the deposit (Scott, 1994). Each hole was purged by removing at least 1 drill hole volume of groundwater to ensure fresh recharge prior to sampling. Samples were pumped from 20 m below the standing water level, which varied from 17 to 23 m below the ground surface. On site pH measurements ranged from 7 to 7.8 (neutral to slightly alkaline), and electrical conductivity (EC) and total dissolved solids (TDS) indicate the water was fresh to slightly brackish (405–484 µS/cm and 324–596 mg/L, respectively). The water temperature was about 29°C. According to the report, eight of the samples were filtered in the field; it is implied that the remaining three, from angled holes and described as “black” and “turbid”, were filtered at the lab (unconfirmed). A 250 ml aliquot of each of the field samples was acidified in the field, presumably for cations. A second, 1 L aliquot was presumably collected for analysis of major anions.

Table 8.1: Abundances of selected metals in groundwater near the Ernest Henry Cu-Au deposit.

Element	Units	[1]Reference groundwater	Ernest Henry 1994	Ernest Henry district 2001
Ca	mg/L	50	10–38	<1–466
Cl^-	mg/L	20	23–170	2–2870
K	mg/L	3	1–9	1–202
Mg	mg/L	7	6–15	<1–302
Na	mg/L	30	52–185	14–1360
SO_4^{2-}	mg/L	30	9–81	<1–1280
HCO_3^-	mg/L	200	160–274	52–677
SiO_2	mg/L	16	-	10–66
TDS	mg/L	350	324–596	88–4610
pH		7.4	7.0–7.8	6.7–9.7
Ag	µg/L	0.3	<1	-
As	µg/L	2	<1–61	<1–303
Au	µg/L	0.002	<1	-
Ba	µg/L	20	61–493	-
Bi	µg/L	0.005	-	-
Co	µg/L	0.1	<1–1	<1–90
Cu	µg/L	3	<1–13	<1–1200
Hg	µg/L	0.07	<0.5	<0.1 & <1
Fe	µg/L	100	<100–600	<10–93900
Mn	µg/L	15	6–1030	<10–7540
Mo	µg/L	1.5	<1–57	<1–712
Ni	µg/L	1.5	<1–4	
Pb	µg/L			<1-412
Se	µg/L	0.4	<10	<10
Sn	µg/L	0.1	<1	-
U	µg/L	0.5	<1–5	<0.1-583
W	µg/L	0.03	<1–184	-
Zn	µg/L	6	4–172	<1–6830

[1] generalised medians (drinkable, various sources, *e.g.,* Smith & Huyck, 1999)

Results

A selection of the results is summarised in Table 8.1, where observed elemental ranges are compared with average groundwater compositions and in mapped format illustrated in Figure 8.2. The following patterns and associations are noted:

1. Fe, Ba, and Mn display reasonably coherent concentration gradients centred on the Ernest Henry supergene resource, with elevated (Fe) and anomalous (Ba and Mn) levels (*e.g.*, Figures 2a, b)
2. As, Mo and W levels are strongly anomalous in groundwater sampled directly above the supergene resource and are elevated in the two drill holes to the NNE (*e.g.* Figures. 2c, d)
3. W is also anomalous in the sample from the northern and unmineralised hole, FTCD2023, which was 60 degree-inclined and produced turbid, particulate-laden groundwater, similar to the water present in two holes drilled into the orebody (Figure 2d)
4. groundwater Cu values are unremarkable, with one slightly elevated result of 13 µg/L in the hole into the northern extreme of the supergene resource (EH115, Figure 2e)
5. total S, sulfate and chloride distributions are similar, and abundances are highest, and perhaps anomalous, in the same three drill holes (Figure 2f).

Apparently, water metal concentrations are not controlled by sample distance to the local basement (shown in labels of Figure 2c, following the hole name). For example, the two anomalous ‘orebody’ samples, EH115 and 126, were collected 2–6 m above the Cretaceous unconformity, as were the metal-poor samples from peripheral and distal holes EH160, FTCD66 and PPK. It was also initially suspected that total drill hole length might control water metal concentrations, particularly if recharge of deep holes (after flushing) occurred in response to the hydraulic head rather than influx from the aquifer(s) above the unconformity. However, water from the deep peripheral holes, EH149 and FTCD2023, sampled 5–10 m below the unconformity, has much reduced Fe, As, and Mo levels (refer to end of hole (EOH) labels of Figure 2c).

In the case of the holes that surround the deposit and barely penetrate the basement, it is reasonable to conclude that recharge is dominated by metal-poor groundwater originating from the overlying cover sediments. In this respect, the results for the PPK borehole (Figure 2c) are expected, being located vertically above deep primary ore (300 m) and ‘up-flow’ of the active metal source.

Interestingly, the patterns of anomalous sulfate (Figure 2f) and Ba (Figure 2b) are almost antithetic, consistent with a pre-mining gradient in groundwater Eh, from relatively reducing conditions over the deposit and paleotopographic high, to more oxygenated conditions to the northeast. This is an expected result given the distinctly reduced conditions under which the Ernest Henry supergene Cu resource formed and the presence of shale in the overburden. More broadly, the anomalous ‘suite’ comprises several metals present in the accessory minerals of the ore deposit’s paragenesis (*viz.,* baryte, molybdenite and scheelite) and defines its secondary dispersion plume (Chapter 6).

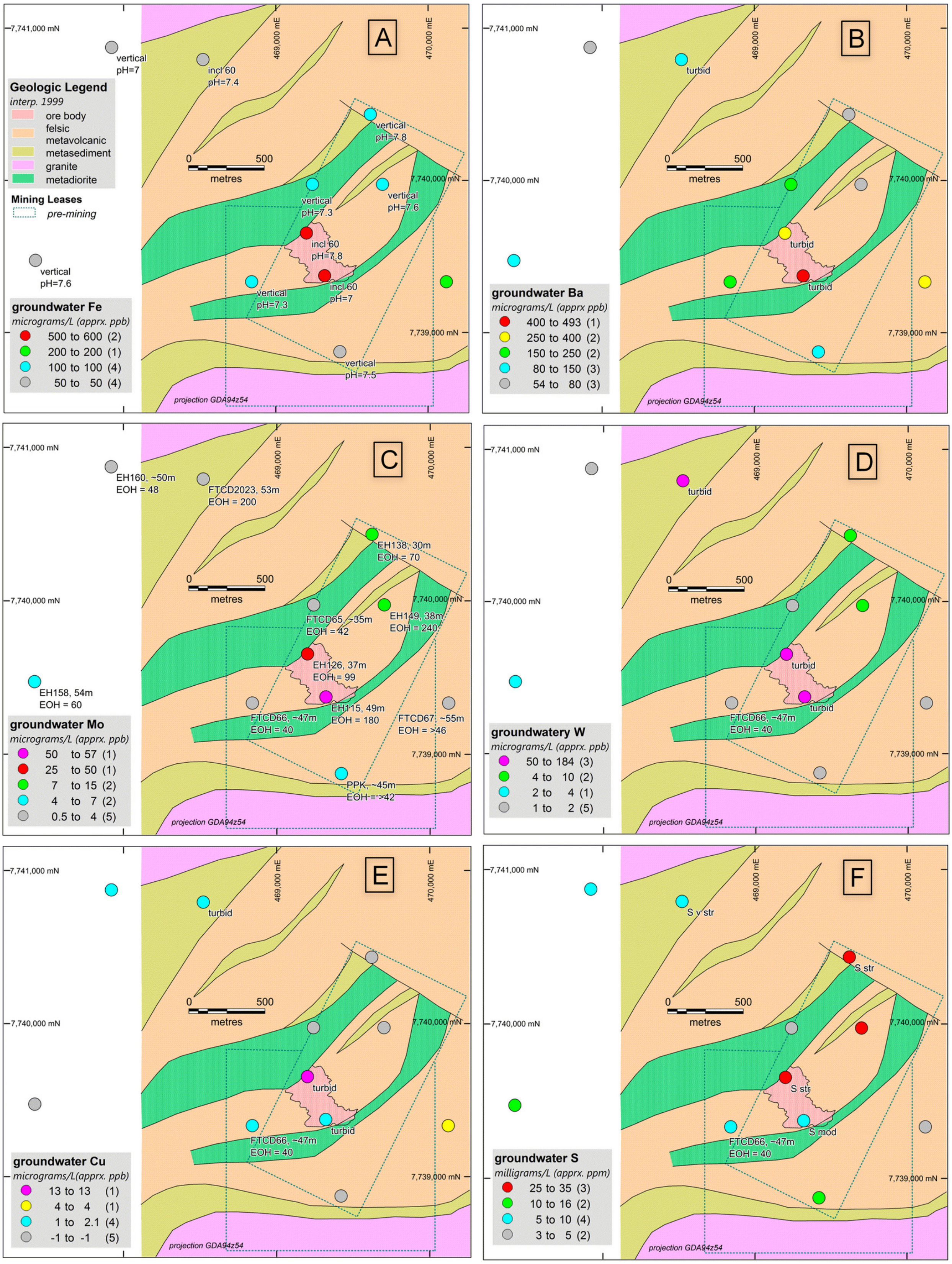

Figure 8.2. Pre-mining abundances of selected metals in groundwater near the Ernest Henry Cu-Au deposit; labels show selected water characteristics (data from Scott, 1994).

Discussion

The groundwater architecture of the extensive Tertiary and Cretaceous cover which onlaps the Eastern Succession is undoubtedly complex. For example, the Cretaceous/Proterozoic unconformity itself is locally a zone of groundwater flow and elevated water pressures were encountered within basement rocks in some sterilisation holes before mining began (Lewis *et al.,* 1994). These deeper waters are the most likely to interact with pre-Mesozoic mineralisation beneath the unconformity, implying that bores which almost reach or penetrate the basement are the most favourable for sampling by mineral explorers.

In summary, the 1994 survey revealed anomalous levels of As, Mo, Ba, Mn, S and W but comparatively low Cu values. The multi-element association is consistent with the groundwater's *measured* neutral to weakly alkaline and *inferred* relatively reduced character, the ore deposit's mineralogy and the geochemistry of its unconsolidated overburden (Chapter 6).

Notwithstanding the limited scope of the survey, and a 'drop-out' on the northern edge of the deposit, it is apparent that groundwater, prior to mining, was chemically anomalous within several hundred metres of the Ernest Henry deposit, except in the up-flow direction, to the south. Elevated levels of S, Mo and W were measured as much as 1000–1200 m down-flow of the deposit to the northeast.

District investigation (2001, during active mining)

Quality and selection of data

By mid-2001, groundwater samples had been collected from 54 station windmill bores, 67 environmental monitoring bores and 11 exploration bores for 506 determinations. Figure 8.3 displays the distribution and type of groundwater bores in relation to RL (to sea level) and approximate total thickness of cover. Although new bores had been regularly added to the program since 1994, only a few were monitored over the entire period.

Water samples collected after 1998 were generally taken from purged and pumped environmental bores. Before then, purging times probably differed and some samples may have been bailed rather than pumped. Samples from active windmills were generally collected by scooping water from the stock watering trough or directly from the outlet pipe.

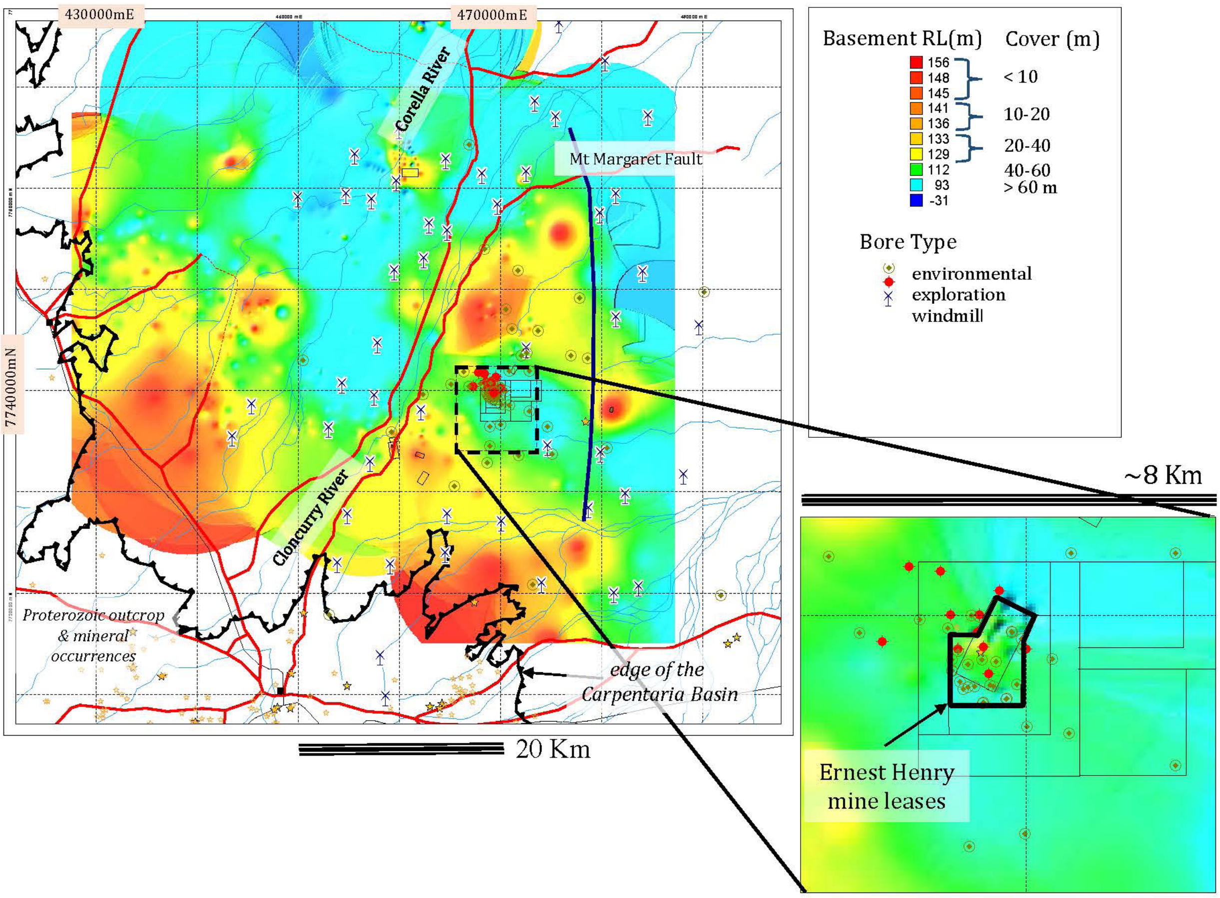

Figure 8.3. Types of water bore within 30 km of the Ernest Henry Cu-Au deposit (from Hannan & Sheppard, 2002).

All samples collected during the monitoring program were filtered before despatch for analysis at the ALS Environmental Laboratory in Brisbane. Significantly, the analytical protocol varied as the program proceeded, as indicated by multiple detection limits for individual trace elements from different batches. The resulting data complexity is to some extent mitigated by the careful recording of sub-detection limit results in the following graphs and maps.

Ternary diagrams for the major cations and anions display tighter groupings for samples from environmental monitoring holes compared to those from windmills. Indeed, the groupings are sufficiently distinct to distinguish a shallow 'Tertiary' aquifer from deeper sources (Figure 8.4); however, to accommodate the variability discussed above only the median value of multiple elemental and water property measurements are utilised for the maps provided herein.

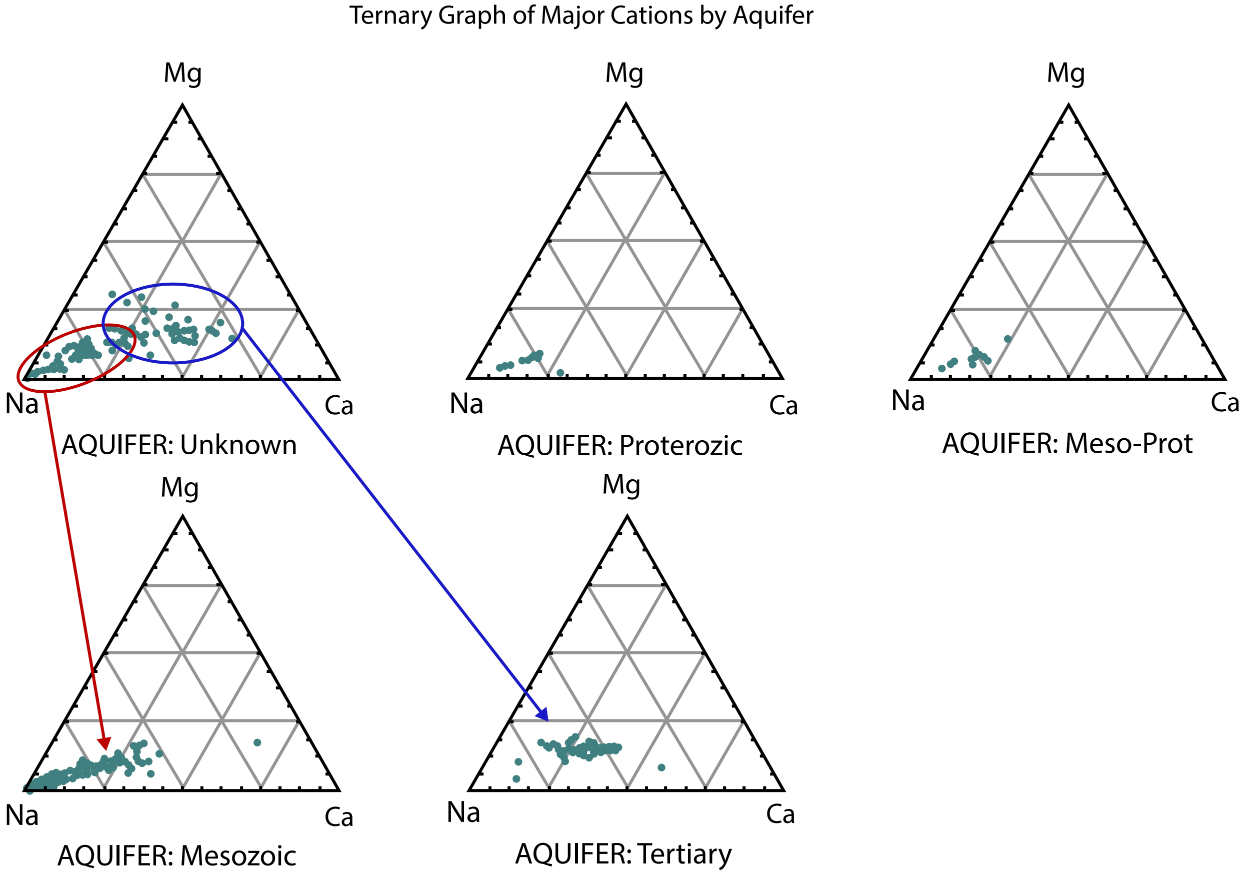

Figure 8.4. Mg-Ca-Na ternary diagrams for various aquifers (after Hannan & Sheppard, 2002).

Close inspection of the dataset reveals discrete batches of results for base metals, such as Cu and Zn, that are anomalously high irrespective of distance from the ore deposit. The outlier batches are excluded from consideration in this document (unlike Hannan & Sheppard, 2002). Significantly, such batch effects are not evident for oxyanion-forming metals such As, Mo and W. Considerable variation is also evident in the metal concentrations measured in multiple samples from the same water bores. Examples of results over time are presented for environmental water bores OB11 and RP03 in Figure 8.5. Bore OB11 was situated above primary ore and just south of the open pit before it was decommissioned in late 1997 and RP03 was located 3 km west of the deposit. Concentrations of major cations (Ca, K and Mg) and anionic species (sulfate and Cl) show evidence of seasonal fluctuation (lower row of graphs, Figure 8.5), whilst those of the base metals are subject to much greater variation (graphs of rows 1 and 2, Figure 8.5). Indeed, the Cu and Zn time profiles of both bores include spikes above 0.05 mg/L (*i.e.*, > 50 ppb), which are anomalous departures from the population medians and far exceed the relevant maxima of the 1994 investigation.

Although natural variation for a single bore could be expected for shallow aquifers due to seasonal rainfall and evaporation trends, the variation in concentrations for specific elements and pH shown in Figure 8.5 are considered to reflect inconsistent sampling practice—particularly given that the base metals are most probably associated with fine particulates and colloids and susceptible to minor variation in the filtering procedure (*e.g.* Puls *et al.,* 1992).

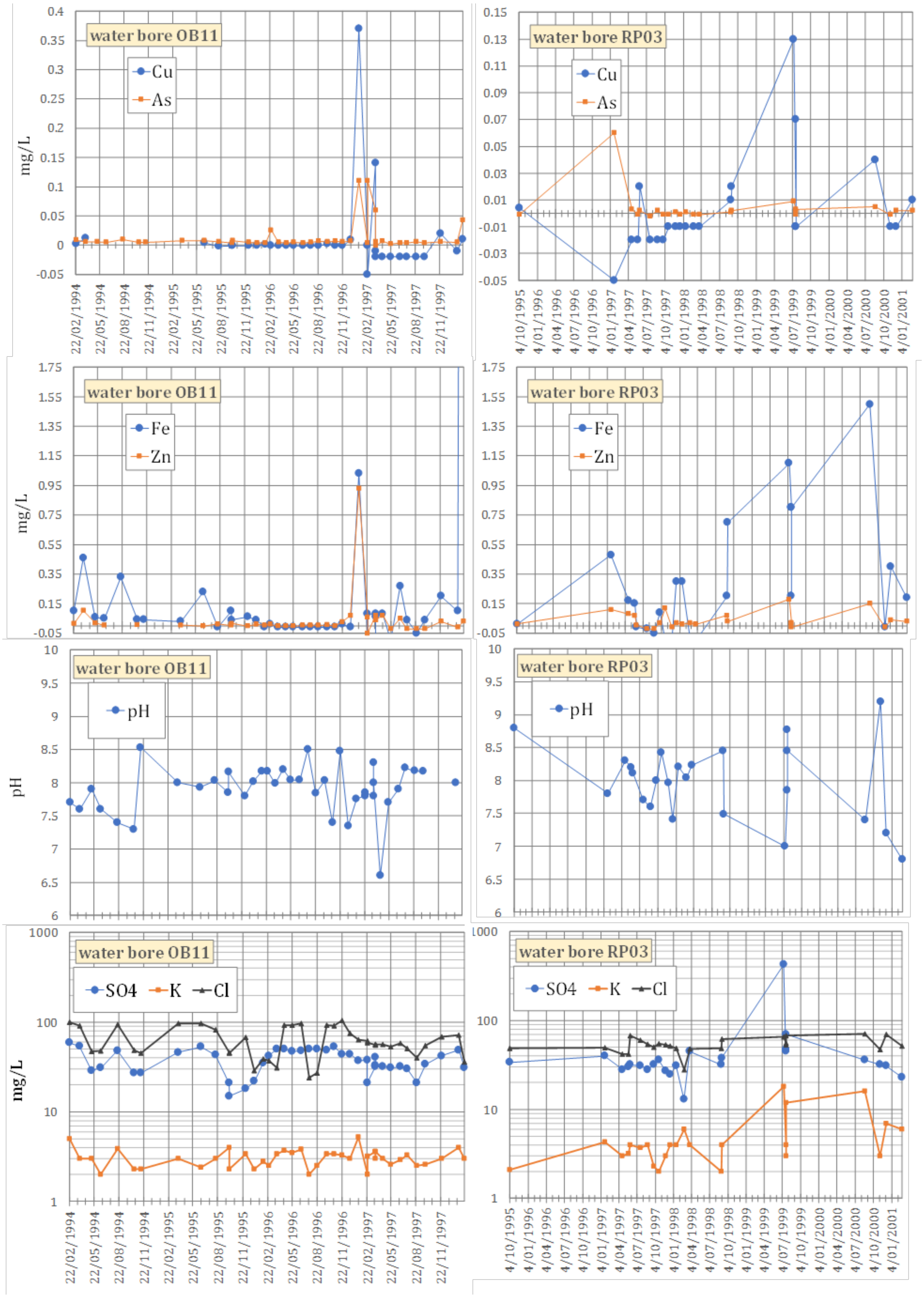

Figure 8.5. Temporal variation in the abundances of selected elements in groundwater from two environmental bores—ore deposit (OB11) and district (RP03) (data from Hannan & Sheppard, 2002).

Notable results

Even after the exclusion of the analytical batch with anomalously high Cu concentrations, it is evident that groundwater samples from near the ore deposit contain metal concentrations elevated relative to most samples from distal environmental and stock bores (Figure 8.6a). However, a gradient is not obvious and the apparent Cu 'bulls-eye' anomaly over the deposit is inconclusive as there are other water bores with concentrations under the detection limit in the same area (inset Figure 8.6a). Changes in analytical procedures over time may explain some of the differences between the metal concentrations found in 1994 and 2001 (Table 8.1).

The spatial distribution of Mo presents a gradient and high concentrations are centred on the mine leases (Figure 8.6b), although Mo concentrations under the detection limits were also recorded in this area (Figure 8.6b).

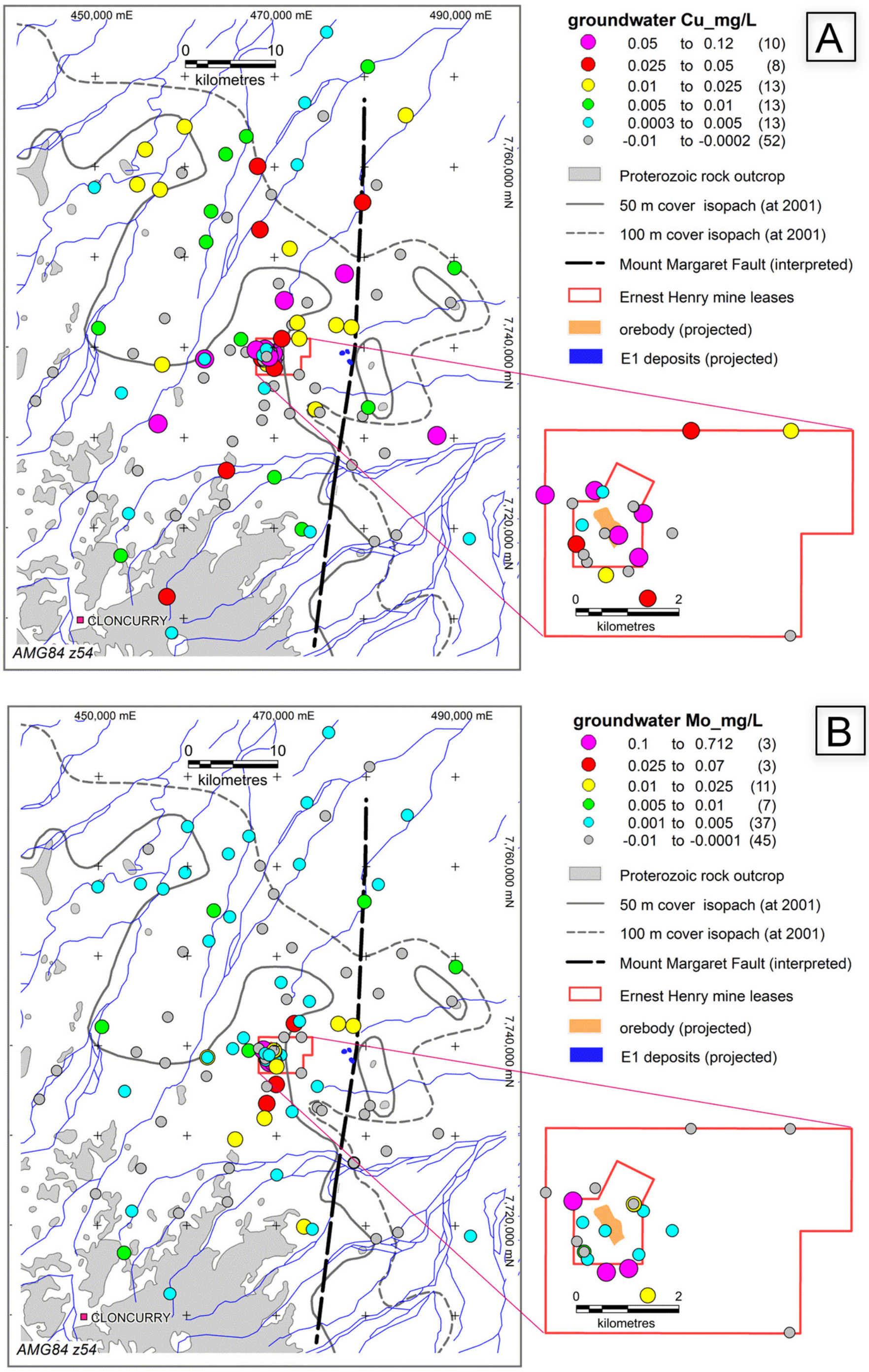

Figure 8.6. Metal abundances in samples of Ernest Henry district groundwater; A–Cu; B–Mo; and thickness of cover isopachs at 2001 (data source—Hannan & Sheppard, 2002).

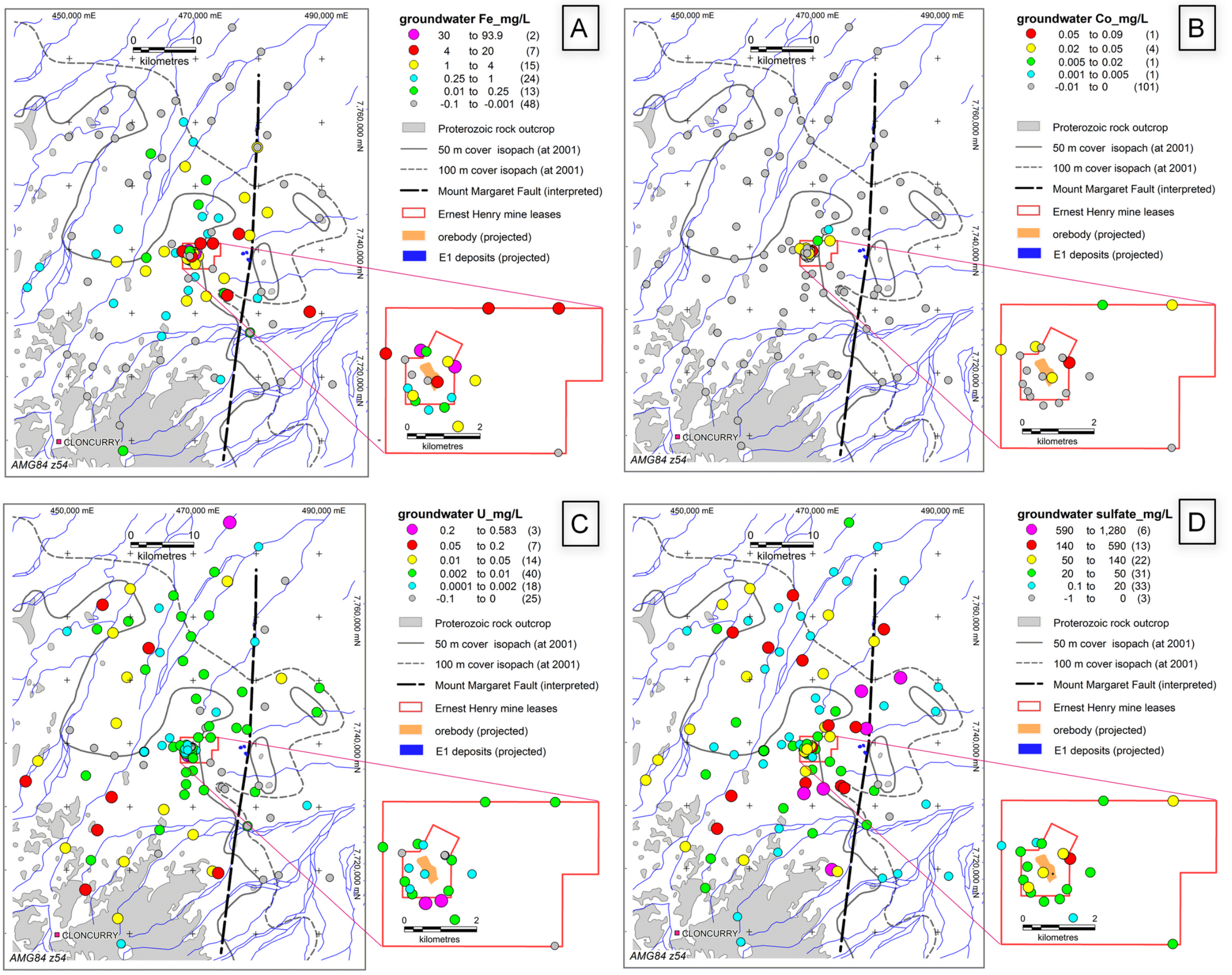

Figure 8.7. Abundances of selected metals and sulfate in samples of Ernest Henry district groundwater (data source Hannan & Sheppard, 2002).

The anomalous Fe and Co results, displayed in Figure 8.7a and 8.7b respectively, and Mn are more convincingly centred on the ore deposit and down-flow to the northeast.

Uranium tends to higher concentrations in areas of thinner total cover (*e.g.* Figure 8.7c); both chloride and sulfate tend to reach anomalous levels in peripheral areas to the south and east of the deposit where cover thickens (*e.g.* Figure 8.7d). Potassium distributions broadly match those of sulfate and chloride.

Discussion

The 2001 investigation confirmed that groundwaters within about 30 km of the Ernest Henry deposit have variable water chemical compositions, most probably related to discrete hydrogeological sub-regions. However, the environmental program data are complicated by inconsistent sampling methods and analytical sensitivities, seasonal variation and the unquantified effects of mine dewatering. For example, several elements highlight the Ernest Henry Mine area, including Fe, Mn, Co, Cu and Mo, but the anomalies are not robust and below detection limit results are frequent at the mine scale (1–2 km). Such variability, especially at individual wells may also be a sign of inconsistent sampling and collection practice over time (*e.g.* Puls *et al.*, 1992). In this regard, it is important that future hydrochemical investigations are consistent and follow rigorous sampling and analytical guidelines (*e.g.* Sandaram *et al.*, 2009, Vail *et al.*, 2013), such as those described in dedicated CSIRO publications (*viz.*, Giblin, 2001, Gray *et al.*, 2011). It is also emphasised that the analysis of an unfiltered sample is necessary to determine the total metal concentration of groundwater, as several metals, such as Fe, Cu, Pb, Zn and Co, and the LREE, are preferentially transported in the suspended colloidal fraction, not as solutes (*e.g.,* Cameron *et al.,* 2004).

It is also evident that neither the anomalies nor the concentrations measured in 2001 match those noted in the pre-mining 1994 investigation, adding to the uncertainty and suggesting some degree of mining impact Although the mixing of the groundwaters from different aquifer sources, such as longer residence time and reducing Mesozoic and younger oxidising Tertiary aquifer waters, and rapidly changing flows as mining progressed, might account for some of the variation, it is concluded that the available data are not reliable to test or model such scenarios.

Critically, however, the highest concentrations of ore-related trace elements tend to be restricted to within 2 km of the mine, so the effects of interaction with mineralisation are apparent despite the complexity and shortcomings of the compiled data.

Conclusions

1. Groundwater compositions vary considerably throughout the Ernest Henry district and within any one of the three main aquifers, reflecting the presence of interactive hydrogeological systems.
2. A pre-mining investigation (1994) showed elevated levels of As, Mo, Ba, Mn, S and W centred approximately on the deposit; dispersion extended up to 2 km to the north and northeast in the 'down-flow' direction.
3. The data of a district scale program of environmental monitoring during mining in the late 1990s (*viz.,* Hannan & Sheppard, 2002) showed that several elements, and to some extent bulk water properties, highlight the Ernest Henry mine area. Water samples contained Cu, Co, Mn, Fe and Mo concentrations which were anomalous up to 3 km 'down-flow', but a spatially coherent pattern was not evident due to analytical drop-outs (results < DL).
4. Collectively, the two programs indicated metal dispersions in groundwater up to 3 km from ore—that is, up to 2 km beyond the 500-ppm geochemical Cu dispersion limit determined at the Mesozoic unconformity in drill holes (Chapter 6).
5. Based solely on the Ernest Henry deposit and district results, the sampling and analysis of groundwater from reconnaissance drill holes is a justifiable activity, with the proviso that low yields of metals and S should not be treated as singular evidence of low basement prospectivity; on the other hand, and assuming verifiably acceptable practices are followed, anomalous concentrations of metals in low salinity and near neutral groundwater may indicate prospectivity.

References

ADSHEAD, N.D., VOULGARIS, P. & MUSCIO, V.N., 1998: Osborne copper-gold deposit. *In*: Berkman, D.A. & Mackenzie D.H. (Editors): *Geology of Australian and Papua New Guinean mineral deposits*. The Australasian Institute of Mining and Metallurgy, Melbourne, 793–800.

ALBAREDE, F. & JUTEAU, M., 1984: Unscrambling the lead model ages. *Geochimica Cosmochimica Acta*, **48**, 207–212.

ANAND, R.R., 2016: Regolith-landform processes and geochemical exploration for base metal deposits in regolith-dominated terrains in the Mt. Isa region, northwest Queensland, Australia. *Ore Deposit Reviews*, **73**, 451–474.

ANAND, R.R., FRASER, S.J., JONES, M.R., LI SHU, MUNDAY, T.J., PHANG, C., ROBERTSON, I.D.M., SCOTT, K.M., VASCONCELOS, P., WILDMAN, J.E. & WILFORD, J., 2002: Geochemical exploration in regolith-dominated terrain, North Queensland. Final Report of AMIRA Project 417. *CRC LEME Open File Report* **120**.

ANAND, R.R. & ROBERTSON, I.D.M., 2012: The role of mineralogy and geochemistry in forming anomalies on interfaces and in areas of deep basin cover: implications for exploration. *Geochemistry: Exploration, Environment, Analysis*, **12**, 45–66.

ANDREW, A.S., HEINRICH, C.A., WILKINS, R.W.T. & PATTERSON, D.J., 1989: Sulfur isotope systematics of copper ore formation at Mount Isa, Australia. *Economic Geology*, **84**, 1614–1626.

ASPANDIAR, M.F., ANAND, R.R. & GRAY, D.G., 2006: Geochemical dispersion mechanisms through transported cover: implications for mineral exploration in Australia. CRC LEME Restricted Report 230. (Reissued as *Open File Report* **246***, CRC LEME, Perth, 2008*).

AUSTRALIAN INSTITUTE OF GEOSCIENTISTS, 2015: www.aig.org.au/librar/seminar-presentations/qld-branch-presentations-events/aig-qld-presentations-pxrf-geochemistry/

BAKER, P.M., BARTSCH, R. & HANCOCK, S., 1995: A proposal for jointly funded geochemical research; Ernest Henry halo study and its exploration relevance. WMC report to MIMEX as part of the - MFC Joint Venture.

BAKER, T., 1994: The geology of the Eloise copper-gold deposit, N.W. Queensland. *Proceedings of the AusIMM Annual Conference, Darwin, August 1994*, 109–204.

BLAKE, D.H., 1982: Review of the Corella Formation. *BMR Journal of Australian Geology & Geophysics*, **7**, 113–118.

BLANCHARD, R., 1968: Interpretation of leached outcrops. *Nevada Bureau of Mines, Bulletin* **66**.

BRESCIANINI, R.F., ASTEN, M.W. & McLEAN, N., 1992: Geophysical characteristics of the Eloise Cu-Au deposit, North-West Queensland. *Exploration Geophysics*, **23**, 33–42.

BROADBENT, G.C., MYERS, R.E. & WRIGHT, J.V., 1998: Geology and origin of shale hosted Zn-Pb-Ag mineralization at the Century deposit, northwest Queensland, Australia. *Economic Geology*, **93**, 1264–1294.

BUTT, C.R.M., SCOTT, K., CORNELIUS, M. & ROBERTSON, I.D.M., 2005: Sample Media. *In*: Butt, C.R.M., Robertson, I.D.M., Scott, K. & Cornelius, M. (Editors): *Regolith Expression of Australian Ore Systems*, CRC LEME, Perth, 53–79.

CAMERON, E.M., HAMILTON, S.M., LEYBOURNE, M.I., HALL, G.E.M. & McClENAGHAN, M.B., 2004: Finding deeply buried deposits using geochemistry. *Geochemistry: Exploration, Environment, Analysis*, **4,** 7–32.

CAMERON, E.M., LEYBOURNE, M.I. & KELLEY, D.L., 2005: Exploring for deposits under deep cover using geochemistry: *Society of Economic Geology Newsletter*, **63**, 5–15.

CANADELL, J., JACKSON, R.B., EHLERINGER, J.R., MOONEY, H.A., SALA, O.E. & SCHULZE, E.D.,1996: Maximum rooting depth of vegetation types at the global scale. *Oecologia*, **108**, 583–595.

CARITAT, P. de, KIRSTE, D., CARR, G. & McCULLOCH, M., 2005: Groundwater in the Broken Hill region, Australia: recognising interaction with bedrock and mineralisation using S, Sr and Pb isotopes. *Applied Geochemistry*, **20**, 767–787.

CARR, G. & DENTON, A, 2002: P618 Meeting 15/07/02 - Cannington case study results. Amira Project P618, Isotopic Discrimination of Partial Leach Geochemical Anomalies in Covered Terrain. Presentation format.

CARR, G.R., 2013: Lead isotope geochemistry: a brave new world? Presentation to Sydney Minerals Exploration Discussion Group (SMEDG), 26 June 2013. CSIRO Exploration and Mining.

CARR, G.R., DENTON, G.J., KORSCH, M.J., GARDNER, B.L., PARR, J.M., ANDREW, A.S., WHITFORD, D.J., WYBORN, L.A.I & SUN S., 2001: User friendly isotope technologies in mineral exploration: Northern Australian Proterozoic Basins. Final Report of AMIRA Project 480. *CSIRO Exploration and Mining Report* **713C**.

CARRANZA, E.J.M., 2009: Geochemical anomaly and mineral prospectivity mapping in GIS. *Handbook of Exploration and Environmental Geochemistry, Volume 11*. Elsevier.

References

CASE, G.N.D., 2016: Genesis of the E1 group of Iron Oxide Copper Gold deposits, Cloncurry district, northwest Queensland. Ph.D. Thesis, College of Science, Technology and Engineering, James Cook University.

CHAPMAN, L.H. & WILLIAMS, P.J., 1998: Evolution of pyroxene-pyroxenoid-garnet alteration at the Cannington Ag-Pb-Zn deposit, Cloncurry district, Queensland, Australia. *Economic Geology*, **93**, 1390–1405.

CLARK, J.R., 1992: Detection of bedrock-related geochemical anomalies at the surface of transported over-burden. *Explore*, **76**, 4–11.

COHEN, D.R., KELLEY, D.L., ANAND, R. & COKER, W.B, 2007: Major Advances in Exploration Geochemistry, 1998-2007. *In*: Milkereit, B. (Editor): *Proceedings of Exploration 07, Fifth Decennial International Conference on Mineral Exploration*, 3–18.

COHEN, D.R., SILVA-SANTISTEBAN C.M., RUTHERFORD, N.F., GARNETT, D.L., & WALDRON, H.M., 1999: Comparison of vegetation and stream sediment geochemical patterns in northeastern New South Wales. *Journal of Geochemical Exploration*, **66**(3), 469–489.

DAVIDSON, G.J. & DIXON, G.H., 1992: Two sulphur isotope provinces deduced from ores in the Mount Isa Eastern Succession, Australia. *Mineralium Deposita*, **27**, 30–41.

DOE, B.R. & STACEY, J.S., 1974: The application of lead isotopes to the problems of ore genesis and ore prospect evaluation: a review. *Economic Geology*, **69**, 757–776.

DRONSEIKA, E., 1998: Assessment of regional partial and total digest soil geochemistry survey carried out by Terra Search PL for Coolgardie Gold in May 1998. In: Beams, S.D. & Henry, R.L.: EPM 11287, Rankin, NW QLD, Annual report for the twelve monthly period ending August 14, 1998, Appendices 1.1 and 1.5. Report held by the Geological Survey of Queensland QDEX Reports System as CR30635.

DUNN, C.E., 2007: *Biogeochemistry in Mineral Exploration. Handbook of Exploration and Environmental Geochemistry, Volume 9*. Elsevier.

EPPINGER, R.G., FEY, D.L, KELLEY, K.D., SMITH, S.M. & GILES, S.A., 2009: An exploration hydrogeochemical study at the giant Pebble porphyry Cu-Au-Mo deposit, Alaska, USA, using high resolution ICP-MS. *Geochemistry: Exploration Environment Analysis*, **12**, 211–226.

ETIOPE, G. & MARTINELLI, G., 2002: Migration of carrier and trace gases in the geosphere: an overview. *Physics of the Earth and Planetary Interiors*, **129**, 185–204.

FOSTER, D. & AUSTIN, J., 2008: The 1800–1610Ma stratigraphic and magmatic history of the Eastern Succession, Mount Isa Inlier, and correlations with adjacent Paleoproterozoic terranes. *Precambrian Research*, **163**(1–2), 7–30.

FUSS, M., 2014: Isotopic (^{87}Sr/^{86}Sr, δ^{13}C and δ^{18}O) indicators of fluid source from carbonates in the Ernest Henry deposit, Queensland, Australia: implications for genesis and exploration. B. Geology Honours thesis, James Cook University, Townsville.

GARSED, I.R., HANNAN, K.W. & FAULKNER, I.L., 1998: EPM 11226 “Mongoona”. Annual report to the Queensland Department of Mines and Energy for the period ending 27th August 1998. Report held by the Geological Survey of Queensland QDEX Reports System as CR30683.

GAZLEY, M.F., BONNETT, L.C., FISHER, L.A., SALAMA, W. & PRICE, J.H., 2017: A workflow for exploration sampling in regolith dominated terranes using portable X-ray fluorescence: comparison with laboratory data and a case study. *Australian Journal of Earth Sciences*, **64**, 903–917.

GAZLEY, M.F. & FISHER, L.A., 2014: A Review of the Reliability and Validity of Portable X-ray Fluorescence Spectrometry (pXRF) Data. *Mineral Reserve and Ore Estimation – The AusIMM Guide to Good Practice*. AusIMM, Melbourne, 69–82.

GIBLIN, A.M., 2001: *Groundwaters: Geochemical pathfinders to concealed ore deposits.* CSIRO Exploration and Mining.

GORE & ASSOCIATES INC., 2006: GORE™ surveys for mineral exploration. A commercial brochure from the W.L. GORE and Associates website.

GRAY, D., NOBLE, R. & GILL, A., 2011: *Field guide for mineral exploration using hydrochemical analysis*. CSIRO Earth Science and Resource Engineering.

GULSON, B.L. & MIZON, K.J., 1979. Lead isotopes as a tool for gossan assessment in base metal exploration. *Journal of Geochemical Exploration*, **11**, 299–320.

HALL, G.E.M. & BONHAM-CARTER, G.F. (Editors) 1998: Selective extractions. *Special Issue of Journal of Geochemical Exploration*, **61**(1–3).

HANNAN, K.W., 1991: Discussion of oxygen isotope data from DDH V334. MIM Exploration Technical Memorandum 1991/005, unpublished (addendum to Technical Report 1593, Halo Project - DDH V334: Distribution of visible sulphides and carbonate, vein orientations and carbonate chemistry).

HANNAN, K.W., 1992a: A discussion of isotope data from the NW Lakes area. MIM Exploration Technical Memorandum 1992/016.

HANNAN, K.W., 1992b: A discussion of mineralisation at Bloodwood Bore. MIM Exploration Technical Memorandum 1992/012.

HANNAN, K.W., 1992c. Reconnaissance S Isotope Data for Corella Formation and Isa Valley South. Informal record of MIM Exploration.

HANNAN, K.W., 1993: Summary of Buckley River Stable Isotope Results. MIM Exploration Technical Memorandum 1993/001.

HANNAN, K.W., 1994a. Summary of partial extraction geochemistry trials at Ernest Henry. MIM Exploration Technical Report 2283.

HANNAN, K.W., 1994b. Ernest Henry groundwater chemistry survey. MIM Exploration PL Technical Memorandum 1994/016.

HANNAN, K.W., 1995. Hydromorphic chemical dispersions above the Ernest Henry Cu-Au Deposit. MIM Exploration Technical Memorandum, 1995/027.

HANNAN, K.W., 1996. Enzyme Leach trial over the Walford Creek Pb-Zn prospect. MIM Exploration Technical Memorandum 1996/020.

HANNAN, K.W., 1997. Plots of drill hole groundwater assays: Ernest Henry area. MIM Exploration PL Technical Memorandum 1997/005.

HANNAN, K.W., 1998. Enzyme Leach Survey ENZ6, EPM 11226 - Mongoona Project. MIM Exploration Technical Report 2867.

HANNAN, K.W., 2003: Discrimination of gossans and ironstones from the Mount Isa Inlier. Unpublished confidential report to Xstrata Copper PL by Geochem Pacific PL.

HANNAN, K.W., 2004. An assessment of the use of Pb isotope analysis for minerals exploration in the Mount Isa region. Draft report to Xstrata Copper PL by Geochem Pacific PL.

HANNAN, K.W., GOLDING, S.D, HERBERT, H.K. & KROUSE, H.R., 1993: Contrasting alteration assemblages in metabasites from Mount Isa, Queensland: implications for copper ore genesis. *Economic Geology*, **88**, 1135–1175.

HANNAN, K.W., HUTTON, D.J. & PERKINS, W.G., 1991: Halo Project - generalised and idealised long and cross sections of Mount Isa mine. MIM Exploration Technical Memorandum 1991/008.

HANNAN, K.W. & SHEPPARD, M., 2002: Study of the chemistry of groundwaters in the vicinity of the Ernest Henry Cu-Au deposit. MIM Exploration PL Technical Report 3109.

HEINRICH, C., ANDREW, A.S., WILKINS, R.W.T. & PATTERSON, D.J., 1989: A fluid inclusion and stable isotope study of the synmetamorphic copper ore formation at Mount Isa, Australia. *Economic Geology*, **84**, 529–550.

HILL, S.M., 2004: Biogeochemical sampling media for regional- to prospect-scale mineral exploration in regolith dominated terrains of the Curnamona Province and adjacent areas in western NSW and eastern SA. *In*: Roach I.C. (Editor): *2004, Regolith 2004*. CRC LEME, 128–133.

JEFFREY, S., 2002: The Cannington Ag-Pb-Zn BHT deposit: a world class discovery with a silver lining. Presentation to 16th AGC, July 2002. Internet pdf.

JONES, D.A., 1986: The Kamarga deposit: stratabound zinc-lead mineralisation in the middle Proterozoic McNamara Group, northwest Queensland. Ph.D. thesis, University of New England, Armidale.

KLUSMAN, R.W., 2009: Transport of ultratrace reduced gases and particulate, near-surface oxidation, metal deposition and adsorption. *Geochemistry, Exploration, Environmental analysis*, **9**, 203–213.

LAWRANCE, L.M., 1999: Multi-element dispersion in Mesozoic basin sediment over the Osborne deposit, northern Queensland, Australia: Implications for regional geochemical exploration in buried terrain. *Australian Institute of Geoscientists, Bulletin*, **28**, 73–81.

LEWIS, D., JENNINGS, K., HANNAN, K., BARBER, A., MAWER, C. & ROWSTON, P., 1994: Ernest Henry supergene project. MIM Exploration Technical Report 2228.

LEYBOURNE, M.I. & CAMERON, E.M., 2010: Groundwater in geochemical exploration. *Geochemistry: Exploration, Environment, Analysis*, **10**, 99–118.

LI SHU & ROBERTSON, I.D.M., 2002: Surficial geology around the Eloise Cu-Au Mine and dispersion into Mesozoic cover from the Eloise mineralisation, N.W. Queensland. In: CRC LEME Open File Report 135. CRC LEME-AMIRA Project P417 1994-1997.

LILLY, R., GASE, G. & MILLER, B., 2017. Ernest Henry iron oxide Cu-Au deposit. *In*: Phillips, N. (Editor): *Australian Ore Deposits, AusIMM Monograph No*. **32**, 501–506.

References

LILLY, R.M. & HANNAN, K.W., 2016: *Geochemistry through cover: Defining geochemical exploration parameters for the Cloncurry Mineral District, Queensland*. Queensland Department of Natural Resources and Mines.

LILLY, R.M., HANNAN, K.W. & A-IZZEDDIN, D., 2010: Geochemistry though cover (GTC) project. Xstrata Copper PL Technical Report 3761.

LORD, R., 2002: Eloise, Queensland, Australia, 2. In: Geochemical dispersions of selected Australian and African stratabound, Fe-oxide, and structurally controlled Cu deposits. MIM Exploration PL. Unpublished, property of Glencore, Mount Isa.

LUCAS, L.M., OLIVER, N.H.S. & DAVIDSON, G.J., 2006: Carbon and oxygen isotope constraints on fluid sources and fluid-wallrock interaction in regional alteration and iron-oxide–copper–gold mineralisation, eastern Mt Isa Block, Australia. *Mineralium Deposita*, **41**, 429–452.

MANN, A.W., BIRRELL, R.D., FEDIKOW, M.A.F. & de SOUZA, H.A.F., 2005: Vertical ionic migration: mechanisms, soil anomalies, and sampling depth for mineral exploration. *Geochemistry: Exploration, Environment, Analysis*, **5**, 201–210.

MANN A.W., MANN A.T., HUMPHREYS, D.B., DOWLING, S.E., STALTARI & MYERS, L., 1997: Soil geochemical anomalies - their dynamic nature and interpretation. *Minerals and Energy Research Institute of Western Australia (MERIWA), Report* **184**.

MARJORIBANKS, R., 2010: *Geological Methods in Mineral Exploration and Mining, 2nd Edition*. Springer-Verlag, 165–177.

MARK, G., FOSTER, D.R.W., POLLARD, P.J., WILLIAM, P.J., TOLAN, J., DARVALL, M. & BLAKE, K.L., 2004: Stable isotope evidence for magmatic fluid input during large-scale Na-Ca alteration in the Cloncurry Fe oxide Cu-Au district, NW Queensland, Australia. *Terra Nova*, **15**, 54–61.

MARK, G., OLIVER, N.H.S. & WILLIAMS, P.J., 2006: Mineralogical and chemical evolution of the Ernest Henry Fe oxide-Cu-Au ore system, Cloncurry district, northwest Queensland, Australia. *Mineralium Deposita*, **40**, 769–801.

NEUERBURG, G.J., 1984: Sampling Chaotic Variation, an Essay into Scientific Methodology for Geochemical Prospecting. *In*: Wauschkuhn, A., Kluth, C. & Zimmermann, R.A. (Editors): *Syngenesis and Epigenesis in the Formation of Mineral Deposits*. Springer, Berlin, Heidelberg, 138–149.

OAKES, B.W. & HALE, M., 1987: Dispersion patterns of carbonyl sulphide above mineral deposits. *Journal of Geochemical Exploration*, **28**, 235–249.

OLIVER, N.H.S., CARTWRIGHT, I., WALL, V.J. & GOLDING, S.D., 1993: The stable isotope signature of kilometre-scale fracture-dominated metamorphic fluid pathways, Mary Kathleen, Australia. *Journal of Metamorphic Geology*, **11**, 705–720.

OLIVER, N.H.S. & WALL, V.J., 1987: Metamorphic plumbing system in Proterozoic calc-silicates, Queensland, Australia. *Geology*, **15**, 793–796.

PAINTER, M.G.M., GOLDING, S.D., HANNAN, K.W. & NEUDERT, M.K., 1999: Sedimentologic, petrographic, and sulfur isotope constraints on fine-grained pyrite formation at Mount Isa Mine and environs, Northwest Queensland, Australia. *Economic Geology*, **94**, 883–912.

PERKINS, W.G. & DENARO, T.J., 2011: Structurally-controlled epigenetic Cu ± Au mineralising system – Western Fold Belt Province. Proterozoic Mount Isa Synthesis. In: Geological Survey of Queensland, 2011: *North-West Queensland Mineral and Energy Province Report*. Queensland Department of Employment, Economic Development and Innovation, Brisbane, Appendix 5d.

PHANG, C., 2005: Tringadee zinc anomaly, NW Queensland. *In*: Butt, C.R.M., Robertson, I.D.M., Scott, K. & Cornelius, M. (Editors): *Regolith expression of Australian ore systems*. CRC LEME, Perth, 197–198.

PPK, 1995: Ernest Henry project draft impact assessment study: available through EHM. PPK Environmental and Infrastructure PL.

PULS, R.W., CLARK, D.A., BERT, B., POWELL, R.M. & PAUL, C.J., 1992: Metals in groundwater: sampling artifacts and reproducibility. *Hazardous Waste and Hazardous Materials*, **9**, 149–161.

READFORD, M. & CURYPKO, T., 2017: Cannington mineral resources and ore reserves update. South 32 Ltd., announcement to Australian Stock Exchange 24/7/17.

ROSE, A.W., HAWKES, H.E. & WEBB, J.S., 1979: *Geochemistry in Mineral Exploration, 2nd Edition*. Academic Press.

RUBENACH, M., ADSHEAD, N., OLIVER, N., TULLEMANS, F. & STEIN, H., 2001: The Osborne deposit: Geochronology, and genesis of mineralisation in relation to host albitites and ironstones. *In*: Williams, P.J. (Editor): A hydrothermal Odyssey. *Extended Conference Abstracts, James Cook University (EGRU)*, 172–173.

RUTHERFORD, N.F., 2002: The regolith, background, anomalies and partial leaches. *ALS–Chemex News 2001*, Issue 1.

RUTHERFORD, N.F., 2009: Partial leaches, sulphur isotopes and regolith controls: a case study from the Osborne Cu□ Au mine far north Queensland. AIG SMEDG Symposium, New Exploration Technologies, Sept. 2009; presentation format.

RUTHERFORD, N.F., 2018: Observing and interpreting geochemical dispersion. AEGC workshop, University of New South Wales: Vectoring to mineralisation. Australian Exploration Geoscience Conference, February 2018. Presentation format.

RUTHERFORD, N.F. & BERKMAN, D., 1999: Finding blind ore bodies with Regoleach. *ALS Mineral Division News*, **8**(4).

RUTHERFORD, N.F., LAWRENCE, L.M. & SPARKS, G., 2005: Osborne Cu-Au deposit, Cloncurry District, NW Queensland. *In*: Butt, C.R.M., Robertson, I.D.M., Scott, K. & Cornelius, M. (Editors): *Regolith expression of Australian ore systems*, 380–382.

RYE, D. & WILLIAMS, N., 1981: Studies of the base metal sulfide deposits at McArthur River, Northern Territory, Australia. III. The stable isotope geochemistry of the H.Y.C. Ridge and Cooley deposits. *Economic Geology*, 76, 826–842.

RYSS, Y.S., VOROSHILOV, N. & SEIGEL, H.O., 1992: Geoelectrochemical Test Programme in Australia, on behalf of The Australian Mineral Industries Research Association Limited, Project P355A.

SCOTT, K., ASHLEY, P. & LAWIE, D., 2002: Gossan maturity and geochemical exploration in the Eastern Lachlan Fold Belt. *Exploration Mining Research News*, **14**, 3–6. CSIRO Division of Exploration and Mining, Wembley, W.A.

SCOTT, K.M., SMITH, J.W., SUN, S.S. & TAYLOR, G.F., 1985: Proterozoic copper deposits in NW Queensland, Australia. *Mineralium Deposita*, **20**, 116–126.

SCOTT, P., 1994: Ernest Henry groundwater geochemistry study. For MIM Exploration by AGC Woodward-Clyde PL. Project 4612.

SEAL II, R.R., 2006: Sulfur Isotope Geochemistry of Sulfide Minerals. *Reviews in Mineralogy & Geochemistry*, **61**, 633–677.

SHEPPARD, M., 2001: Ernest Henry Cover Project, Final report. MIM Exploration, Miscellaneous Report 2001/020.

SHEPPARD, M. & HANNAN, K.W., 2001: Significant findings of the Ernest Henry Cover Project – preliminary to the final report. MIM Exploration, Technical Memorandum 2001/005.

SKRZECZYNSKI, R.H., 1993: From concept to Cannington: a decade of exploration in the Eastern Succession. Symposium on recent advances in the Mount Isa Block. *Australian Institute of Geoscientists Bulletin*, **13**, 35–38.

SMITH, K.S. HUYCK, H.O.L., 1999: An overview of the abundance, relative mobility, bioavailability, and human toxicity of metals. *In*: Plumlee, G.S. & Logsdon, M.J. (Editors): The Environmental Chemistry of Mineral Deposits. *Reviews in Economic Geology*, **6A**, 29–70.

SUNDARAM, B., FEITZ, A., CARITAT, P. de, PLAZINSKA, A., BRODIE, R., CORAM, J. & RANSLEY, T., 2009: Groundwater Sampling and Analysis – A Field Guide. *Geoscience Australia, Record* **2009/27**.

SUTHERLAND, D., 2011: Soil Gas Hydrocarbons: An Organic Geochemistry that Detects Hydrocarbon Signatures in Surficial Samples to Locate .and Identify Deeply Buried Targets. Search and Discovery Article #40684, Activation Laboratories Ltd. Presentation format.

SUTHERLAND, D. & HOFFMAN, E., 2009: Evaluation of SGH soil sample data, Golden Hope Mines VMS/Base Metal Project. Supplemental Report of work order A09-4379. Activation Laboratories Ltd, Ontario.

TAYLOR, G.F. & SCOTT, K.M., 1982: Evaluation of gossans in relation to lead-zinc mineralisation in the Mount Isa Inlier, Queensland. *BMR Journal of Australian Geology and Geophysics*, **7**, 159–180.

TAYLOR, G.F. & THORNBER, M.R., 1992: Gossan and Ironstone Surveys. *In*: Butt, C.R.M. & Zeegars, H. (Editors): *Handbook of Exploration Geochemistry. Volume 4. Regolith Exploration Geochemistry in Tropical and Subtropical Terrains*. Elsevier, Amsterdam, 139–202.

TAYLOR, R.G., 2016: *Gossans and leached cappings – field assessment*. Springer-Verlag.

THIEDE, D.S., 1999: A critical review of penetrative geochemical exploration techniques. Consulting report to MIM Exploration.

THORNBER, M.R., 1992: The chemical mobility and transport of elements in the weathering environment. *In*: Butt, C.R.M. & Zeegers, H. (Editors): *Regolith Exploration Geochemistry in Tropical and Subtropical Terrains, Handbook of Exploration Geochemistry Volume 4*, 79–96. Elsevier, Amsterdam.

TULLEMANS, F.J, AGNEW, P. & VOULGARIS, P., 2001: The role of geology and exploration within the mining cycle at the Osborne Mine, NW Queensland. *In*: Edwards, A.C. (Editor): *Mineral resources and ore estimation – the AusIMM guide to good practice,* 157–168. The Australasian Institute of Mining and Metallurgy, Melbourne.

VAIL, J., FRANCE, D. & LEWIS, B., 2013: Groundwater Sampling. Operating Procedure SESDROC-301-R3, U.S.

WALTERS, S., SKRZECZYNSKI, R., WHITING, T., BUNTING, F. & ARNOLD, G., 2002: Discovery and geology of the Cannington Ag-Pb-Zn deposit, Mount Isa Eastern Succession, Australia: Development and application of an exploration model for Broken Hill-type deposits. *Society of Economic Geologists Special Publication* **9**, 95–118.

WALTERS, S.G. & BAILEY, A., 1998: Geology and mineralisation of the Cannington Ag–Pb–Zn Deposit: an example of Broken Hill-type mineralisation in the Eastern Succession, Mount Isa Inlier, Australia. *Economic Geology*, **93**, 1307–1329.

WAN, W., WANG, M., HU, M. & GAO, Y., 2017: Identification of metal sources in Geogas from the Wangjiazhuang copper deposit, Shandong, China: Evidence from lead isotopes. *Journal of Geochemical Exploration*, **172**, 167–173.

WANG, M., GAO, Y. & LIU, Y., 2008: Progress in the collection of Geogas in China. *Geochemistry: Exploration, Environment, Analysis*, **8**, 183–190.

WANG, M., HANNAN, K.W. & LILLY, R.M., 2012: A test of metals in soil gas (MSG) at Mount Isa mine, Australia. *Proceedings of the 34th International Geological Congress: Unearthing our Past and Future — Resourcing Tomorrow. Brisbane 2012*.

WANG, X., CHANG, Z., LU, Y., XU, L. & XIE, X., 1997: Nanoscale metals in Earthgas and mobile forms of metal in overburden in wide-spaced regional exploration for giant deposits in overburden terrains. *Journal of Geochemical Exploration*, **38**, 157–171.

WARING, C.L., 1990: Genesis of the Mt. Isa Cu Ore System. Ph. D. Thesis, Monash University.

WARING, C.L., 1991: Carbonate isotopic and major element geochemical exploration technique. A report to MIM Exploration Pty Ltd. Geosphere Pty Ltd.

WARING, C.L., ANDREW, A.S. & EWERS, G.R., 1998: Use of O, C, and S stable isotopes in regional mineral exploration. *AGSO Journal of Australian Geology & Geophysics*, **17**(4), 301–313.

WARREN, J.K., 2016: *Meta-evaporites. Chapter 14 of Evaporites – A geological compendium*, 1375–1468. Springer, Switzerland.

WILDMAN, J.E., 2002: The geochemical discrimination of mineralised and barren ironstones from the Selwyn Au-Cu deposit, N.W. Queensland. A report of AMIRA Project 417. *CRC LEME Open File Report* **128**.

ZAHOROWSKI, W., HYDE, M. & WHITTLESTONE, S., 1996: Radon survey of the Ernest Henry copper-gold deposit. Report C442 by ANSTO for MIM Exploration PL.

Appendix A

Sampling procedures for the GORE, MSG and SGH methods

extracts of Section 3 of:
Lilly, R.M., Hannan, K.W. and A-Izzeddin, D., 2010. Geochemistry though cover (GTC) project. Xstrata Copper PL Technical Report 3761, 97 pp. Unpublished property of Glencore.

GEOCHEMICAL TECHNIQUES, FIELD SAMPLING PROCEDURES AND LAB ANALYSIS

3.1 SCOPE (abridged)

Seven analytical techniques were used and evaluated for this project. Because of the different geochemical methods, sample sites and sample mediums it was very important that field sampling procedures were standardised and that systematic site observations were recorded at each sample site for future reference (see Table 9).

To determine sample site repeatability (sampling precision) and facilitate a comparison of sampling precision between each geochemical method, field Duplicates (DUPs) and replicates (REPs) were collected approximately every 8th sample site.

- DUP soil samples were taken from sieved material from the same excavation as the original sample. DUP GORE modules and MSG samples were inserted/collected <50cm from the primary sample site.
- REP soil samples were taken from another sample hole located between 3 and 5m from the primary sample site. REP GORE modules and MSG samples were inserted/collected between 3 and 5m from the primary sample site. Field qualifier information should be the same for all primary samples and DUP/REP samples

3.2 GORE SOIL GAS SURVEY

(LABORATORY: W.L.GORE & ASSOCIATES, INV. MARYLAND, USA)

3.2.1 TECHNIQUE

The premise of the GORE method is that sulphide systems at depth will release compounds (ranging from aromatics, oxygenated, inorganic and sulphur compounds) by oxidation reaction processes that will migrate to surface through post mineralisation cover and cover sequence rocks. Modules are analysed via automated thermal desorption gas chromatographic separation, mass selective detection (ATD_GC/MS). A total of 86 organic compounds are analysed during this survey including several hydrocarbon types (the aliphatics – alkanes, alkenes, cycloalkanes, aromatics and polyaromatics). The sampling module was originally developed in the early 1990's for environmental and hydrocarbon surveys and contains a gas adsorbing sorbent-based collector that is porous to vapours but excludes water and soil particles. The passive GORE soil gas method involves the emplacement of the GORE module (Figure 28) to a depth of approximately 45-60cm for the duration between 10 and 60 days.

3.2.2 SAMPLING

Because of the nature of the GORE and SGH soil gas techniques it is vital that the storage, instillation and retrieval of the GORE module is carried out in a meticulous and conscientious manner. The module is highly sensitive to gases and vapours so field personnel should avoid smoking and the use of insect repellents, sunscreen and other substances containing volatile organic or oily substances while working with the modules. Handling of modules should be kept to a minimum and a new pair of surgical (latex) gloves must be worn for each sample.

Field procedure requires a (paint, oil and grease free) tool to make a hole in the regolith to the depth of 45-60cm. For this study a pointed steel rod was used with a heavy sledge hammer, which proved successful in all terrains. However, where smectitic or soils with a high clay content were encountered (such as black-soil plains), the rod would occasionally become stuck and require digging out. Implanting the GORE module requires organizational consistency, firstly putting on clean gloves and removing the module from its container and making sure all sample numbers are recorded correctly. A piece of pre-cut (approx 1.5m) fluorescent string ('brickies line') is looped through the loop in the module before the insertion rod is put into the pre-cut pocket at the base of the module (Figure 28). The module is them pushed into the hole and the insertion rod is removed (usually requiring a twisting action). It was common for stones and soil to drop into the hole, especially in unconsolidated regolith requiring another hole to be driven. The top of the hole would then be covered by simply kicking over loose surface material and the protruding string would also be covered, often by loose rocks. This was intended to prevent the string being found and the module disturbed or removed. The site was then marked by a marker and flagging tape. In areas close to habitation or tracks on the Mount Isa 1100 OB grid the markers were placed discretely to reduce the chance of passers by disturbing the sample.

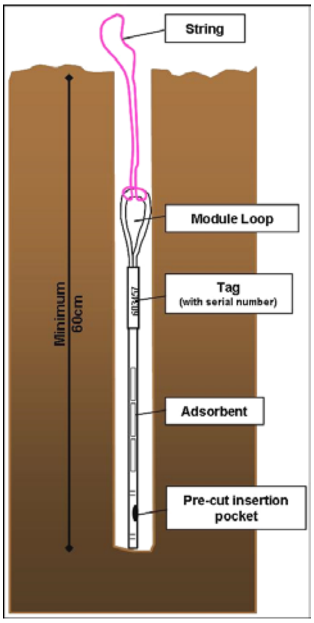

Figure 28, key components of the GORE module

Figure 29, the process of implanting a GORE module. (A) Making hole with heavy sledge hammer, rod and collar.

(B) Removing GORE module from glass vial, placing insertion rod into insertion pocket at base of module. (C) Inserting module. (D) Removing insertion rod, leaving module in place (while keeping hold of retrieval string).

GORE modules were left in situ for 28 days prior to retrieval. Upon collection the site was identified and the string located. A new pair of surgical (latex) gloves was put on and the corresponding glass container that had previously contained the individual module was opened. Modules were easily removed from the hole by pulling the string (with only light resistance). The string was then removed and discarded and the module was pushed into the container and the lid screwed on tightly. During this process handling was limited to the upper loop and lower pocket portions of the module to minimise any contact with the sorbent containing part.

3.3 METAL SOIL GAS (MSG)

(LABORATORY: UNIVERSITY OF QUEENSLAND, BRISBANE)

3.3.1 TECHNIQUE

This study provides the first trial of the technique in Australia although the technique has been applied in China and Asia for over 15 years (Wang et al, 2008). The MSG method is a direct product of the Geogas sampling method, first described by Malmqvist and Kristiansson, (1984). The development of the method is described in Wang et al (1995).

The technique involves passing 'geogas' through an ultra-pure liquid collector, in this case dilute triple distilled Nitric acid (HNo_3) sourced and analysed by ICP-MS (to ppb detection limits) at the University of Queensland (UQ). The suite of elements analysed by MSG is mainly chalcophile metals, making it especially suited to metal exploration. There is still some academic debate as to whether only gaseous species are sampled and whether a sub 0.45ɥm solid particle component is captured (Wang et al, 2008).

3.3.2 SAMPLING

The sampling technique requires a hole of <5cm diameter to be made to a depth of around 60cm in the regolith (i.e. same rods and hammer as GORE survey). Early in the survey it was found that the hole would often collapse prior to the sampler being screwed into place. This was simply solved by pouring a few ml of drinking water around the rod prior to removal. The water consolidated the loose soil surface material making for a better seal with the screw sampler. A cone-shaped screw sampler is then inserted into the hole and screwed in to the regolith to a depth of 30-40cm (Figure 30), when an effective seal was reached in all but the loosest sands. Silica-gel tubes are then attached to the sampler, sample collection bottle and pump. The 1.5l pump is drawn up 3 times per sample site for a total of 4.5l gas passing through the collector per sample hole. The gas is pumped through a 0.45ɥm micropore filter to remove coarse particles entering the liquid collectors. This process is completed 3 times at each sample site, with all holes made within 2m of one another, for a total of 13.5l of gas passed through the liquid collector. The repetition of sampling at each site improves reproducibility of the data (Wang et al, 2008).

Between samples the gas filtering device was cleaned using spare ultra-clean nitric acid from a separate bottle specifically labled for cleaning. Latex gloves were worn for safety to prevent contact of acid with skin. While the use of Nitric acid in the field is a safety concern, it can simply be washed off with water if spillage occurs. Overall, the sampling method for MSG proved very robust and practical in the field, with the advantage that the sample collected in the field requires no further preparation prior to analysis by ICP-MS.

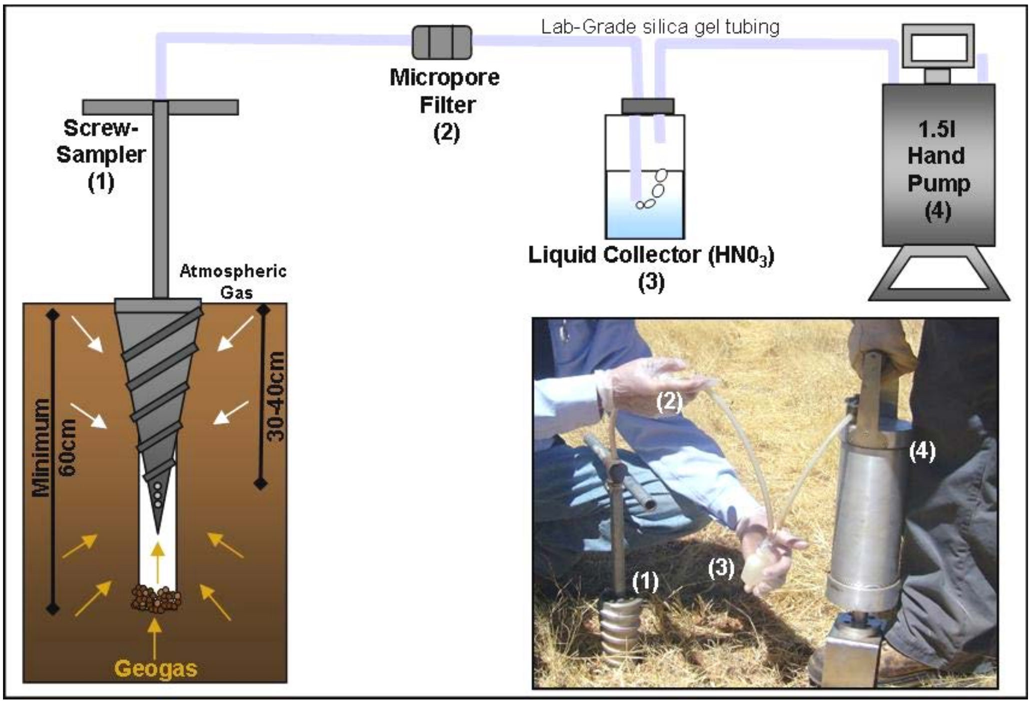

Figure 30, Simplified schematic for MSG collection process used in GTC project (after Wang et al, 2008). Inset picture illustrates sample collection in the field with numbers correlating to main diagram

3.8 SOIL GAS HYDROCARBON (SGH)

(LABORATORY: ACTIVATION LABORATORIES Ltd. ONTARIO, CANADA)

3.8.1 TECHNIQUE

The Soil Gas Hydrocarbon technique is based on the extraction of organic compounds absorbed within soil. Samples are heated to release and detect up to 162 complex hydrocarbon compounds (in the C5-C17 range) with detection limits of parts per trillion (ppt). The process is cost effective as very little sample preparation is required and has been in development for over 25 years.

3.8.2 SAMPLING

The sampling method for SGH was for the most part the same as the main soil sampling procedure (Section 3.4.2 and Figure 31) except that the sample material was not to be in contact with any plastic materials. This was to reduce the risk of contamination by hydrocarbons present in the plastic. The sample was collected from the homogenised secondary excavation placed through a 5mm steel and aluminium sieve and collected on a stainless-steel plate (Figure 33) prior to being bagged (in standard plastic zip-lock bags). The average SGH sample weighed 240g.

Figure 33, showing the 5mm metal sieve (steel wire, aluminium body) and the stainless-steel collection plate. The items were wiped clean between samples with cloth.

Appendix B

The calculation of QA parameters - precision and bias

Background

Precision is a measure of the ability of a sampling process or analytical technique to produce the same result on repeated determinations. Mathematically, it corresponds to the Relative Standard Deviation (RSD) of a standard normal distribution. It is typically expressed as 2RSD or '*two-sigma precision'*, being the percent relative variation at the two standard deviations confidence level, at the stated concentration "C" (*i.e.,* Pc = 100*2σ/C). This means, for example, that if the precision at 1000 ppm is determined to be 20% then the 95 out of 100 determinations are expected to lie between 800ppm and 1200 ppm.

The following procedure is based on the formulation of precision by Thompson and Howarth (1978) and an evolution of the 'HARD' method (Shaw *et al.*, 1998) by Australian practitioners - that is, the use of paired assays for the calculation of precision and bias. The step-by step procedure produces two key results, MPD and Med-2APD, corresponding to bias and precision, respectively.

Calculation instructions

1. Place the paired results in separate columns in a spreadsheet
2. In the third column, calculate the difference between the pair: X1-X2.
3. In the fourth column, calculate the average of the pair: (X1+X2)/2.
4. In the fifth column, calculate the percentage difference (PD) by dividing the difference by the average and multiplying by 100 (*i.e.,* column3 ÷ column4 x 100).
5. In the sixth column, calculate the 2 x Absolute value of column 5 – this is the twice Absolute Percent Difference (2APD) for each QA data pair (*n.b.,* these values can be directly used for APD plots, such as Figure 10 of Chapter 5).
6. At the bottom of column 5 (PD), calculate the mean of all values in that column. This is the **MPD** or mean percent difference, which is a measure of bias (*n.b.,* the median PD can also be used, especially if the population contains extreme outliers).
7. At the bottom of column 6 (2APD), calculate the median of all values in that column. This will produce the **Med-2APD** of the entire data set. This is a measure of precision, as Med-2APD is a robust and unbiased estimation of standard deviation, in particular, the two-sigma precision (above citations).

Notes

- Assay data that are less than four times the lower-detection limit (LDL) should not be included in any final precision calculations as most of the variance will be related to these samples.
- Pairs that produce a 2APD value of more than 100% and at concentrations >4 LDL (lower detection limit), should be checked for sample transposition errors. Values that lie outside of this range will be comparatively common in chemical leachant and soil-gas data but should be immediately scrutinised for data errors or sample site peculiarities.
- If one of a pair is below the detection limit it can be recoded to 0.5 LDL to ensure the pair contributes to the precision calculation (an important consideration for gold).
- Precision is **not** additive in the sampling and assaying process (unlike variance).

References

Shaw, W.J., Khosrowshahi, S., Horton, J., and Waltho, A., 1998. Predicting and monitoring variability in sampling, sample preparation and assaying. Aust. Institute of Geoscientists Bulletin 22, pp. 11-20.

Thompson, M and Howarth, R.J., 1978. A new approach to the estimation of analytical precision. Journal of Geochemical Exploration, 9, pp. 23-30.

Maps of drill hole collars and leachant soil surveys - Mount Isa region

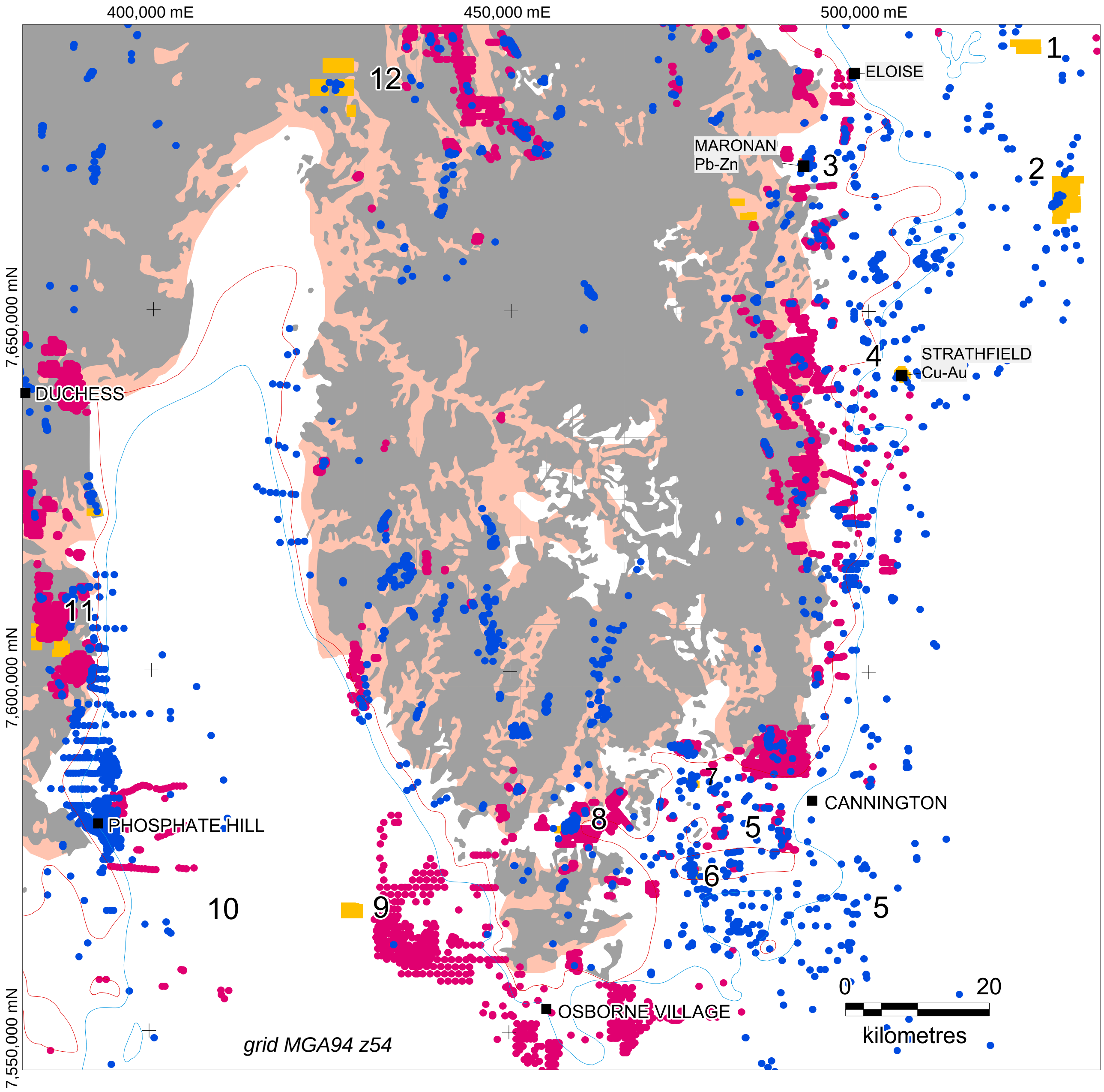

Legend

- ■ 0 m cover (at 2001)
- ■ very thin cover (mostly < 10 m)
- — 100 m cover isopach at 2001
- — 50 m cover isopach at 2001
- ● **target drill hole**
- ● **bedrock geochem drill hole**
- ■ **leachant grid (detail Fig. 7.2)**

sub region southeast

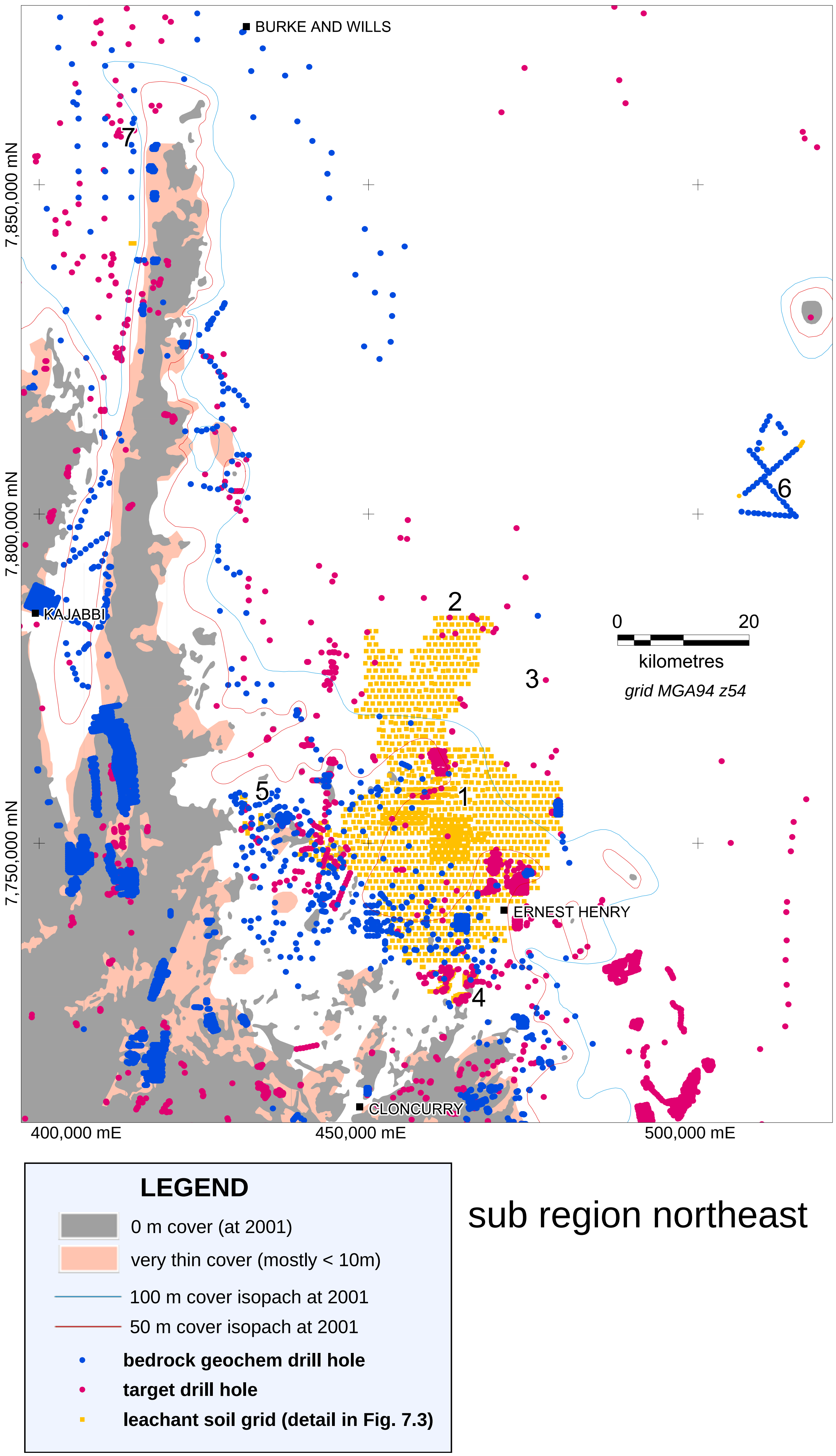

sub region northeast

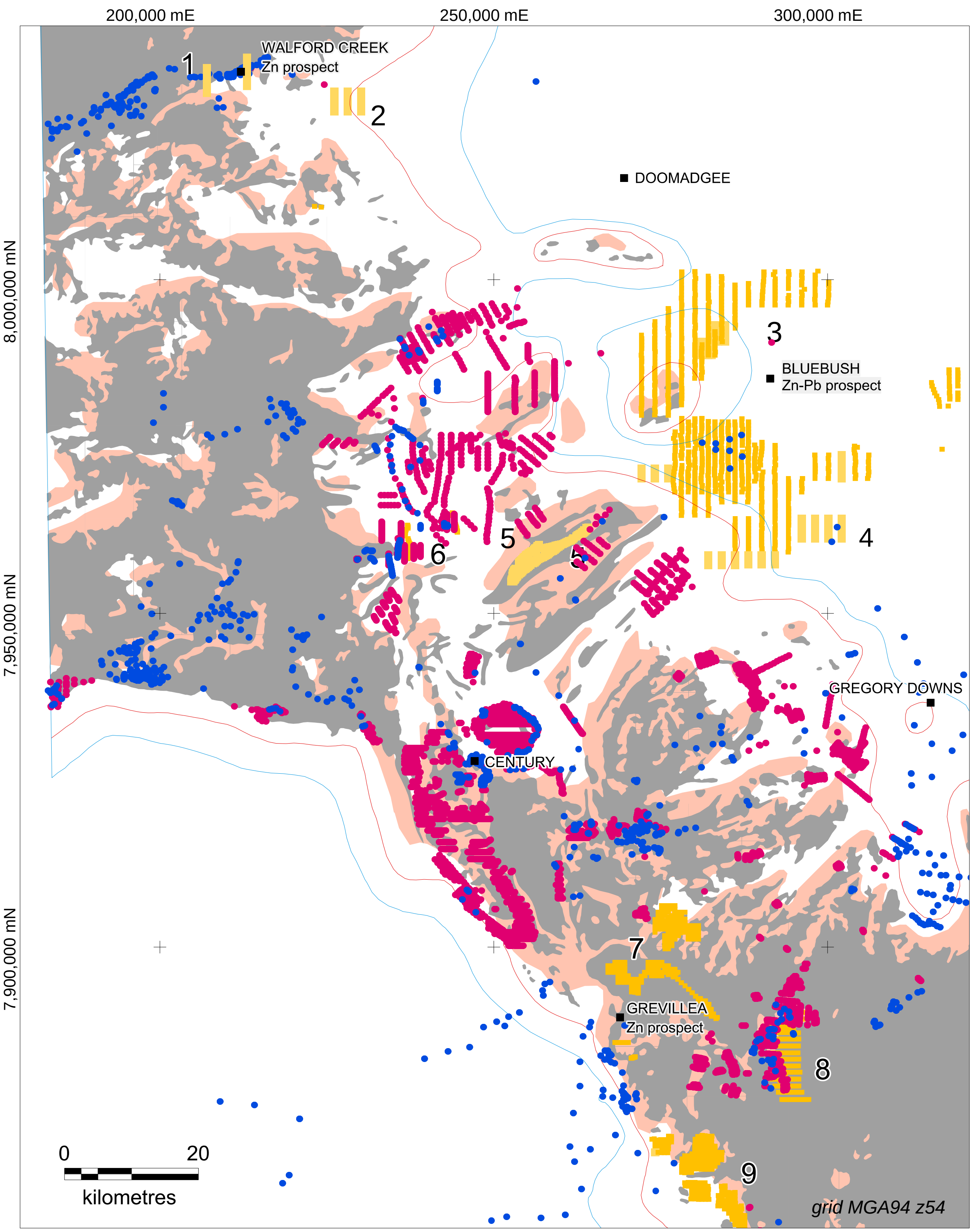

LEGEND

▨ 0 m cover (at 2001)

▨ very thin cover (mostly < 10m)

— 100 m cover isopach at 2001

— 50 m cover isopach at 2001

● **target drill hole**

● **bedrock geochem drill hole**

■ **leachant soil grid (detail in Fig. 7.4)**

sub region northwest

M.I.M. Exploration Pty. Ltd.
MEMORANDUM

Enzyme Leach Trial Over the Walford Creek Zn-Pb Prospect

Keith Hannan
15th March 1996

IMPORTANT - 2018 April
original tables and figures missing
selected figures recovered from "overhead" film copies
schematic map added (ex-film)
field photos added (scans of photographs)

CONTENTS

Survey Costs (excludes field logistics and support)

KWH time in field	: 8 days	2540
KWH report	: 16 days	5080
Airfare and photos		700
Assays enzyme leach	US$5180	7045
Assays Total Digest		2928
Drafting and Secretarial: 2days		400
		$18693

M.I.M. Exploration Pty. Ltd.

Memorandum

From : Keith Hannan
To : Ian Willis
Date : March 15th, 1996
Subject : Walford Creek Orientation Geochemical Survey

Title : **Enzyme Leach Trial Over the Walford Creek Pb-Zn Prospect**

Conclusions

Enzyme leachable Zn in alluvial sands constitutes a geochemical anomaly that extends several hundred metres south of the Fish River Fault at the Walford Creek Pb-Zn prospect. Total zinc, by contrast, drops sharply to background levels 50 metres beyond the Fault. The anomaly appears to extend across the surface projection of an extensive pyrite lens and associated mineralisation of the Mount Les Siltstone beneath more than 70 metres of overburden.

When normalised to Mn (metal/Mn+metal), enzyme leachable Zn, Cu and V display a combined pattern similar to the unprocessed Zn data. That is, an anomaly occurs at the surface, with blind mineralisation 70m below, and extends up to 1 kilometre southward above an extensive pyrite lens of the Mount Les Siltstone. The anomaly is attributed to either horizontally- or vertically-directed hydromorphic dispersion of metals from primary mineralisation into the cover sands. There is no convincing evidence of electrochemical dispersion at Walford Creek (*c.f.,* Ernest Henry).

The enzyme leach anomaly represents a large increase in the area of explorable secondary dispersion. Undiscovered sediment-hosted Pb-Zn deposits in the Gulf region are likely to occur next to faults with a complex movement history. Therefore, hydromorphically redistributed metals may occur over extensive areas at various levels in cover materials and may be laterally offset from ore. The dispersions are easily accessed and are likely to have preserved chemical gradients. They are therefore valid targets for early-stage ground assessment in appropriate settings such as the Gulf of Carpentaria.

There is a 300m wide enzyme leach anomaly in the southwest of the survey area (Line 6900E) which should be assessed in relation to existing targets derived from geophysical data and basin reconstructions.

Introduction

Survey Rationale, Location and Geology

As part of a continuing programme of technique development for covered terrain geochemical exploration, sampling of two lines over blind parts of Walford Creek prospect mineralisation was carried out in early May 1995 to test metal responses to the enzyme leach method.

The plan, overleaf, shows the location of the survey lines relative to the Fish River Fault and the vertically projected upper pyrite lens (inferred from a TEM survey). The schematic cross section (also overleaf) shows relationships between different rock units, structures and mineralisation. Near the Fish River Fault, survey line 12900E transects strong mineralistion beneath a few metres of alluvium and about 70m of Mount Les Siltstone. The associated pyrite lens extends more than 1000 metres to the south. Survey line 6900E, on the other hand, transects only very weak mineralisation (<1 wt% combined) and a deeper and weakly pyritic horizon.

Regolith Characteristics and Sampling Methodology

The cross sections of Figures 1 and 6 summarise topographic and shallow geologic features along each survey line. Samples were taken 25m apart within a few hundred metres of the Fish River Fault, and 50m apart elsewhere.

Most of the survey was conducted on a broad plain of fine-grained, pale-coloured, quartzose alluvial sand (Plate 1a). Except for abundant grass roots, the surficial sand does not have the appearance of a true soil. A colour change is not normally observed until a depth of 25cm or more, where irregular patches of faint orange mottling is observed (Plate 1b). Locally, these mottles are centred by dark brown to redddish sooty hematite and have developed at some sample sites to harder pisoliths and pisolith clusters. Similar pisolith development was observed in our N.T. gulf country tenements and probably results from high level ground water stands during the wet season.

Samples on the alluvial flats were generally taken at the first appearance of mottling, with the assumption that it represents an oxidation-reduction interface suitable for scavenging mobile metal compounds.

In areas of outcrop (*e.g.,* Plate 2a), samples were dug from patches of colluvium, or where necessary, from large cracks and joints within the rock pavement. Generally, a stoney soil with a moderate organic content was present, and the sample was taken at the colour transition to brown or red-brown silty colluvium beneath (Plate 2b).

Most samples were sieved to -0.25mm and stored in a zip-lock plastic bag (100-200g). Damp samples were sieved to -2mm (3-400g) and resieved at the lab to -0.25mm before analysis. Sample depths, regolith characteristics, and sample sieve fraction were all recorded at each station and are reported in Tables 1-4.

Quality Assurance

The effect of sample site variation on enzyme leach and total assay responses was tested by two excavations, 2-5m apart to the same depth, every 10-20 stations (recorded in the QC column of Tables 1-4). As noted for other surveys (*e.g.,* Hannan, 1995a,b), enzyme leach responses are quite robust over areas of tens of square metres. The results of 13 site replicates for Cu and Zn are displayed in Figures 10-12 (see QA and Assay section at end of report). Only station 29400N on line 6900E shows poor replicate correspondence (Fig.12).

Given that samples were taken at a large range of depths, there was some concern that an additional source of variation had been introduced into the assay data. However, a plot of sample depth versus enzyme leach Zn for one line indicates that depth does not control the enzyme leach response at the survey scale (Fig.13).

Line 12900E

Observations

(1) *Zn:* Enzyme leach and total zinc responses in the alluvial sands south of the Fish River Fault differ markedly. Total Zn values drop sharply 50m beyond the Fault to less than 20ppm, whereas enzyme leach Zn decays from elevated values over several hundred metres before dropping to a possible background level at 31000N (see Figure 1, upper).

(2) *Cu:* The enzyme leach Cu profile is similar to that of Zn (Figure 1, middle). By contrast, total Cu values increase slightly but progressively from the south towards the Fish River Fault (refer Figure 5a for clarity). The highest total Cu values occur in samples just south of the Fault, in an area with a slightly subdued enzyme leach Cu and Zn response.

(3) *V:* The total vanadium profile is almost flat, without a discernible change across the alluvium-outcrop transition (Figure 1, lower). By contrast, enzyme leach V increases steadily in the sands south of the Fault, and there is a discernible base-level change at the alluvium-outcrop transition. Enzyme leach V abundances do not appear to respond to known or inferred faults, and are not anomalous above known mineralisation like Zn and Cu.

(4) *Normalised profiles:* Normalisation against Mn highlights the enzyme leachable Zn- and Cu-anomalous nature of the sands south of the Fish River Fault (Figure 2). Normalised V values are also emphasised in samples up to 1000m south of the Fault (Figure 2, lower). In the combined plot of Figure 3, the 800-1000m wide anomalous zone is highlighted as well as isolated peaks that may correspond to geological features; *viz.*, the 29550 peak occurs at the transition from older to younger alluvium to the south, and the outcropping subunit Pff_3 at 32250N is slightly anomalous.

(5) *Other features:* Samples betwen 29750 and 29950N have elevated halogen levels (Figure 4). The alluvium at this location is pisolite rich and corresponds to a gradual elevation drop of about 2m to younger alluvium associated with the flood plain of a large creek at 29250N. South of this transition the alluvium has progressively higher total Fe, Mn, K, Ba, and V abundances consistent with a provenance change (Figure 5b-d). Samples from this area also have unusually elevated enzyme leach Sb, Ba and Mn values, presumably also a provenance feature (Figure 4).

Interpretation

The lack of a total Zn dispersion south of the Fault indicates that clastic input to the recent sands from mineralised rocks in the vicinity of the Fish River Fault is minimal. This argument is supported by:

(a) higher levels of some lithophile elements south of the Fish River Fault that are inconsistent with mechanical derivation from the north (*e.g.*, total K and total Ba, Figure 5c,d);
(b) an opposing, abrupt decrease of other chalcophile elements across the Fault in common with total Zn (*e.g.*, total As, Figure 5b);
(c) maximum enzyme leach Zn values offset some 150m to the south of the Fault; and
(d) visible mechanical dispersion limited to pebbly ferruginous colluvium within 50-75m of the Fault.

Therefore the anomalous enzyme leach Zn pattern in the alluvial sands is not a product of lateral mechanical dispersion of primary mineralisation. Lateral hydromorphic or vertical transport of Zn from depth (hydromorphic or vapour-assisted) must be responsible.

A minor mechanically dispersed component from the north could account for the total Cu pattern south of the Fault. As noted for Zn however, *the enzyme leach and total Cu profiles diverge in detail*, suggesting independent mechanisms of dispersion.

The broadly coincident normalised Zn, Cu and V anomalies of line 12900E provide an even stronger argument against provenance control of the enzyme leach patterns. Firstly, individual Cu-Zn and V peaks from the anomalous zone do not always coincide. Secondly, the normalised metal pattern is not simply an artifact of lower Mn abundances because equally low Mn values occur in samples beyond the main anomalous zone (Figure 4c, upper).

The single station anomaly at 29550N may be related to a local wet season flooding level. Local pisolite development above creek beds and enzyme leach halogen anomalies at breaks in gentle slopes above gulley systems and creeks were also observed in similar surveys at HYC and Lorella (to be reported).

Line 6900E

Observations:

(1) *Zn and Cu:* The enzyme leach profiles for Zn and Cu on this line differ markedly from those of line 12900E. Firstly, alluvial sand south of the Fish River Fault is only anomalous within 100m of the Fault (Figure 6). The samples from this area also have high total Zn and Cu responses and were dug from pebbly and ferruginous colluvium. Secondly, elevated enzyme leach responses in the order of those on Line 12900E occur on the north end of line 6900E within skeletal soil developed on mostly outcroppping unit 3 of the Fish Fiver Formation (Pff$_3$). Another, narrower, anomalous zone occurs on the southern end of the line between 28500 and 28800N.

(2) *V:* Elevated enzyme leach V is only observed in samples from the south-facing colluvial slope of the Fish River Fault. These samples also have high total Mn levels.

(3) *Normalised Profiles:* Unlike line 12900E, normalised Zn anomalous areas lack a strong Cu response. The normalised V anomaly at 28600E occurs within a Zn-anomalous zone, and in detail corresponds to a poorly drained and wet clay-rich area 100m north of a low pavement of Constance Range Sanstone.

(4) *Other Features:* As noted for line 12900E, elevated total K, Ba and low base metal levels in samples south of the Fish river Fault indicate that that much of the sand must be distally derived. Neither the sediments of outcropping Constance Range Sandstone to the south nor Fickling Group to the north explain these chemical patterns unless complex chemical redistribution accompanies the erosion-sedimentation process.

Interpretation

The lack of an enzyme leach Zn anomaly comparable to the 12900E line is attributed to the much weaker and deeper mineralisation of the Mount Les Siltstone at this location (<1wt.% combined Pb-Zn). The Zn-Cu anomalies on the ends of this line are difficult to account for. The northern anomaly may simply be related to outcropping Pff$_3$ and Pfw$_b$, because Pff$_3$ samples also seem to be anomalous on line 12900E (see previous section). The association of the southern Zn-Cu anomaly with a strong normalised vanadium spike is a feature shared by the line 12900E anomaly. Could it be a hydromorphic feature related to mineralisation, or is it just a quirk of local drainage conditions?

Discussion

The enzyme leach patterns for Zn and, to a lesser degree, Cu, reveal a secondary dispersion halo far larger in area than that produced by erosion of mineralised material from the exposed Fish River Fault. The critical question is whether the loosely bound metal of the halo was introduced hydromorphically (*i.e.,* by groundwater) or electrochemically as some kind of vapour phase.

Apart from the coincidence of vanadium- and zinc-anomalous sands (where normalised to Mn) south of the Fish River Fault, none of the so-called 'oxidative suite' metals like As and Mo display patterns of interest. Therefore it is probably safe to conclude that the Walford Creek Zn-Pb (Cu) resource is not coupled to the surface electrochemically.

If the surface enzyme leach anomaly is a hydromorphic feature, was the metal transported vertically into the cover materials or horizontally? At Ernest Henry there is strong evidence of vertical hydromorphic dispersion of ore metals into unconsolidated overburden (Hannan, 1995c). However, at Walford Creek the present topography indicates that there could be groundwater flow from north to south, with outcropping Fickling Group rocks and the mineralised Fault as part of the catchment. If so, it cannot be concluded from this survey that hydromorphic metal halos will necessarily occur vertically above blind mineralisation at other locations. However, it is likely that Walford Creek analogues with extensive hydromorphic halos await detection, because most of the significant Pb-Zn deposits in the Gulf are bound by faults with complex movement histories.

The 300m wide enzyme leach anomaly on the south end of Line 6900E could be an artifact of local drainage conditions, but it should be checked against existing target models because of it's similar chemical make-up to the large 12900E anomaly.

References

Hannan, K.W., 1995a, Partial Extraction Soil Surveys: Covered Copper Deposits, Northern Chile: MIMEX Technical Report 2670.

Hannan, K.W., 1995b, Ernest Henry Enzyme Leach Survey II: MIMEX Memorandum 28/12/95 (7pp, 5 figs.).

Hannan, K.W., 1995c, Hydromorphic Chemical Dispersions above the Ernest Henry Cu-Au deposit: MIMEX Memorandum 1/8/95 (6pp, 5 figs.).

Webb, W. and Rohrlach, B., 1992, The Walford Creek Prospect - an exploration overview: Exploration Geophysics, v.23, 407-412.

K.W. Hannan

cc. ***K. Hannan***
Adelaide and Darwin Offices (via John Anderson)
Brisbane Library

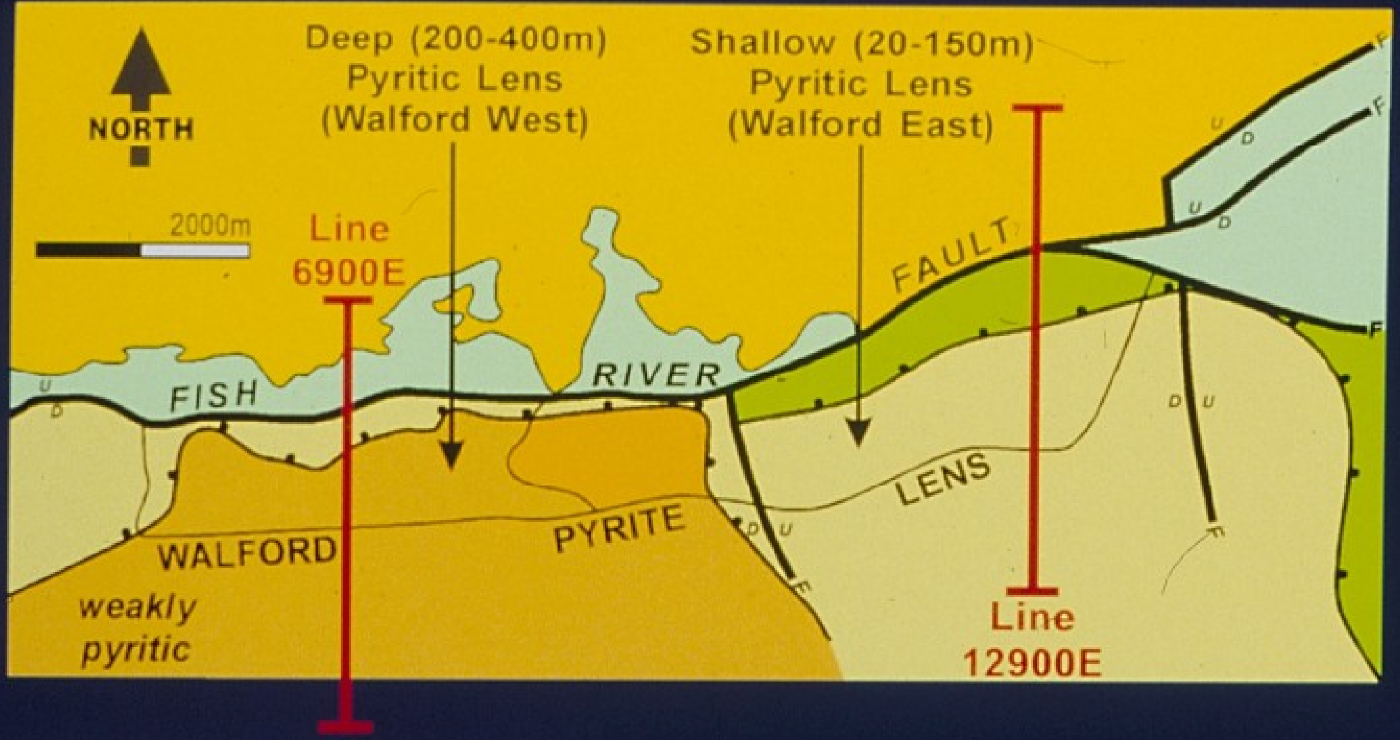

SUMMARY GEOLOGICAL PLAN
WALFORD CREEK PROSPECT
ILLUSTRATING THE EXTENT OF THE PYRITE

Psa	Constance Sandstone
Pfd	Doomadgee Formation
Pfl	Mt Les Siltstone
🟦 🟥	Pyritic Pb-Zn Mineralisation >5% Combined Pb-Zn
✱ ✱	Stockwork Mineralisation
🟧	Dolomite Breccia
Pfw	Walford Dolomite
Pff	Fish River Formation

SCHEMATIC
GEOLOGICAL CROSS SECTION
WALFORD CREEK PROSPECT
(11250mE)

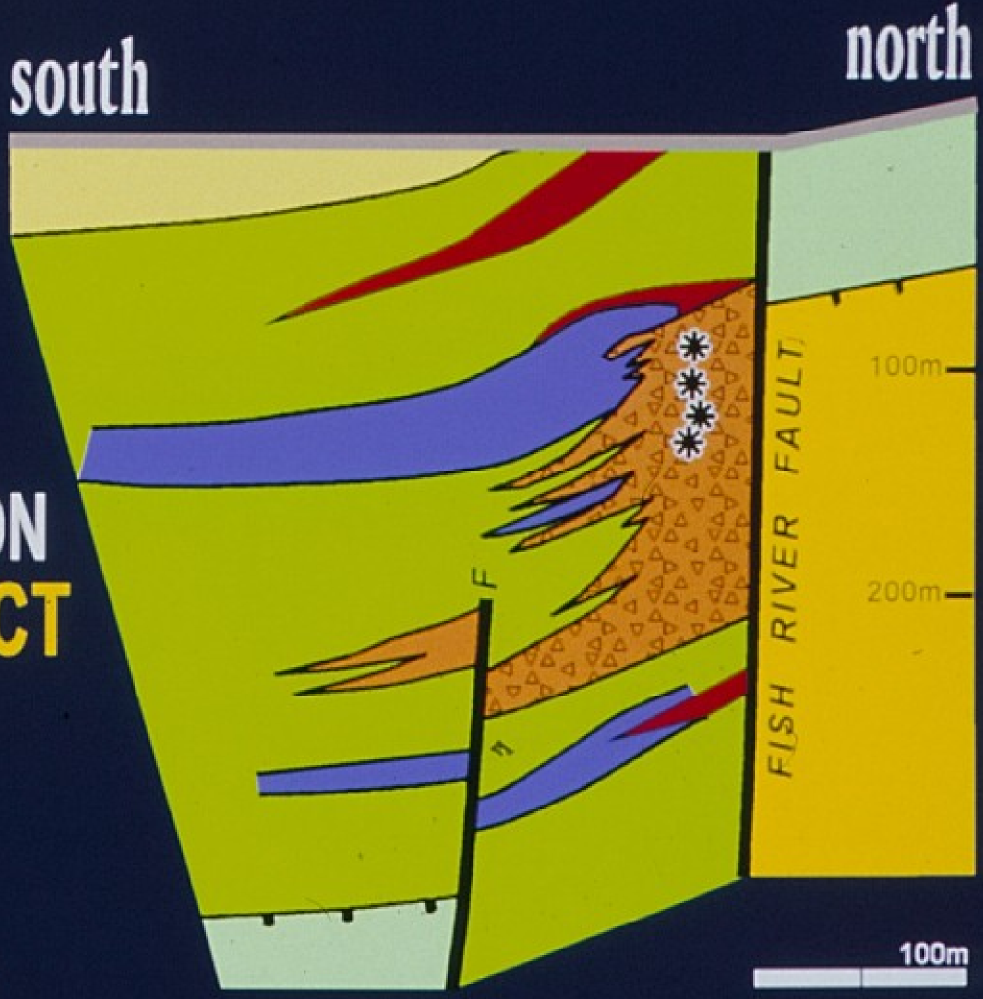

Taken from Webb and Rohrlach (1992)

Plate 1

Plate 2

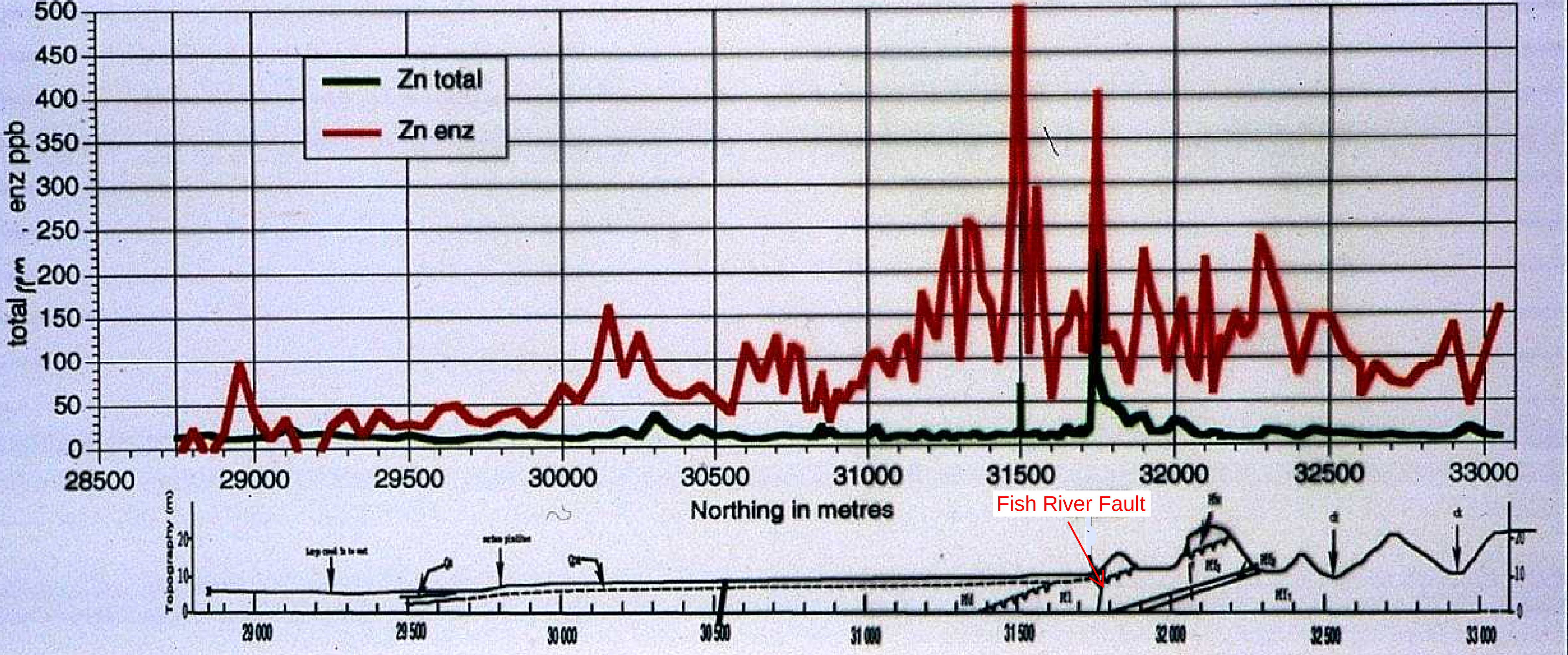

Figure 1 upper

Walford Creek : Line
12900 E Orientation

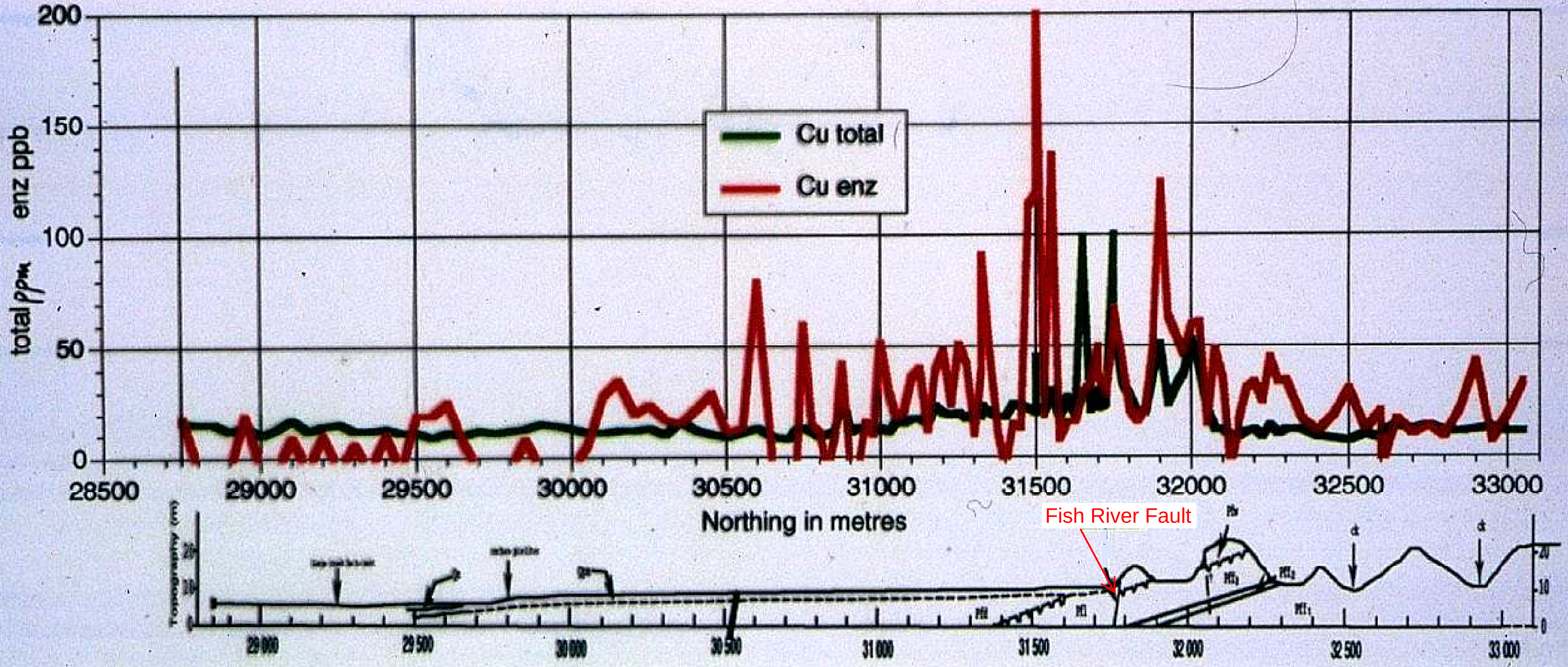

Figure 1 middle

Walford Creek : Line
12900 E Orientation

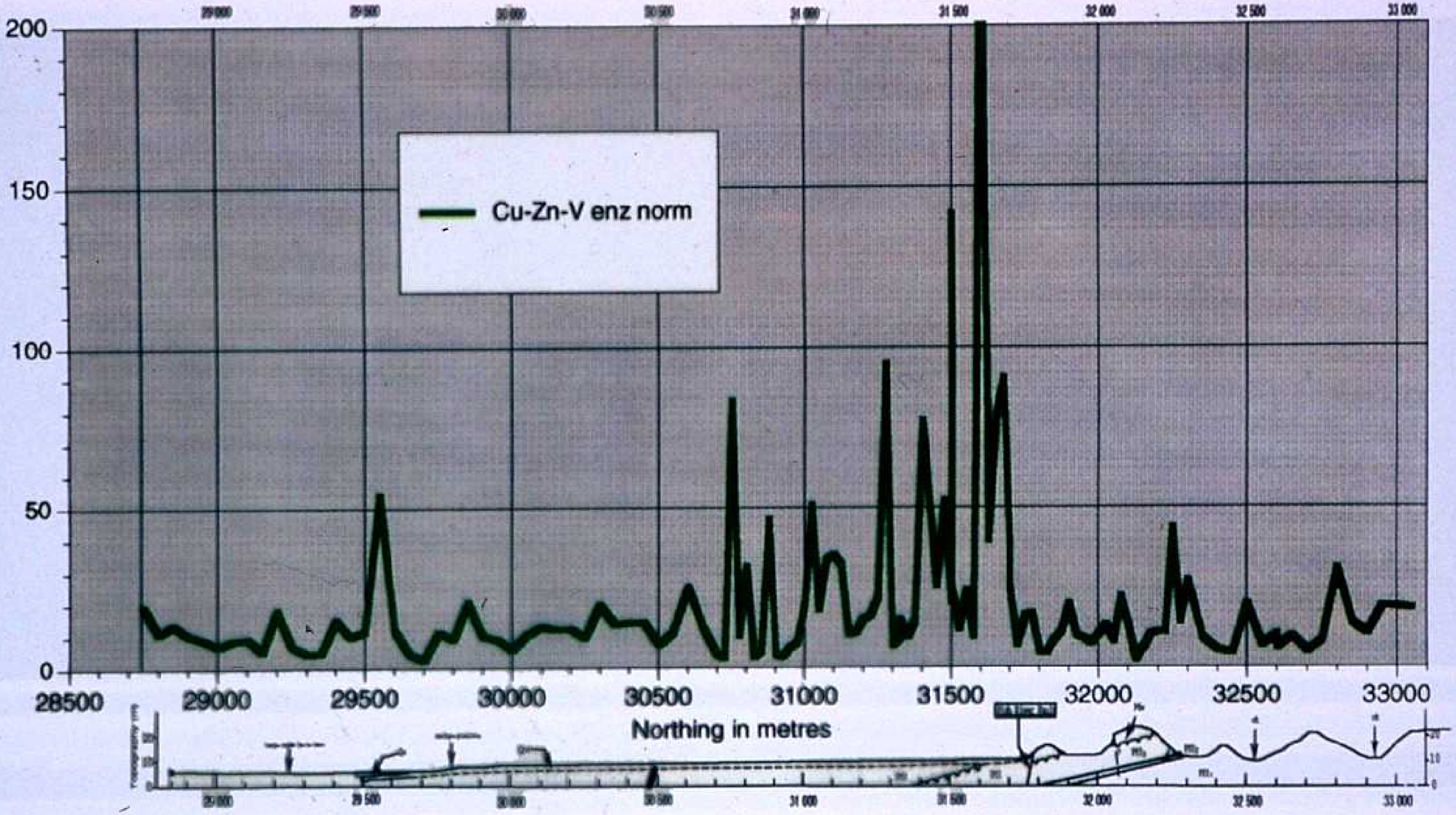

Walford Creek : Line
12900 E Orientation

Figure 3